Studying the interaction of Api5 with TopBP1 and its functional characterization in apoptosis signaling upon DNA damage

A thesis submitted in partial fulfillment of the requirements

for the degree of

Doctor of Philosophy

By

Abhinav Parivesh

20103082

IISER PUNE

Indian Institute of Science Education and Research

2017

Declaration

I declare that this written submission represents my idea in my own words and where others' ideas have been included; I have adequately cited and referenced the original sources. I also declare that I have adhered to all principles of academic honesty and integrity and have not misrepresented or fabricated or falsified any idea/data/fact/source in my submission. I understand that violation of the above will be cause for disciplinary action by the institute and can also evoke penal action from the sources which have thus, not been properly cited or from whom proper permission has not been taken when needed.

The work reported in this thesis is the original work done by me under the guidance of Dr. Mayurika Lahiri.

Date   **Signature of the student**

Certificate

I certify that the thesis entitled **"Studying the interaction of Api5 with TopBP1 and its functional characterization in apoptosis signaling upon DNA damage"** presented by **Mr Abhinav Parivesh** represents his original work which was carried out by him at IISER, Pune under my guidance and supervision during the period from **2nd August 2010** to **26th June 2016.**

The work presented here or any part of it has not been included in any other thesis submitted previously for the award of any degree or diploma from any other university or institutions. I further certify that the above statements made by him in regard to his thesis are correct to the best of my knowledge.

Date: **Dr. Mayurika Lahiri**

                                                          (Supervisor)

Dedication

To my parents for making me believe in my dreams and Encouraging to realize them

Acknowledgements

Synopsis

Studying the interaction of Api5 with TopBP1 and its functional characterization in apoptosis signaling upon DNA damage

Name of the student: Abhinav Parivesh

Student ID: 20103082

Name of the thesis superwiser: Dr Mayurika Lahiri

Date of registration: 2nd August 2010

Indian Institute of Science Education and Research (IISER) Pune

Introduction

The genome is constantly subject to a massive onslaught of DNA damaging agents, extrinsic as well as intrinsic (Ciccia and Elledge, 2010). Intrinsic genotoxic agents include products of metabolism like Reactive oxygen species (ROS), Nitric oxide (NO), alkylating agents to name a few, and the resulting replication fork arrests, whereas external DNA damaging agents include UV causing TT dimerization and single strand breaks (SSB), Ionising radiations causing double-strand breaks (DSB) and a host of various different chemicals (Giglia-mari et al., 2011). The cell has evolved elegant genomic integrity surveillance mechanisms to take care of the DNA-damaging insults it is subjected to so as to preserve its nuclear genome in its current state and pass it on to next generation with minimal changes.

Upon DNA damage, the cell exhibits a DNA damage response (DDR) (Fig 1.1), which begins with activation of checkpoint signaling that communicates with the cell cycle checkpoints to halt the cell cycle, this is followed by activation of DNA repair mechanisms, if however, the extent of damage is too large to be repaired, checkpoint signaling triggers apoptosis (Zhou and Elledge, 2000). In the rare scenario, if the DNA is still not repaired, DNA damage is accumulated that can pass on to subsequent generations, leading to accumulation of genomic instability, which can be a cause for cancer (Kastan and Bartek, 2004). Deregulation of any of the components of cell cycle checkpoint machinery causes genomic instability that may lead to disease (Massauge et al., 2004).

ATM-Chk2 and ATR-Chk1 constitute the two canonical checkpoint signaling pathways, which respond to DSB and SSB/replication fork arrests respectively and a lot of crosstalk is involved between the two owing to inter-conversion of damage structures, making the whole pathway too complex with multiple levels of checks and controls (Fig 1.2). ATM and ATR belong to the family of phosphatidylinositol 3-OH kinase-like kinases (PIKKs). These apical checkpoint kinases act as *sensors* which sense the DNA damage through some higher order chromatin structure changes with the help of other sensor proteins, some of which are also shown to double up as the *mediators* along with other mediator proteins to relay the signal to the downstream *transducer* serine/threonine kinases Chk1 and Chk2. The transducer kinases ultimately phosphorylate the *effectors* like cyclins, p53, E2F1 among others that control cell cycle or DNA repair or Apoptosis.

TopBP1 is a key mediator in the ATR-Chk1 pathway. Human Topoisomerase II β binding protein 1 (TopBP1) is a BRCA1 C-terminus (BRCT) –domain rich protein that is structurally and functionally conserved throughout eukaryotic organisms. Human TopBP1 has 9 BRCT domains, 3 BRCT related regions and 1 poly (ADP-ribose) polymerase homologous region. TopBP1 plays diverse roles in DNA metabolism (Fig 1.4). TopBP1 is expressed at the highest levels during S phase and interacts with DNA Pol ε, possibly helping in loading Pol α, implicating its role in initiating DNA replication; its co-localization with BRCA1 at replication forks when replication is inhibited shows its function in DNA replication fork maintenance (Makiniemi et al., 2001). TopBP1 is phosphorylated by ATM at S405 by ATM in response to DNA damage stabilizing it which otherwise gets degraded through ubiquitylation (Yamane et al., 2002). TopBP1 forms IR irradiation-induced foci (IRIFs) in the nucleus at sites of DNA damage or replication fork arrests through its BRCT 5, which interestingly is not dependent upon its ATM-mediated phosphorylation or Rad9 interaction, but upon its interaction with Nbs1 at the later's N-terminal domain (Morishima et al., 2007; Wardlaw et al., 2014; Yamane et al., 2002). TopBP1 also has a role as transcriptional regulator. Reporter assay studies have identified BRCT domain 4 to be an activator and adjacent BRCT domains 2 and 5 to be repressors of transcription, it has been shown it to activate transcription of HPV E2 transcription factor while repressing the transcription of c-abl (Boner et al., 2002; Wright et al., 2006; Zeng et al., 2005).

Two important transcriptional regulation targets of TopBP1 are p53 and E2F1. TopBP1 interacts with the DNA binding domain (DBD) of p53 via BRCT 7-8 and inhibits its promoter binding activity, thus preventing activation of p53 cell cycle and apoptosis transcriptional targets (Liu et al., 2009a). p53 is mutated in almost 50% of tumors and TopBP1 mediates mutant p53 gain of function through NF-Y and p63/p73 (Liu et al., 2011). Akt phosphorylates TopBP1 at S1159 inducing its oligomerization through BRCT 7-8 (Liu et al., 2006). The oligomerized TopBP1 can no longer bind to chromatin and carry out its DNA damage response, it instead interacts with E2F1 (Liu et al., 2013). It interacts with the amino terminus of E2F1 through its BRCT 6 and inhibits E2F1 functions like induction of S-phase entry and apoptosis (Liu et al., 2003). TopBP1 represses E2F1 mediated cell cycle control and apoptosis by recruiting SWI/SNF chromatin remodeling complex proteins Brg1/Brm onto E2F1 responsive cell cycle and apoptosis target promoters and hence, repressing their activation (Liu et al., 2004).

Other than the Rb-E2F1 pathway, MDM2-p53 is the other key pathway that is activated by checkpoint signaling (Yoshida and Miki, 2010). Both of them have extensive crosstalk between each other and determine the cell fate; survival or apoptosis (Polager and Ginsberg, 2009). E2F1 signals the transcription of p14^{ARF} ,that is an inhibitor MDM2: the E3 ubiquitin ligase of p53. E2F1 thus brings about a stabilization of the downstream p53 indirectly which otherwise undergoes constant turnover by MDM2 (Beckerman and Prives, 1995; Fridman and Lowe, 2003; Haupt et al., 2003; Oren, 1999; Yoshida and Miki, 2010). E2F1 and p53 are two key tumor suppressors in the cell and their functions overlap, both regulate cell cycle as well as apoptosis induction by working as transcription factors to regulate overlapping sets of proteins. Upon low level of DNA damage, checkpoint pathway phosphorylates p53, disrupting its interaction with its degrader MDM2, hence stabilizing it (Moll et al., 2003). p53 upregulates p21 transcriptionally bringing about G1 arrest so as to buy time for the DNA repair to happen (Garner and Raj, 2008; Rodier et al., 2007). If however, the extent of damage is high, p53 accumulates above a particular threshold and now functions to instead up-regulate the transcription of pro-apoptotic proteins like BAX, PUMA, NOXA, FAS (which can also be transcribed by E2F1 independently) (Roos and Kaina, 2013).

One of the regulators of E2F1 is Api5. Api5 is known to influence both the cell cycle regulation as well as the apoptosis induction functions of E2F1 (Arconde et al., 2013; Morris et al., 2006). Apoptosis inhibitor 5 (Api5) or Antiapoptotic clone 11 (AAC11) or FGF2 interacting factor (FIF) is a 1575bp, 60kDa nuclear protein which was first identified as a novel inhibitor of apoptosis induced by growth factor withdrawal by Tewari et al (1997). Api5 was also observed to inhibit apoptosis induced by DNA damage (Berghe et al. 2000). This protein is highly conserved across species as diverse as humans, mouse, frog, fly, mosquito and plants, but they are absent in worms or yeast (Li et al., 2011; Morris et al., 2006). The N-terminal half of the protein is identical to HEAT repeats, while C-terminal is identical to ARM repeats; two known protein-protein interaction motifs, hence Api5 is also predicted to scaffolding function for protein binding (Han et al., 2012b). Over-expression of Api5 inhibits E2F1 overexpression mediated apoptosis indicating that Api5 might be functioning downstream of E2F1 mediated transcriptional control, at least of apoptosis target genes (Morris et al., 2006). Api5 was indeed shown to negatively influence one such E2F1 downstream apoptotic transcriptional target APAF-1, which is involved in the formation of apoptosome (Mayank et al., 2015). The known interactor proteins of Api5 include Fibroblast growth factor 2 (FGF2), apoptotic protein Acinus, chromatin remodeling enzyme ALC1 (a member of SNF2 family of chromatin modifiers), while its plant homologue has been shown to interact with two DEAD-box RNA helicases AIP1/2 (Ahel et al., 2012; Berghe et al., 2000; Li et al., 2011). While Api5 inhibited acinus mediated DNA fragmentation and apoptosis, it was activated by Pim-2 to inhibit apoptosis through NF-kappaB pathway (Ren et al., 2010; Rigou et al., 2009).

Apoptosis or programmed cell death (PCD) is an evolutionarily conserved mechanism of cell death in mammals that normally occurs during development and aging as a part of the homeostatic mechanism of the body to maintain cell numbers. It can also get activated in response to several physiological as well as pathological stimuli (Elmore, 2007). There are two main pathways of apoptosis: death receptor or extrinsic pathway mitochondrial or intrinsic pathway, both of which converge at the execution pathway. The extrinsic pathway is activated in presence of a number of extracellular apoptosis-inducing stimuli which act as ligands for transmembrane death receptors whereas intrinsic pathway is activated by nonreceptor-mediated stimuli like DNA

damage, radiation, toxins, hypoxia, hypothermia, viral infections, free radicals to name a few. Apoptosis activates cysteine proteases called Caspases, which cleave their targets at specific Aspartic acid residues so as to bring about proteolysis associated with apoptosis. The intrinsic pathway of apoptosis begins with the opening of mitochondrial permeability transition (MPT) pore and loss of transmembrane potential (Elmore, 2007). This releases Cytochrome c from inter-membrane space, which then interacts with APAF-1 to form the heptameric backbone of apoptosome (Bratton and Salvesen, 2010). Mitochondrial damage and pore formation are governed by the Bcl2 family of proteins. A total of 25 Bcl2 family proteins are known as yet, some of them are pro-apoptotic meaning they help in opening of mitochondrial pore for example,. Bcl-10, Bax, Bak, Bid, Bad, Bim, Bik to name a few,, while the others are anti-apoptotic which means that they either stabilize the mitochondrial membrane or antagonize the function of pro-apoptotic Bcl2 proteins for example, Bcl-2, Bcl-x, Bcl-xl, Bcl-xs, Bcl-w, BAG among others, (Elmore, 2007; Fulda and Debatin, 2006). Apoptosis pathway regulators like p53 and E2F1 govern the transcription of Bcl2 family of proteins (Fulda and Debatin, 2006; Polager and Ginsberg, 2009).

A GST TopBP1 pulldown screen performed in the lab with HeLa nuclear extracts identified Api5 as a novel interactor upon DNA damage. Owing to this and evidences of them affecting the same axis of apoptosis induction signaling: the one governed by E2F1, it will be intriguing to further validate this interaction and investigate the mechanism how it affects the DNA damage-induced apoptotic pathway as this may be one of the novel ways by which DNA damage induced checkpoint pathway signals to the apoptotic pathway that gets activated upon the failure of repair.

Following are the specific objectives of this study:

1. To confirm the interaction between Api5 and TopBP1 *in vitro* and determine the interacting domain(s)/region(s) of each of the proteins.

2. To elucidate Api5 and TopBP1 interaction *in vivo* in the context of DNA damage in mammalian cells.

3. To investigate the binding of Api5 protein with DNA *in vitro* and its foci formation *in vivo* on damaged DNA and/or its co-localization with TopBP1 DDR foci.

4. Functional characterization of Api5 in response to DNA damage.

Results

1. Api5 interacts with BRCT 7-8 domains of TopBP1 *in vitro* through a region between its N-terminal and LZD.

Full length and truncation mutant constructs of Api5 and TopBP1 were cloned into bacterial expression pGEX-2Tkcs vector (Fig 3.2.2.1 B, C, D, E). Api5 deletion constructs were designed so as to include or exclude the LZD in combination with rest of the regions of the protein. The constructs were transformed into *E Coli* BL21 DE3 bacteria and grown in a culture. Recombinant protein expression was induced by IPTG and purified by affinity purification using GST-agarose beads so as to obtain GST Api5 (88kDa), GST Api5 Δ2-3 (68kDa), GST Api5 LZD (31 kDa), GST Api5 Δ1-2 (42 kDa), GST Api5 Δ3 (72 kDa), GST Api5 Δ1 (46 kDa) and GST (28kDa) proteins (Fig 3.2.1.1 A and 3.2.2.2 B, C, D). The GST affinity tag of full-length GST Api5 protein was removed by thrombin cleavage (Fig 3.2.1.1 B) so as to avoid the possibility of interaction through GST oligomerization while performing protein interaction studies with GST TopBP1 recombinant protein. TopBP1 truncation mutants were designed so as to achieve progressive deletion of the canonical pairs of BRCT domains. The pGEX-2Tkcs-TopBP1 truncation mutant clones were similarly used to express and purify GST TopBP1 (193 kDa), GST BRCT Δ1-2 (167 kDa), GST BRCT Δ1-3 (149 kDa), GST BRCT Δ1-5 (117 kDa), GST BRCT Δ1-6 (88 kDa), GST BRCT Δ7-8 (168 kDa), GST AAD (64 kDa) and GST BRCT 7-8 (58 kDa) recombinant proteins (Fig 3.2.2.5 B,C,D,E,F and 3.2.2.6 D). Reciprocal far western blotting was performed to validate the interaction *in vitro,* as well as to elucidate the interacting domain(s)/region(s). Full-length Api5 and its truncation mutants were used as "prey" along with full-length TopBP1 as "bait" protein (Fig 3.2.1.3 B and 3.2.2.4 B). Reciprocally, full-length TopBP1 and its truncation mutants were used as "prey" together with Api5 as "bait" protein (Fig 3.2.2.6 B,C). The reciprocal far western revealed that Api5 shows direct biochemical interaction with TopBP1. BRCT7-8 of TopBP1, N-terminal portion as well as LZD+C terminal portion of Api5 were responsible for this interaction though the region between N-terminal and LZD was sufficient for interacting with TopBP1. While *in vitro* interaction study validated the interaction and revealed the interacting regions as well, it didn't tell about the

physiological standing and relevance of this interaction. So this interaction study needed to be performed *in vivo* in response to DNA damage.

2. Api5 shows an interaction with TopBP1 *in vivo* that gets enhanced upon DNA damage

In vivo interaction studies were performed in HeLa cells as the GST –TopBP1 pulldown screen was performed with HeLa nuclear extracts. Camptothecin (CPT) was used as a source of DNA damage to induce the apoptotic pathway. The first step towards using CPT for current studies is determining the dosage that is just sufficient to induce apoptosis and is not as high so as to induce cell death by necrosis. This is critical because Api5 is an anti-apoptotic protein and is supposed to carry out its function at the threshold of induction of apoptosis by DNA damage and not when that threshold has been breached and necrosis has set in as a result of excessive DNA damage The threshold dosage of CPT to induce apoptosis was determined by staining the cells with AnnexinV-PI and flow cytometry analysis (Fig 4.2.1B). 10μM CPT for 16 hours was chosen as the dose of damage to be used for IP experiments since this dose was just able to induce apoptosis while keeping the extent of necrosis quite low.

Immunoprecipitation (IP) was performed on HeLa cell lysates to check the Api5-TopBP1 interaction *in vivo*. TopBP1 was observed to co-immunoprecipitate with Api5 (Fig 4.2.2A) without or with CPT-induced DNA damage. Image J based densitometric quantification of biological triplicates indicated that TopBP1 showed an increased interaction with Api5 upon 16 hours of CPT-induced DNA damage (Fig 4.2.2B).

Since both TopBP1 and Api5 are known nuclear proteins, it is further interesting to investigate whether the interaction happens on chromatin or elsewhere in the nucleus.

3. Api5 binds to DNA and hence the chromatin, but it does not form damage dependent or cell cycle-dependent nuclear foci unlike TopBP1

Our previous studies showed that Api5 interacts with TopBP1 in normal asynchronous cells and the interaction increases after damage. Given the formation of TopBP1 replication and DDR foci, it is pertinent to investigate whether Api5 co-localizes at such foci. Before looking for the possibility of Api5 foci co-localization with that of TopBP1, it should be evaluated whether Api5 forms damage dependent or

cell cycle dependent foci at the first place. If at all Api5 is found to form foci, it can further be investigated whether they are formed owing to its ability to bind to DNA by its own or whether its foci formation is dependent upon its protein-protein interaction(s).

EMSA studies were performed with a linear 1.5kB DNA as well as with annealed oligos to create 70mer dsDNA or 70mer fork and bubble that mimic DNA intermediate structures formed upon DNA damage. EMSA results showed that Api5 can bind directly to DNA and it does so preferably to normal dsDNA in comparison to any intermediate DNA structures (Figure 5.2.1 A, B, C, D).

Chromatin fractionation studies revealed that Api5 is bound to the chromatin and is present in the nucleoplasm as well, both in presence and absence of DNA damage (Fig 5.2.2).

Immunofluorescence and live cell imaging revealed that Api5 did not form nuclear foci under any circumstance of DNA damage or cell cycle phase. Neither did global and prolonged DNA damage caused by CPT nor localized and instantaneous damage caused by laser made Api5 to form cytologically discernible "foci" anywhere close to those formed by TopBP1 or γH2AX under such circumstance (Fig 5.2.3). It did not form foci during different phases of the cell cycle with or without damage (Fig 5.2.5 A). Over-expressed recombinant Api5 protein also did not form nuclear foci upon CPT or laser-induced DNA damage (Fig 5.2.6). From these observations, it can be argued that the interaction between Api5 and TopBP1 might be happening on the chromatin in a way that is not cytologically discernible, possibly in a way similar to that of some of the checkpoint and DNA repair proteins.

4. Functional characterization of Api5 in response to DNA damage

siRNA-mediated knockdown of Api5 and rescue studies were performed in p53 proficient U2OS cells. Api5 knockdown did not affect CPT-induced activation of checkpoint pathway in the way TopBP1 knockdown did. While TopBP1 knockdown inhibited the activation of Chk1, Api5 knockdown did not affect the activation of Chk1 or Chk2 upon CPT induced damage (Fig 6.2.1.2). Functional characterization of Api5 in the apoptosis pathway was done at a dose of CPT that was just sufficient of inducing apoptosis as evidenced by activation of caspases (Fig 6.2.1.3). Rescue experiment was performed by introducing an Api5-mVenusC1 clone which had been

mutagenized to make it siRNA-resistant (Fig 6.2.1.1). Ectopically expressed recombinant Api5 exhibited a significant decrease in protein levels upon damage. (Fig 6.2.1.4 A, D, E). Rescue experiment was also performed with truncation mutants of Api5 so as to determine the region of Api5 responsible for its function in the apoptosis pathway as discovered from siRNA knockdown and full length Api5 rescue experiments performed earlier. Deletion mutants of Api5 were cloned into mVenusC1 plasmid (Fig 6.2.2.1 C, D, E, F, G) to express Api5 Venus (89kDa), Api5 Venus Δ2-3 (69kDa), Api5 Venus LZD (32 kDa), Api5 Venus Δ1-2 (43 kDa), Api5 Venus Δ3 (73 kDa) and Api5 Venus Δ1 (47 kDa) proteins. The Δ1-2, Δ1 and LZD deletion constructs that lacked the region of Api5 between its N-terminal and LZD showed a significant decrease in protein levels upon DNA damage in comparison to those containing the above region namely,. Δ2-3 and Δ3 (Fig 6.2.2.2 F, G, H, I, J). This indicates the region between its N-terminal and LZD is important for the stability of protein. This could be explained due to the presence of a LxxLL motif in that region which is supposed to impart stability to the protein structure (Han et al., 2012a). Several markers like active caspase 3, active caspase 9, PARP1 were monitored to elucidate the role of Api5 in the apoptosis pathway (Fig 6.2.1.5 and 6.2.2.3). Levels of p53, its activation (p53pS15) and its upstream negative regulator MDM2 were also monitored (Fig 6.2.1.6, 6.2.1.7 and 6.2.2.4). These studies revealed that Api5 knockdown activated caspases and its re-introduction reduced caspase activation as deduced from the levels of cleaved caspases upon DNA damage. The region of Api5 between its N-terminal and LZD was responsible for this function. Api5 knockdown also stabilized p53 over and above that achieved due to DNA damage and it reverted back upon rescue with recombinant Api5.

Discussion and future perspectives

As discussed earlier TopBP1 is a BRCT rich protein. BRCT domains can occur as single as well as canonical pairs, single BRCT domains do not, but canonical pairs do have the potential to recognize and bind phosphorylated proteins at sequence motif pSXXF (Wu et al., 2015; Zhang et al., 1998). TopBP1 was observed to interact with Api5 *in vivo* that showed an enhancement upon DNA damage. Protein phosphorylation prediction databases (UniProt and PhosphSite Plus) predict phosphorylation of Api5 at multiple residues and considering the phospho-protein

binding nature of TopBP1, it could be speculated that interaction between the two may be dependent upon this PTM. However, the dependence of their interaction on phosphorylation of Api5 can be ruled out by the findings of *in vitro* interaction studies which showed that the two *in bacto* purified recombinant proteins interacted with each other as shown by far western blotting analysis. Interestingly, BRCT 7 and 8 of TopBP1 were involved in this interaction that forms a canonical pair and is supposed to bind to phosphorylated proteins. It will be interesting to investigate the phosphorylation state of Api5. Api5, on the other hand, was observed to interact with TopBP1 through a region between its N-terminal and LZD. This region of Api5 has a sequence that resembles both the HEAT and ARM protein-protein interaction motifs towards the N terminal and C terminal respectively. It will be interesting to elucidate which amongst the two regions is responsible/sufficient for its interaction with TopBP1 and further investigate the role of the LxxLL motif within the HEAT repeat in this. Cell fractionation studies showed that Api5 is bound to chromatin and this could be because of its direct binding to DNA as evidenced by EMSA studies proving that lack of basic DNA binding region in its LZD does not limit its interaction with DNA as it happens anyway. EMSA studies were performed with annealed oligos to generate dsDNA and intermediate structures like fork and bubble. It will be useful to broaden the repertoire of DNA structures tested for their binding to purified Api5 protein as different kinds of genotoxic damages can produce a wide variety of DNA damage structures which are not limited to stalled forks and bubbles; varying lengths of ssDNA-dsDNA junctions will be of particular interest. Api5 is believed to be a nuclear protein, just like TopBP1 but it was observed to be present in the cytoplasmic fraction as well unlike TopBP1 which could possibly be due to its nuclear export by piggybacking on some unknown interactor or directly through the CRM pathway because of presence of a putative NES, that will be an interesting aspect to investigate. Ectopically expressed Api5 showed a decrease in protein levels upon DNA damage and this was even more pronounced in the deletion constructs that did not have the region between its N-terminal and LZD. The decrease in protein levels can either happen because of repression of transcription or because of degradation of the protein. Prior reports, however, support the concept of Api5 degradation as a means of its function upon apoptotic stimuli, whereas the deletion construct observation is supported by the fact that the constructs showing more degradation

lack the LxxLL motif that has been reported to be important for providing stability to the protein. Api5 knockdown led to an increase in active Caspase 3 levels upon DNA damage that were reduced upon Api5 rescue, proving negative regulation of DNA damage-induced apoptosis by Api5. The region between N-terminal and LZD was responsible for this anti-apoptotic activity. Api5 knockdown increased the levels of p53 significantly over and above its stabilization upon DNA damage without much affecting its activation measured by its phosphorylation at S15, however, TopBP1 didn't have that effect. This effect could either be because of a comparable down-regulation of its primary degrador MDM2 or because of its transcriptional up-regulation. MDM2, however, did not show a concomitant change in levels under the same experimental conditions as would be expected to bring about the change in p53 levels that was observed. Hence the possibility of transcriptional up-regulation of p53 because of Api5 knockdown could not be ruled out. Interestingly, TopBP1 has also been reported to inhibit E2F1 transcriptional targets by recruiting Brg1/Brm to E2F1 responsive promoters. Interactions of TopBP1 and Api5 with different components of SWI/SNF complex and with each other as shown in this study, may point towards them working in a protein complex with the multiple components of chromatin remodeling complex so as to aid and complement each other in bringing about transcriptional regulation of apoptotic promoters leading to inhibition of apoptosis in the face of DNA damage.

Bibliography

Ahel, D., Hořejší, Z., Wiechens, N., Polo, S.E., Garcia-, E., Owen-hughes, T., and Boulton, S.J. (2009). Poly (ADP-ribose) -dependent regulation of DNA repair by the chromatin remodelling enzyme ALC1. Science *325*, 1240–1243.

Arconde, T., Touriol, C., Perez, G., Navarro, M.G., and Lacazette, E. (2013). Api5 Contributes to E2F1 Control of the G1 / S Cell Cycle Phase Transition. PLoS One *8*, 1-10.

Beckerman, R., and Prives, C. (1995). Transcriptional Regulation by p53. J. Biol. Chem. *270*, 6966–6974.

Berghe, V. Den, Laurell, H., Huez, I., Zanibellato, C., and Cedex, T. (2000). FIF [Fibroblast Growth Factor-2 (FGF-2) -Interacting-Factor], a Nuclear Putatively Antiapoptotic Factor , Interacts Specifically with FGF-2. Mol. Endo. *14*, 1709–1724.

Boner, W., Taylor, E.R., Tsirimonaki, E., Yamane, K., Campo, M.S., and Morgan, I.M. (2002). A Functional interaction between the human papillomavirus 16 transcription/replication factor E2 and the DNA damage response protein TopBP1. J. Biol. Chem. *277*, 22297–22303.

Bratton, S.B., and Salvesen, G.S. (2010). Regulation of the Apaf-1-caspase-9 apoptosome. J. Cell Sci. *123*, 3209–3214.

Ciccia, A., and Elledge, S.J. (2010). Review The DNA Damage Response : Making It Safe to Play with Knives. Mol. Cell *40*, 179–204.

Elmore, S. (2007). Apoptosis: A Review of Programmed Cell Death. Toxicol Pathol. *35*, 495–516.

Fridman, J.S., and Lowe, S.W. (2003). Control of apoptosis by p53. Oncogene *22*, 9030–9040.

Fulda, S., and Debatin, K.-M. (2006). Extrinsic versus intrinsic apoptosis pathways in anticancer chemotherapy. Oncogene *25*, 4798–4811.

Garner, E., and Raj, K. (2008). Protective mechanisms of p53-p21-pRb proteins against DNA damage-induced cell death. Cell Cycle *7*, 1–6.

Giglia-mari, G., Zotter, A., and Vermeulen, W. (2011). DNA Damage Response. Cold Spring Harb. Perspect. Biol. *3,* 1-19.

Han, B., Kim, K.H., Lee, S.J., Jeong, K., Cho, J., Hee, K., Woo, T., Kim, S., Yoon, H., Suh, S.W., et al. (2012). Helical Repeat Structure of Apoptosis Inhibitor 5 Reveals

Protein-Protein Interaction Modules * □. J. Biol. Chem. *287*, 10727–10737.

Haupt, S., Berger, M., Goldberg, Z., and Haupt, Y. (2003). Apoptosis - the p53 network. J. Cell Sci. *116*, 4077–4085.

Kastan, M.B., and Bartek, J. (2004). Cell-cycle checkpoints and cancer. Nature *432*, 316–323.

Li, X., Gao, X., Wei, Y., Deng, L., Ouyang, Y., Chen, G., Li, X., Zhang, Q., and Wu, C. (2011). Rice APOPTOSIS INHIBITOR5 coupled with two DEAD-box adenosine 5'-triphosphate-dependent RNA helicases regulates tapetum degeneration. Plant Cell *23*, 1416–1434.

Liu, K., Lin, F., Ruppert, J.M., and Lin, W. (2003). Regulation of E2F1 by BRCT Domain-Containing Protein TopBP1. Molecular and Cellular Biology *23*, 3287–3304.

Liu, K., Luo, Y., Lin, F., and Lin, W. (2004). TopBP1 recruits Brg1 / Brm to repress E2F1-induced apoptosis , a novel pRb-independent and E2F1-specific control for cell survival. Genes Dev. *18*, 673–686.

Liu, K., Paik, J.C., Wang, B., Lin, F.-T., and Lin, W.-C. (2006). Regulation of TopBP1 oligomerization by Akt/PKB for cell survival. EMBO J. *25*, 4795–4807.

Liu, K., Bellam, N., Lin, H.-Y.Y., Wang, B., Stockard, C.R., Grizzle, W.E., and Lin, W.-C.C. (2009). Regulation of p53 by TopBP1: a potential mechanism for p53 inactivation in cancer. Mol Cell Biol *29*, 2673-2693.

Liu, K., Ling, S., and Lin, W. (2011). TopBP1 Mediates Mutant p53 Gain of Function through NF-Y and p63 / p73   . Mol Cell Biol *31*, 4464–4481.

Liu, K., Graves, J.D., Scott, J.D., Li, R., and Lin, W.-C. (2013). Akt switches TopBP1 function from checkpoint activation to transcriptional regulation through phosphoserine binding-mediated oligomerization. Mol. Cell. Biol. *33*, 4685–4700.

Mäkiniemi, M., Hillukkala, T., Tuusa, J., Reini, K., Vaara, M., Huang, D., Pospiech, H., Majuri, I., Westerling, T., Mäkelä, T. P., et al. (2001). BRCT Domain-containing Protein TopBP1 Functions in DNA Replication and Damage Response. J. Biol. Chem. *276*, 30399-30406.

Mayank, A.K., Sharma, S., Nailwal, H., and Lal, S.K. (2015). Nucleoprotein of influenza A virus negatively impacts antiapoptotic protein API5 to enhance E2F1-dependent apoptosis and virus replication. Nat. Cell Death Dis. *6*, 1–11.

Moll, U.M., Petrenko, O., Moll, U.M., and Petrenko, O. (2003). The MDM2-p53 Interaction. Mol Cancer Res. *1*, 1001–1008.

Morishima, K., Sakamoto, S., Kobayashi, J., and Izumi, H. (2007). TopBP1 associates with NBS1 and is involved in homologous recombination repair. Biochemical and Biophysical Research Communications *362*, 872–879.

Morris, E.J., Michaud, W.A., Ji, J., Moon, N., Rocco, J.W., and Dyson, N.J. (2006). Functional Identification of Api5 as a Suppressor of E2F-Dependent Apoptosis In Vivo. PLoS Genetics *2*, 1834-1848.

Oren, M. (1999). Regulation of the p53 tumor suppressor protein. J. Biol. Chem. *274*, 36031–36034.

Polager, S., and Ginsberg, D. (2009). p53 and E2f : partners in life and death a V. Nat. Rev. Cancer *9*, 738–748.

Ren, K., Zhang, W., Shi, Y., and Gong, J. (2010). Pim-2 activates API-5 to inhibit the apoptosis of hepatocellular carcinoma cells through NF-kappaB pathway. Pathol. Oncol. Res. *16*, 229–237.

Rigou, P., Piddubnyak, V., Faye, A., Rain, J.-C., Michel, L., Calvo, F., and Poyet, J.-L. (2009). The antiapoptotic protein AAC-11 interacts with and regulates Acinus-mediated DNA fragmentation. EMBO J. *28*, 1576–1588.

Rodier, F., Campisi, J., and Bhaumik, D. (2007). Two faces of p53 : aging and tumor suppression. Nucleic Acids Res. *35*, 7475–7484.

Roos, W.P., and Kaina, B. (2013). DNA damage-induced cell death : From specific DNA lesions to the DNA damage response and apoptosis. Cancer Lett. *332*, 237–248.

Wardlaw, C.P., Carr, A.M., and Oliver, A.W. (2014). TopBP1 : A BRCT-scaffold protein functioning in multiple cellular pathways. DNA Repair (Amst). *22*, 165–174.

Wright, R.H.G., Dornan, E.S., Donaldson, M.M., and Morgan, I.M. (2006). TopBP1 contains a transcriptional activation domain suppressed by two adjacent BRCT domains. Biochem. J. *400*, 573–582.

Wu, Q., Jubb, H., and Blundell, T.L. (2015). Phosphopeptide interactions with BRCA1 BRCT domains: More than just a motif. Prog. Biophys. Mol. Biol. *117*, 143–148.

Yamane, K., Wu, X., and Chen, J. (2002). A DNA Damage-Regulated BRCT-Containing Protein , TopBP1 , Is Required for Cell Survival. Molecular and Cellular Biology *22*, 555–566.

Yoshida, K., and Miki, Y. (2010). The cell death machinery governed by the p53 tumor suppressor in response to DNA damage. Cancer Sci. *101*, 831–835.

Zeng, L., Hu, Y., and Li, B. (2005). Identification of TopBP1 as a c-Abl-interacting protein and a repressor for c-Abl expression. J. Biol. Chem. *280*, 29374–29380.

Zhang, X., Moréra, S., Bates, P.A., Whitehead, P.C., Coffer, A.I., Hainbucher, K., Nash, R.A., Sternberg, M.J.E., Lindahl, T., and Freemont, P.S. (1998). Structure of an XRCC1 BRCT domain: A new protein-protein interaction module. EMBO J. *17*, 6404–6411.

Zhou, B.S., and Elledge, S.J. (2000). The DNA damage response: putting checkpoints in perspective. Nature *408*, 433–439.

Contents

List of figures

Abbrevations

Api5..Apoptosis inhibitor 5

AAC11..Anti-apoptotic clone 11

FIF..FGF2 interacting factor

LZD..Leucine zipper domain

TopBP1...Topoisomerase II β-binding protein

BRCT..BRCA1 C-terminal

PTM..Post translational modification

CPT...Camptothecin

DSB...Double strand break

SSB..Single strand break

RFA...Replication fork arrest

DDR...DNA damage response

ATM..Ataxia telangiectasia mutated

Chk2..Checkpoint kinase 2

ATR...ATM and Rad3 related

Chk1..Checkpoint kinase 1

ORC2...Origin recognition complex

9-1-1..Rad9-Hus1-Rad1

TNN...Tris NaCl NP-40 buffer

RIPA..Radio immunoprecipitation assay buffer

BCA...Bicinchoninic acid

IP...Immunoprecipitation

IF..Immunofluorescence staining/imaging

WB...Western blotting

TAE..Tris Acetic acid EDTA buffer

TE...Tris EDTA buffer

PCR..Polymerase chain reaction

dNTP..deoxy-nucleotide triphosphate

SDM...Site directed mutagenesis

IPTG...Isopropyl β-D-1-thiogalactopyranoside

GST..Glutathione S-transferase

xxx

SDS... Sodium dodecyl sulfate

TEMED..Tetramethylethylenediamine

APS... Ammonium persulfate

PAGE...Polyacrylamide gel electrophoresis

CBB...Coomassie brilliant blue

TBS-T..Tris buffered saline-Tween-20

6X SB... 6X Sample buffer (Laemmli buffer)

PVDF...Polyvinylidene fluoride

NFDM..Non-fat dry milk

DMEM...Dulbecco's modified eagle's medium

DPBS...Dulbecco's phosphate buffered saline

PBS...Phosphate buffered saline

FBS...Fetal bovine serum

BSA...Bovine serum albumin

EMSA..Electro-phoretic mobility shift assay

ssDNA...single-stranded DNA

dsDNA...double-stranded DNA

STEB...Sucrose Tris EDTA gel loading buffer

TBE...Tris boric acid EDTA buffer

siRNA..small interfering RNA

FACS...Fluorescence activated cell sorting

PI...Propidium iodide

G1 phase...Growth 1 phase

G2 phase...Growth 2 phase

S phase...Synthesis phase

GFP..Green fluorescence protein

ECFP..Enhanced cerulean fluorescence protein

H2B..Histone 2-B

Chapter 1. Introduction

1.1 Prelude

Every human cell contains around three billion base pairs of DNA housed inside its nucleus which is the master database of cell and a signature of the individual and the species, that has stood all the evolutionary forces to shape up in its current form to shape the being of the individual. So, the utmost responsibility of every cell is to preserve its nuclear genome in its current state and pass it on to next generation with minimal changes. But, at the same time the DNA is constantly subject to a massive onslaught of DNA damaging agents, extrinsic as well as intrinsic (Ciccia and Elledge, 2010). Intrinsic genotoxic agents include products of metabolism like reactive oxygen species (ROS), nitric oxide (NO) and alkylating agents to name a few, that result in replication fork arrests, whereas examples of external DNA damaging agents include ultraviolet radiation (UV) that cause TT dimerization and single strand breaks (SSB), ionising radiation (IR) that cause double-strand breaks (DSB) and a host of various different chemicals (Giglia-mari et al., 2011).

 Therefore, the cell has evolved elegant genomic surveillance mechanisms to take care of the DNA-damaging insults it is subjected to. This mechanism involves an intricate network of proteins which can be broadly classified as tumor suppressors and oncogenes to exert their control at the cell cycle checkpoints, halting the cell cycle and providing it time and resources to repair its damaged DNA. Only, when success is not achieved in mending the mistakes, the cell goes down the path of death (apoptosis) or proliferation (tumorigenesis).

Deregulation of any of the components of cell cycle checkpoint machinery causes genomic instability that may lead to disease (Massauge et al., 2004). Ataxia telangiectasia (A-T) for example is characterized by neurodegeneration, radiosensitivity, immunodeficiency and cancer predisposition, and is caused by a mutation in the checkpoint gene ATM (Zhou and Elledge, 2000). Hypomorphic mutations in the gene NBS1 leads to a disease called Nijmegen breakage syndrome (NBS) characterized by microcephaly, immunodeficiency, radiation sensitivity and predisposition to cancer (Nyberg et al., 2002).

Cellular responses to DNA damage constitute one of the most important fields in cancer biology. While DNA damage causes cancer (supported by epidemiological

1

data), it is also used for the treatment of cancer (radio and chemotherapy), which is responsible for the most of the side effects of the therapy (hair loss, bone marrow suppression, gastrointestinal toxicities attributed to cell death of the progenitors in these tissues) (Hanahan and Weinberg, 2011; Kastan and Bartek, 2004). So, unraveling the incompletely understood cellular response to DNA damage remains a challenging field of study.

The extraordinary ability of genome maintenance systems to detect and resolve defects in the DNA ensures a very low rate of spontaneous mutations and a breakdown in any or several of its components leads to increased mutability of the cells in response to mutagenic agents.

1.2 History

This field was too fast to emerge as a promising field in science hardly after a decade since the elucidation of the structure of DNA by Watson and Crick in 1953. Lee Hartwell in 1960's performing genetic screens in budding yeast identified mutants that blocked specific stages of cell cycle progression. He called this "checkpoints" and the genes responsible for it as cell division cycle (cdc) genes. Beginning in 1972 Paul Nurse identified mutants in fission yeast that could speed up the cell cycle, he named them cdc2 and subsequently discovered its first human homolog CDK1 gene in 1987 which controls the G2/M transition. Tim Hunt working with Sea Urchin egg extracts identified proteins the levels of which varied throughout the cell cycle, he named them "Cyclins". The three shared the 2001 Nobel Prize in medicine *"for their discoveries of key regulators of the cell cycle"*. Brian, Cox, John Game and Robert Mortimer among others identified a collection of radiation-sensitive mutants of yeast in the late 1960s in genetic screens calling them as rad genes. Ted Weinert in association with Lee Hartwell did additional genetic screens in yeast to characterize Rad mutations that were required for the checkpoint response to cell cycle arrest following a DNA damage signal and named them "mec" mutants (mitotic entry checkpoints). Weinert further used genetic screens with the damage inducing cdc mutants and identified mec1, mec2, and mec3 mutants as defective for the G2/M checkpoint. In the following decades, other players of the cell cycle and checkpoint signaling pathways were discovered in yeast and subsequently in higher eukaryotes including humans. One of the most important players being p53, discovered in 1979

and its mutation implicated in almost 50% of solid tumors. Sequencing of the Human Genome in 2001 gave a second major thrust in an identification of the huge number of proteins involved in genome maintenance. About 130 different Human repair genes with unknown functions were identified and cloned then (Wood et al., 2001).

1.3 The DNA damage response and cell cycle checkpoints

Upon DNA damage, the cell exhibits a DNA damage response (DDR) (Fig 1.1), which begins with activation of checkpoint signaling that communicates with the cell cycle checkpoints to halt the cell cycle, this is followed by activation of DNA repair mechanisms, if however, the extent of damage is too large to be repaired, checkpoint signaling triggers apoptosis (Zhou and Elledge, 2000). In the rare scenario, if the DNA is still not repaired, DNA damage is accumulated that can pass on to subsequent generations, leading to accumulation of genomic instability, which can be a cause for cancer (Kastan and Bartek, 2004).

The cell cycle checkpoint is a mechanism evolved by the cell by which it can halt the cell from progressing to the next stage of the cell cycle until it can ensure that an earlier process, such as DNA replication or mitosis is complete. These checkpoints comprise of G1/S, S, G2/M and mitotic or spindle assembly checkpoints and passage through each of them is regulated by the activation of cyclin-dependent kinases by respective cyclins whose levels keep changing throughout the cell cycle (Kops et al., 2005). During G1 phase, Cyclin D is expressed which in complex with CDK4/6 ensures protein synthesis and growth. Expression of Cyclin E by the end of G1 phase initiates DNA synthesis and thus Cyclin E - CDK2 govern G1/S transition. During replication, Cyclin A expression comes up and Cyclin A – CDK2 control the onset and transition of DNA replication during S phase. Cyclin B expression rises by the end of S phase into the G2 phase and Cyclin B – CDK1 control G2/M transition (Warmerdam and Kanaar, 2010). The different cyclins and their levels are governed by components of checkpoint signaling.
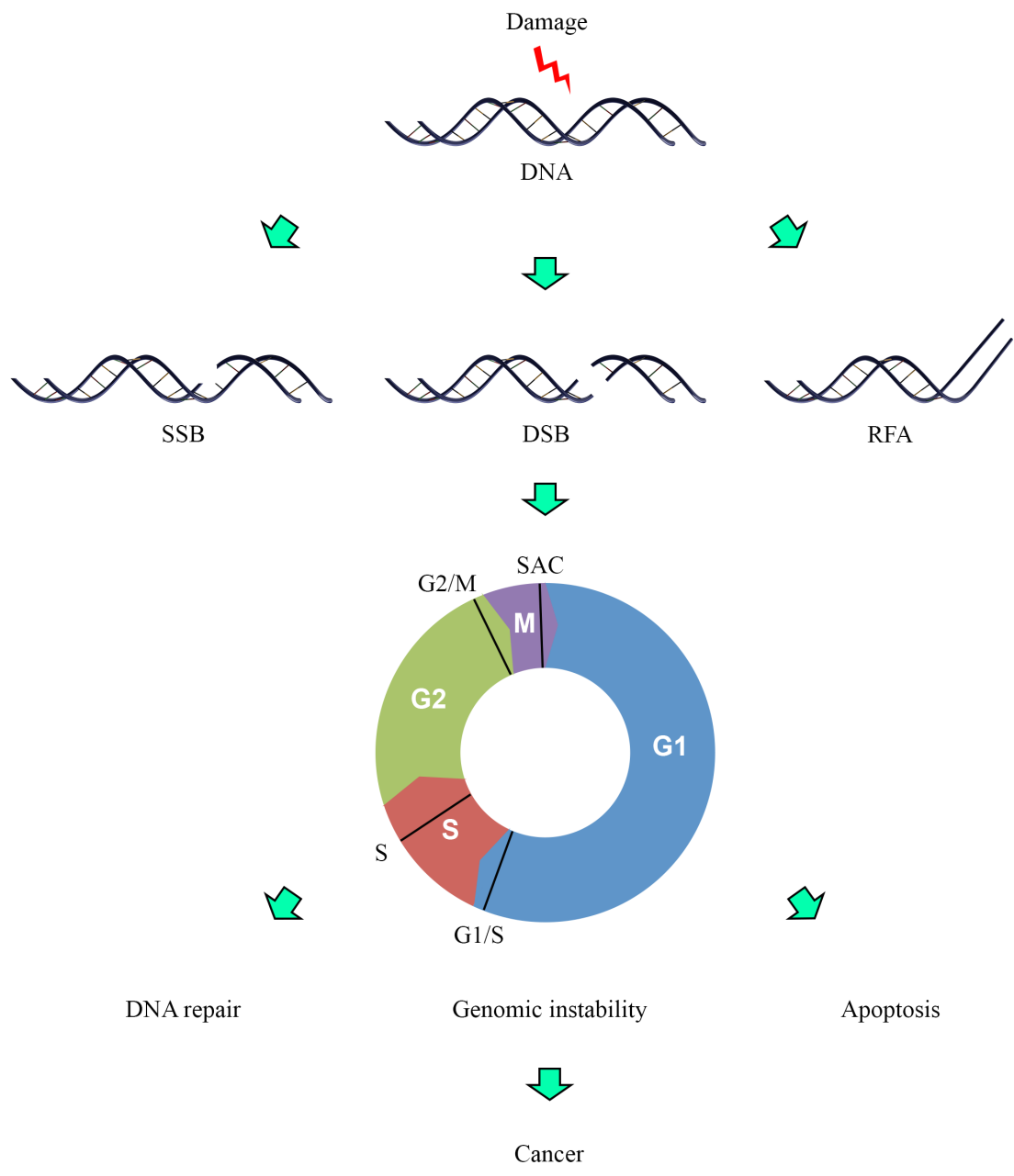
Figure 1.1: The DNA damage response (DDR).

DNA damaging agents may cause single strand breaks (SSB), double strand breaks (DSB) or replication fork arrest (RFA), all of which activate the checkpoint signaling halting the cell cycle at G1/S, S, G2/M or spindle assembly checkpoint (SAC). This is followed by the onset of DNA repair, if however, the extent of damage is large, apoptosis is induced. Failure of either of them leads to accumulation of genomic instability, which can lead to cancer (modified from Kastan and Bartek, 2004; Liang et al., 2009; Malumbres and Barbacid, 2009; Warmerdam and Kanaar, 2010; Zhou and Elledge, 2000).

1.4 Checkpoint signaling

ATM (Ataxia telangiectasia mutated) and ATR (ATM and Rad3 related) are extremely large 301 and 350 kDa phosphatidylinositol 3-OH kinase-like kinases (PIKK) (Kastan and Bartek, 2004). Other members of this family include DNA-PK and mTOR (Iijima et al., 2008). These proximal checkpoint kinases act as *sensors* which sense the DNA damage through some higher order chromatin structure changes with the help of other sensor proteins, some of which are also shown to double up as the *mediators* along with other mediator proteins to relay the signal to the downstream *transducer* serine/threonine kinases Chk1 and Chk2. The transducer kinases ultimately phosphorylate the *effectors* like cyclins, p53, E2F1 among others, that control cell cycle or DNA repair or Apoptosis. ATM-Chk2 and ATR-Chk1 constitute the two canonical checkpoint signaling pathways, which respond to DSB and SSB/replication fork arrests respectively and a lot of crosstalk is involved between the two making the whole pathway too complex with multiple levels of checks and controls (Fig 1.2). As is evident, ATM-Chk2 but not ATR-Chk1 is dispensable for the normal being of the cell (Kastan and Bartek, 2004).

DSB	**DNA damage structures**	SSB, RFA
	⬇	
MRN, γH2AX, ATMIN	**Sensors**	RFC-RAD17, 9-1-1
	⬇	
ATM	**Apical kinases**	ATR
	⬇	
MDC1, 53BP1, BRCA1	**Mediators**	TopBP1, Claspin
	⬇	
Chk2	**Transducer kinases**	Chk1
	⬇	
	Effectors p53, E2F1, CDC25s...	
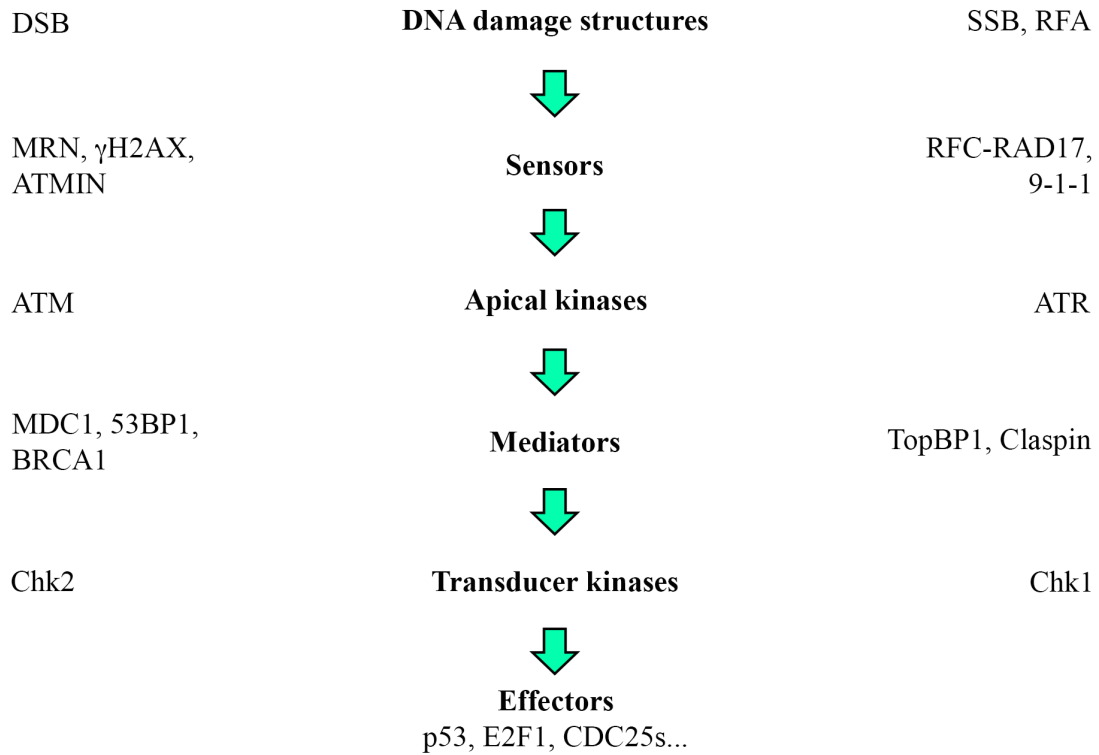
Figure 1.2: Simplified overview of the checkpoint-signaling pathway.

DNA damage structures are identified by sensor proteins which then activate apical kinases ATM or ATR that activate the transducer kinases Chk2 or Chk1 respectively through the mediators, the effectors are ultimately activated that regulate cell cycle checkpoints, DNA repair or apoptotic pathways. ATM-Chk2 and ATR-Chk1 are the two parallel canonical pathways of checkpoint signaling that are activated in response to DSBs and SSBs/Replication fork arrests respectively, though there are extensive crosstalk between the two pathways (modified from Abraham, 2001; Kastan and Bartek, 2004; Liang et al., 2009).

1.5 ATM-Chk2 signaling

The ATM-Chk2 response is activated rapidly in response to double-strand breaks (DSB) across the G1/S, S or G2/M phases of the cell cycle. ATM activation is a two-step process. DSB leads to phosphorylation of H2AX (γH2AX), which is identified by NBS1 of the MRN complex (MRE11-RAD50-NBS1) leading to tethering of MRN on DSBs and its concentration. DSBs lead to monomerization of inactive ATM dimers leading to their partial activation (Iijima et al., 2008). In a second step, the C-terminal ATM interacting motif (AIM) of NBS1 leads to autophosphorylation of ATM at S1981 leading to its full activation. AIM on NBS1 or AIM like motifs on ATM interacting protein (ATMIN), Ku80 and ATRIP which activate ATM, DNA PKcs, and ATR respectively could be a conserved domain in DNA damage recognition proteins which activate PIKKs (Kanu and Behrens, 2007). ATM activation leads to further phosphorylation of mediator/transducer proteins like p53, c-Abl, MDC1, 53BP1, BRCA1, Chk2 as well as γH2AX leading to the further amplification of signal as well as DNA repair and checkpoint response. DSB repair in eukaryotes occurs primarily by Nonhomologous end joining (NHEJ) or Homologous recombination (HR). NHEJ is an error-prone repair mechanism occurring throughout the cell cycle carried out by recruitment of factors like DNA PKcs, Ku70/Ku80, Artemis, XRCC IV/ DNA ligase IV, XLF, whereas HR is an error-free DNA repair pathway occurring in S or G2 phases and has following steps: DNA end resection carried out by NBS1, Exo1; 3'overhang coating by single strand binding protein RPA; strand invasion felicitated by RAD51; new strand synthesis initiated by the recruitment of RAD51C, RAD51D, BRCA1; Holliday junction resolution by helicases and nucleases (Christmann, 2003).

1.6 ATR-Chk1 signaling

ATR has different roles in DNA damage response via arresting the cell cycle, preventing firing of late replication origins, stabilization of stressed replication forks, promoting DNA repair and restart of DNA replication (Flynn and Zou, 2011). This signaling cascade is activated slowly mainly in response to Single strand breaks (SSB) or replication fork arrests predominantly in the S phase of the cell cycle. ssDNA are coated by RPA which in turn lead to localization of ATRIP and its

heterodimeric partner ATR. In the presence of ssDNA-dsDNA junctions, RFC like protein Rad17 acts as a clamp loader to load the PCNA like RAD9-RAD1-HUS1 (9-1-1) sliding clamp onto the DNA lesion. This acts as a scaffold for recruitment of other regulators like TopBP1 in the vicinity of ATR-ATRIP to ultimately bring about efficient activation of ATR (Liang et al., 2009). The ATR activation domain in TopBP1 between BRCT VI and VII interacts with ATRIP as well as the PRD (PIKK regulatory domain) of ATR bound to RPA coated ssDNA. On the other hand, TopBP1 BRCT domains I and II interact with RAD9 C-terminus of the 9-1-1 via a phosphorylated residue (S387). These two interactions mediated by TopBP1 lead to the full-fledged activation of ATR (Flynn and Zou., 2011). Furthermore, TopBP1 and Claspin function as mediators to activate Chk1, which in turn phosphorylates its downstream effectors like cdc25A and cdc25C affecting the cell cycle (Liang et al., 2009).

A number of parallel pathways mediated by the different components of the checkpoint signaling network work simultaneously to orchestrate a global checkpoint response to DNA Damage and bring about a G1 /S, S or G2/M arrest.

1.7 DNA structures activating checkpoint responses and the ATM – ATR switch

SSB or replication fork arrests leading to ssDNA and ssDNA-dsDNA junctions are the key DNA structures activating the ATR pathway. The strength and timing of ATR activation depend upon the length of ssDNA, the number of ssDNA-dsDNA junctions or their association with replication forks (Flynn and Zou, 2011). The DSB leading to dsDNA blunt ends also activate ATM in a dsDNA-ssDNA junction length-dependent manner and provide an opportunity for biphasic DSB response wherein the instant ATM activation by virtue of dsDNA leads to a more prolonged ATR activation as a result of resection of the dsDNA by exonucleases MRN-CtIP and ExoI of the ATM pathway. Increasing length of single strand overhangs (SSOs) at the dsDNA and ssDNA junction attenuates ATM activity and potentiates ATR activity through a swap of DNA damage sensors. Thus single stranded DNA orchestrates an ATM to ATR switch which constitutes a biphasic response to DSBs (Shiotani and Zou, 2009). This fact is further supported by *in vitro* studies of the preferential binding of the different sensor/mediator/effector proteins of ATM and ATR pathway to different kinds of

DNA structures (Sancar and Kemp, 2011) also providing an evidence for the occurrence of a lot of crosstalk between the ATM-Chk2 and ATR-Chk1 pathways.

1.8 Regulation of the cell cycle checkpoints

The G1 checkpoint response targets two major tumor suppressor pathways: p53 and pRB. In response to the damage, the ATM/ATR and Chk1/Chk2 phosphorylate p53 transcription factor within its amino-terminal transactivation domain as well as its ubiquitin ligase MDM2. These changes lead to stabilization and accumulation of p53, whose key transcriptional target is the p21 CIP1/WAF1 inhibitor of the Cdk2 kinase, leading to G1 arrest. Additionally, DNA damage also preserves E2F transcription factors bound to RB, to ensure sustained G1 blockage. Mitogenic signals cause activation of Cdk4/6-CyclinD causing phosphorylation of RB and release of E2F which in turn bring about the transcription of its targets ORC, MCM, DNA Pol α which support DNA replication (Massagué, 2004).

S phase checkpoint also has two parallel branches. In response to damage, Chk1 and Chk2 enhance the physiological level of phosphorylation and hence turnover of Cdk2-CyclinA activator cdc25A. The inhibition of the activity of CDK2 activity blocks the loading of cdc45 onto chromatin blocking DNA Pol α and hence new origin firing. Another branch involves phosphorylation of NBS1 and FANCD2 leading to S-phase block (Abraham, 2001; Nyberg et al., 2002).

The G2 checkpoint block in response to genotoxic stress involves inhibition of activation of CyclinB-CDK1 by ATM/ATR and Chk1/Chk2. This is carried out by p38 kinase mediated subcellular sequestration, degradation and/or inhibition of CDK1 activator cdc25 family of phosphatases at the M phase boundary. Several upstream regulators of CyclinB-CDK1 like Polo-like kinases as well as cell cycle inhibitors p21, GADD4a, and 14-3-3 sigma proteins are implicated in G2 checkpoint response (Abraham, 2001; Kastan and Bartek, 2004; Nyberg et al., 2002).

1.9 Different kinds of DNA lesions and Repair mechanisms

The different exogenous and endogenous stresses lead to different kinds of DNA lesions. For example. hydrolysis leads to spontaneous DNA depurination, ROS induce base oxidation and DNA breaks, replication defects can cause mismatches, replication

forks collapse can result in strand breaks, UV can cause single strand breaks, mismatches, and cyclobutane pyrimidine dimers (CPD), IR can lead to double strand breaks. SN1 and SN2 alkylating agents can lead to O-alkylated and N-alkylated purines and pyrimidines (Fu et al., 2012). The choice of which repair system to use depends both on the type of lesion and on the cell cycle phase of the cell. There are several single step repair mechanisms that take care of some lesions. For example, MGMT (Pegg et al., 1995) and AlkB homolog ABH (Duncan et al., 2002) repair alkylation lesions. DNA photolyases repair UV-induced CPD and 6-4 photoproducts in a light-dependent manner (Thompson and Sancar, 2002). Base Excision repair (BER) majorly removes oxidized DNA bases in nondividing cells by employing enzymes such as DNA glycosylases and AP endonucleases (Fishel et al., 2007). Nucleotide excision repair on the other hand repairs bulky DNA adducts arising from UV-induced photolesions and intrastrand crosslinks in G1 cells (Friedberg et al., 2001). It comprises of a global genomic repair (GGR) and a transcription-coupled repair (TCR). If left unrepaired during the G1 phase, bulky DNA lesions can block DNA polymerases. Replication then proceeds by bypassing these lesions using specialized translesion synthesis (TLS) polymerases or template-switch mechanisms that use the newly synthesized sister chromatid as a template. Mismatch Repair, basically functional in the S phase removes base mismatches caused by spontaneous and induced deamination, oxidation, methylation and replication errors (Modrich and Lahue, 1996). DNA double strand breaks are highly potent inducers of genotoxic stress (chromosome breaks and translocation) and cell death. Depending upon the cell cycle phase they are repaired by the error-prone non-homologous end joining (NHEJ) which occurs in G0/G1 phase or by error free homologous recombination (HR) occurring in late S or G2 phases using the homologous DNA strand as a template for repair synthesis (Johnson and Jasin, 2000).

1.10 TopBP1: A key mediator of the checkpoint response

Human Topoisomerase II β binding protein 1 (TopBP1) is a BRCA1 C-terminus (BRCT) domain rich protein that is structurally and functionally conserved throughout eukaryotic organisms. Human TopBP1 has 9 BRCT domains, 3 BRCT related regions and 1 poly (ADP-ribose) polymerase homologous region.
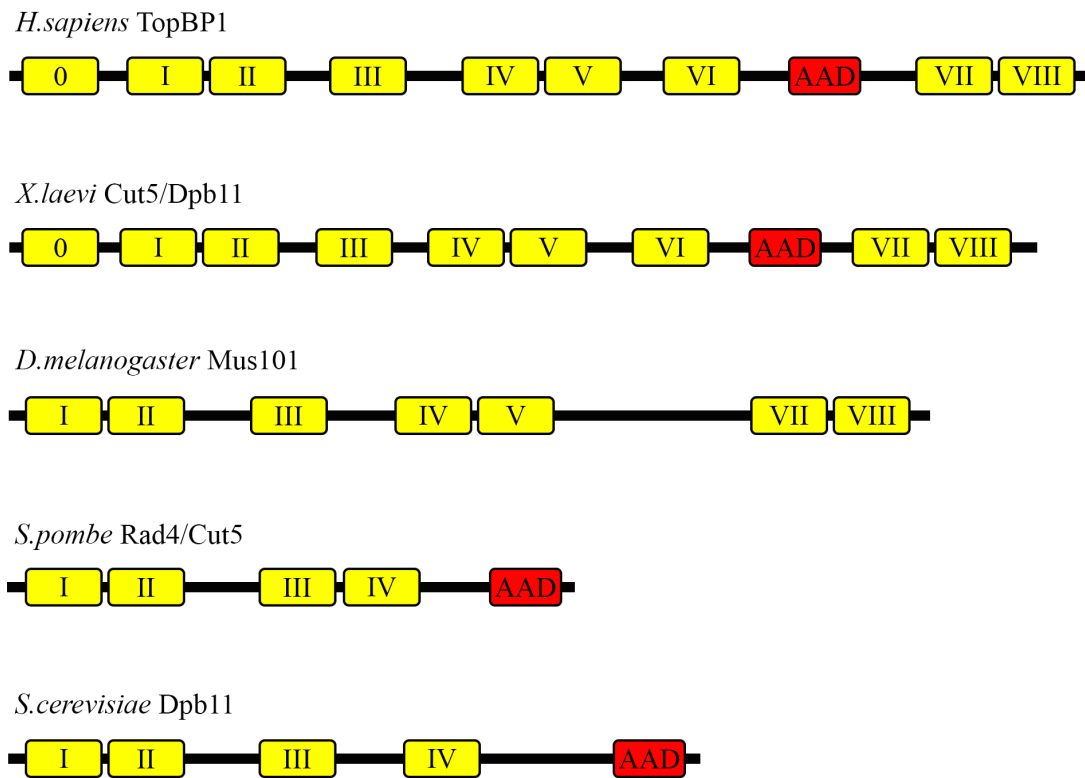
Figure 1.3: Human TopBP1 and its homologs in other eukaryotes.

Diagrammatic representation showing the component domains of TopBP1 in Human, Xenopus, Fruit fly, fission and budding yeast (adapted from Garcia et al., 2005; Lin et al., 2012; Mordes et al., 2008; Wardlaw et al., 2014)

Its structure and its other eukaryotic homologs are shown in Figure 1.3 (Garcia et al., 2005; Wardlaw et al., 2014). TopBP1 binds to the C-terminus of Topoisomerase II β, which is a member of Type II subfamily of Topoisomerases that generate transient DSBs to catalyze topological changes in DNA. TopBP1 is a chromatin-bound protein and is capable of binding to DNA directly (Yamane and Tsuruo, 1999). The BRCT domains of the TopBP1 are a common feature of many of the DNA damage repair and checkpoint proteins and they play an important role in their protein interactions as well as DNA damage foci localization (Sheng and Zhao; Wardlaw et al., 2014). TopBP1 plays diverse roles in DNA metabolism (Fig 1.4). TopBP1 functions as a sensor and mediator in checkpoint signaling activated upon DNA damage and is manifest by its interaction with the C-terminal of Rad9 component of the PCNA like clamp loader 9-1-1 through its BRCT 1-2 and ATR through its ATR activation domain (AAD) leading to activation of ATR (Greer et al., 2003; Kumagai et al., 2006). TopBP1 is expressed at the highest levels during S phase and interacts with DNA Pol ε, possibly helping in loading Pol α, implicating its role in initiating DNA replication (Makiniemi et al., 2001). Its co-localization with BRCA1 at replication forks when replication is inhibited shows its function in DNA replication fork maintenance (Makiniemi et al., 2001). TopBP1 is phosphorylated by ATM at S405 by ATM in response to DNA damage stabilizing it which otherwise gets degraded through ubiquitylation (Yamane et al., 2002). TopBP1 forms IR irradiation-induced foci (IRIFs) in the nucleus at sites of DNA damage or replication fork arrests through its BRCT 5, which interestingly is not dependent upon its ATM-mediated phosphorylation or Rad9 interaction, but upon its interaction with Nbs1 at the latters N-terminal (Morishima et al., 2007; Wardlaw et al., 2014; Yamane et al., 2002). TopBP1 also has a role as transcriptional regulator. Reporter assay studies have identified BRCT domain 4 to be an activator and adjacent BRCT domains 2 and 5 to be repressors of transcription, it has been shown it to activate transcription of HPV E2 transcription factor while repressing the transcription of c-abl (Boner et al., 2002; Wright et al., 2006; Zeng et al., 2005).

Two important transcriptional regulation targets of TopBP1 are p53 and E2F1. TopBP1 interacts with the DNA binding domain (DBD) of p53 via BRCT 7-8 and inhibits its promoter binding activity, thus preventing activation of p53 cell cycle and apoptosis transcriptional targets (Liu et al., 2009a). p53 is mutated in almost 50% of

tumors and TopBP1 mediates mutant p53 gain of function through NF-Y and p63/p73 (Liu et al., 2011). Akt phosphorylates TopBP1 at S1159 inducing its oligomerization through BRCT 7-8 (Liu et al., 2006). The oligomerized TopBP1 can no longer bind to chromatin and carry out its DNA damage response, it instead interacts with E2F1 (Liu et al., 2013). It interacts with the amino terminus of E2F1 through its BRCT 6 and inhibits E2F1 functions like induction of S-phase entry and apoptosis (Liu et al., 2003). TopBP1 represses E2F1 mediated cell cycle control and apoptosis by recruiting SWI/SNF chromatin remodeling complex proteins Brg/Brm onto E2F1 responsive cell cycle and apoptosis target promoters and hence, repressing their activation (Liu et al., 2004).
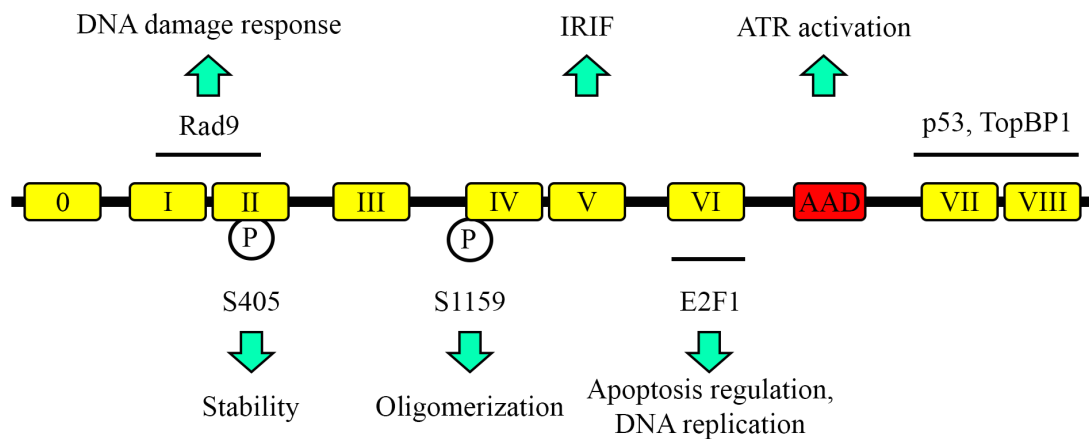
Figure 1.4: Salient features of TopBP1.

TopBP1 interacts with Rad9 through BRCT 1-2 and with ATR through AAD leading to ATR activation and checkpoint response. ATM phosphorylates TopBP1 at S405 in response to DNA damage contributing to its stability. BRCT 5 is responsible for the formation of ionizing radiation induced foci (IRIF). It is phosphorylated by Akt at S1159 leading to its oligomerization through BRCT 7-8. Oligomerized TopBP1 can interact with E2F1 through BRCT6 and p53 through BRCT 7-8 rspectively and inhibit transcription from their target promoters (modified from Garcia et al., 2005; Liu et al., 2003, 2009, 2013; Morishima et al., 2007; Wardlaw et al., 2014; Yamane and Tsuruo, 1999; Yan and Michael, 2009; Yoo et al., 2009).

13

1.11 Anti-apoptotic clone 11 (AAC11) or Apoptosis inhibitor 5 (Api5)

Apoptosis inhibitor 5 (Api5) or Antiapoptotic clone 11 (AAC11) or FGF2 interacting factor (FIF) is a 1575bp, 60kDa nuclear protein in humans. It was first identified as a novel inhibitor of apoptosis in murine fibroblasts as a 1023bp cDNA in a library corresponding to 25kDa protein; a 55kDa "long" variant of the protein was also identified in the same screen (Tewari et al., 1997). The short form of the protein was shown to support cell viability upon growth factor removal, while the long form did not show this property. Api5 was also observed to inhibit apoptosis induced by DNA damage (Berghe et al., 2000). This protein is highly conserved across species as diverse as humans, mouse, frog, fly, mosquito and plants, but they are absent in worms or yeast (Li et al., 2011; Morris et al., 2006).

Human Api5 protein has four isoforms: a, c, d and b, corresponding to four different splice variants (NCBI). Han *et al* solved the crystal structure of Api5 (PDB ID: 3U0R) and showed it to be composed of 19 α helices and two 3_{10} helices (Fig 1.5A). The N-terminal half of the protein is identical to HEAT repeats, while C-terminal is identical to ARM repeats; two known protein-protein interaction motifs, hence Api5 is also predicted to have scaffolding functions for protein binding. The concave side of Api5 protein has highly positive surface charge, whereas the convex side has negative surface charge, providing an opportunity for electrostatic attraction to its binding proteins. Api5 has a LxxLL motif in α6 helix, a Leucine Zipper Domain (LZD) in α18 helix and a Nuclear localization signal (NLS) beyond the 19th α helix (Fig 1.5B). The three leucines of LxxLL motif are embedded inside the protein and not likely to play a role in protein interactions, but instead involved in providing stability to protein by forming hydrophobic interactions with neighboring α helices. The heptad repeat of leucine residues in α18 is predicted to be a leucine zipper without a basic DNA binding region and was not found to be involved in Api5 dimerization (Han et al., 2012).

The known interactor proteins of Api5 include Fibroblast growth factor 2 (FGF2), apoptotic protein Acinus, chromatin remodeling enzyme ALC1 (a member of SNF2 family of chromatin modifiers), while its plant homologue has been shown to interact with two DEAD-box RNA helicases AIP1/2 (Ahel et al., 2012; Berghe et al., 2000; Li et al., 2011).

Api5 was observed to be upregulated in a broad spectrum of human carcinomas including those of lung and colon (Koci et al., 2012), B-cell chronic lymphoid leukemia (Krejci et al., 2007) and nonsmall cell lung carcinoma (Sasaki et al., 2001). Overexpression of Api5 was shown to not only protect cancer cells from undergoing apoptosis but also inducing invasiveness and metastasis via Erk-mediated MMP expression (Kim et al., 2000; Song et al., 2015). These pieces of evidence led to the prediction that Api5 could be functioning as a metastatic oncogene (Faye and Poyet, 2010). Poor prognosis of cancers expressing Api5 was a good enough reason to exploit inhibition of Api5 as a means of cancer therapeutics. A cell-penetrating peptide named RT53 derived from LZD region of Api5 indeed demonstrated specific cancer cell killing ability (Jagot-Lacoussiere et al., 2016).

The mechanism of apoptosis inhibition by Api5 is however poorly understood. Tewari *et al* hypothesized that it might be functioning either by preventing proto-oncogenic transcriptional activation, linked to apoptotic phenotype or in light of its alleged lack of a DNA binding domain, it could be working by acting as a novel competitive inhibitor of leucine zipper factors for gene transactivation. Even though the Api5 LZD was predicted to be lacking basic DNA binding domain, reporter assays with deletion constructs of Api5 revealed it to contain transcription activation and repression regions, though any transcriptional regulation target of Api5 is yet to be discovered (Berghe et al., 2000). Api5 has been observed to target several pathways under different conditions to carry out its anti-apoptosis function. Api5 was shown to downregulate APAF-1 which is a transcriptional target of E2F1 and is involved in the formation of apoptosome required for the activation of the intrinsic pathway of apoptosis (Mayank et al., 2015; Morris et al., 2006). While Api5 inhibited acinus mediated DNA fragmentation and apoptosis, it was activated by Pim-2 to inhibit apoptosis through NF-κB pathway (Ren et al., 2010; Rigou et al., 2009).

Api5 was shown to inhibit E2F1 mediated apoptosis using fly genetic screens as well as mammalian cells (Morris et al., 2006). Api5 and E2F1 did not have any reciprocal regulation over each other, their protein levels were observed to exhibit a similar pattern across the cell cycle peaking at G1, Api5 aided in transcription from the cell cycle targets of E2F1 in contrast to those of its apoptotic targets, and it inhibited E2F1 mediated apoptosis by probably working downstream of E2F1 (Arconde et al., 2013; Morris et al., 2006). One target of Api5 downstream of E2F1 is APAF-1 (Mayank et

al., 2015), but there could be others that might be even more important regulator(s) of apoptosis pathway.

Api5 interactor FGF2 is another downstream E2F1 transcriptional target that has been found to be upregulated following modulation of E2F1 binding to FGF2 promoter by Api5. This activates the downstream FGFR1/PKCδ/ERK effector pathway leading to degradation of pro-apoptotic Bim protein and inhibition of apoptosis. This constitutes a mechanism by which tumor cells escape immune detection by tumor antigen-specific T cells and hence evade apoptosis (Noh et al., 2014). Activation of FGFR1 signaling further induces Cancer stem cell (CSC) property in the cells, which is marked by increase in NANOG expression, frequency of CD44-positive cells and sphere-forming capacity in suspension cultures (Song et al., 2017). Api5 thus not only has an anti-apoptotic function, it may have roles in tumor development and progression as well.

Another mechanism of Api5 anti-apoptotic function is through its interaction with the CARD domain of Caspase 2 through its C terminal region and hence inhibiting the dimerization and auto-activation of Caspase2. Caspase2 is unique among caspases as it shows features of both initiator and effector caspases (discussed in section 1.14). Interestingly Api5 was not observed to interact or inhibit the function of the other two caspases (9 and 1) that also have CARD domain (Imre et al., 2017).

The only PTM of Api5 known till now is its acetylation at Lysine 251 (Choudhary et al., 2012; Han et al., 2012b). Api5 is acetylated after its synthesis, which renders it stable and inactive. Upon the onset of apoptotic signals, it is de-acetylated and undergoes degradation while carrying out its anti-apoptotic function. The mechanism of its degradation, as well as its acetyltransferases and deacetylases, are unknown.
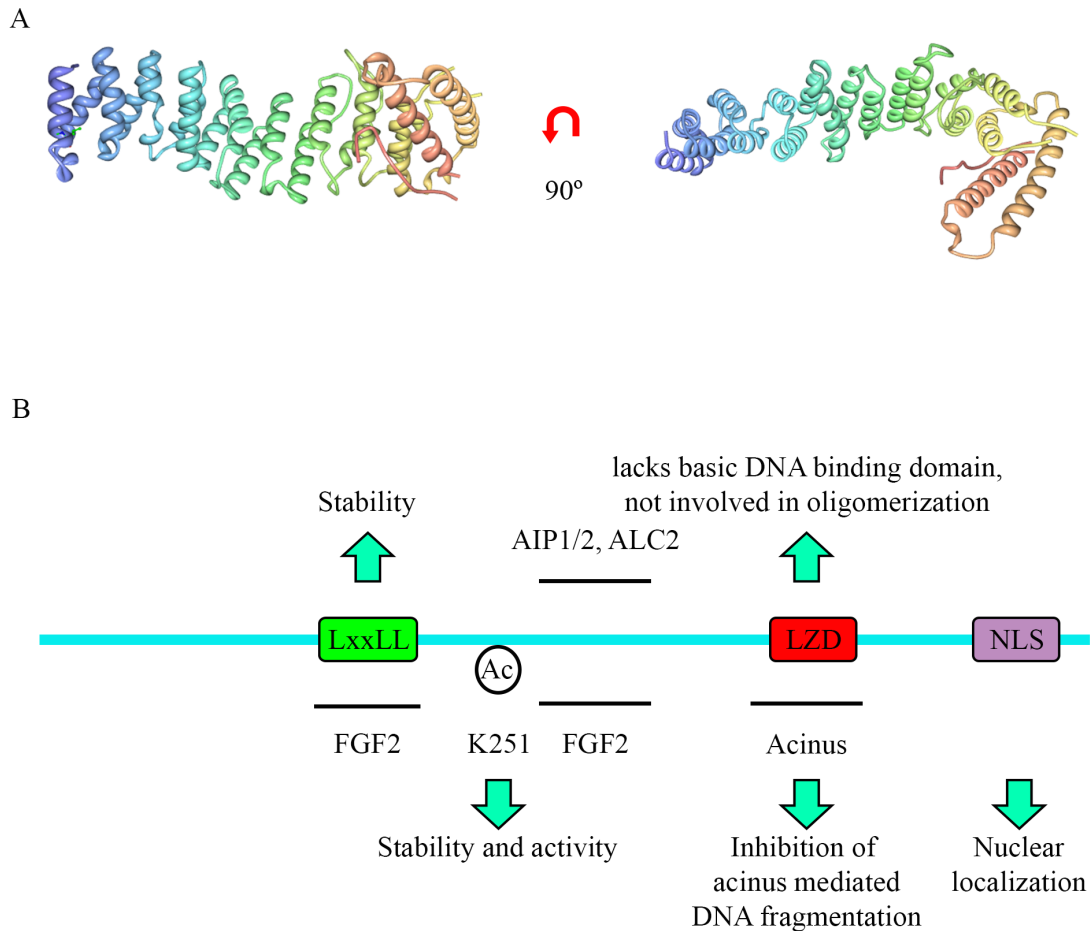
Figure 1.5: Structure and salient features of Api5.

(A) All α-helix structure of Api5 protein as derived from PDB, N-terminal is colored violet and C-terminal is red (Han et al., 2012; Moreland et al., 2005) (B) Simplified schematic of Api5 showing relative positions of the LxxLL, LZD and NLS domains, LxxLL motif forms internal hydrogen bonds with surrounding α helices to provide stability to the protein, LZD is speculated to lack the basic DNA binding domain and is not involved in Api5 oligomerization, it is responsible for the interaction with Acinus, inhibiting its DNA fragmentation function. Api5 interacts with FGF2, ALC1, while its rice homologue interacts with AIP1/2, it is acetylated at Lys251 imparting it stability, its NLS at the C-terminal felicitates nuclear localization (modified from Ahel et al., 2012; Berghe et al., 2000; Han et al., 2012; Li et al., 2011; Rigou et al., 2009; Tewari et al., 1997)

1.12 E2F family of transcription factors: roles in cell cycle, growth control, and apoptosis

E2F comprises of a family of 6 proteins (E2F1-6) and at least two heterodimeric partners DP1 and DP2. E2F1, E2F2, and E2F3 are efficient inducers of S phase while E2F4 and E2F5 do so only weekly. The E2F1 transcription factor is best known for its role in regulating almost every phase of the cell cycle. E2F1 mediates induction of apoptosis which is its intrinsic function rather than a consequence of an abnormal S phase entry (DeGregori et al., 1997). E2F1 hence might be functioning as a tumor suppressor in conjunction with Rb. Apoptotic function of E2F1 has also been implicated by affecting the accumulation of p53, which under normal conditions is controlled by Mdm2 (Kowalik et al., 1998). E2F1 induced apoptosis is not well characterized though it has been reported to be p53 dependent and independent, APAF-1 dependent and independent and p73 dependent depending upon the context.

Under normal conditions, TopBP1 interacts with E2F1 (and not other E2F factors) through its BRCT domains and represses its transcriptional activity through Rb-independent but Brg1/Brm (key components of SW1/SNF chromatin remodeling complex) dependent mechanism, thereby inhibiting apoptosis (Liu et al., 2004). In response to DNA damage, both TopBP1 and E2F1 (through its N-terminus ATM phosphorylation site) are phosphorylated by ATM. TopBP1 represses E2F1 and recruits it to the BRCA1 repair complex. TopBP1 thus recruits checkpoint activation machinery to activate Chk1 during DNA damage at the same time it also inhibits E2F1 mediated apoptosis to allow completion of DNA repair. This provides a novel mechanism of coupling of the DNA damage- repair pathway to the Cell cycle checkpoint pathway (Liu et al., 2003; 2004).

The regulation of E2F1 induced apoptosis is although not fully understood. Several potential players have been implicated, TopBP1 being one of them. Morris reported another protein Apoptosis inhibitor 5 (Api5) to be a critical determinant of E2F1 induced apoptosis.

1.13 Role of E2F1/p53 in inducing apoptosis

When success is not achieved in repairing the damaged DNA, the checkpoint machinery directs the activation of apoptosis. Earlier it was believed that the

18

determination of cell fate in response to the stress depended upon the downstream effectors like p53 and E2F1, but there have been recent reports that the players of the cell cycle checkpoints, checkpoint signaling as well as repair are involved in direct/indirect activation of apoptosis in a transcriptionally dependent/independent way and vice versa. p53 is mutated in more than 50% of cancer cases and hence it called as the "guardian of the genome" (Yoshida et al., 2010) which has also been proved by tumor susceptibility of p53 knockout mice (Donehower et al., 1992). The exact cell fate specified by p53 activation is dictated by cell type, environment milieu and the nature of stress (Brady et al., 2010) and is governed by its post-translational modifications like phosphorylation, acetylation, ubiquitylation (Yoshida et al., 2010). Many different signaling pathways modulate the p53 signaling to choose between apoptosis/quiescence/senescence depending upon the intensity of stress (Erol, 2011). These modulators include MDM2, p21, TGFβ, mTOR, cMyc among others. Under lower stress conditions it shows a pro-survival response by acting as a tumor suppressor halting the cell cycle at G1/S checkpoint and also activating several DNA-repair and antioxidant genes. Under potent stress it activates proteins like p21, PAI1, PML leading to senescence (Kortlever., 2006; Riley., 2008), under severe stress it activates apoptosis. p53 stimulates both the intrinsic as well as extrinsic pathways of apoptosis, both in a transcription-dependent and independent manner (Yoshida et al., 2010). It transcriptionally upregulates intrinsic pathway pro-apoptotic proteins like BAX, NOXA, PUMA, APAF-1 (Nakano et al., 2001; Oda et al., 2000; Robles et al., 2001; Toshiyuki and Reed, 1995), PERP, DR5 receptor (Haupt et al., 2003) as well as TRAIL and FAS ligand (Kuribayashi et al., 2008; Maecker et al., 2000) of the extrinsic pathway. Else it can directly interact with anti-apoptotic proteins Bcl2, Bcl-XL or proapoptotic protein Bak, compromising the mitochondrial membrane stability and hence the release of cytochrome c (Wolff et al., 2008). This pro-apoptotic function of p53 is further supported by another transcription factor E2F1 which supports its accumulation in response to stress which otherwise has a tumor suppressor function in conjunction with pRb (Kowalik., 1998). E2F comprises a family of 8 members (E2F1-8) and at least 2 heterodimeric partners DPN1 and 2. E2F1-3a are transcriptional activators while the rest are transcriptional repressors (Wu et al., 2009). Induction of apoptosis by E2F1 is its intrinsic function rather than a consequence of an abnormal S phase entry (DeGregory et al., 1997). E2F1 induced

apoptosis is not well characterized though it has been reported to be p53 dependent and independent, APAF-1 dependent and independent and p73 dependent depending upon the context.

There could be several more layers of regulations and several more players in the regulation of apoptosis between E2F1/p53 and Bcl2 family proteins that are not completely understood. Some downstream effectors of the E2F1 pathway like p73 are known but much more are yet to be found out.

1.14 Apoptosis

Apoptosis or programmed cell death (PCD) is an evolutionarily conserved mechanism of cell death in mammals that normally occurs during development and aging as a part of the homeostatic mechanism of the body to maintain cell numbers. It can also get activated in response to several physiological as well as pathological stimuli (Elmore, 2007). Apoptosis is associated with cell shrinkage and pyknosis, plasma membrane blebbing, chromatin condensation and fragmentation, breakage of the cell into apoptotic bodies called "budding" which are promptly phagocytosed by macrophages, parenchymal cells or neoplastic cells thus preventing the release of apoptotic cell constituents into the surroundings and resultant inflammation (Elmore, 2007). These attributes distinguish apoptosis from necrosis, which involves rupturing of cells, releasing its constituents outside and causing inflammation response (Gobeil et al., 2001). A low dose of injurious stimuli often induces apoptosis, which is an energy consuming process whereas necrosis is energy passive and is triggered by high doses of injurious stimuli (Soldani and Scovassi, 2002).

There are two main pathways of apoptosis: death receptor or extrinsic pathway and mitochondrial or intrinsic pathway, both of which converge at the execution pathway, though there is also a report of a perforin/granzyme pathway of apoptosis (Elmore, 2007). The extrinsic pathway is activated in presence of a number of extracellular apoptosis-inducing stimuli which are in the form of ligands like certain cytokines, drugs, hormones, pathogens or native activities compounds like vitamins and anti-oxidants (Hongmei, 2012). The intrinsic pathway is activated by nonreceptor-mediated stimuli which can be negative in nature: i.e, the absence of certain growth factors, hormones, and cytokines that can lead to failure of suppression of cell death programs triggering apoptosis. Other stimuli like DNA damage, radiation, toxins,

hypoxia, hypothermia, viral infections, and free radicals can act in a positive fashion as their presence induces the intrinsic pathway (Fulda and Debatin, 2006).

Apoptosis activates cysteine proteases called Caspases, which cleave their targets at specific Aspartic acid residues so as to bring about proteolysis associated with apoptosis. There are 10 major caspases that are broadly categorized as initiator caspases (2,8,9,10), effector caspases (3,6,7) and inflammatory caspases (1,4,5) (Parrish et al., 2016).

The extrinsic pathway of apoptosis involves transmembrane death receptors belonging to TNF receptor gene superfamily (Fulda and Debatin, 2006). Fas receptor and TNF receptor are common examples. They bind to their specific ligands Fas and TNF respectively and undergo oligomerization. This leads to clustering of FADD or TRADD adapter proteins on the intracellular domains of Fas and TNF receptors respectively which in turn leads to binding and dimerization of procaspase8 to form the death induced silencing complex (DISC). DISC activates caspase8 due to autolytic cleavage of the proenzyme. active caspase 8 activates the downstream executioner caspase cascade beginning with caspase 3 (Parrish et al., 2016).

The intrinsic pathway of apoptosis begins with the opening of mitochondrial permeability transition (MPT) pore and loss of transmembrane potential (Elmore, 2007). This releases Cytochrome c from inter-membrane space, which then interacts with APAF-1 to form the heptameric backbone of apoptosome (Bratton and Salvesen, 2010). procaspase 9 is recruited to apoptosome and undergoes dimerization leading to its autolytic cleavage and partial activation (Zou et al., 2003). Active caspase 9 again triggers the execution pathway caspase cascade beginning with caspase3. MPT opening also releases proteins like Smac/DIABLO that function as antagonists to inhibitors of apoptosis proteins (IAPs) (Silke and Meier, 2013). IAPs are a family of proteins characterized by a presence of Baculovirus IAP repeat (BIR) domain and RING domain. There are eight known human IAPs with XIAP being a prominent example (Salvesen and Duckett, 2002). Mitochondrial damage and pore formation are governed by the Bcl2 family of proteins. A total of 25 Bcl2 family proteins are known as yet, some of them are pro-apoptotic meaning they help in opening of mitochondrial pore,. Bcl-10, Bax, Bak, Bid, Bad, Bim, Bik as examples,, while the others are anti-apoptotic which means that they either stabilize the mitochondrial membrane or antagonize the function of pro-apoptotic Bcl2 proteins, for example, Bcl-2, Bcl-x,

Bcl-xl, Bcl-xs, Bcl-w, BAG to name a few (Elmore, 2007; Fulda and Debatin, 2006). Apoptosis pathway regulators like p53 and E2F1 govern the transcription of Bcl2 family of proteins (Fulda and Debatin, 2006; Polager and Ginsberg, 2009). Activated Caspase 8 of the extrinsic pathway cleaves Bid - a pro-apoptotic Bcl2 family protein, that leads to mitochondrial damage, cytochrome c release and subsequent activation of the intrinsic pathway. This is an example of the "crosstalk" between the extrinsic and intrinsic pathways of apoptosis (Parrish et al., 2016).

Both the extrinsic and intrinsic pathways end up in activating the execution pathway of apoptosis, which involves activation of the effector caspases 3, 6 or 7 (Elmore, 2007). Caspase 3 activates several downstream enzymes and proteins whose actions bring about the morphological and biochemical changes characteristic of apoptosis. Caspase 3 cleaves proteins like PARP, plasma membrane cytoskeletal protein alpha fodrin, nuclear protein NuMA. Gelsolin protein acts as a nucleus for actin polymerization and its cleavage by Caspase 3 destroys the cytoskeletal assembly. Caspase 3 cleaves the pro-enzyme ICAD to activate the CAD cytoplasmic endonuclease. CAD degrades chromosomal DNA and leads to chromatin condensation. Acinus further acts on it to shred DNA into fragments (Rigou et al., 2009). All of this is followed by phospholipid asymmetry and externalization of phosphatidylserine on the outer lamella. The appearance of these residues on the outer leaflet of apoptotic cells felicitates non-inflammatory phagocytic recognition, early uptake, and disposal. These residues also serve as markers to identify apoptotic cells by biochemical methods in the lab such as that by Annexin V (Fig 1.6).
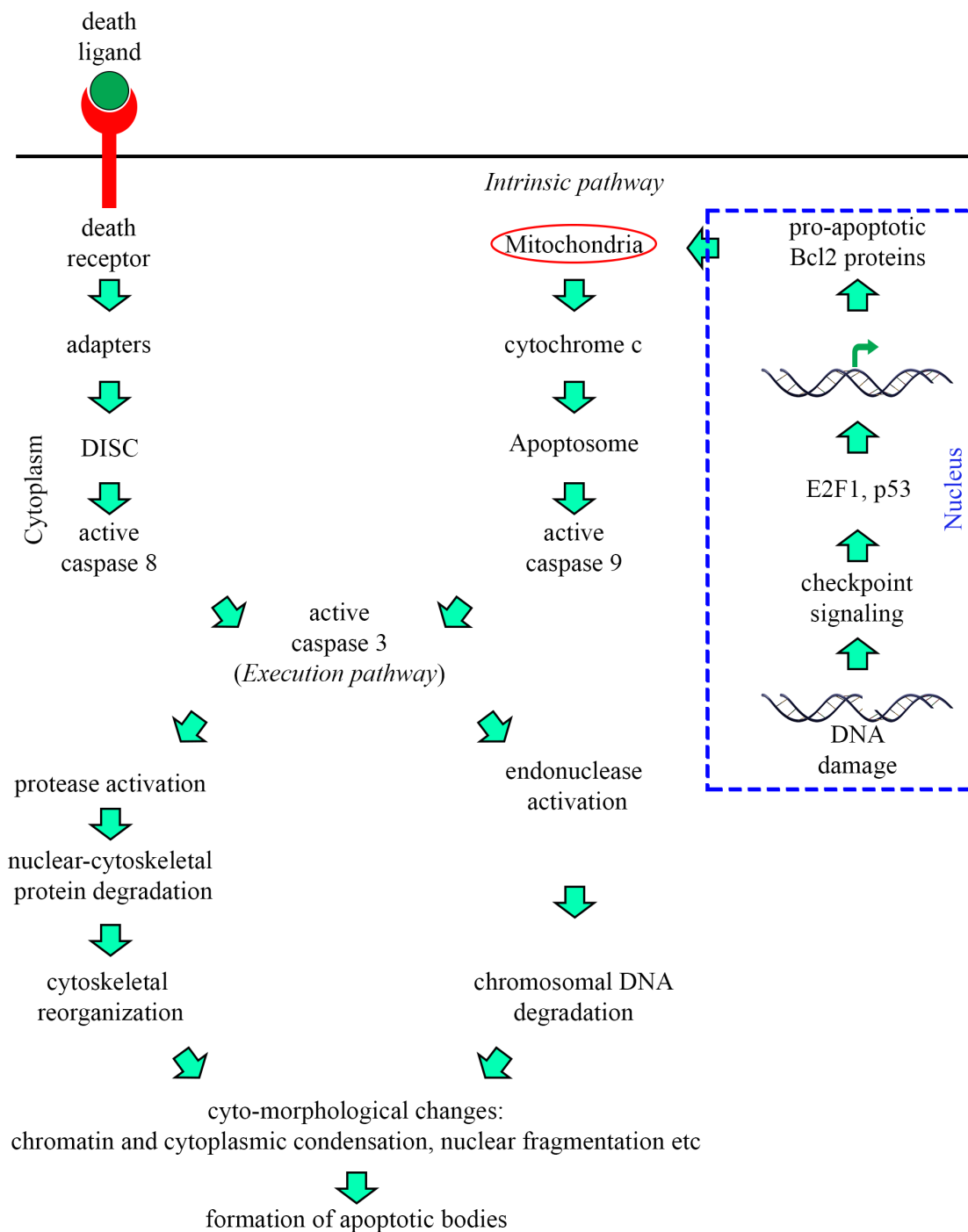
Figure 1.6: Simplified schematic of apoptosis pathway.

The two major pathways of apoptosis are extrinsic and intrinsic pathway that get activated in response to external stimuli (death domain ligands) or intrinsic stimuli (DNA damage or physiological conditions) respectively activating their initiator caspases 8 and 3 respectively that culminate in the activation of caspase 3 to set on

the execution pathway; caspase 3 and downstream proteases bring about protein and DNA degradation forming apoptotic bodies that are phagocytosed by non-inflammatory macrophages (modified from Elmore, 2007; Parrish et al., 2016)

1.15 Rationale of the study and specific objectives

HeLa nuclear extracts were prepared (Méndez and Stillman, 2000) and their activity was confirmed by ATR activation assay (Shiotani and Zou, 2009). The extracts were incubated without or with poly d[A/T] annealed oligos which mimic damaged DNA so as to activate the checkpoint pathway proteins in the extract. GST-TopBP1 recombinant protein was expressed and purified from bacteria and was incubated with the above extracts. A GST pull-down was performed and analyzed on SDS-PAGE. The bands showing enrichment upon DNA damage were excised from the gel, trypsin digested and subjected to LC-MS/MS to screen for the peptides. The analysis revealed several known as well as novel interactors of TopBP1. Api5 was discovered as one such novel interactor.

Both Api5 and TopBP1 have anti-apoptotic functions. Api5 is predicted to inhibit E2F1 mediated apoptosis at a level below E2F1 whereas TopBP1 while primarily being a checkpoint mediator protein, is known to inhibit E2F1 mediated apoptosis by repressing transcription from its target promoters (Liu et al., 2003; Morris et al., 2006). In light of their interaction upon DNA damage and reports of them affecting the same axis of apoptosis induction signaling: the one governed by E2F1, it will be intriguing to further validate this interaction and investigate the mechanism how it affects the DNA damage-induced apoptotic pathway as this may be one of the novel ways by which DNA damage induced checkpoint pathway signals to the apoptotic pathway that gets activated upon the failure of repair.

Following are the specific objectives of this study:

1. To confirm the interaction between Api5 and TopBP1 *in vitro* and determine the interacting domain(s)/region(s) of each of the proteins.
2. To elucidate Api5 and TopBP1 interaction *in vivo* in the context of DNA damage in mammalian cells.
3. To investigate the binding of Api5 protein with DNA *in vitro* and its foci formation *in vivo* on damaged DNA and/or its co-localization with TopBP1 DDR foci.

24

4. Functional characterization of Api5 in response to DNA damage.

Chapter2: Materials and Methods

2.1 Chemicals and Reagents

Following chemicals were purchased from Sigma: Ampicillin (9518), Kanamycin (K 1377), DTT (11583786001), DMSO (M81802), Trizma base (T 1503), EDTA (E 9884), Ethidium bromide (E 8751), Potassium chloride (P9541), Calcium chloride (C 3306), Magnesium chloride (M 9272), CBB-R250 (27816), Bromophenol blue (B 0126), Xylene cyanol (X 4126), Triton X (X 100), Tween-20 (P 2287), NP-40 (NP40S), Sodium citrate (W 302600), PEG 8000 (P 5413), BSA lyophilized powder (A 9418), SDS (L 3771), Sodium azide (S 2002), HEPES (H 3375), Sucrose (S 0389), Sodium fluoride (450022), Sodium orthovanadate (S 6508), PMSF (P7626), Protease inhibitor cocktail (P8340), EGTA (E 3889), Boric acid (B 6768), Acrylamide (A 9099), bis-Acrylamide (146072), TEMED (T 9281), Sodium deoxycholate (D 6750), Sodium chloride (S 9888).

Glacial acetic acid (11005), Methanol (32407), Iso-propanol (13825), Hydrochloric acid (29508), Glycerol (15457), Glycine (12835), Sodium hydroxide (15895) and Ammonium persulphate (15055) were procured from Qualigens Chemicals.

SeaKem LE Agarose (50004) was bought from Lonza while LB broth base (12780029) came from Invitrogen and LB broth with agar (L 2897) was from Sigma.

2.2 Antibodies

active Caspase 9 (ab2302), ORC2 SB46 (ab31930) and GFP (ab290) antibodies were purchased from Abcam. Api5 (PAB7951) antibody was procured from Abnova. The TopBP1 antibody was attained from both BD Biosciences (611874) and Bethyl Laboratories (A300-111A) while p53 (A300-247A) antibody and Rabbit IgG (P120-201) was from Bethyl Laboratories. PARP1 (AM30) antibody was acquired from Calbiochem. Following antibodies were purchased from Cell Signaling Technology: pChk1 S345 133D3 (2348S), pChk2 T68 (2661S), Chk2 1C12 (9271S), p53 pS15 (9284S), cleaved Caspase 3 Asp 175 5A1E (9664S), Bax (2772S). 53BP1 (4937S). GST (05-782) and γ H2AX-FITC (16-202A) antibodies were obtained from Merck Millipore. Chk1 G4 (sc8408) and E2F1 C20 (sc193) antibodies were acquired from Santacruz Biotechnology whereas MDM2 (sc-813) was a kind gift from Dr. Manas

Santra (NCCS). GAPDH (G9545) and α Tubulin (T6199) antibody was procured from Sigma Aldrich. Anti-Mouse (115-035-003) and anti-Rabbit (111-035-003) HRP conjugated secondary antibodies were bought from Jackson ImmunoResearch. HRP-Protein A (10-1023) was purchased from Invitrogen. Alexa Fluor 488 (A-11034), Alexa Fluor 568 (A-11004) and Alexa Fluor 632 (A-21071) conjugated secondary antibodies were bought from Invitrogen.

2.3 Plasmids and Constructs

AAC11 pGEX 4T11 construct was a kind gift from Jean-Luc Poyet, INSERM UMRS1160, Paris, France. pGEX-2TKcs, Full-length TopBP1, and its deletion constructs namely,. BRCT Δ1-2, Δ1-3, Δ1-5, Δ1-6, Δ7-8 and AAD cloned into pGEX-2TKcs as well as pUNI50 were a gift from the lab of Lee Zhou, MGH Cancer Centre, USA. pCATCH NLS-S and pCDNA3.1 HAC1 cloning vectors were was gifted by Walter Schaffner, University of Zurich and Jomon Joseph, National Centre for Cell Science, Pune respectively. mVenusC1, mCherryN1 cloning vectors, and H2B ECFP construct were gifted by Jennifer Lippincott-Schwartz, NIH, USA.

2.4 Cloning

Full-length Api5 Isoform1 cds (1575bp) and its different regions were cloned into relevant vectors for carrying out the *in vitro*, *in vivo* interaction and functional studies. These deletion mutants were designed so as to include or exclude the putative Leucine Zipper Domain (LZD) of the protein in different combinations with rest of the regions of the protein. The resultant deletion constructs were named as Api5 Δ2-3 (1-1079bp), Api5 LZD (1080-1172bp), Api5 Δ1-2 (1173-1575bp), Api5 Δ3 (1-1172 bp), and Api5 Δ1 (1080-1575bp).

Full-length Api5 was cloned between EcoRI and NcoI restriction sites on the MCS of pGEX-2TKcs Vector. Api5 was PCR amplified using 1μL pGEX4T11 plasmid miniprep as template, 0.5μM each of Api5 For2 (Bioserve) and GST Api5 Rev (IDT) primers, 0.5mM of dNTP mix (Bangalore Genei 610602500051730), 1X Pfu Polymerase buffer and 1μL cloned Pfu polymerase (Stratagene 600154) and making up the volume to 50μl with milli-Q water in a 200μl microfuge tube (Axygen 10011-816). The tube was placed in a PCR machine (Eppendorf master cycler gradient

E950000015) and subject to the following thermocycling conditions: Initial denaturation at 95°C for 2min followed by 30 cycles of denaturation at 95°C for 1 minute, primer annealing at 60°C for 1 minute and extension at 72°C for 3 minutes, a penultimate final extension at 72°C for 6 minutes ultimately ending the cycle by holding at 4°C. Two of such 50μL PCR reactions were pooled together and purified using a PCR purification kit (Qiagen 28104) following manufacturer's instructions and eluted in 15 μL prewarmed Elution Buffer. 10μL of the purified amplicon (~200-300ng Insert DNA) was double digested with 1uL each of EcoRI-HF (NEB R3101) and NcoI-HF (NEB R3193) in 1X suitable NEB Buffer (following manufacturer's instructions) for 3.5 hrs at 37°C. 5uL of pGEX-2TKcs plasmid miniprep was simultaneously digested in a similar reaction for 2.5 hr followed by additional incubation with 1μL of Calf Intestinal Alkaline Phosphatase (NEB M0290) for 1 hr. Both the digested insert DNA and the vector were subsequently purified using PCR purification kit and eluted in 15μL prewarmed elution buffer. Ligation was set up in Vector: Insert molar ratios of 1:1, 1:3 and 1:6 along with an empty Vector control using T4 DNA Ligase (NEB M0202) following manufacturer's instructions to a total volume of 10μl for 16 hours at Room Temperature. *E.coli* DH5α were then transformed with ligation reactions and plated on LB-Agar Amp (100μg/ml) plates. The plates that had been plated with vector plus insert ligation were observed for the appearance of a small number of colonies whereas the one plated with only vector ligation product was observed for the absence of any colonies. The colonies were numbered and a replica plate was prepared while simultaneously re-suspending each numbered colony in a correspondingly numbered tube containing 5μL milli-Q water. The tubes were heated to 95°C for 2 minutes and spun down to collect the supernatant containing the plasmid to be used for subsequent colony PCR. Each colony PCR reaction was set up using the above supernatant with 1X Taq B Buffer, 1.5mM MgCl₂, 0.5mM dNTP mix, 0.2μL Taq polymerase (Bangalore Genei 610602500051730) and 0.5μM each of same forward and reverse primers that had been used for cloning, making up the volume to 10μL with milli-Q water and subjected to the same thermocycler conditions. Colonies corresponding to the clones showing positive amplification were picked and inoculated in 3mL LB-ampicillin (100μg/ml). Plasmid miniprep was performed by alkaline lysis followed by phenol-chloroform extraction and ethanol precipitation. The plasmid pellet was dissolved in

50μL TE buffer. TE buffer was composed of 100mM Tris-Cl pH 7.4 and 10mM EDTA pH 8.0 made up in milli-Q water. The clones were confirmed by restriction digestion. 2μL of the purified plasmid was digested with the same set of restriction enzymes (EcoRI-HF and NcoI-HF) for 3 hours at 37°C in a 10μL reaction. 2μl of 6X gel loading dye (Bangalore genei) was mixed with digestion reaction and loaded onto a 0.8% agarose gel made up in 1X TAE and containing Ethidium bromide (0.5μg/ml) along with Supermix DNA ladder (Bangalore Genei 612652171001730) and subjected to electrophoresis. 50X TAE buffer was made by adding 242g Tris base, 57.1ml glacial acetic acid, and 100ml EDTA pH8.0 to distilled water up to 1L. The gel was observed under a UV trans-illuminator (Syngene G-box). The clones showing the release of the insert at a size corresponding to the PCR amplicon used for cloning were marked as positive clones.

The positive clones were used for subsequent protein expression and stored by making plasmid glycerol stocks. 1μL of plasmid miniprep was used to transform *E coli*DH5α cells using 5XKCM and plated as described earlier. 5X KCM was composed of 0.5M KCl, 0.15M CaCl$_2$ and 0.25M MgCl$_2$. a single colony was picked to inoculate 3mL of LB-amp culture and grown overnight at 37°C. 700μl of the culture was mixed by vortexing with sterilized 50% glycerol in a tube. This was flash frozen in liquid nitrogen and stored away at -80°C as the plasmid glycerol stock for Api5-pGEX-2Tkcs plasmid construct.

2.5 Site-directed mutagenesis (SDM)

Site-directed mutagenesis PCR reaction was set up using 1μL of Api5 mVenusC1 plasmid miniprep as template, 0.5μM each of mut Api5 1-F and mut Api5 1-R primers (IDT), 0.8mM of dNTP mix (Bangalore Genei 610602500051730), 1X Pfu Polymerase buffer and 1μL Pfu turbo (Stratagene 600252-52), making up the volume to 50μl with milli-Q water in a 200μl microfuge tube (Axygen 10011-816). A negative control was kept in which PCR reaction had all the ingredients except Pfu turbo. The tubes were placed in a PCR machine (Eppendorf master cycler gradient E950000015) and subject to the following thermocycling conditions: Initial denaturation at 95°C for 1min followed by 18 cycles of denaturation at 95°C for 30 seconds, primer annealing at 55°C for 1 minute and extension at 68°C for 15 minutes and ending the cycle by holding at 4°C. The PCR reactions were taken out and

digested with 1μl of DpnI (NEB R0176) at 37°C for 1 hour. Each reaction was used to transform 100μl of *E.coli* DH5α competent cells and plated onto LB agar-kanamycin (33μg/ml) plates. The negative control plate was observed for the absence of any colonies whereas the colonies that appeared on the experimental plate were inoculated into LB-Kan media. Plasmid was isolated by using miniprep kit (Qiagen 27104) and the clones checked for mutagenesis by sending them for sequencing using Api5-1 mutseqchk (IDT) primers to a third party vendor (1st BASE).

2.6 Expression and purification of GST fusion proteins in bacteria

Competent *E.coli* BL21 DE3 cells were transformed with 1μl of the Api5-pGEX2Tkcs plasmid miniprep and plated to LB-agar-Ampicillin to obtain colonies as described previously. A single colony was used to inoculate 20ml of LB-Amp (250ug/ml) and grown overnight in a conical flask in a shaker incubator at 37°C. Next day, 5ml of the above culture was used to inoculate 200ml of LB-Amp (250ug/ml) in a conical flask and was incubated in a 37°C shaker-incubator at 210 rpm. The culture was grown for 2-3 hours till it reached OD 600 of 0.6-0.7. 1ml of culture was aliquoted out, spun down and the bacterial cell pellet resuspended in 50μL 2X Laemmli buffer and stored at -40°C as "uninduced culture". 6X laemmli buffer was composed of 0.35M Tris-Cl pH6.8, 36% Glycerol, 11% SDS, 0.6M DTT, and 0.012% bromophenol blue made up of milli-Q water. Isopropyl β-D-1-thiogalactopyranoside (Sigma 15502-56) was added to the culture to a final concentration of 0.4mM so as to induce protein expression from the plasmid construct. The culture was incubated at 25°C for 10 hours in the shaker incubator at 180 rpm. 1ml of induced culture was taken out to prepare "induced culture" sample similarly as the one for "uninduced culture" as described earlier. Rest of the culture was spun down in a centrifuge (Eppendorf 5810R) at 4000 rpm for 15 minutes at 4°C in a falcon tube to harvest the bacterial cells. The cell pellet was stored away at -80°C after flash freezing it in liquid nitrogen. On the day of protein purification, the bacterial pellet was thawed and resuspended in 20mL (i.e, 1/10th the volume of original bacterial culture) of Extraction buffer made up of 20mM HEPES pH 7.6, 0.5M NaCl, 0.5mM EDTA, 10% Glycerol, 0.5% NP-40, and 1X protease inhibitor cocktail (Sigma P8340). The tube was thoroughly vortexed to resuspend the cells homogeneously. The tube was kept in an ice bath and subjected to sonication to disrupt the bacterial cells. The cell

suspension was sonicated using a 6mm probe of the Vibracell sonicator (Sonics VCX130) with an amplitude of 50% for the duration of 2 minutes with the pulse on for 50 seconds and pulse off for 30 seconds. This cycle was repeated once so as to get a viscous bacterial cell lysate. The cell lysate was transferred to Oak Ridge tubes (Nalgene 3119-0030) and spun at 12,000 rpm for 30 min at 4°C in a tabletop centrifuge (Eppendorf 5810R). The supernatant (cleared lysate) was transferred to a fresh falcon tube. The pellet was resuspended in 20ml of PBS. 40μl each of this suspension and cleared lysate was taken out, added with 8μl of 6X laemmli buffer and stored away at -40°C as "pellet" and "supernatant" respectively. Meanwhile, 500μl of Glutathione-agarose settled resin (Pierce 16101) was taken in a falcon tube and prewashed/equilibrated with extraction buffer. This was done by adding 5ml of extraction buffer to the resin and spinning it down at 700g for 2 minutes at 4°C. The supernatant was aspirated out using a pinched-gel-loading tip attached to a vacuum aspirator so as to avoid loss of beads during aspiration. 20ml of the cleared bacterial lysate prepared previously was added to the equilibrated glutathione agarose beads in a falcon tube and incubated on an end to end shaker at 4°C for 1 hour. In the meantime wash buffer I and II were prepared and kept on ice. Wash buffer I was made up of 20mM Tris-Cl pH 8.0, 150mM Sodium chloride, 1% Triton-X 100 and 1X protease inhibitor cocktail (Sigma P8340). Wash buffer II was made up of 100mM Tris-Cl pH7.6, 100mM Sodium Chloride and 5% Glycerol. After an hour of incubation, the glutathione beads-cell lysate suspension was spun down at 700g for 2 minutes at 4°C. 40μl of the supernatant was aliquoted out and stored at -40°C as "flow through" after adding 8μL of the 6X laemmli buffer. Rest of the supernatant was aspirated out. The protein-coated glutathione beads were washed thrice with 10ml each of Wash buffer I and subsequently once with 10ml Wash buffer II as described earlier. 20μL of the washed beads resuspended in Wash buffer II was aliquoted out, added with 10μl of 2X laemmli buffer and stored away at -40°C as "bead-bound protein". Rest of the protein-bound glutathione bead slurry was pipetted out to a microfuge tube with a cut 1ml tip, flash frozen in liquid nitrogen and stored away at -80°C for future use.

2.7 Thrombin cleavage of GST-Api5 fusion protein

The pGEX-2Tkcs vector has a linker region between GST-encoding sequence and MCS that codes for an amino acid sequence, which is a consensus recognition motif for thrombin cleavage. Thrombin (GE Healthcare 27-0846-01) was reconstituted in a suitable volume of thrombin storage buffer following manufacturer's instructions so as to prepare a concentration of 1 Unit/μl of thrombin enzyme, aliquoted and stored at -40°C. Thrombin storage buffer was made up of 50mM sodium citrate, 200mM sodium chloride, 0.1% PEG 8000 and 50% Glycerol at a final pH of 6.5. The thrombin cleavage reaction was set up in a thrombin cleavage buffer. Thrombin cleavage buffer was prepared of 5mM Calcium chloride, 150mM Sodium chloride, 50mM Tris-Cl pH7.5 and 1% Triton-X 100. Equal volumes of thrombin cleavage buffer and protein bound bead slurry were mixed with the suitable volume of reconstituted thrombin enzyme in a microfuge tube so as to achieve a concentration of 1 Unit of thrombin per 100μg of bead-bound protein. The tube was incubated in an end to end shaker at room temperature (25°C) for 16 hours after which the mixture was spun down at 700g for 2 minutes at 4°C and the supernatant collected, flash frozen in liquid nitrogen and stored away at -80°C for future use as the GST removed purified Api5 protein.

2.8 Elution of GST-Api5 fusion protein from Glutathione agarose beads

GST Api5 protein was eluted from the Glutathione agarose beads with GST elution buffer. This buffer was composed of 50mM Tris-Cl pH 8.0 and 20mM L-Glutathione reduced (Sigma G4251-50G). Equal volumes of protein bound Glutathione agarose bead slurry and GST elution buffer was incubated together in a microfuge tube at room temperature (25°C) on a rocker for 30 min. The mixture was then centrifuged at 700g for 2 minutes and the supernatant collected. The supernatant contained eluted GST fusion protein. It was flash frozen in liquid nitrogen and stored at -80°C for future use.

2.9 Analyzing and quantifying purified proteins

The purified proteins were analyzed by resolving them in SDS-PAGE. SE 260 mini-vertical units for running 10x10.5 cm slab gels and allied apparatus for casting the gels (multiple gel caster, glass plates, notched silica plates, 1mm spacers, 10 well and 15well combs) were purchased from GE Healthcare Life Sciences. 10% gel was cast from a 30% (29% acrylamide-1%bisacrylamide) stock solution. 20μl each of the samples prepared during protein purification namely, "Un-induced culture", "Induced culture", "lysate", "pellet", "flow-through" and "bead-bound protein" were loaded on the gel along with BSA quantitative standards and run in 1X SDS-running buffer at 120V. 10X SDS running buffer was composed of 0.25M Tris, 1.92M glycine and 1% SDS (w/v) made up in distilled water. The gel was stained with CBB staining solution for 3 hours to overnight. The staining solution was made up of 0.25% coomassie brilliant blue R-250 (w/v), 50% methanol, 10% glacial acetic acid and 40% distilled water. The stained gel was then given multiple washes with the de-staining solution (50% methanol, 10% glacial acetic acid, 40% distilled water) so as to remove the background staining. It was then imaged with trans-white illumination under ImageQuant LAS 4000 biomolecular imager (GE Healthcare Life Sciences). The gel was analyzed for protein induction, fractionation of the induced protein into bacterial cell lysate vs pellet, the size of the protein and its purity. The protein was visually quantified by comparing the intensity of the purified protein band at expected size with that of the known BSA quantity standards. The bead eluted as well as the thrombin-cleaved protein were similarly run on the gel and analyzed. The protein concentration of the GST eluted and thrombin-cleaved protein was also quantified using BCA protein assay kit (Pierce 23225) following manufacturer's instructions.

2.10 Far western blotting

1μg each of "Prey" proteins were electrophoresed on a 10% denaturing protein gel. The separated proteins were wet transferred to Immobilon-P PVDF membrane (Millipore IPVH00010). The membrane was first activated by immersing it in methanol and then into transfer buffer. The transfer sandwich was set up in a TE-22 Mini tank transfer unit (GE Healthcare Lifesciences 80-6204-26) filled up with 1X transfer buffer and subjected to 110 mAmp constant electricity overnight or 250 mAmp for 3 hours with constant stirring at 4°C. 10X transfer buffer was prepared by

dissolving 58g Tris and 293g Glycine in distilled water and making up the volume to 2L. Working dilution of transfer buffer was prepared by diluting 10X transfer buffer to 1X with water and adding 20%(v/v) of methanol. The transferred proteins were sequentially denatured and then renatured *in situ*. This was achieved by incubating the membrane with a set of AC buffers. AC buffers were composed of 10% glycerol, 100mM NaCl, 20mM Tris-Cl pH7.5, 1 mM EDTA, 0.1% tween-20, 1mM DTT, 2% non-fat dry milk (Saco USA) and 6M, 3M, 1M, 0.1M or 0M Guanidine-HCl made up to a total volume of 25ml. The membrane was incubated in AC buffers containing 6M, 3M and 1M Guanidine-HCl, one after the other for 30 minutes each at room temperature in a 50ml falcon tube on a rotator. It was incubated in AC buffer with 0.1M guanidine-HCl for 30 min at 4°C and ultimately in AC buffer without Guanidine-HCl at 4°C overnight to bring about slow renaturation of the proteins bound to the membrane. The membrane was then blocked for 1 hour in 5% nonfat dry milk (NFDM) dissolved in 1XTBS-0.1% Tween-20(TBS-T). 10X TBS (Tris-buffered saline) was prepared by dissolving 30g Tris, 80g NaCl and 2g KCl in distilled water, adjusting the pH to 7.6 and making up the volume to 1L. The membrane was now incubated overnight with 3ml of protein binding buffer containing 3μg of "bait protein" (1μg/ml) sealed in a plastic sachet at 4°C on a nutator mixer. This was followed by washing the membrane thrice in 1X TBS-T for 10 minutes each on a rocker. The membrane was next incubated with primary antibody against the bait protein suitably diluted in 10ml of 5%NFDM dissolved in 1X TBS-T in a falcon tube and incubated for 3 hours at room temperature on a rotator. The membrane was again washed with 1X TBS-T four times, 10 minutes each and then incubated with suitable HRP conjugated secondary antibody (1:10,000 dilution in 10ml of 5% NFDM-TBST). The membrane was similarly washed again four times with 1X TBS-T. Immobilon western chemiluminescent HRP substrate (Millipore WBKLS0500) was added to the membrane following manufacturer's instructions and the resulting chemiluminescence was imaged under ImageQuant LAS 4000 biomolecular imager (GE Healthcare LifeSciences).

2.11 Cell lines and cell culture

HeLa cells were purchased from ECACC and U2OS cells were a kind gift from Dr. Jomon Joseph, NCCS, India. Cells were cultured in 10ml of complete media. The

complete media was prepared by supplementing DMEM (Lonza 12604) with 10% fetal bovine serum (Gibco 10270106) and 1X penicillin-streptomycin antibiotic (Gibco 514022). They were grown in monolayers in 100 mm dishes (Eppendorf/Corning) at 37°C in a humidified CO_2 incubator (New Brunswick Galaxy 170R) with 5% CO_2 and 95% air. 90% confluent cultures were harvested by first rinsing the culture with 5ml DPBS (Lonza 17512F), incubating with 1ml of 0.05% Trypsin-EDTA (Lonza 17161) at 37°C for 2min to dislodge the cells, pool the cell suspension in 5ml media to a falcon tube, spin it down at 1000rpm in a swing bucket rotor centrifuge (Beckman Coulter Allegra X-12), resuspending the cell pellet in 1ml of media and finally replating the cells in 10ml of fresh media at a 1:1000 dilution so as to get a confluent monolayer culture within 4-5 days.

2.12 Immunoblotting (Western blotting)

The protein samples were made in Laemmli buffer and run on SDS-PAGE. The proteins separated on the gel were transferred to PVDF membrane as described earlier. The membrane was blocked in 10ml of 5% nonfat dry milk (NFDM) dissolved in 1X TBS-0.1% Tween-20 (TBS-T) in a 50 ml falcon tube on a rotator for 1 hour. 10X TBS (Tris-buffered saline) was prepared by dissolving 30g Tris, 80g NaCl and 2g KCl in distilled water, adjusting the pH to 7.6 and making up the volume to 1L. The membrane was then moved to a 50ml falcon tube containing the primary antibody diluted in 5ml of 5% NFDM-TBST at an appropriate concentration and incubated for three hours at room temperature or overnight at 4°C on a rotator. 4% Block-ACE (AbD Serotec / BioRad BUF029) dissolved in 1X TBS-T (instead of NFDM) was used as blocking solution or for making primary antibody dilutions in the case of probing for phosphoproteins. The membrane was now taken out in a washing dish and given four washes of 10 minutes each in 1X TBS-T by placing the dish on a rocker. It was next incubated in 1:10,000 dilution of either HRP conjugated secondary anti-mouse antibody (Jackson 115-035-003) or anti-rabbit antibody (Jackson 111-035-003) made up in 10 ml of 5% NFDM-1X TBST in 50 ml falcon tube for 1 hr on a rotator (depending upon the origin of primary antibody). The membrane was similarly washed in 1X TBS-T four times followed by rinsing in distilled water before developing for chemiluminescence. Immobilon western chemiluminescent HRP substrate (Millipore WBKLS0500) was prepared by mixing 500µl each of hydrogen

peroxide and luminol with 1ml of distilled water in a vial in the dark. 2ml of the above was spread over the membrane by using a p1000 pipette for less than a minute. The membrane was immediately placed inside ImageQuant LAS 4000 biomolecular imager (GE Healthcare LifeSciences) and chemiluminescence was captured under "precision" as well as "increment" exposure settings. Multiple images were taken under "increment" exposure until the chemiluminescence signal started getting saturated. The penultimate image before the appearance of a saturated signal was considered for analysis.

2.13 Immuno-fluorescence staining and imaging

Borosilicate glass coverslips (22mm x 22mm) were acid washed by immersing them in 1N HCl and incubating for 2-3 hours at 65°C in a water bath with stirring. This was followed by multiple washes in milli-Q water to remove the acid and storing away in 70% ethanol at -30°C. A single coverslip was taken out from alcohol and placed in a 35mm dish (Corning) or in a well of 6 well dishes (Corning/Eppendorf) and was left for air drying for 10-15 mins. $2x10^5$ cells were suspended in 2ml of complete DMEM media and added to the dish and grown overnight in the tissue culture incubator followed by desired treatment. The experimental set to be stained was taken out from the incubator and rinsed thrice with 1ml of ice cold PBS. 4% Formaldehyde was made by diluting the 37% stock (Thermo Fisher) in PBS. 1ml of this was added to the adherent cells for 20 mins at room temperature to fix the cells. The cells were then rinsed with 1ml of ice cold PBS once and then incubated with 2ml of 0.1% Glycine-PBS for 5 min to quench the fixation reaction. They were washed with 1ml PBS for 5 min each with gentle rocking. The PBS was replaced with 1ml of 0.5% TritonX-100-PBS and incubated at RT for 10 min to permeabilize the cells, followed by washing thrice with 1ml PBS for 5 min each. The PBS was aspirated out and cells were now blocked by adding 200µl of 10% goat serum (Abcam ab7481) or FBS (Gibco 10270106) made in PBS to the coverslip and incubating in a humidified chamber for 1hr at RT. The blocking solution was then replaced with the suitable dilution of primary antibody made in 200µl of 10% goat serum/FBS made in PBS and incubating similarly for 1 hour. After this primary antibody staining, the cells were washed thrice with 1ml of 1X Immunofluorescence(IF) buffer for 5 min each with gentle rocking. The 1X IF buffer was composed of 1X PBS, 0.05% NaN_3, 0.1% BSA, 0.2% TritonX-

100 and 0.05% Tween-20 at a final pH of 7.4. The samples were next subjected to secondary antibody staining. Suitable Alexa Fluor 488/568/632 conjugated secondary antibody (Invitrogen A-11034/A-11004/A-21071) was mixed with 200 μl of 10% goat serum/FBS at a dilution of 1:1000 and added to the samples and incubated similarly for 1 hour. The samples were subsequently washed similarly with 1X IF buffer and then counterstained with Hoechst 333258 (Invitrogen H3569) diluted in 1ml of 1X IF buffer at 1:5000 for 10 min. The staining solution was then replaced with 1X IF buffer. The coverslip containing stained adherent cells was carefully picked up with a pointed tweezer, inverted and mounted on a glass slide with 7μl of the mounting media. Mounting media was prepared with a composition of 90% glycerol, 10% 10X PBS and 0.125% n-propyl gallate (Sigma P3130). The coverslip was sealed with transparent nail paint (Elle 18), air-dried and the slide stored away in a slide box at 4°C.

The slides were imaged under a confocal microscope (LSM 780 Carl Zeiss) Each set of experimental and control samples were imaged under the same exposure and acquisition settings.

For the laser-induced DNA damage followed by fixed cell imaging, 12,500 cells resuspended in 500μl of complete DMEM were spotted on each well of the 12 well multi-test slide (MP biomedical sciences 96041205), the slide was placed inside a 100 mm dish with its lid closed and kept away in the incubator overnight. Next day, the slide was taken out, its media was replaced with fresh DMEM containing BrdU labeling agent (Invitrogen 000103) at a dilution of 1:100. The cells were incubated for another 24 hours. The slide was now transferred to the stage of a laser capture microdissection (LCM) microscope (PALM MicroBeam Carl Zeiss). The cells were observed under DIC, laser tracks (ROI) were marked in the nuclei and then subjected to the PALM laser at an energy not too high that could obliterate the cells but just sufficient so as to cause DNA damage. This was standardized after multiple experiments. The damaged cells were put back in the incubator, taken out after designated time points and proceeded for IF staining as described previously.

For laser-induced damage coupled with live cell imaging, $1x10^5$ cells were seeded in 1ml of complete DMEM in each chamber of a 2-chambered coverglass (Lab-tek 155380) and grown overnight. Necessary transfections were carried out as described in section 2.16. BrdU labeling agent was added to the media at a dilution of 1:100, 24

hours before the beginning of imaging. The slide was placed on the heated and humidified stage of a confocal microscope (LSM 780 Carl Zeiss). Live cell imaging at relevant channels was initiated while damage was inflicted by the multi-photon laser of LSM 780 on a predefined ROI in the nucleus at an energy that did not physically damage the cells. The cells were imaged at regular intervals after the damage to look for recovery.

2.14 Immunoprecipitation (IP)

Immunoprecipitation was performed with Api5 and IgG antibodies from cells subjected with or without damage. 8×10^5 HeLa cells resuspended in 5ml of DMEM media each were seeded into four 60mm dishes. The culture was grown overnight. CPT was added the next day to two of the dishes to a final concentration of 10μM, whereas the equal volume of DMSO was added to the other two as vehicle control. The culture was incubated further for 16 hours for the cells to amass CPT-induced DNA damage.

The media was aspirated out from the dishes and culture was rinsed with 3ml of chilled DPBS thrice. The IP experiment was performed with whole cell lysate (WCL) of the cells lysed in TNN buffer. TNN buffer was composed of 50mM Tris pH7.6, 150mM NaCl, 0.5% NP-40, 1X protease inhibitor cocktail (Sigma P8340) and 0.1mM PMSF made up in milli-Q water. 100μl of TNN buffer was added to the dish and kept on ice for 20 minutes for the cells to lyse. The cells were scraped off using a cell scraper and collected into 1.5ml microfuge tube. The tube was briefly vortexed and incubated in ice further for 10 minutes. It was now centrifuged in a pre-cooled tabletop centrifuge at 15,000g for 15 minutes so as to settle the cell debris. The supernatant was transferred to a fresh tube, protein content quantified by BCA assay, and volume made up to 200μl with TNN buffer (corresponding to 350μg of total protein). 10μl (corresponding to 5% of the total volume of WCL to be used for IP) of the above lysate was set aside and stored at -40°C as "Input" after adding 2μl of 6X SB. The WCL was pre-cleared with 1μg of anti-rabbit IgG before using it for IP. 0.2μl of anti-rabbit IgG (Bethyl P120-201) was added to the WCL and incubated at 4°C on a nutating rocker for 1 hour. PAG magnetic beads were used to extract IgG so as to pre-clear the WCL. 10μl of BioAdembeads PAG slurry (Ademtech 611874) was taken out in a microfuge tube and washed thrice with 15μl TNN buffer by placing the

tubes in DynaMag-2 Magnetic Particle Concentrator (Invitrogen 123.21D) kept on the ice. The beads were finally equilibrated in 15µl of TNN buffer. After 1 hour of incubation with IgG, the WCL was transferred to the tube containing PAG beads and incubated further for 1 hour on the nutating rocker at 4°C. The tubes were placed on the magnetic rack so as to extract out the beads and the pre-cleared WCL was transferred to fresh tubes. The IP was performed with 1µg of anti-Api5 or anti-rabbit IgG antibodies. 2µl of anti Api5 antibody raised in rabbit (Abnova PAB7951) or 0.2µl of anti-rabbit IgG (Bethyl P120-201) was added to respective tubes and incubated at 4°C on a nutating rocker for 4 hours. The immunoprecipitates were captured by incubating the above with 10µl of washed and TNN buffer equilibrated PAG beads for another hour at 4°C on a nutating rocker. The lysate was aspirated out and the beads bound with immunoprecipitates were washed thrice with 200µl TNN buffer similarly by using the magnetic rack kept on ice. The immunoprecipitates were finally lysed by resuspending the beads in 20µl of 2X SB after which they were stored away at -40°C.

2.15 Sub-cellular fractionation

Mendez & Stillman's (Méndez and Stillman, 2000) chromatin fractionation protocol was followed. $5x10^5$ cells were seeded in 60 mm dish (Corning) in 5ml of complete DMEM and grown overnight. They were subsequently subjected to the required treatment(s). The dish was now taken out, media was removed and cells were rinsed once with 3ml of ice-cold PBS. The cells were scraped off with the help of cell scraper (Corning) in 1ml of cold PBS on the ice and collected in a microfuge tube. The tube was centrifuged at 1000 rpm in a swing bucket rotor centrifuge (Eppendorf 5810R) for 5 min at 4°C. The supernatant was carefully aspirated out and cell pellet was resuspended in 200µl of buffer A. Buffer A was composed of 10mM HEPES pH7.9, 10mM KCl, 1.5mM $MgCl_2$, 0.34M sucrose, 10% glycerol, 1mM DTT, 10mM NaF, 1mM Sodium orthovanadate, 1X protein inhibitor cocktail (Sigma P8340) made up of milli-Q water. TritonX-100 was subsequently added to the cell suspension to a final concentration of 0.1%, mixed well and incubated on ice for 5 min to lyse the cells. This cell lysate was divided into two equal volumes. 100µl of this total cell extract (TCE) was taken away and stored at -40°C after adding the 6X laemmli buffer. The 6x laemmli buffer was composed of 0.35M Tris-Cl pH6.8, 36% Glycerol, 11%

SDS, 0.6M DTT, and 0.012% bromophenol blue made up of milli-Q water. Residual 100μl was centrifuged at 1300g for 5min at 4°C in a fixed angle rotor centrifuge (Eppendorf 5430). The supernatant taken out in a fresh tube was the cytoplasmic fraction (S1) while pellet was the nuclear fraction (P1). S1 was centrifuged at 20,000g for 15 min at 4°C to clarify the cytoplasmic fraction. The resultant supernatant was taken out as soluble cytoplasmic proteins fraction (S2) and was stored away after adding the laemmli buffer. The pellet contained cell debris (P2) and was discarded. Meanwhile, 100μl of Buffer B was added to P1 and incubated on ice for 30 min to lyse the nuclei. Buffer B was composed of 3mM EDTA, 0.2mM EGTA, 1mM DTT made up in milli-Q water. After 30 min, P1 was centrifuged at 1700g for 5 min at 4°C. The supernatant containing solubilized nuclear proteins was transferred to a fresh tube (S3) and stored after adding the laemmli buffer. The pellet containing chromatin-bound proteins or chromatin-enriched fraction (P3) was washed once again with buffer B. This was done by adding 100μl of buffer B to the pellet, re-suspending it, spinning it down at 1700g for 5 min at 4°C and then discarding the supernatant. The pellet was dissolved in 100μl of the 1X laemmli buffer. This suspension was sonicated in Vibracell sonicator (Sonics VCX 130) using 3mm probe at an amplitude of 25% for 15 seconds. The sonicated P3 was then heated at 70°C for 10 min and stored away at -40°C.

2.16 Electrophoretic mobility shift assay (EMSA)

EMSA was performed with 1.5kb linear dsDNA as well as with 70mer annealed oligos. 1595bp long DNA was amplified by PCR using Api5 HAC1 NLS forward/reverse primers and AAC11-pGEX4T11 plasmid as template. 3x50μl PCR reactions were pooled and purified using PCR purification kit (Qiagen 28104) and eluted in 50μl of elution buffer. The concentration was quantified using Nanodrop and volume was adjusted with elution buffer so as to make a 100nM stock of dsDNA. A set of EMSA reactions were set up in 600μl microfuge tubes (Axygen) using indicated concentrations of proteins from a 10μM stock along with 10nM DNA, 1X BSA (NEB), 1mM ATP (Sigma A2383) and 1X EMSA buffer made up to a total volume of 10μl with milli-Q water. 1X EMSA buffer contained 50mM Tris-Cl pH8.0, 100mM KCl and1mM DTT. Each reaction was incubated in a water bath at 37°C for 20 min. The reaction was quenched by adding 2μl of cold 6X STEB. 6X STEB was

made up of 0.1M Tris-Cl pH8.0, 0.2M EDTA, 40% sucrose (w/v) and 0.4mg/ml Bromo-phenol-Blue in milli-Q water. The samples were now loaded on 0.8% agarose gel made in 1X TAE buffer and containing 0.5μg/ml Ethidium bromide alongside with Supermix DNA ladder (Bangalore Genei 612652171001730), electrophoresed at constant 80V and observed under a UV trans-illuminator (Syngene G-box).

EMSA was also performed using annealed oligos as probes. ds70-1/ds70-2, ds70-1/70-Fork and 70-Bubble/ds70-2 oligo pairs (all Sigma) were annealed to create dsDNA, dsDNA-Fork, and dsDNA-Bubble-dsDNA structures. Each of the lyophilized oligos was resuspended in milli-Q water following manufacturer's instructions so as to make 100μM stock. 10X annealing buffer was used to anneal the oligos. It was composed of 100mM Tris-Cl pH7.5, 1M NaCl, made up of milli-Q water. 25μl each of the two 100μl re-suspended oligo stocks was added with 10μl of 10X annealing buffer and 40μL of milli-Q water in a microfuge tube. The tube was heated to 95°C for 3 min, then cooled to 60°C for 3 min, followed by 37°C for 30 min. Resulting annealed oligos were diluted to 5μM with 1X annealing buffer, aliquoted and stored away at -40°C. Set of EMSA reactions were set up using increasing concentrations of the protein with a constant concentration of annealed oligos. Each set consisted of indicated concentration of protein, 0.5μM of indicated annealed oligo, 1X BSA (NEB), 1mM ATP and 1X EMSA buffer made up to a total volume of 10μl with milli-Q water. The reaction was incubated at 37°C on a water bath for 20 min and then quenched by adding 2μl of ice-cold 6X non-denaturing DNA PAGE gel loading dye. The dye was composed of 10mM Tris-Cl pH8.0, 0.06% Bromophenol blue (Sigma), 0.06% Xylene cyanol (Sigma), 60% glycerol, 60mM EDTA pH8.0 and water. Each set of reactions was loaded onto a pre-cooled 5% non-denaturing polyacrylamide gel and electrophoresed at 20mA constant current at 4°C along with GeneRuler Ultra Low Range DNA Ladder (Fermentas SM1213). The electrophoresis buffer of choice was Tris-Boric acid-EDTA (TBE). 5X TBE stock solution was prepared by dissolving 54g Tris, 27.5g Boric acid and 20ml of 0.5M EDTA pH8.0 in distilled water and making up the volume to 1L. The gel was cast and run in PROTEAN ii xi Cell (Biorad) midi gel apparatus following manufacturer's instructions. 5% gel was cast using appropriate volumes of 30% acrylamide-bisacrylamide solution, 1X TBE, 10% APS and TEMED. The electrophoresis tank was filled with 0.5X TBE. The gel was removed from the apparatus after

electrophoresis and stained with Ethidium bromide diluted in milli-Q water at a concentration of 0.5μg/ml in a glass tray placed on a rocker for 10min. The stained gel was imaged under GE Typhoon FLA 9500 platform.

2.17 siRNA knockdown and rescue

Gene knockdown was carried out by transient transfections with siRNA and their rescue was carried out by transiently co-transfecting mammalian expression constructs cloned with the siRNA-resistant target gene. siRNA was purchased from Dharmacon. 5X siRNA resuspension buffer (Sigma) was diluted to 1X with DNase RNase free water (Sigma W4502). Lyophilized siRNA was reconstituted using this buffer following manufacturer's instructions so as to prepare 20μM stock solution which was then aliquoted into double autoclaved microfuge tubes and stored away at -80°C.

1.0×10^5 cells resuspended in 1ml of complete DMEM were seeded in each well of the 12-well dish (Corning) and grown overnight in the tissue culture incubator.

6μl of Lipofectamine® RNAiMAX Transfection Reagent (Invitrogen 13778150) was diluted with 100μl of prewarmed OPTI-MEM (Gibco 31985062) in a microfuge tube (Axygen) to make solution I and was incubated for 5min. In the meantime, 2μl of 20μM siRNA stock was diluted in 100μl of prewarmed OPTI-MEM to make solution II. The solution I & II were now mixed and incubated at room temperature for another 5 min. 100μl of the above mixture was then added drop-wise to each well-containing 1ml complete media, mixed and then put back in the incubator. 24 hours after the first transfection for the knockdown, transfection mixture from 1st transfection was aspirated out and replaced with 1ml of fresh complete media and the dish put away in the incubator. The second transfection was carried out for a second knockdown and rescue. The solution I was prepared as previously and Solution II was prepared by adding 2μg of rescue plasmid along with 2μl of siRNA stock to 100μl of OPTI-MEM. Solutions I & II were mixed, incubated for 10 min and 100μl of the mixture was added dropwise to each well. The culture was incubated for another 48 hours and then the experimental treatments were carried out. The cell lysate was prepared in RIPA buffer. RIPA buffer was composed of 50mM Tris-Cl pH7.4, 150mM NaCl, 0.1% SDS, 0.01% Sodium azide, 0.5% Sodium deoxycholate, 1mM EDTA pH8.0, 1% NP-40 and 1X protein inhibitor cocktail (Sigma P8340). The culture dish was kept on ice

and media was aspirated out. It was rinsed twice with ice-cold PBS. 45μl of freshly prepared RIPA buffer was added to the dish dropwise and was left for 15min. The cells were scraped off using a cell scraper (Corning) and collected in a microfuge tube. The tube was vortexed briefly and incubated on ice for another 15 min. It was now centrifuged at 4°C at 12000 rpm for 15 min in a centrifuge (Eppendorf 5430). The supernatant was transferred to a fresh tube and pellet containing cell debris was discarded. The amount of protein in cell lysate was quantified by BCA protein assay kit (Pierce 23225) following manufacturer's instructions. The lysate was diluted with appropriate volumes of PBS and 6X laemmli buffer so as to make a mixture with the protein concentration of 1.5μg/μl. 10μl (corresponding to 15μg of protein) of the lysate was to be loaded per lane for SDS-PAGE and western blotting analysis.

2.18 Plasmid transfection for transient overexpression

The gene of interest was cloned into a mammalian expression plasmid. Plasmid midiprep was performed using NucleoBond Xtra midi (Macherey Nagel 740410.50) kit, following manufacturer's instructions to purify plasmid and prepare a stock of 1μg/μl concentration.

For live cell imaging, $1x10^5$ cells were seeded in 1ml of complete DMEM in each chamber of a 2-chambered coverglass (Lab-tek 155380) and grown overnight. 4μl of Lipofectamine® 2000 (Invitrogen 11668-019) was diluted with 96μl of OPTI-MEM (Gibco 31985062) to make Solution I in a microfuge tube. The solution I was incubated at RT for 5 min. Meanwhile, plasmid DNA to a total amount of 1μg was dissolved in 100μl of OPTI-MEM in another microfuge tube to make Solution II. 100μl each of solution I and II were mixed thoroughly by pipetting and incubated at RT for 20 min. Meanwhile, complete DMEM was removed from the chambered coverslip and replaced with 1ml of OPTI-MEM and incubated in the TC incubator for 20 min. After 20 min, 800μl OPTI-MEM was added to Solution I+II and this mixture was added to the cells in the chamber after aspirating out its OPTI-MEM with which it had been kept for acclimatization for 20 min. The culture was incubated for 4 hours after which, 0.5ml of DMEM-30%FBS was added to the culture and kept away in the TC incubator for another 48 hours for the protein to express.

For doing chromatin fractionation of cells containing the several deletion mutants of Api5 mVenusC1 NLS, 4×10^5 cells were seeded in 5ml of complete DMEM in a 60 mm dish (Corning) and grown overnight. 18µl of Lipofectamine® 2000 (Invitrogen 11668-019) was diluted with 388µl of OPTI-MEM in 15 ml falcon tube to make Solution I and incubated at RT for 5 min. In the meantime, 4µg of plasmid DNA to be transfected was dissolved in 400µl of OPTI-MEM in a microfuge tube to make solution II. 400µl of Solution II was now added to 400µl of Solution I and incubated at RT for another 20 min. Meanwhile, the culture was acclimatized with 5ml of OPTI-MEM. After 20 min, 4.2ml of OPTI-MEM was added to Solution I+II mixture and added to the culture dish after removing its acclimatizing OPTI-MEM. The dish was incubated for 4hr in the TC incubator and after this duration, 2.5ml of DMEM-30%FBS was added to the culture to replenish serum, and the culture kept away in TC incubator for another 48 hours for the protein to express.

2.19 Cell cycle synchronization-FACS and AnnexinV staining-FACS

Cells were synchronized by thymidine-nocodazole block and Fluorescence-activated cell sorting (FACS) was performed on a BD Accuri flow cytometer instrument.
16×10^5 cells were seeded in a 100mm dish (Corning) in 10ml of complete media and grown for 16-20 hr to get a 40% culture. The media was then aspirated out, culture rinsed twice with 5ml of DPBS and replaced with complete media supplemented with 2mM Thymidine. The culture was grown for 24 hours, after which the media was removed, rinsed twice with 5ml of DPBS and replenished with 10 ml of fresh complete media and kept away in the incubator. After 3 hours, the media was removed, the culture was rinsed again twice with 5 ml of DPBS and replenished with 10 ml of complete media supplemented with 100 ng/ml Nocodazole. The culture was further grown for another 12 hours and after which the synchronized culture was harvested. To harvest the cells, the culture dish was gently tapped against a hard surface to dislodge the cells. The floating cells were collected and spun down at 500g for 5 min in a swing bucket centrifuge (Beckman Coulter Allegra X-12). The supernatant was aspirated out and the cell pellet was rinsed with 6 ml of DPBS. The washed cell pellet was resuspended in 10 ml of fresh complete media. In the meantime, two 60 mm dishes (Corning) were prepared by putting an acid washed coverslip to each of the dishes and left to air dry. 10ml of the synchronized cell

suspension was divided into two, and 5ml was added to each of the two 60mm dishes. After thus releasing the synchronized cells into fresh media with required drug regimen, it was harvested after indicated time points. At each time point of harvest, the coverslip was picked and subjected to immunostaining while rest of the adherent cells were harvested by gentle trypsinization. The harvested cells were fixed by resuspending the cell pellet in 500μl of 70% ethanol in a microfuge tube and storing it away at 4°C. To acquire FACS profile of the samples, propidium iodide (PI) staining was carried out. The ethanol fixed samples were spun at 500g for 5 min at 4°C, ethanol aspirated out and rinsed once with 500μl of PBS. The washed cells were resuspended in 500μl of PBS, 10μl of RNase A (10mg/ml stock) and 20μl of PI (1mg/ml stock) were added and incubated in the dark at 37°C for 1 hour with gentle tapping at regular intervals. The FACS profile of samples was acquired on BD Accuri C6 flow cytometer using manufacturers instructions.

For determining apoptosis induction, 2.5×10^5 cells resuspended in 2ml of complete DMEM media were seeded into each well of a 6 well dish (Corning). The cells were grown overnight and then subjected to different dosages of CPT. They were subsequently harvested and freshly stained using Annexin-V-FLUOS staining kit using manufacturer's instructions (Roche 1858777). The FACS profile of stained cells was acquired within 10 minutes on BD FACSCalibur flow cytometer following manufacturer's instructions.

Chapter 3: *In vitro* interaction studies between Api5 and TopBP1

3.1 Background

Cells are the functional units of life and protein-protein interactions (PPI) drive biological processes thus determining the cellular outcome. They are important for all the intra and extracellular functions such as DNA replication, transcription, translation, splicing, secretion, cell cycle control, signal transduction to name a few. (Phizicky and Fields, 1995; Shoemaker and Panchenko, 2007; Westermarck et al., 2013). PPIs can be variously categorized depending upon the context. They can be permanent or transient based upon their strength and temporal longevity, they can be specific or non-specific, they can further be homo or hetero-oligomeric depending upon the similarity between the interacting subunits/polypeptides (Shoemaker and Panchenko, 2007). Strong PPIs are a result of the formation of covalent bonds like SUMOylation and Ubiquitylation. However, a lot of PPIs are weak and are made by ionic interactions, dipole interactions, hydrogen bonds, Van der Waals forces, and hydrophobic interactions (Chen et al., 2008).

Even though the PPIs and their resultant functions are enormously diverse, the interacting protein interfaces share some common properties. Proteins generally have a modular structure. The human genome has 20,000-30,000 genes encoding for a proteome consisting of around 500,000 different proteins of which the cell can encode around 10,000 proteins at a given time (Berggård et al., 2007). This staggering diversity of the proteome in comparison to the genome is made possible by the existence of a modular structure of proteins. Relatively conserved sets of such modules/domains can come together in different permutations and combinations to make this diversity of proteins and thus enable the full spectrum of functional capability. This kind of setup aids in the rapid evolution of new signaling pathways while ensuring their conserved regulation. Efficient signaling in response to stimuli is enabled by the formation of protein complexes of up to several megadaltons in size in which a scaffold protein holds together upstream as well as downstream signaling proteins in a dynamic spatiotemporally regulated fashion. PPIs mostly are mediated by distinct PPI domains but can also happen between regions outside such domains in the unstructured/unfolded region of the proteins. There are over 80 known PPI domains (Westermarck et al., 2013). PTB, PDZ, SH2, SH3, LZD, RING, BRCT are

some prominent PPI domains which occur in different proteins in a combinatorial manner (Pawson and Nash, 2000; Phizicky and Fields, 1995; Westermarck et al., 2013).

Api5 and TopBP1 also have modular structures. Api5 is made up of all alpha helices that are held together by unstructured loops. The tertiary structure of the protein has concave and convex surfaces that are positively and negatively charged respectively. It has a LxxLL motif and an LZD. The N-terminal of the protein resembles HEAT repeats while the C-terminal is identical to ARM repeats (Han et al., 2012a). LxxLL motif, LZD, HEAT, and ARM are all well known PPI domains (Neuwald and Hirano, 2000a; Plevin et al., 2005; Tewari et al., 2010). TopBP1 is made up of pairs of BRCT domains joined by unstructured regions (Wardlaw et al., 2014). BRCT domains are known phosphoprotein interacting domains (Leung and Glover, 2011; Mesquita et al., 2010).

The LC-MS analysis of GST-TopBP1 pull-down screen identified Api5 as a novel interactor of TopBP1. The presence of putative PPI domains in both the proteins and other attributes like charge-properties and unstructured regions makes it even more interesting to further elucidate the region(s) of either of the proteins involved in the possible interaction. The first step towards this is validating the interaction between full-length TopBP1 and Api5 using a suitable method, followed by further analysis to elucidate the interacting region(s).

Protein interactions can be detected and validated by a variety of genetic, biochemical and biophysical tools. Novel protein interactors can generally be detected by using a bait protein. Bait proteins can be purified using single tag affinity purification or Tandem affinity purification. Methods like cross-linking, 2D-native PAGE or quantitative proteomics like LC-MS may be utilized to identify interactors of the bait protein. Library based methods and looking up public PPI databases can also help us identify new PPIs (Berggård et al., 2007; Miernyk and Thelen, 2008). Validation of these interactions is an important step towards the discovery of new PPIs. This should be confirmed both *in vivo* and *in-vitro*. *In vivo* methods like two-hybrid systems (yeast and mammalian), co-immuno-precipitations, confocal microscopy, surface plasmon resonance to name a few, are commonly used to validate PPIs (Chen et al., 2008; Shoemaker and Panchenko, 2007; Tobergte et al., 2013). Commonly used *in vitro* interaction strategies to validate PPIs include affinity pulldown of purified

proteins and protein affinity chromatography like far western blotting (Phizicky and Fields, 1995; Wu et al., 2007). A major drawback of *in vivo* interaction studies like co-IP from mammalian extracts or microscopy is that it can't distinguish direct PPI between two proteins of interest from an indirect interaction through another scaffolding protein. This makes *in vitro* interaction studies important as this can prove or disapprove direct biochemical interaction potential between two proteins of interest in a cell-free system.

3.2 Results

3.2.1 *In vitro* interaction study of full-length Api5 and TopBP1

3.2.1.1 Overexpression and purification of GST Api5

Api5 pGEX 4T11 plasmid was a kind gift from Prof Jean Luc-Poyet, INSERM Paris. Full-length Api5 was amplified from Api5 pGEX 4T11 plasmid by PCR using Api5 For2 (Bioserve) forward and GST Api5 rev (IDT) reverse primers. This was cloned between NcoI and EcoRI restriction sites of pGEX 2Tkcs plasmid. Api5 pGEX 2Tkcs plasmid construct was used to express GST Api5 protein in *E.coli* BL21 DE3 cells. This was a fusion protein of Api5 and GST affinity tag. Protein expression from the plasmid was induced by IPTG and overexpressed protein was purified from the bacterial lysate by affinity purification using GST agarose resin. The molecular weight of Api5 protein is 60 kDa and that of GST is 28 kDa, resulting in the molecular weight of GST-Api5 being 88 kDa. The bead-bound purified protein along with some samples collected during the different steps of protein purification was run on 10% SDS-PAGE alongside protein marker and stained with Coomassie brilliant blue R-250 (CBB). The gel was subsequently destained with aceto-methanol to reveal the protein bands (Fig3.2.1.1A). The other protein of interest, TopBP1 with which we had to study the *in vitro* interaction of Api5, was to be expressed with GST affinity tag as well. This posed a challenge of showing a false positive interaction between the two fusion proteins while performing the *in vitro* interaction experiments, owing to GST-GST oligomerization. To overcome this challenge, GST Api5 fusion protein was digested with Thrombin to remove its GST tag. This was possible because of the presence of a thrombin recognition linker sequence between the GST tag and multiple cloning site (MCS) in the pGEX 2Tkcs plasmid. Bead-bound GST Api5 was digested with Thrombin in thrombin cleavage buffer and the thrombin-cleaved Api5 protein fraction was eluted. The eluted fraction, along with residual beads and BSA quantitative standards were run on 10% SDS-PAGE and stained with CBB and analyzed (Fig3.2.1.1B). We were able to achieve a robust expression of GST Api5 and sufficiently clean purification profile of both GST-Api5 and thrombin-cleaved Api5 proteins.
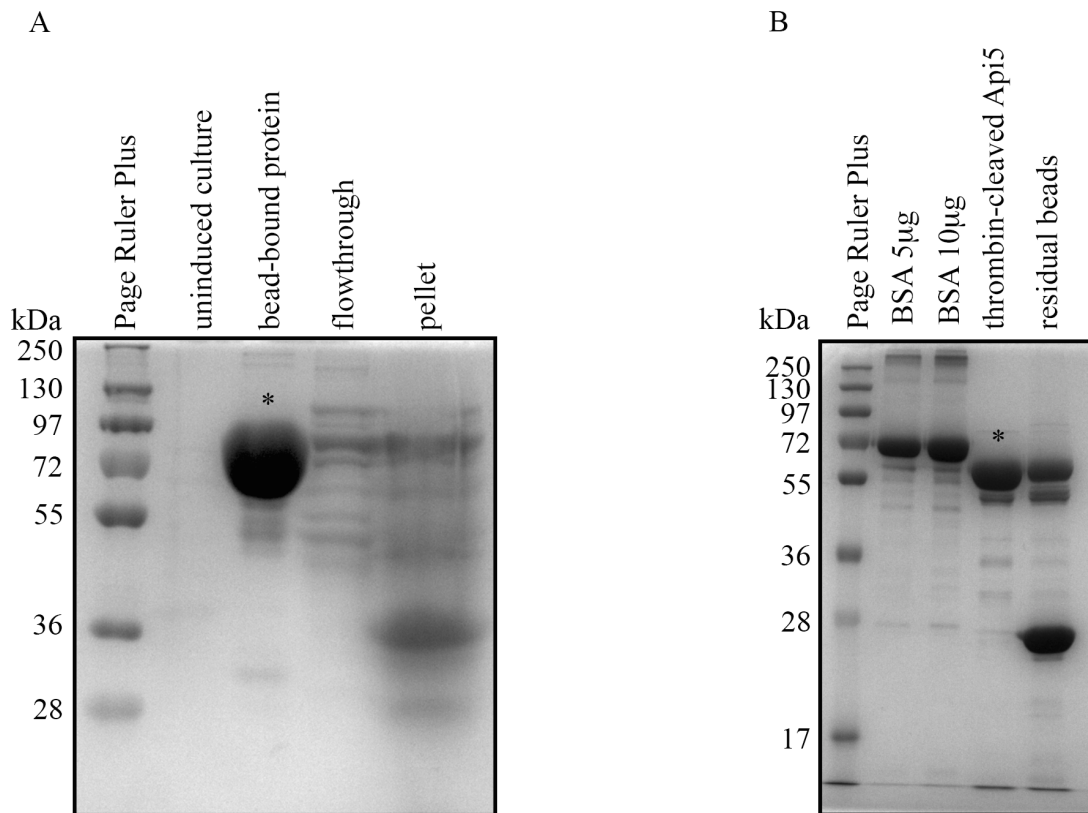
Figure 3.2.1.1: Purification of GST Api5 and its thrombin cleavage.

(A) GST Api5 protein was purified from bacterial lysate; protein ladder, uninduced culture, bead-bound protein, flow through and sonicated bacterial cell pellet were run on the gel and stained with CBB. Band for purified Api5 protein at expected size (86kDa) is marked with an asterisk. (B) protein ladder, 5μg BSA, 10μg BSA, thrombin-cleaved eluted Api5 protein and residual beads were run on the gel and stained with CBB. The band for thrombin-cleaved Api5 at expected size (60kDa) is marked with an asterisk.

3.2.1.2 Overexpression and purification of GST TopBP1

TopBP1 pGEX-2Tkcs bacterial expression plasmid was a kind gift from Prof. Lee Zou, MGH Cancer Center, USA. This plasmid was used to express GST TopBP1 protein in *E Coli* BL21 DE3 cells after induction of the culture with IPTG. The bacterial cells were lysed by sonication and the GST-tagged TopBP1 protein was purified from the lysate by affinity purification with the help of GST agarose affinity resin. Purified bead-bound protein, as well as samples collected across various steps of protein expression and purification experiment, were run on 10% SDS-PAGE, stained with CBB and destained with aceto-methanol to reveal the bands and imaged (Fig 3.2.1.2). The level of protein expression was fair enough but not as strong as GST Api5. It also showed multiple bands at lower molecular weights than the expected size (210kDa), which could have been degradation products owing to the relatively big size of the fusion protein. Multiple attempts were made with changed induction and purification conditions to achieve better yield and purity of GST TopBP1 protein only to a limited success. Thrombin cleavage of bead-bound GST TopBP1 protein to release TopBP1 was attempted, but sufficient amount of cleaved protein could not be detected in the eluted fraction possibly due to relatively low concentration of GST TopBP1 protein at the first place.
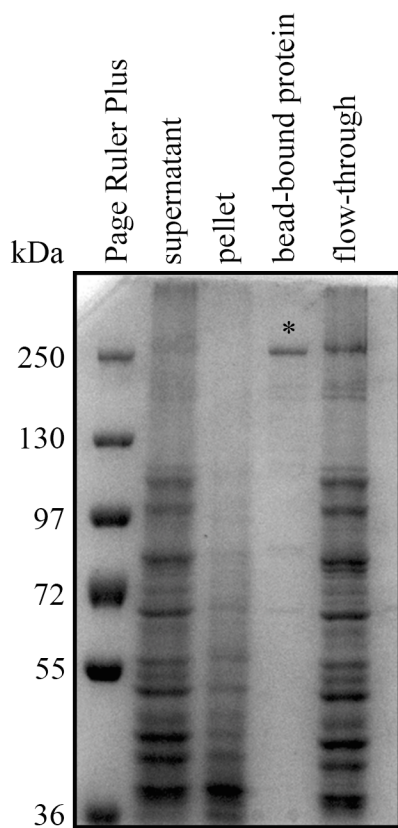
Figure 3.2.1.2: Expression and purification of GST TopBP1.

TopBP1 pGEX 2Tkcs plasmid was expressed in bacteria to express GST TopBP1 protein. Protein ladder sonicated supernatant, sonicated pellet, bead-bound purified protein and flow through were run on SDS-PAGE, stained with CBB, destained with aceto-methanol and imaged. Band for bead-bound purified GST TopBP1 at expected size (210kDa) is marked with asterisk

3.2.1.3 Api5 and TopBP1 interact *in vitro*

Api5 and TopBP1 proteins obtained by batch purification using GST affinity resin in the previous section showed that while they had decent quantitative yield, they were not of high order qualitatively. They showed some non-specific bands below their expected sizes, which could have been either because of the presence of impurities during purification or protein degradation. *In vitro* interaction technologies like GST affinity pull-down of the bait GST fusion protein-prey protein mixture to look for co-precipitation of prey protein requires relatively higher levels of protein purity. Higher order purification of bait and prey proteins (Api5 and TopBP1 respectively) that were obtained by batch purification was attempted by gel filtration chromatography as well as ion exchange chromatography only to a limited success. So an alternative strategy of far western blotting (Wu et al., 2007) was employed to study the *in vitro* interaction between Api5 and TopBP1. In far western blotting technology, the prey protein is first electrophoresed on an SDS-PAGE to separate the protein of interest from (any) impurities present in the preparation according to size, and then transferred and immobilized on a solid support (PVDF membrane). While probing the membrane with the antibody against bait protein with which it had been incubated, the signal appearing only at the expected size of prey protein is considered, ignoring non-specific bands at any other size. This reduces the requirement of high levels of purity of proteins needed for *in vitro* interaction studies.

GST Api5 and thrombin-cleaved Api5 were used as prey protein. BSA, Msh2Δ4, and GST served as the negative controls. 1μg each of these proteins was electrophoresed on SDS-PAGE and transferred to PVDF membrane. The proteins are partially or fully denatured when subjected to denaturing SDS-PAGE and denatured proteins are not in a state of showing protein-protein interactions. Hence, the proteins immobilized on the membrane were subjected to serial dilutions of a strong denaturant guanidinium hydrochloride to firstly ensure a proper denaturation and then a gradual and slow renaturation of the proteins to their native state, thus enabling them to exhibit their protein binding properties. The membrane was now incubated with eluted GST TopBP1 protein (bait) dissolved in protein binding buffer at a concentration of 1μg/ml. The membrane was now immunoblotted with an antibody against TopBP1 (Bethyl A300-111A) at a dilution of 1:5000 and the chemiluminescence was imaged (Fig 3.2.1.3B). Another gel was run with the same experimental and control prey

proteins in the same quantity in parallel and stained with CBB to get a profile of the proteins used for the binding experiment (Fig 3.2.1.3A). As is evident from Fig GST Api5 as well as thrombin-cleaved Api5 showed an interaction with GST TopBP1 as concluded from the appearance of chemiluminescence bands at their expected sizes of 86 kDa and 60 kDa respectively. This was unlike any of the negative controls and validated a direct biochemical interaction between Api5 and TopBP1 *in vitro*.
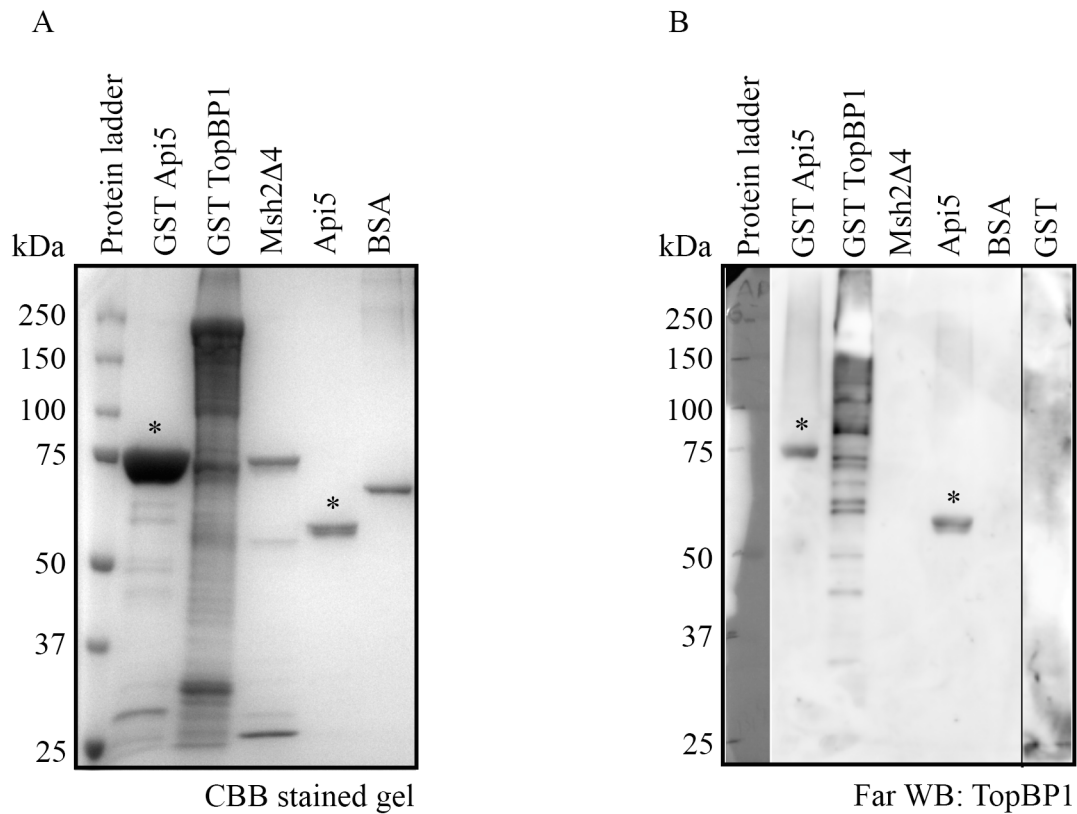
Figure 3.2.1.3: Api5 interacts with TopBP1 *in vitro*.

(A) Protein ladder, 1µg each of purified GST Api5, GST TopBP1, Msh2Δ4, thrombin-cleaved Api5 and BSA were run on 10% SDS-PAGE and stained with CBB. (B) similar loading as in (A) along with 1µg GST was run on 10% SDS-PAGE and subjected to far western blotting, using TopBP1 as bait protein followed by immunoblotting with TopBP1 antibody. Asterisks on (B) indicate the bands of GST Api5 and Api5 that show an interaction with GST TopBP1. These bands also correspond to the asterisks on (A) indicating the same proteins at expected sizes

3.2.2 Mapping the region(s)/domain(s) of Api5 and TopBP1 involved in the *in vitro* interaction

3.2.2.1 Cloning of deletion constructs of Api5 into pGEX-2Tkcs

Far western studies validated the interaction between Api5 and TopBP1 *in vitro*. As discussed earlier both Api5 and TopBP1 have such motifs/domains, which are known to have protein-protein interaction functions. *in vitro* interaction studies so far showed that full-length proteins can bind with each other. Owing to the presence of PPI domains in both Api5 and TopBP1 it would be interesting to map the region(s)/domain(s) of either of the protein that are involved as well as sufficient for showing this interaction.

The first dimension of this study was to find the region(s) of Api5 involved in its interaction with full-length TopBP1 and the second dimension was to find the region(s) of TopBP1 involved in its interaction with full-length Api5

To address the first dimension, a series of Api5 truncation mutants were created (Fig 3.2.2.1A). These were designed so as to include or exclude the LZD in combination with rest of the regions of the protein. The full-length Api5 cloned into pGEX 2Tkcs consisted of 524 amino acids. The deletion constructs designed were as follows:

i)   Api5 Δ2-3: portion of Api5 from before the beginning of LZD, comprising of 358 amino acids spanning between 1-358

ii)   Api5 LZD: only the LZD portion, comprising of 31 amino acids spanning between 358-389

iii) Api5 Δ1-2: portion of Api5 after the LZD, comprising of 135 amino acids spanning between 389-524

iv)   Api5 Δ3: portion of Api5 without the region after LZD, comprising of 389 amino acids spanning between 1-389

v)   Api5 Δ1: portion of Api5 from LZD to the end, comprising of 166 amino acids spanning between 358-524

Api5 pGEX 4T11 was used as a template to PCR-amplify the different regions and cloned between NcoI and EcoRI sites of the pGEX-2Tkcs plasmid. Api5 Δ2-3 was amplified using Api5 For2 (Bioserve) and LZD rev2 (Bioserve) primer pair, Api5 LZD was amplified with GSLZDfor (Bioserve) and GSLZDErev (Bioserve) primer pair, Api5 Δ1-2 was amplified using GS-6 for (Bioserve) and GST Api5 rev (IDT)

primer pair, Api5 Δ3 was amplified using Api5 For2 (Bioserve) and GSLZDErev (Bioserve) primer set and lastly Api5 Δ1 was amplified using GSLZDfor (Bioserve) and GST Api5 rev (IDT) primer pair. GST Api5 Δ2-3 had already been cloned in the lab, while rest of the deletion constructs were cloned as part of this work. The clones obtained were confirmed by restriction digestion with NcoI and EcoRI and looking for insert release at expected size (Fig 3.2.2.1 B, C, D, E).
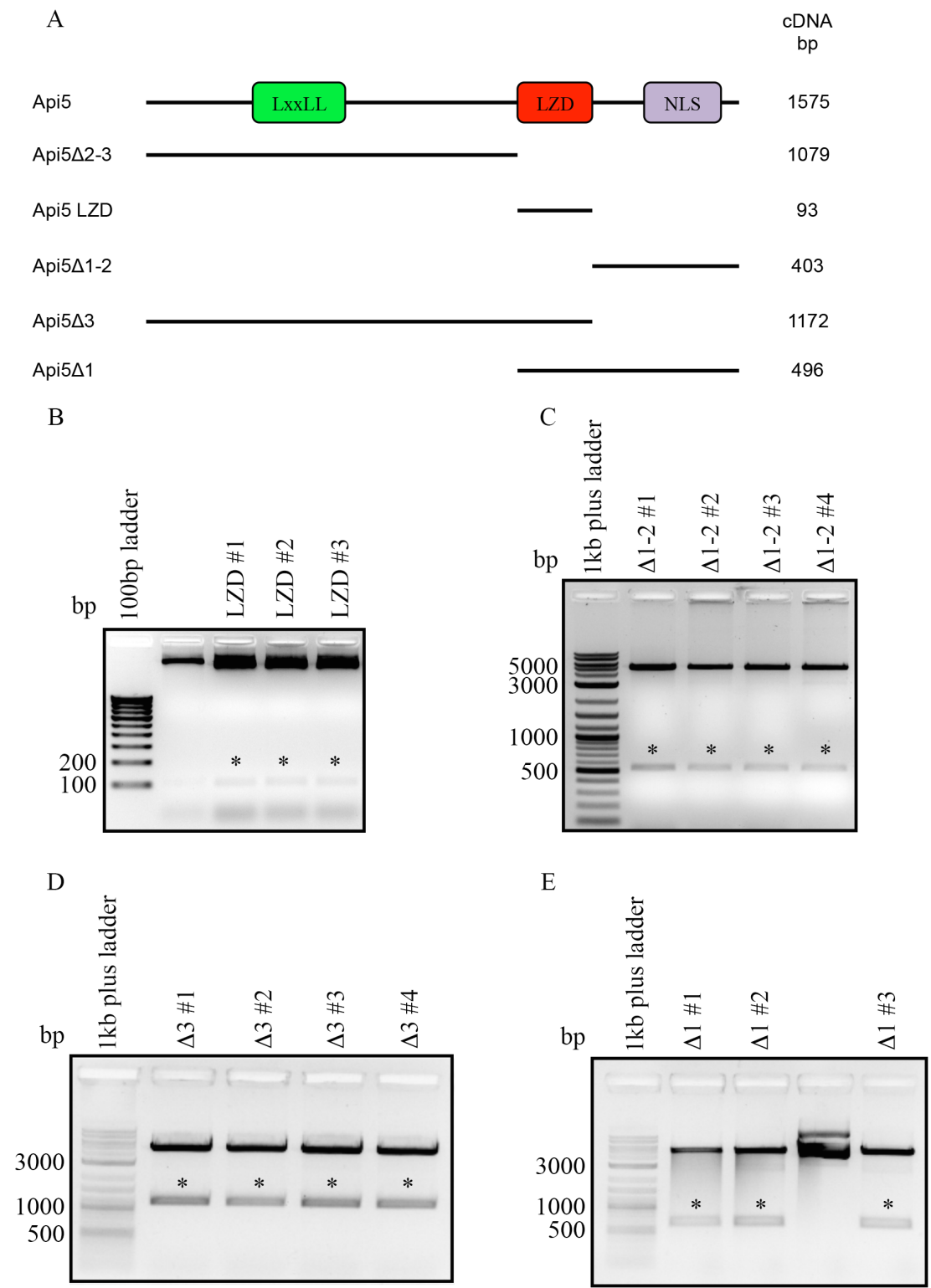
Figure 3.2.2.1: Cloning of Api5 deletion constructs into pGEX-2Tkcs.

(A) Schematic of Api5 and its deletion constructs indicating each of their cDNA sizes which correspond to the size of amplicon used for cloning as well as the size of fragment release upon restriction digestion to confirm the cloning. (B-E) EtBr-stained

agarose gels imaged under UV trans-illuminator showing insert release from pGEX-2Tkcs vector upon restriction digestion: (B) three different positive clones of LZD construct showing release of 93bp fragment, (C) four different positive clones of Δ1-2 construct showing release of 403bp fragment, (D) four different positive clones of Δ3 construct showing release of 1172 bp fragment and (E) three different positive clones of Δ1 construct showing release of 496bp fragment.

3.2.2.2 Overexpression and purification of GST Api5 deletion constructs

Full length and deletion constructs of Api5 cloned into pGEX 2Tkcs that were prepared in the previous section were used to express the GST fusion truncation mutant proteins of Api5 (Fig 3.2.2.2A). The constructs were similarly expressed in *E coli* BL21 DE3 bacterial cells and expression was induced by IPTG. The cells were lysed by sonication and the over-expressed protein in the lysate was purified by affinity purification. Batch purification using GST-agarose beads was performed. Several samples during the different steps of bacterial protein expression and purification were collected and run on 10% SDS-PAGE and visualized after CBB staining. The purified truncation mutant proteins of Api5 showed more non-specific bands in comparison to the full-length GST Api5 protein purified earlier. Among the truncation mutants themselves, Δ1 and Δ1-2 showed more non-specific bands in comparison to Δ2-3, Δ3, and LZD. Protein expression and purification conditions were tweaked around to get the best purification profile as is represented in Fig 3.2.2.2(B, C, D).

A

	protein kDa	+GST kDa
Api5 — LxxLL — LZD — NLS	60	88
Api5Δ2-3	40	68
Api5 LZD	3	31
Api5Δ1-2	14	42
Api5Δ3	44	72
Api5Δ1	18	46

B

GST Api5 Δ2-3   GST Api5 LZD

C

GST Api5 Δ1-2
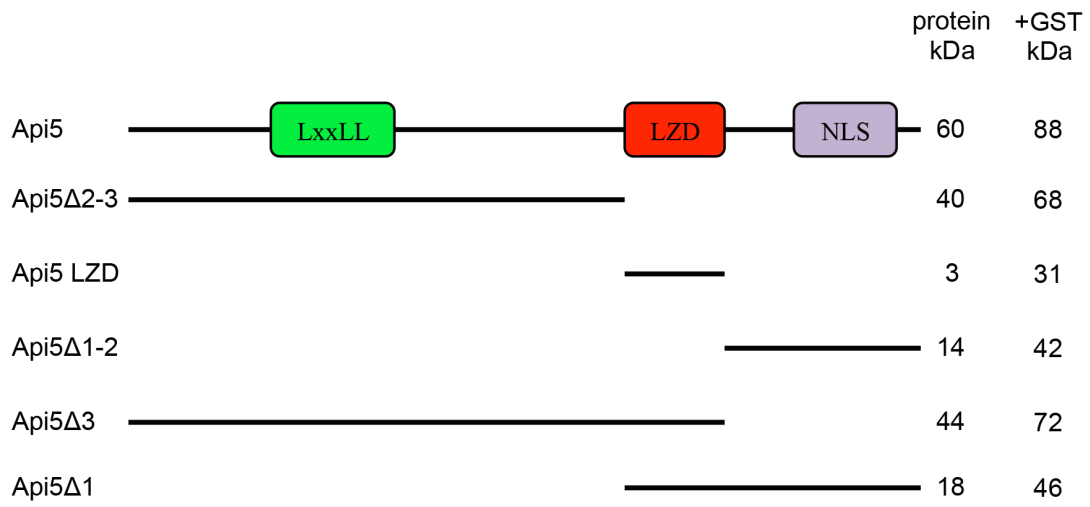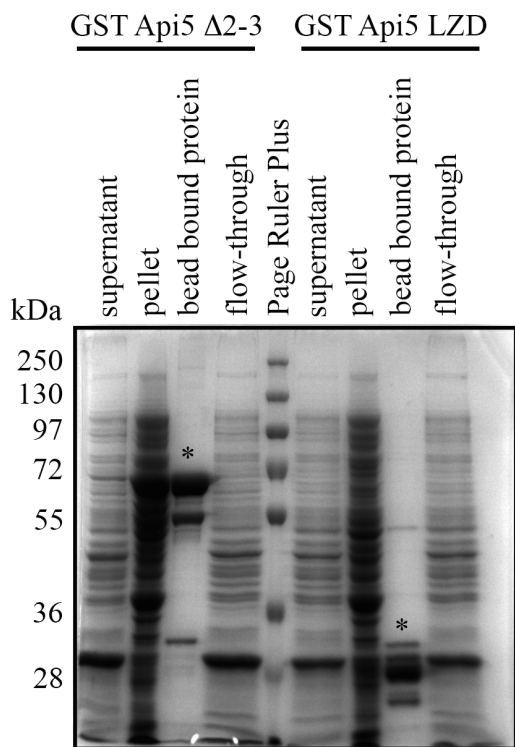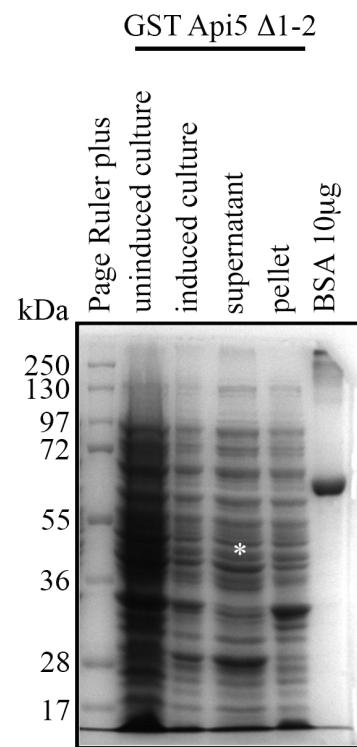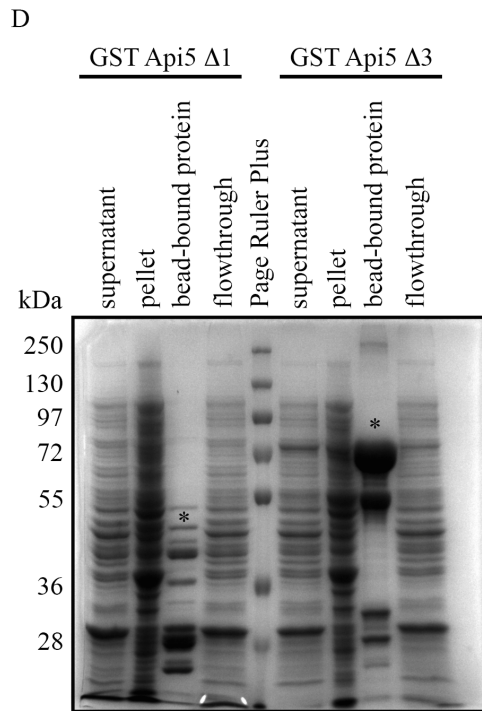
Figure 3.2.2.2: Expression and purification of Api5 truncation mutant proteins.

(A) Schematic of Api5 and its truncation mutants indicating the molecular weight of proteins. GST fusion adds additional 28 kDa to each of the proteins and the molecular weights of each of the GST fusion Api5 truncation mutants are also mentioned. (B-D) protein purification samples were run on 10% SDS-PAGE and visualized after CBB staining. (B) Lanes 1-4: sonicated supernatant, bead-bound protein and flow-through of GST Api5 Δ2-3 protein. Purified protein at the expected size of 68kDa is marked with an asterisk, Lane5: protein ladder, Lanes 6-9: sonicated supernatant, sonicated pellet, bead-bound protein and flow through of GST Api5 LZD. Purified protein at the expected size of 31kDa is marked. (C) Protein ladder, followed by uninduced culture, induced culture, sonicated supernatant and sonicated pellet of GST Api5 Δ1-2 protein. Overexpressed protein at the expected size of 42 kDa is marked in the supernatant lane, the last lane has BSA protein standard. (D) Lanes 1-4: sonicated supernatant, sonicated pellet, bead-bound protein and flow through of GST Api5 Δ1 protein preparation, purified protein at the expected size of 46kDa is marked, Lane5: protein ladder, Lane6-9: sonicated supernatant, sonicated pellet, bead-bound protein and flow through of GST Api5 Δ3 protein preparation. Overexpressed protein at the expected size of 72kDa is marked with an asterisk.

3.2.2.3: Western blotting of GST Api5 truncation mutant proteins and probing with GST antibody to validate the proteins

As observed in the previous section, the purified truncation proteins showed non-specific bands. Analyzing the protein preparations for their sizes by observing CBB stained gel did not give any information about the nature of those nonspecific bands as to whether they were just impurities present in the preparation or they were products of protein degradation. Moreover, the purified proteins: the full-length GST Api5 as well as its truncation mutants, that appeared at expected sizes on CBB stained gel needed to be validated. This was achieved by immuno-blotting the purified truncation mutation proteins against GST antibody (Fig 3.2.2.3A,B). Anti-GST antibody (Millipore 05-782) was used at a dilution of 1:5000.

Probing the western blot with GST antibody caught up bands for each of the samples, proving that the purified products were indeed GST fusion proteins that we intended to purify. For almost all the protein preps, non-specific bands appeared only at molecular weights lower than the expected size and never at higher weights. This proved that the nonspecific bands present in our protein preparations were products of protein degradation, and this ruled out the chances of them being protein impurities. It was also observed that the Δ1 and Δ1-2 truncation mutants showed more protein degradation in comparison to others. This proved that the 1st region of Api5 is responsible for providing stability to the protein, as the mutants lacking it, that is to say, Δ1 and Δ1-2, showed degradation *in vitro*. This could be explained by taking into consideration an earlier speculation (Han et al., 2012a) that the LxxLL motif, which is present in the first region of Api5 is responsible for the stability of Api5 protein.
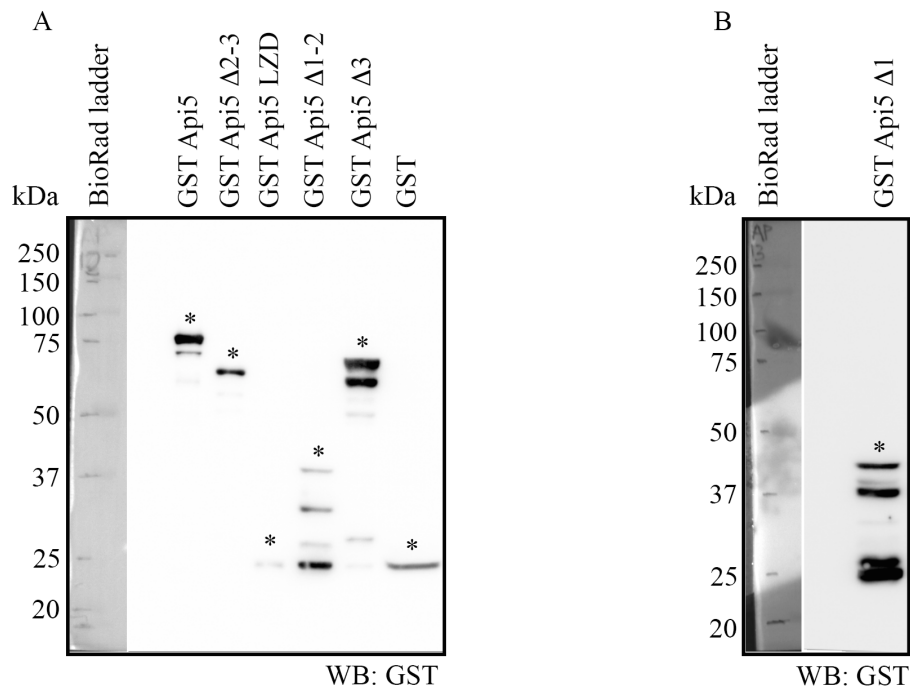
Figure 3.2.2.3: Validation of GST Api5 and its truncation-mutation proteins by immunoblotting.

Purified proteins were run on 10% SDS-PAGE, western blotted, and probed with GST antibody. (A) Protein ladder, GST Api5 (88kDa), GST Api5 Δ2-3 (68 kDa), GST Api5 LZD (31 kDa), GST Api5 Δ1-2 (42 kDa), GST Api5 Δ3 (72 kDa), GST (28 kDa) and (B) protein ladder, GST Api5 Δ1 (46 kDa). Expected bands are marked with an asterisk.

63

3.2.2.4 Mapping of Api5 region(s) required for it's *in vitro* interaction with TopBP1

Some of the GST Api5 truncation mutation proteins showed higher levels of protein degradation that contributed to a lower yield of the intact protein. Changing the expression and purification conditions only improved the qualitative and quantitative yield of the deletion constructs to a certain extent and absolute purity could not be achieved. Because of this reason, far western blotting was again used as a method of choice for studying the *in vitro* biochemical interaction between full-length TopBP1 and Api5 deletion mutants. The design of these Api5 deletion mutants that involved truncation of portions or Api5 one each at a time or in combinations, allowed us to map the region(s) of Api5 that were involved in or were sufficient for interaction with TopBP1 by analyzing the which one(s) of the truncation mutants showed or not an interaction with TopBP1. GST fusion full-length and truncation mutants of Api5 were used as prey proteins, immobilized on the membrane, whereas full-length GST TopBP1 was used as the bait protein. As mentioned in the previous section, this strategy had a potential pitfall of showing false positives owing to possible GST-GST interaction under certain conditions. So, GST was kept as a control along with all the other Api5 prey proteins to look out for the possibility of protein interaction via GST tags.

The purified proteins were quantified by visual estimation of their band at expected size with respect to a known BSA quantity standard. 1µg each of the prey proteins were run on the gel, transferred to membrane, denatured and renatured using serial dilutions of guanidinium hydrochloride, incubated with eluted bait protein (GST TopBP1) at a concentration of 1µg/ml, and then probed with TopBP1 antibody (Bethyl A300-111A) at a dilution of 1:5000 (Fig 3.2.2.4B). Another gel was run in the parallel, with the same loading of prey proteins as the one used for far western; it was visualized after staining with CBB to get the prey protein profile (Fig 3.2.2.4A).
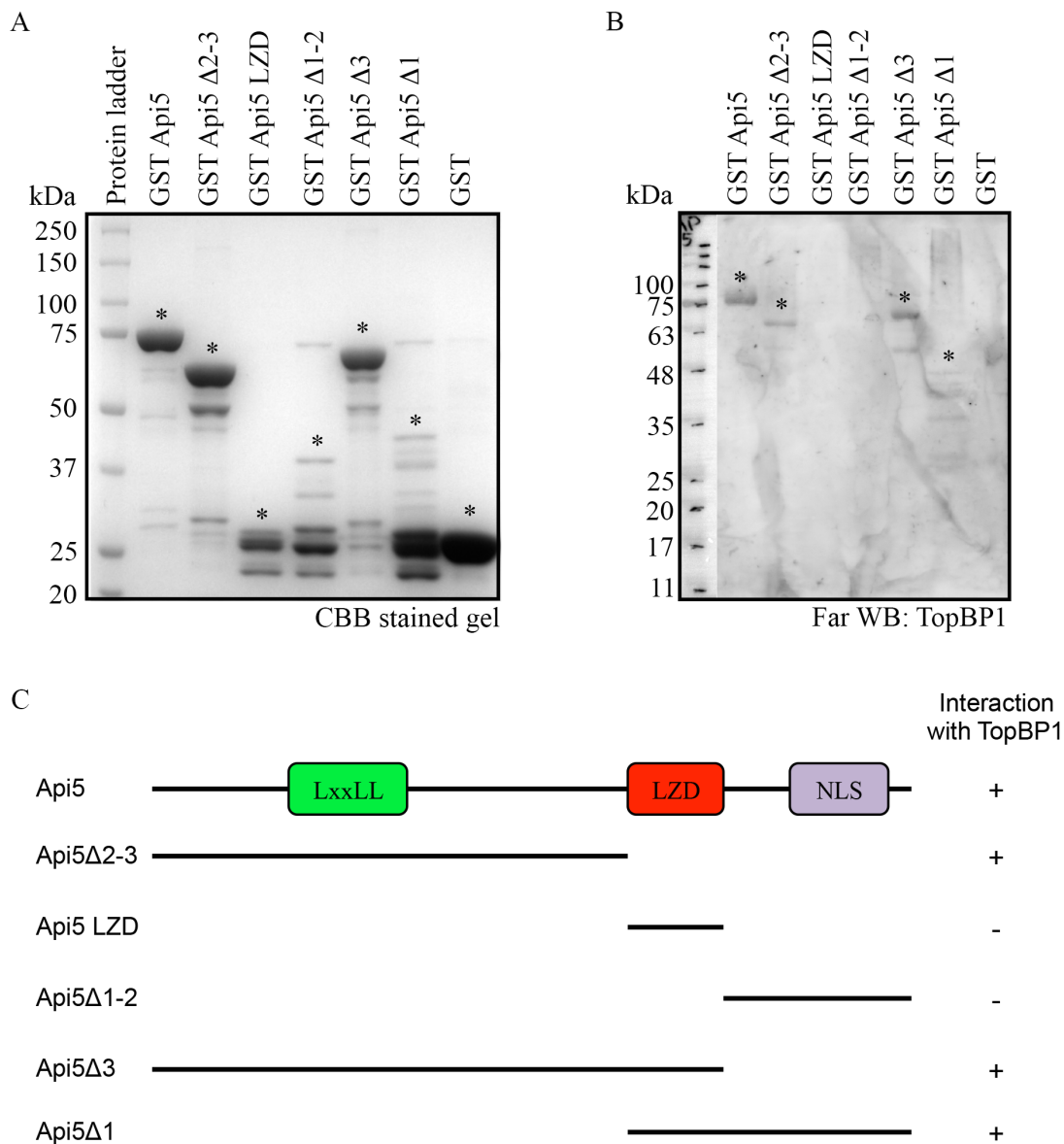
Figure 3.2.2.4: Mapping of region(s) of Api5 that interact with TopBP1.
(A) 1µg each of GST Api5 (88kDa), GST Api5 Δ2-3 (68kDa), GST Api5 LZD (31 kDa), GST Api5 Δ1-2 (42 kDa), GST Api5 Δ3 (72 kDa), GST Api5 Δ1 (46 kDa) and GST (28kDa) run on a 10% SDS-PAGE and visualized after CBB staining. The protein bands are marked with asterisks. (B) Far-western blot having the same loading as in (A) as prey proteins, and incubated with GST TopBP1 as bait protein and probed with TopBP1 antibody. Bands corresponding to the expected size of prey proteins that show an interaction with GST TopBP1 show the chemiluminescence signal. (C) Schematic highlighting the observations from (B).

GST did not show an interaction with GST TopBP1 ruling out the chance of interactions via GST-GST oligomerization happening under the experimental conditions used here (Fig 3.2.2.4 B). Of the Api5 deletion mutants, Δ2-3, Δ3, and Δ1 showed the interaction with TopBP1, whereas LZD and Δ1-2 did not. Analysis of this interaction profile revealed the region(s) of Api5 involved in/sufficient for interaction with TopBP1. Δ2-3 as well as Δ3 showed an interaction meaning that the region of Api5 from its N-terminal till the beginning of LZD is sufficient for interacting with TopBP1. Interestingly, that is also the region, which contains the LxxLL motif. LZD or the region beyond LZD to the C-terminal (Δ1-2) did not show interaction with TopBP1 separately indicating that these two regions were not self-sufficient of showing the interaction with TopBP1. However, when both of these regions came together as in Δ1, they made the resultant protein competent of interacting with TopBP1. So it can be concluded that the N-terminal region of Api5 is sufficient for interacting with TopBP1, while LZD and C-terminal by themselves are not. However, the LZD and C-terminal together are involved in interacting with TopBP1.

3.2.2.5 Overexpression and purification of GST TopBP1 and its deletion constructs

As mentioned in section 3.2.1, the other dimension of addressing the question of elucidating the region(s)/domain(s) of Api5 and TopBP1 involved in interaction with each other was to map the regions of TopBP1 that interact with Api5 biochemically. As has been mentioned earlier, TopBP1 protein is composed of 9 BRCT domains and an ATR activation domain (AAD) between BRCT 6 and 7. A set of truncation mutants of TopBP1 present in the lab were used that contained progressive deletions of BRCT domains (Figure 3.2.2.5A):

i)   BRCT Δ1-2: TopBP1 without BRCT domains 0,1 and 2

ii)   BRCT Δ1-3: TopBP1 without BRCT domains 0,1,2 and 3

iii)   BRCT Δ1-5: TopBP1 without BRCT domains 0,1,2,3,4 and 5

iv)   BRCT Δ1-6: TopBP1 without BRCT domains 0,1,2,3,4,5 and 6

v)   BRCT Δ7-8: TopBP1 without domains 7 and 8

vi)   AAD: TopBP1 with only AAD and without any BRCT domains

vii)   BRCT 7-8: TopBP1 with only BRCT 7 & 8 and without BRCT 0,1,2,3,4,5,6 and AAD

BRCT Δ1-2, BRCT Δ1-3, BRCT Δ1-5, BRCT Δ1-6, BRCT Δ7-8 and AAD cloned into pGEX 2Tkcs bacterial expression vector constructs were kind gifts from Prof Lee Zou, MGH Cancer Center, USA. BRCT 7-8 pGEX 2Tkcs construct was prepared in the lab by PCR amplifying BRCT 7-8 region from the full-length TopBP1 template using TopBP1 BRCT7-8 pGEX-2Tkcs For (Sigma) & TopBP1 pGEX-2Tkcs Rev (Sigma) primer pair and cloning it between BamHI and EcoRI sites of pGEX 2Tkcs vector.

BRCT deletion constructs cloned in pGEX 2Tkcs as mentioned in Fig 3.2.2.5A were used to express GST fusion TopBP1 BRCT truncation mutant proteins. The constructs were transformed into *E. coli* BL21 DE3 bacterial cells and the cultured. Exogenous protein expression was induced with IPTG, the cells were lysed by sonication and the GST-tagged overexpressed proteins were purified from the bacterial lysate by affinity purification using GST agarose affinity beads. Each of the purified GST TopBP1 BRCT deletion mutant protein along with several samples collected during the different steps of protein expression and purification was run on 10% SDS-PAGE, stained with CBB and visualized (Fig 3.2.2.5 B,C, D, E, F, G).

A

		cDNA kB	protein kDa	+GST kDa
TopBP1	0 I II III IV V VI VII VIII	4308	165	193
BRCTΔ1-2		3756	139	167
BRCTΔ1-3		3276	121	149
BRCTΔ1-5		2394	89	117
BRCTΔ1-6		1635	60	88
BRCTΔ7-8		3777	140	168
AAD		924	36	64
BRCT 7-8		792	30	58
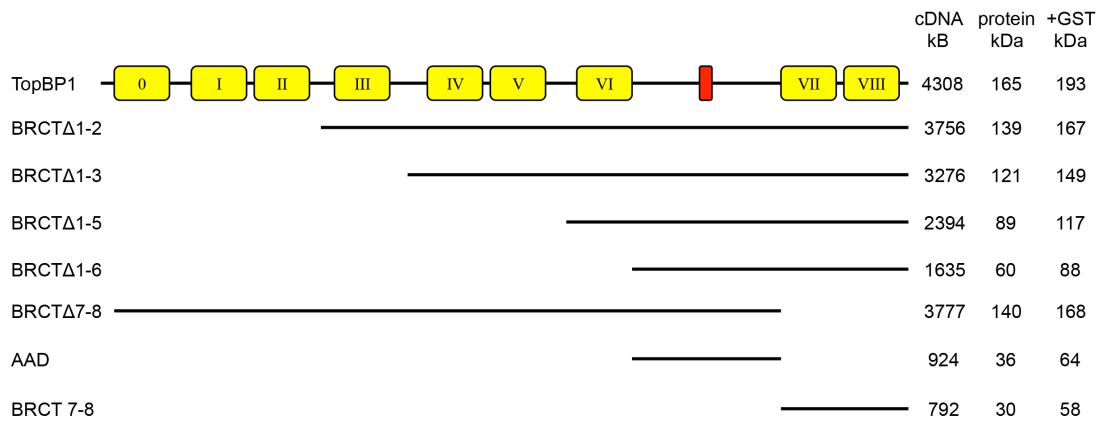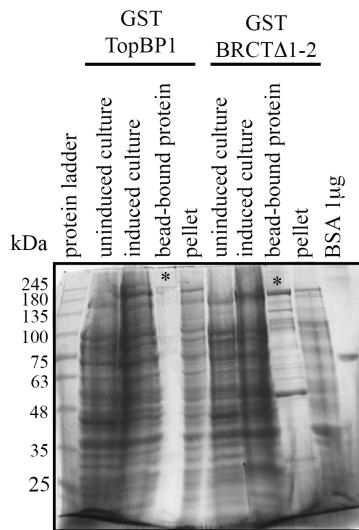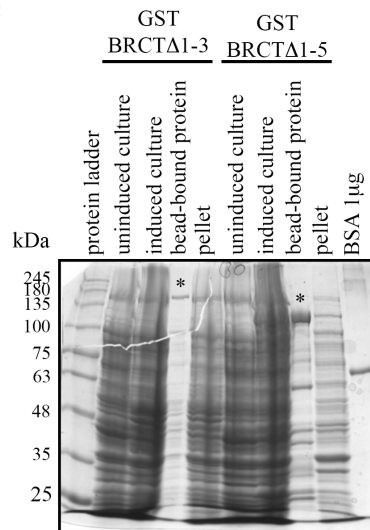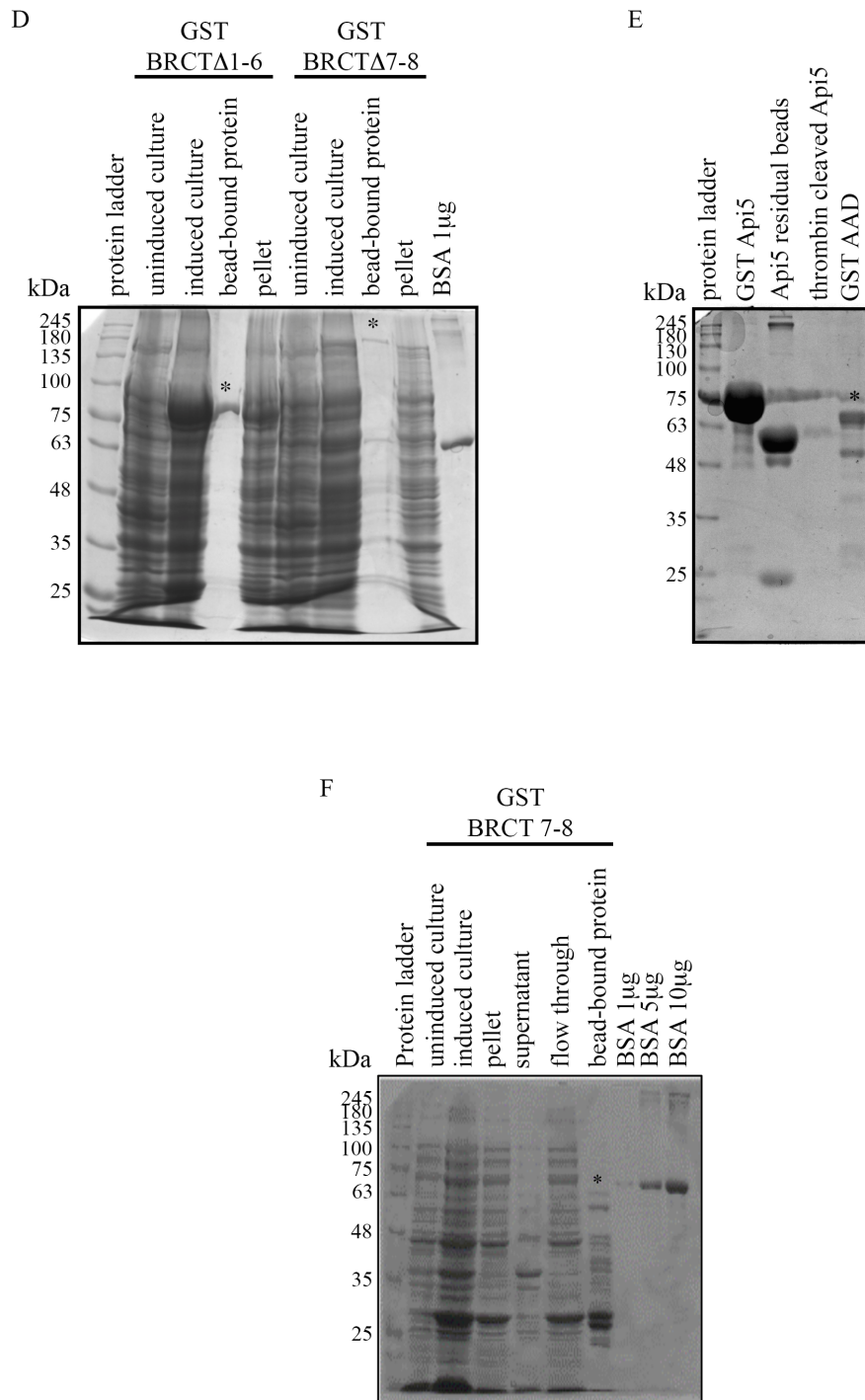
Figure 3.2.2.5: Overexpression and purification of GST fusion deletion constructs of TopBP1.

(A) Schematic of TopBP1 showing its domain organization and the BRCT deletion constructs, showing each of their cDNA lengths, molecular weight of proteins coded by each one of them as well as that of their GST fusion proteins. B, C, D, E, F: samples for protein purification of different GST TopBP1 BRCT truncation mutants

were run on 10% SDS-PAGE, stained with CBB and visualized. (B) Lanes 1-5: ladder, uninduced culture, induced culture, bead-bound protein (marked at 193kDa), and sonicated pellet of GST TopBP1 protein preparation, Lanes 6-9: uninduced culture, induced culture, bead-bound protein (marked at 167 kDa), sonicated pellet of GST BRCT Δ1-2 protein preparation., Lane 10: 1μg BSA. (C) Lanes 1-5: ladder, uninduced culture, induced culture, bead-bound protein (marked at 149kDa), and sonicated pellet of GST BRCT Δ1-3 protein preparation, Lanes 6-9: uninduced culture, induced culture, bead-bound protein (marked at 117 kDa), sonicated pellet of GST BRCT Δ1-5 protein preparation., Lane 10: 1μg BSA. (D) Lanes 1-5: ladder, uninduced culture, induced culture, bead-bound protein (marked at 88kDa), and sonicated pellet of GST BRCT Δ1-6 protein preparation, Lanes 6-9: uninduced culture, induced culture, bead-bound protein (marked at 168 kDa), sonicated pellet of GST BRCT Δ7-8 protein preparation., Lane 10: 1μg BSA. (E) Lane 1: protein ladder, Lane 4: purified bead-bound GST AAD protein marked with asterisk at its expected size of 64kDa. (F) protein preparation samples for GST BRCT 7-8: Ladder, uninduced culture, induced culture, sonicated pellet, sonicated supernatant, flow through, bead-bound protein marked at it expected size of 58 kDa, followed by 1μg, 5μg and 10μg of BSA as quantity standard.

3.2.2.6 Mapping the domains of TopBP1 required for it's *in vitro* interaction with Api5

The additive truncation of BRCT domains to create the several GST TopBP1 deletion mutant constructs allowed us to map the domains of TopBP1 required for its direct biochemical interaction with Api5. Since Thrombin cleavage of GST Api5 protein eluted abundant amounts of Api5 protein (as discussed earlier), Api5 protein without the GST tag was used as bait protein. This saved the trouble of ruling out PPI happening because of GST oligomerization between bait and prey proteins. The GST fusion BRCT deletion constructs were used as prey protein. GST and BSA were kept as negative controls. The GST and thrombin eluted proteins were quantified by comparing the visual estimation of density of the band at expected size with that of known quantity of BSA. 1μg each of the GST TopBP1, GST BRCT Δ1-2, GST BRCT Δ1-3, GST BRCT Δ1-5, GST BRCT Δ1-6, GST BRCT Δ7-8 and GST AAD pray proteins, as well as GST and BSA negative controls, were run on 10% SDS-PAGE, stained with CBB and visualized (Fig 3.2.2.6 A). Another gel was run in the parallel with the same loading, transferred to PVDF membrane, and subjected to denaturation and renaturation using serial dilutions of guanidinium hydrochloride. The renatured proteins immobilized on the blot were incubated with Api5 protein in a suitable Protein binding buffer at a concentration of 1μg/ml. The blot was now probed with Api5 antibody (Abnova PAB7951) at a dilution of 1:2500. Chemiluminescence signal at the expected size of prey proteins was scored to figure out the constructs that showed an interaction (Fig 3.2.2.6 B). 1μg GST BRCT 7-8 construct was separately run on a gel along with a positive control GST TopBP1 and a negative control GST, the proteins were transferred to PVDF membrane and stained with Ponceau S to reveal the prey protein profile (Fig 3.2.2.6 C). The blot was now washed thoroughly and subject to the same far western blotting routine as for rest of the BRCT deletion mutants earlier (Fig 3.2.6 D).

Far western blotting results with TopBP1 BRCT truncation mutants (Fig 3.2.6 E) showed that the mutants BRCT Δ1-2, BRCT Δ1-3, BRCT Δ1-5 and BRCT Δ1-6, all of whom contained BRCT 7 and BRCT 8 showed an interaction with Api5 whereas, the mutants like BRCT Δ7-8 and AAD, which had other domains except for BRCT 7 and BRCT 8, did not interact with Api5. This led to the conclusion that BRCT 7 and 8 are required for interaction with Api5. However, the interaction between BRCT 7-8

71

construct with Api5, which only had BRCT7 and BRCT8, made it clear that BRCT7 and 8 are required and sufficient for the interaction of TopBP1 protein with Api5.

A — CBB stained gel

B — Far WB: Api5

C — Ponceau S stained blot

D — Far WB: Api5

E

	Interaction with Api5
TopBP1	+
BRCTΔ1-2	+
BRCTΔ1-3	+
BRCTΔ1-5	+
BRCTΔ1-6	+
BRCTΔ7-8	-
AAD	-
BRCT 7-8	+
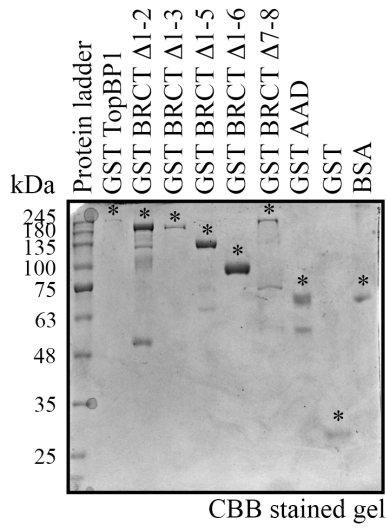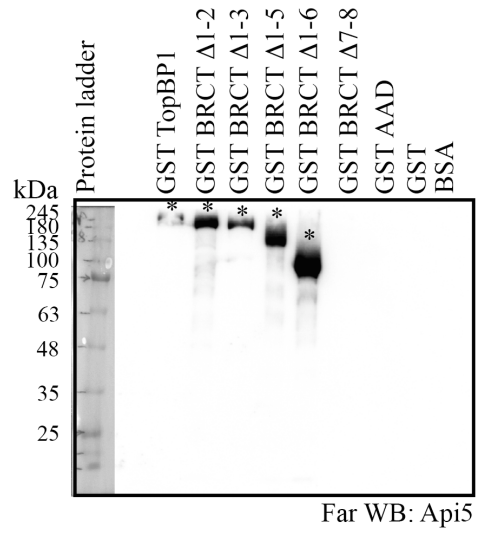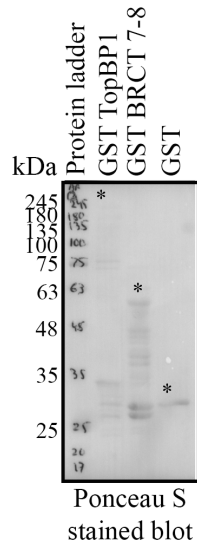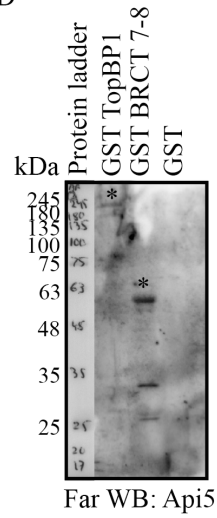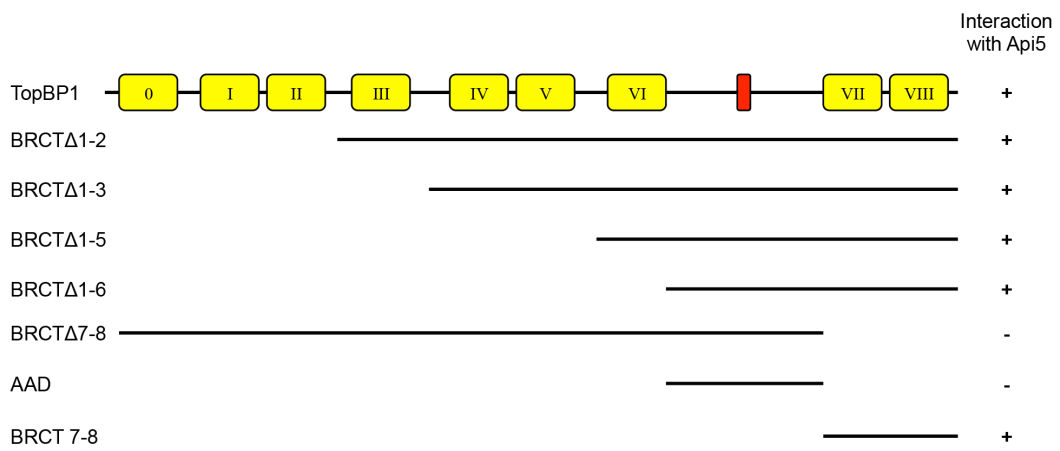
Figure 3.2.2.6: Mapping the domains of TopBP1 required for it's *in vitro* interaction with Api5.

(A) 1μg each of indicated "prey" proteins were run on 10% SDS-PAGE, stained with CBB and visualized. (B) 1μg each of indicated "prey" protein were run on gel, transferred to PVDF membrane, subjected to far western blotting using Api5 as "bait" protein and probed with Api5 antibody, proteins showing an interaction are marked with asterisk. (C) 1μg of indicated "prey" proteins were run on 10% SDS-PAGE, transferred to PVDF membrane and stained with Ponceau S (D) the blot in (C) was subjected to far western blotting using Api5 as "bait" protein and probing with Api5 antibody, proteins showing interaction are marked with asterisk (E) schematic concluding the results of far western blotting showing the interaction status of TopBP1 BRCT deletion constructs with Api5.

3.3 Discussion

Out of the several PPI validation strategies available, affinity purification of tagged proteins was chosen because this was a standardized and robust way of testing the biochemical ability of two proteins of interest to interact directly with each other in a cell-free system without the influence of any other scaffolding or catalyzing protein in the milieu. However, the protein preparations performed didn't yield high-grade purity of the tagged proteins. This led us to consider far western blotting as a method of choice for studying the interaction between "bait" and "prey" proteins as this involved separation and immobilization of protein preparation on a solid support, thus enabling distinction between true interaction readout and false positives emanating from nonspecific proteins at unexpected sizes. However, a major drawback of the technique is that it involves strong denaturation and renaturation of the protein while immobilized on solid support (PVDF membrane). Proteins sometimes may not refold properly after being denatured with a strong denaturant (like guanidinium hydrochloride). This concern was however addressed while standardizing the far western protocol. Control experiment was performed with GFP protein immobilized on the membrane: loss of fluorescence was observed after denaturation and reappearance of fluorescence was considered as a read out for proper renaturation (data not shown). This however only partially addresses the concern because different proteins may show different refolding kinetics.

Human TopBP1 has 9 BRCT domains with BRCT 1 and 2, 4 and 5, 7 and 8 forming pairs while BRCT 3 and BRCT 9 being "singletons". Of the three BRCT pairs, only BRCT 7 and 8 display a canonical arrangement (Wardlaw et al., 2014). Under such arrangement, the first BRCT domain of the pair facilitates binding to phosphoproteins whereas the second BRCT provides sequence specificity. TopBP1 was shown to interact with Api5 through its BRCT 7 and 8 domain. Api5 is not known to exhibit any phosphorylation as yet. So it will be interesting to look for phosphorylation of Api5 owing to our finding

BRCT 7 and 8 of TopBP1 is known to have several interacting partners. TopBP1 is known to interact with important tumor suppressor p53 through BRCT 7 and 8 and thus repress p53 mediated apoptosis induction in response to DNA damage (Liu et al., 2009b). It will be interesting to investigate any parallels between the anti-apoptosis

role of Api5 and that of p53 in response to DNA damage, mediated by their interaction with the same domains of TopBP1.

Api5 is also known to have several interactors. FGF2 interacts with Api5 through the LxLL motif and another region in its N-terminal (Berghe et al., 2000). The N-terminal region of Api5 was observed to be sufficient for interaction with TopBP1, though the C-terminal together with LZD were also able to interact with TopBP1. The crystal structure of Api5 indicates that it has almost consistent positive and negative charge properties along its length on the two opposite concave and convex surfaces respectively (Han et al., 2012a). This could be the reason why large portions of the protein towards N-terminal as well as C-terminal showed binding potential towards TopBP1.

In vitro interaction study revealed the region(s) of both Api5 and TopBP1 involved in the interaction. But it did not give any information about the dynamic state of their association/dissociation *in vivo* and how does that change in response to external stimuli like DNA damage. So, Api5- TopBP1 interaction needed to be further investigated *in vivo* to reveal its physiological relevance.

3.4 Summary

Full length and truncation mutant constructs of Api5 and TopBP1 were prepared in bacterial expression pGEX 2Tkcs vector. The constructs were transformed into *E Coli* BL21 DE3 bacteria and grown in a culture. Exogenous protein expression was induced by IPTG. The overexpressed proteins were purified by using affinity purification using GST-agarose beads. The GST affinity tag of full-length GST Api5 protein was removed by thrombin cleavage. Reciprocal far western blotting was performed to validate the interaction *in vitro,* as well as to elucidate the interacting domain(s)/region(s). Full-length Api5 and its truncation mutants were used as "prey" along with full-length TopBP1 as "bait" protein. Reciprocally, full-length TopBP1 and its truncation mutants were used as "prey" together with Api5 as "bait" protein. The reciprocal far western revealed that Api5 shows direct biochemical interaction with TopBP1. BRCT 7-8 of TopBP1, N-terminal portion as well as LZD+C terminal portion of Api5 were responsible for this interaction. While *in vitro* interaction study validated the interaction and revealed the interacting regions as well, it didn't tell about the physiological standing and relevance of this interaction. So this interaction study needed to be performed *in vivo* in response to DNA damage.

Chapter 4: *In vivo* interaction studies between Api5 and TopBP1

4.1 Background

Protein-protein interactions (PPIs) form the basis of cellular signaling and function. As discussed in the previous chapter several approaches are available for identifying and validating novel PPIs. Whereas *in vitro* approaches like far western blotting or pull-down of affinity purified tagged proteins can validate a direct physical interaction, it does not address the question of its physiological relevance.

PPIs inside cells are regulated by several mechanisms. Apart from the biochemical considerations of the proteins involved, it also depends upon factors such as post-translational modifications (PTMs) and subcellular localization (SCL) at a given space and time, presence or absence of certain stimuli that govern them, all of which, together make the physiological conditions under which PPIs happen inside the cell (Berggård et al., 2007). *In vitro* interaction studies address the role of biochemical and biophysical factors like surface properties of the interacting proteins of interest, they do not address the physiological considerations of PTMs, SCLs, presence of other proteins in the milieu potentially posing a competitive kinetics for PPIs.

PTMs like phosphorylation, acetylation, SUMOylation, ubiquitination among others, are often employed by regulatory proteins as means of increasing or decreasing their affinity toward the target protein. PTMs hence, function as molecular switches to turn on or off or shuffle or intercross certain signaling pathways in response to different stimuli (Jensen; Karve and Cheema, 2011; Mann and Jensen, 2003; Spektor and Rice, 2009; Walsh et al., 2005). These signaling pathways function on the basis of dynamic protein interactions between a couple of proteins or in big protein complexes around a central scaffold protein. These scaffold proteins themselves can be subject to PTMs. TopBP1, for example, is a central scaffold protein in the checkpoint pathway that undergoes phosphorylation and can regulate several functions: DNA replication, cell cycle checkpoints and DNA damage response by virtue of its interaction with different proteins under different conditions (Garcia et al., 2005; Wardlaw et al., 2014). Api5 is also known to undergo acetylation (Choudhary et al., 2012; Han et al., 2012b). Studying their interaction *in vivo* takes into consideration their putative PTMs that can be of different kinds under physiological versus pathological conditions, which in turn can be an effect of presence or absence of relevant stimuli (Westermarck et al., 2013).

In vivo interaction can be investigated by a number of approaches. There are methods like two-hybrid (yeast or mammalian), split protein complementation, fluorescence resonance energy transfer (FRET), surface plasmon resonance (SPR), co-immuno-precipitation, to name a few (Berggård et al., 2007; Chen; Chen et al., 2008; Miernyk and Thelen, 2008; Phizicky and Fields, 1995; Piehler, 2005; Westermarck et al., 2013; Xing et al., 2016). Most of the *in vivo* studies require the introduction of tagged proteins of interest and then detecting/monitoring it in a live system, the presence of tag might potentially hinder with the normal function/interaction/localization of the protein (Berggård et al., 2007). This drawback, however, does not perturb co-IP because it can be performed using antibodies specific to endogenous proteins. Co-IP can be considered a chimera of *in vitro* and *in vivo,* because while the interaction is detected *in vitro* using the cell lysate, the interaction itself is allowed to happen *in vivo* inside live cells under physiological conditions (Xing et al., 2016).

Since the basis of this interaction study was a pull-down screen in the presence or absence of DNA damage, it is imperative that we use DNA damaging agent as the stimulus to activate DNA damage response (DDR) pathways just at the sub-apoptotic levels and then investigate the state of interaction between TopBP1 and Api5 in comparison to that without damage so as to investigate their physical binding as a basis of their function in the possible interplay between DDR and apoptosis pathways. Camptothecin (CPT) was chosen as the DNA damaging drug because of its lethality caused by the formation of a combination of single-strand break (SSB) and double strand break (DSB) and ensuing ability to induce apoptosis even at low doses (explained below).

Camptothecin is a plant alkaloid isolated from the Chinese plant *Camptotheca acuminata.* It was shown to have anti-leukemic and anti-tumor activities in animals making it suitable to be used for chemotherapeutic purposes (Janmuarv; M.E.Wall, Wani, C.E. Cook, K.H. Palmer, A.T. McPhail, 1966). CPT has a novel ring structure and exists in inter-convertible lactone (active) and carboxylate (inactive) forms (Hsiang et al., 1985; M.E.Wall, Wani, C.E. Cook, K.H. Palmer, A.T. McPhail, 1966; Pommier, 2009) (Fig 4.1A). The anti-tumor activity of CPT is a manifestation of its TopoisomeraseI (TopI) poison function.

A

B

Step I — TopIcc formation and strand swiveling

Step II — TopIcc stabilization and formation of transient SSB

Step III — Fork collision and formation of permanent DSB
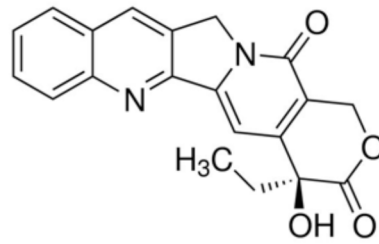
■ : CPT   ● : Topoisomerase I
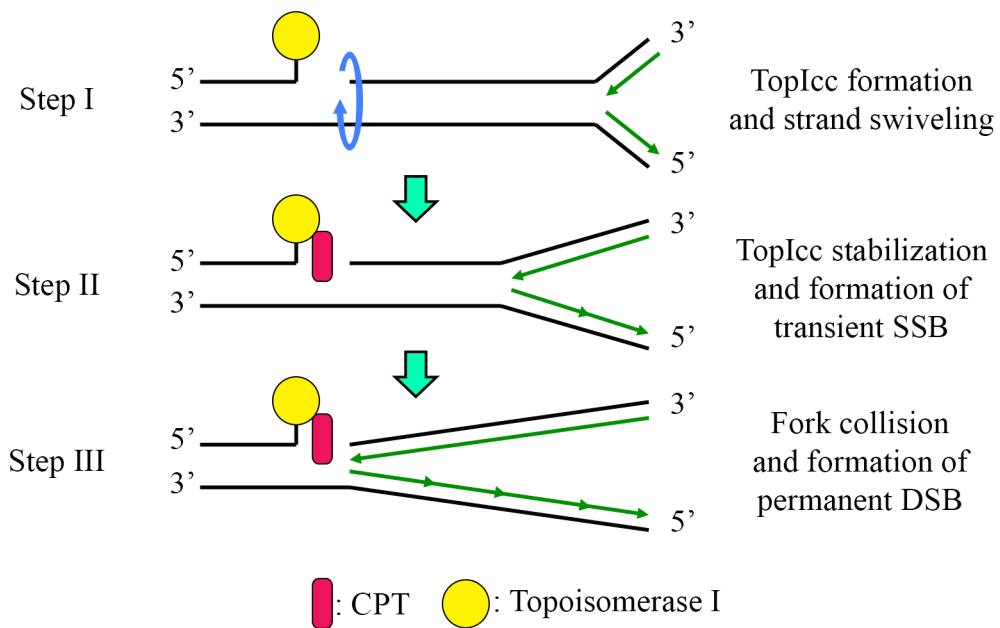
Figure 4.1: Mechanism of the function of Camptothecin.

(A) Chemical structure of CPT representing the Lactone (active) form. (B) Mechanism of SSB and DSB formation by CPT illustrated by fork collision model. CPT: Camptothecin, TopIcc: Topoisomerase I cleavable complex, SSB: single strand break, DSB: double strand break

DNA replication or transcription requires opening up of the chromatin and formation of replication/transcription bubble. This creates a positive/negative supercoil in the DNA helix on either side of bubble leading to torsional strain that needs to be relieved. This torsional strain is relieved by Topoisomerases: humans having Topoisomerase I (TopI) and Topoisomerase II (TopII) (Pommier, 2009; Ryan et al., 1991). TopI does its function by nicking and resealing one of the strands of DNA. TopI carries out a nucleophilic attack on the sugar-phosphate backbone of one of the strands of DNA through its catalytic tyrosine residue so as to break the phosphodiester bond and form a covalent bond with the 3' end of the broken DNA strand (Parchment and Pessina, 1998). This is a transient structure and is called Topoisomerase I-DNA cleavable complex (TopIcc) (Pommier, 2009; Rothenberg, 1997). The TopIcc formation is followed by swiveling of the other 5'-OH end of broken DNA around the complimentary intact strand of DNA leading to the release of torsional strain (Fig 4.1B StepI) (Koster et al., 2005). TopI now re-ligates the two broken ends restoring the double-stranded structure of DNA and coming out of the TopIcc.

CPT, however, interferes with the TopI function resulting in temporary single strand breaks (SSB) and permanent double strand breaks (DSB). The mechanism of DNA damage caused by CPT is best explained by "Fork collision model" (Pommier, 2009; Rothenberg, 1997). CPT binds to the TopIcc and stabilizes it. This inhibits the religation step leading to the formation of SSBs (Fig 4.1B StepII) (Hsiang et al., 1985). This SSB is, however, short-lived as it gets converted into permanent DSB as soon as the leading strand of the moving replication fork collides with the CPT stabilized TopIcc (Fig 4.1B StepIII) (Hsiang et al., 1989; Ryan et al., 1991). This leads to fork collapse, which is highly toxic and this leads to cell death by apoptosis (Bino et al., 1992; Morris, 1996), or necrosis if the dose of CPT is higher (Mirakabadi et al., 2012). Because of the ability of CPT to induce apoptosis even at the comparatively low dosage, it is a drug of choice for studying DNA damage-induced apoptosis pathways. CPT is cell cycle specific DNA damage causing agent and it induces DSBs and the resultant apoptosis at S phase of the cell cycle when DNA replication is happening (Hsiang et al., 1989; Johnson et al., 1997; Ryan et al., 1991), so treatment with CPT generally involves long incubation times for asynchronous

cultures as most of the cells in that population are in G1 phase at any given time and they have to move to S phase to acquire the permanent DSBs.

4.2 Results

4.2.1 10μM CPT induces apoptosis in HeLa Cells

CPT is a potent drug that is commonly used when studying DNA damage-induced apoptosis pathways. CPT is capable of inducing apoptosis as well as necrosis at lower and higher dosages respectively. The first step towards using CPT for current studies is determining the dosage that is just sufficient to induce apoptosis and is not as high so as to induce cell death by necrosis. This is critical because Api5 is an anti-apoptotic protein and is supposed to carry out its function at the threshold of induction of apoptosis by DNA damage and not when that threshold has been breached and necrosis has set in as a result of excessive DNA damage.

Conventional methods of measurement of cytotoxicity of a drug like Trypan blue dye exclusion or MTT assay work on the principle of their ability to differentiate between live versus dead cells. These can't differentiate between apoptotic versus necrotic cells within the population of "dead" cells. Hence AnnexinV-Propidium iodide staining followed by flow sorting of cells was performed as this technique can differentiate between apoptotic versus necrotic cells.

HeLa cells were chosen for performing IP experiments because the initial GST TopBP1 pull-down that identified Api5 as a novel interactor was performed with HeLa nuclear extracts. HeLa cells were treated with 0, 1, 2.5, 5, 7.5, 10, 12.5, 15, 17.5 and 20 μM of CPT for 16 hours, harvested, stained with AnnexinV-PI and analyzed by flow cytometry within 10 minutes. Cells that were AnnexinV-PI negative were scored as live, AnnexinV positive and PI negative cells were scored as apoptotic while both AnnexinV-PI cells were scored as necrotic (Fig 4.2.1A,B). Increasing dosage of CPT was observed to induce gradually increasing the extent of apoptosis and necrosis (Fig 4.2.1C). 10μM CPT for 16 hours was chosen as the dose of damage to be used for IP experiments since this dose was just able to induce apoptosis while keeping the extent of necrosis quite low.
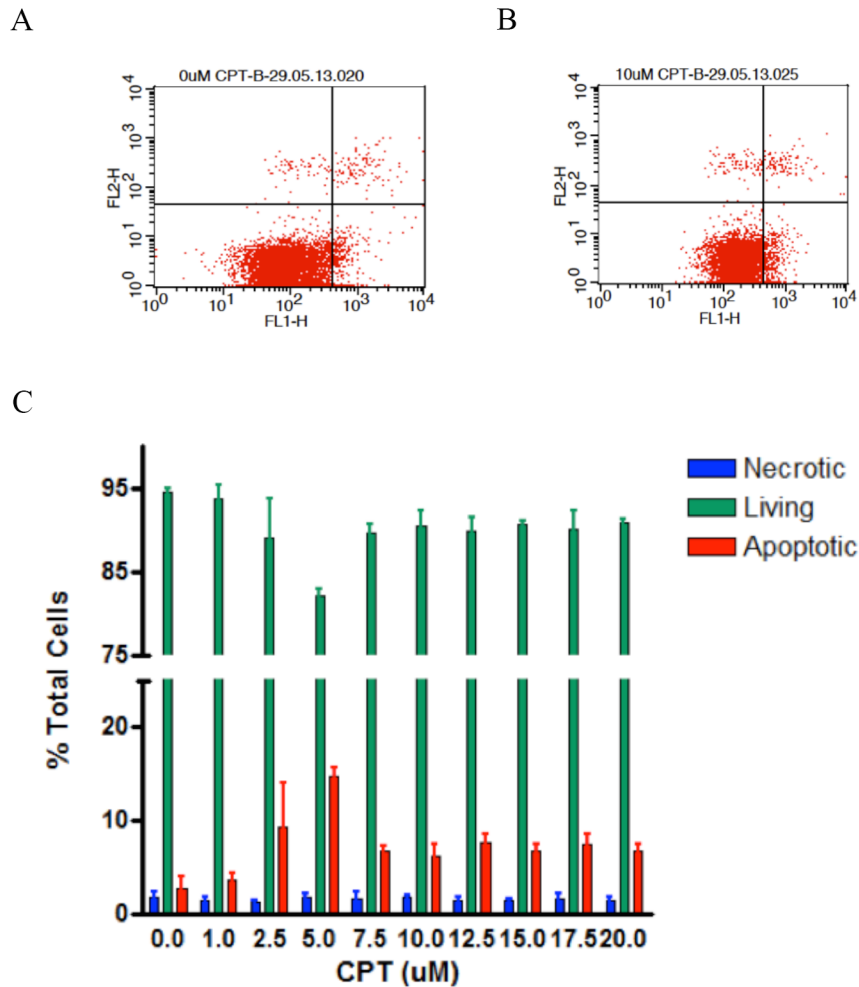
Figure 4.2.1: CPT dosage determination by Annexin V-PI staining and FACS.

(A, B): Scatter plot showing FACS profile of cells treated without and with CPT respectively. FL1-H (X-axis) represents fluorescence of AnnexinV. FL2-H (Y-axis) represents PI fluorescence, lower left quadrant shows live cell population, lower right quadrant shows apoptotic cells, upper right quadrant shows necrotic cell population. (C) Graph showing the distribution of necrotic, live and apoptotic cells as a percentage of the total cell population. Experiments were carried in biological triplicates (N=3) and error bars represent SEM.

4.2.2 Api5 and TopBP1 interact *in vivo* and this interaction shows an increase upon CPT-induced DNA damage

Immunoprecipitation (IP) was performed on HeLa cell lysates to check the Api5-TopBP1 interaction *in vivo*. HeLa cells were grown on 60mm dishes, incubated with or without CPT for 16 hours, lysed in TNN buffer and pre-cleared with suitable IgG. Api5 was immunoprecipitated with 1μg of anti Api5 antibody (Abnova PAB7951). IgG IP control samples were pulled down with an equal amount of anti-rabbit IgG antibody (Bethyl P120-201). The IP along with their respective "Input" samples were separated on a 10% PAGE and subjected to western blotting. The blot was cut according to the expected size of TopBP1 and Api5 and probed with anti TopBP1 (Bethyl A300-111A) at a dilution of 1:5000 and anti Api5 (Abnova PAB7951) at a dilution of 1:2500.

TopBP1 was observed to have co-immunoprecipitated with Api5 immunoprecipitate (Fig 4.2.2A) without or with CPT-induced DNA damage. Image J based densitometric quantification of biological triplicates indicated that TopBP1 showed an increased interaction with Api5 upon 16 hours of CPT-induced DNA damage (Fig 4.2.2B).

 The interaction was also observed after 4, 8 and 12 hours of CPT damage (data not shown). Reverse IP was also performed. Api5 was observed to co-immunoprecipitate with TopBP1 immunoprecipitates with or without CPT damage (data not shown).

This result proved that Api5 and TopBP1 interacted *in vivo* inside the cells, indicating towards a possible physiological significance. The physiological relevance of Api5 and TopBP1 interaction was exemplified by its ability to show an increase upon DNA damage.

A

B
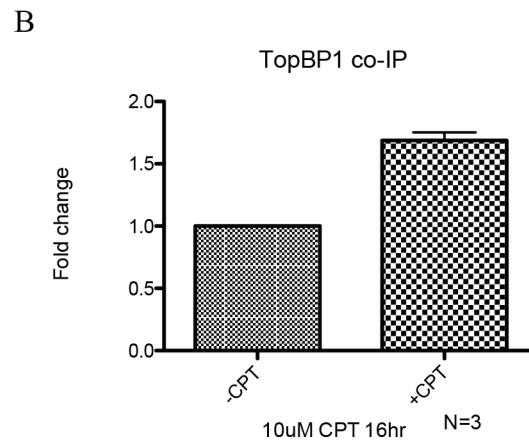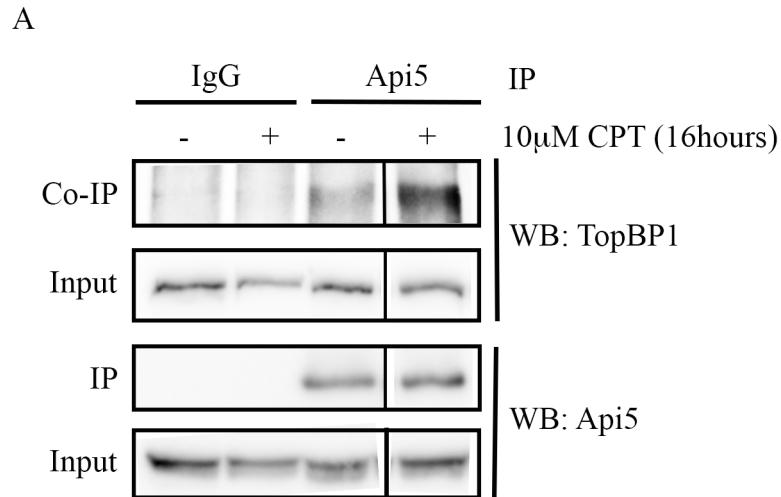
Figure 4.2.2: TopBP1 interacts with Api5 *in vivo.*

(A) Lanes1-2: IgG IP samples treated without and with 10μM CPT for 16 hours, Lanes 3-4: Api5 IP samples treated without and with 10μM CPT for 16 hours. Box1-2: Co-IP and corresponding 5% Input samples probed for TopBP1. IgG and Api5 IP (Box3) and corresponding 5% input samples (Box4) probed for Api5. (B) Fold increase in TopBP1 co-IP upon CPT treatment, calculated after normalizing TopBP1 co-IP western blot densitometric quantification with that of corresponding TopBP1 inputs and averaged across three biological replicates (N=3).

4.3 Discussion

We were able to show an interaction between Api5 and TopBP1 *in vivo* and also that it increases upon DNA damage. This was achieved by antibody affinity-based purification of Api5 bound protein complex. Such affinity based purification can have a strong bias towards detecting the protein interactions that exhibit high binding affinity and slow dissociation kinetics (Berggård et al., 2007). Weak and transient protein interactions can escape detection by this method, more so if stringent washing conditions are used (Phizicky and Fields, 1995). Detecting protein interactions by co-IP require preservation of pre-formed protein complexes within the cells as a result of the physiological process even after cell lysis. Such maintenance requires a delicate balance of salts and detergents to maintain the protein concentration and pre-formed complexes at a configuration closest possible to that in the cell. These conditions were met after a lot of standardizations of salt, detergent and electrolyte concentrations.

The difference in the binding states of TopBP1 and Api5 upon DNA damage may indicate a possible role of this interaction in the signaling triggered upon DNA damage that connects checkpoint and apoptosis pathways.

In vivo interaction study using whole cell lysates only prove the interaction but it doesn't give any information about the cellular sub-compartment where the interaction happens. Since both TopBP1 and Api5 are known nuclear proteins, it is further interesting to investigate whether the interaction happens on chromatin or elsewhere in the nucleus. TopBP1 is known as chromatin binding protein which forms foci at sites of DNA damage, whereas Api5 is not known to be having that attribute, so it is imperative to first find out whether Api5 protein can bind to DNA and then further investigate whether their interaction happens at such sites of TopBP1 foci.

4.4 Summary

To summarize, a suitable concentration of the Topoisomerase I poison CPT was determined by AnnexinV-PI staining and FACS that is just sufficient to induce apoptosis in HeLa cells. This concentration of CPT was used as a source of DNA damage for conducting *in vivo* interaction studies. Co-IP was employed to prove the interaction between Api5 and TopBP1 in mammalian cells, which showed an increase upon CPT-induced DNA damage. This indicated towards a possible role of this interaction at the interface between checkpoint and apoptosis pathways. Since this experiment was carried out using whole cell lysates, it did not shed any light upon the sub-cellular compartment where this interaction might happen. Given the foci formation capability of TopBP1 upon DNA damage, and increased interaction of Api5 with TopBP1 following damage, it is imperative to determine whether Api5 co-localizes at such sites.

Chapter 5: Api5 DNA binding, foci formation, and TopBP1 foci co-localization studies

5.1 Background

DNA damage triggers DDR. This leads to the formation of cytologically discernible nuclear "foci" that firstly are formed by the accumulation of certain DDR proteins at sites of lesion that can, later on, spread up to several megabases along the chromatin from the site of damage (Kollenstart, 2009). These foci can be visualized by methods of microscopy after either IF staining of fixed cells or tracking them in real-time using fluorescently tagged proteins and live-cell imaging (Rothkamm et al., 2015; Jensen, 2013). DDR foci follow a tight spatiotemporal regulation. DSB, for example, are populated by γH2AX within seconds after damage and can remain there for hours together till the lesion is repaired (Francisco and Francisco, 2008; Huang et al., 2004; Turinetto and Giachino, 2015).

Some DDR proteins can assemble at such foci owing to their ability to recognize the lesion directly. The sensor and mediator proteins of checkpoint signaling pathway like γH2AX, MRN complex, 9-1-1 complex, RPA, 53BP1, TopBP1 are examples,which comprise the upstream players of DDR pathway. Alternatively, some DDR proteins are assembled at such foci through protein-protein interactions with proteins of the first category. Most downstream proteins of the DDR pathway are recruited in such way, for example, checkpoint-signaling apical kinases ATR and ATM, or repair proteins like Rad51, Ku70/80 among others. The dynamic assembly and disassembly of proteins at foci is often controlled by the state of their PTMs like phosphorylation, ubiquitylation, SUMOylation, methylation, acetylation and PARylation (Polo and Jackson, 2011).

TopBP1 is a chromatin-associated nuclear protein (Garcia et al., 2005). Api5 is a nuclear protein while its chromatin association state is ambiguous and its levels change across the cell cycle peaking at G1 (Arconde et al., 2013). It has an unconventional LZD, which lacks a basic DNA binding domain (Tewari et al., 1997). The IP in our earlier study was performed with whole cell lysates and given the nuclear nature of both the proteins the next logical step is to determine the nature of

the interaction between the proteins within the nucleus in the context of DNA damage.

TopBP1 is a scaffolding checkpoint phosho-protein that has function across several aspects of DNA metabolism and cell function. It has roles in DNA replication, checkpoint signaling mediated DDR, maintenance of stalled replication forks, DNA repair and transcription regulation (Liu et al., 2004; Makiniemi et al., 2001; Morishima et al., 2007; Yamane et al., 2002; Yan and Michael, 2009) TopBP1 is known to form replication as well as DDR foci inside the nucleus (Makiniemi et al., 2001; Yamane and Tsuruo, 1999; Yamane et al., 2002). It's DDR foci are formed in response to DSB caused by IR (Greer et al., 2003; Morishima et al., 2007) as well as SSB caused by HU or UV (Forma et al., 2010; Makiniemi et al., 2001). Though TopBP1 is primarily a mediator in the ATR-Chk1 pathway that gets activated in response to SSB or replication fork stress (Kumagai et al., 2006), it also has a role in activating ATR through its activation by ATM in response to DSB (Yoo et al., 2007; 2009). One of the markers for distinguishing replication vs DDR induced TopBP1 foci is 53BP1. TopBP1 DDR foci are known to co-localize with 53BP1 foci upon DNA damage across all the phases of the cell cycle but peaking at G1 (Cescutti et al., 2010; Rappold et al., 2001; Schultz et al., 2000; Ward et al., 2003).

For studying such DDR foci, damage can be inflicted upon a "global" scale to the whole nucleus by exposing the cells to radiations or DNA damaging drugs. Alternatively, a localized damage can be inflicted by using site-specific nucleases like I-SceI or localized UV laser micro-irradiation after photosensitization with Thymidine homologs like BrdU or DNA intercalating agents like Hoechst (Rastogi et al., 2010; Suzuki et al., 2010, 2011).

However, not all DDR proteins accumulate at DNA lesions in a form that can be visualized under the microscope as foci, for example, NHEJ components, Chk1, Chk2 to name a few (Kollenstart, 2009; Polo and Jackson, 2011). Under such circumstances, another approach of analyzing protein dynamics in response to DNA damage is by comparing their chromatin binding state with or without damage using chromatin/sub-cellular fractionation.

Our previous studies showed that Api5 interacts with TopBP1 in normal asynchronous cells and the interaction increases after damage. Given the formation of TopBP1 replication and DDR foci, it is pertinent to enquire whether the Api5

interaction with TopBP1 happens at the latters DNA foci or elsewhere, whether Api5 forms damage dependent or cell cycle dependent foci at the first place and whether it co-localizes with TopBP1 foci. If at all Api5 is found to form foci, it can further be investigated whether they are formed owing to its ability to bind to DNA by its own or whether its foci formation is dependent upon its protein-protein interaction(s).

DNA-protein interactions can be studied by a number of *in vitro* and *in vivo* methods like nitrocellulose filter binding assay, DNase footprinting assay, Electrophoretic mobility shift assay (EMSA), Chromatin immunoprecipitation (ChIP), DNA adenine methyltransferase identification (DamID), Surface plasmon resonance (SPR), Systematic evolution of ligands by exponential enrichment (SELEX), Yeast one-hybrid system, DNA microarrays, Protein microarrays, Proximity ligation, Atomic force microscopy (AFM), X-ray crystallography, nuclear magnetic resonance among others (Alves and Cunha; Carey et al., 2016; Hellman and Fried, 2009; Helwa and Hoheisel, 2010). Since our study was not aimed at identifying DNA sequence specific binding of Api5 protein, but just limited to investigate it's binding potential to normal DNA and/or intermediate structures non-specifically, EMSA was the method of choice. This was performed in a cell-free system using purified Api5 protein and DNA.

If however, Api5 is not found to form foci altogether, it will still be relevant to investigate its chromatin binding state *in vivo* within the cells. Co-occupation of both the proteins on chromatin and discovery of their interaction under the same conditions of DNA damage might point towards their interaction on the chromatin in a form that is not cytologically discernible as "foci".

CPT was used as a source of "global" DNA damage for reasons discussed in the previous chapter. U2OS osteosarcoma cells were used for the experiment owing to their p53 proficiency given the important role of p53 in apoptosis pathways where Api5 is hypothesized to be functioning (Polager and Ginsberg, 2009). The dosage of CPT was kept at 10μM for 16 hours following the regimen of previous studies of the Api5 function using U2OS cells (Rigou et al., 2009).

5.2 Results

5.2.1 Api5 interacts with DNA *in vitro*

Api5 protein contains a Leucine Zipper Domain (LZD) that lacks a basic DNA binding domain and its DNA binding status is ambiguous. Whereas it can still be bound to the chromatin owing to (any) protein interaction(s), it needs to be investigated whether it can bind to DNA by itself.

This was studied by employing electrophoretic mobility shift assay (EMSA). A non-specific 1.5kB dsDNA fragment probe was incubated with increasing concentrations of bacterially purified and thrombin-cleaved Api5 protein for 20 min at 37°C in a suitable EMSA master mix that contained Tris buffer, KCl, DTT, and ATP. The reaction was quenched with STEB gel loading buffer and loaded on 0.8% Agarose gel and subject to electrophoresis and imaged after incubation with EtBr. A broad range of Api5 protein concentrations (0.25, 0.5, 0.75. 1, 1.5 μM) was used along with 0.5μM & 1μM of a positive control protein EcoP50 I, to standardize the EMSA conditions (Fig 5.2.1A) EcoP50 I is a restriction enzyme so it's a known DNA binding protein. Elaboration of Api5 protein concentration range (0, 0.1, 0.2, 0.3, 0.4, 0.5, 0.6, 0.7, 0.7, 0.8, 0.9, 1.0, 1.5, 2.0, 2.5, 3.0, 3.5, 4.0 μM) used in similar EMSA helped further resolve that it caused a shift in dsDNA mobility from 0.3μM onwards and a super-shift from 0.9μM onwards (Fig 5.2.1B). This proved that Api5 is capable of a direct biochemical interaction with dsDNA.

An important aspect of the present study involved investigating the effect of DNA damaging agent like CPT, which formed intermediate DNA structures such as stalled replication forks or bubbles (as discussed in the previous chapter), so it was also pertinent to look for Api5 protein binding to such structures in comparison to normal dsDNA. Pairs of random sequence oligos were designed and annealed so as to produce dsDNA, fork and bubble structures. Increasing concentration of Api5 protein (0, 0.5, 1.0, 1.5, 2.0, 2.5, 3.0, 3.5, 4.0, 5.0, 5.5, 6.0, 6.5 μM) were incubated with dsDNA(70bp), dsDNA(20bp)-fork(50bp) and dsDNA(20bp)-bubble(30bp)-dsDNA(20bp) probes and run on 5% non-denaturing PAGE in TBE buffer, stained with EtBr and imaged under UV light (Fig 5.2.1 C, D, E).

A

B

C

DNA probe: _____ 70 bp

D

DNA Probe: 20bp / 50bp

E

DNA Probe: 20bp 30bp 20bp
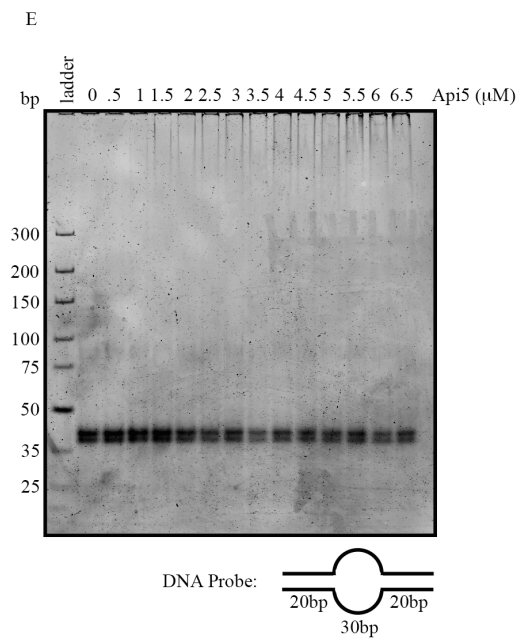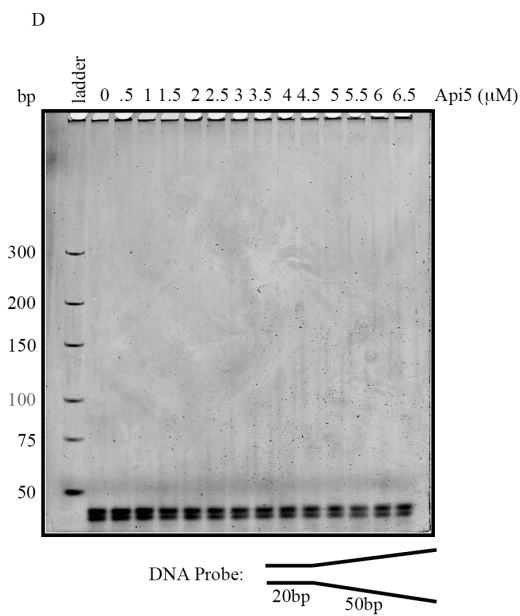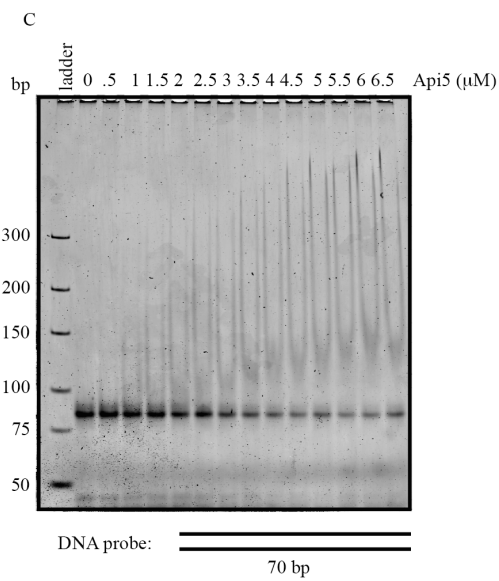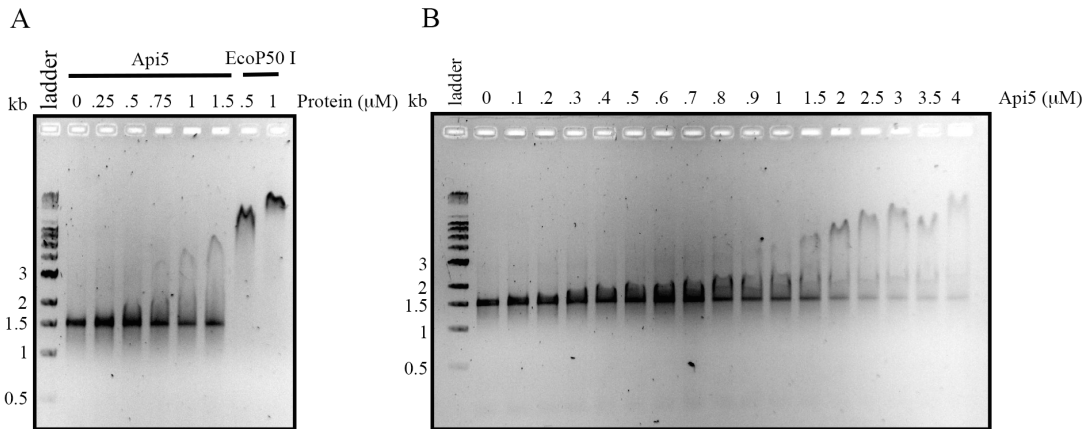
Figure 5.2.1: Api5 interacts with DNA *in vitro*.

(A) Api5 causes DNA probe mobility shift comparable to that of known DNA binding protein under the experimental conditions of EMSA. Supermix DNA ladder (lane1), EMSA reactions consisting of indicated concentrations of purified Api5 (lanes 2-7) and EcoP50 I protein (lanes 8-9) incubated with 10nM of 1.5kB dsDNA probe each were run on 0.8% Agarose gel in TAE buffer, stained with EtBr and imaged under UV. (B) Api5 causes shift as well as supershift of DNA probe. Supermix DNA ladder (Lane 1) and EMSA reactions as in (A) with indicated concentrations of purified Api5 protein (lanes 2-18) were similarly run and imaged. (C, D, E) Api5 associates with dsDNA preferably in comparison to intermediate fork and bubble structures. Generuler ultra low range DNA ladder (lane1), EMSA reactions consisting of indicated concentrations of Api5 protein (lanes 2-15) incubated with 0.5μM each of dsDNA (C), dsDNA-fork (D) and dsDNA-bubble-dsDNA (E) probes were run on 5% non-denaturing PAGE, stained with EtBr and imaged under UV.

Equivalent concentrations of Api5 protein was observed to cause a higher shift to dsDNA probe in comparison to fork or bubble DNA probes. This led to the conclusion that Api5 binds preferably to normal dsDNA in comparison to any intermediate DNA structures.

5.2.2 Api5 is chromatin bound *in vivo*

Results from the previous section showed that Api5 is associated with DNA *in vitro*. It was interesting to explore what is the condition *in vivo*, as to what is its chromatin binding status within the cells. This question can be answered only to a limited success using the techniques of microscopy, owing to its limitations of visualizing protein interaction with DNA in case it is not visually discernable. For this, we employed a simple yet robust biochemical method of chromatin or sub-cellular fractionation that separated out the chromatin, nucleoplasmic and cytoplasmic fractions from the whole cell lysate (WCL). ORC2 and GAPDH were the controls for the technique as ORC2 is a known chromatin-bound and GAPDH is a known cytoplasmic protein.

U2OS cells were subjected or not to CPT-induced DNA damage, and fractionated following Stillman & Mendez's protocol (Méndez and Stillman, 2000). The samples were western blotted and probed for Api5, TopBP1, ORC2 (Abcam ab37355 at a dilution of 1:500) and GAPDH (Sigma G9545 at a dilution of 1:20,000) respectively (Fig 5.2.2). The presence of ORC2 in chromatin and its absence from cytoplasmic and nucleoplasmic fractions, together with the presence of GAPDH in cytoplasmic, while absence from nucleoplasmic or chromatin fractions was an indication of the authenticity of the procedure.

Observation of TopBP1 in chromatin and its near absence in rest of the fractions was in accordance with the earlier reports. Interestingly, Api5 was present abundantly in the chromatin fraction proving its DNA binding *in vivo*. It, however, was present in lesser amounts in the nucleoplasmic as well as cytoplasmic fractions.
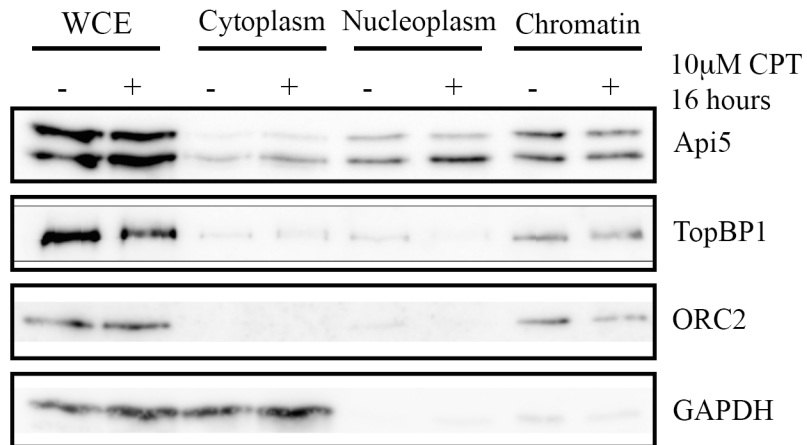
Figure 5.2.2: Api5 is chromatin bound *in vivo* both in presence or absence of DNA damage.

Whole cell extracts (lanes 1-2), cytoplasm (lanes 3-4), nucleoplasm (lanes 5-6) and chromatin (lanes 7-8) treated without or with CPT-induced damage subjected to WB and probed for Api5, TopBP1, ORC2, and GAPDH respectively.

5.2.3 Api5 does not form DDR nuclear foci or co-localize with TopBP1 DDR foci

U2OS cells were treated or not treated with 10μM CPT for 16 hours, fixed and co-immuno-fluorescently stained for TopBP1 (using TopBP1 antibody BD 611874 at a dilution of 1:200) along with Api5 (using Api5 antibody Abnova PAB7951 at a dilution of 1:1000). The slides were imaged under a confocal microscope. TopBP1 was observed to be forming distinct nuclear foci upon damage whereas Api5 did not form morphologically similar foci with or without damage in the nucleus (Fig 5.2.3A). TopBP1 showed a significant increase in foci formation upon CPT-induced DNA damage (Fig 5.2.3B). Api5 and TopBP1 foci formation were also looked upon another kind of DNA damage that is caused by UV irradiation. CPT causes DSBs while UV forms labile photoproducts that lead to fork stalling and formation of SSBs. U2OS cells were irradiated or not with UV light at the energy of 50 J/m^2 for 6 seconds followed by incubation for 2 hours and then fixation and staining. UV also did not induce Api5 foci formation like those of TopBP1 (Fig 5.2.3C), though TopBP1 did not show a significant increase in foci formation upon damage (Fig 5.2.3E). As discussed earlier, TopBP1 can form DDR as well as replication foci hence it was important to elucidate the nature of TopBP1 foci that showed an increase upon CPT-induced DNA damage. This was achieved by co-IF staining with 53BP1, which forms DDR foci and is known to co-localize with TopBP1 DDR foci. U2OS cells were similarly treated with CPT and stained for TopBP1 (using TopBP1 antibody BD 611874 at a dilution of 1:200) and 53BP1 (using 53BP1 antibody Cell signaling 4937 at a dilution of 1:100) and imaged (Fig 5.2.3D). TopBP1 and 53BP1 foci co-localization was measured using Jacop plugin of ImageJ. TopBP1 and 53BP1 foci showed a significant increase in colocalization upon CPT-induced DNA damage (Fig 5.2.3F) indicating that the increase in TopBP1 foci observed upon CPT damage were indeed DDR foci and not replication foci.

The above foci formation studies were performed upon DSB formation following prolonged exposure to CPT. There was a possibility that Api5 foci might not be as persistent as TopBP1 foci to last after 16 hours of drug exposure. The transient nature of Api5 foci induced upon damage needs to be explored. This was achieved by employing another strategy of inducing instantaneous DSBs and then staining for Api5 along with other markers after a short time span of the damage (in minutes range). For this, U2OS cells were first photosensitized with BrdU for 24 hours and

97

then UV-C laser of a Zeiss laser capture microdissection (LCM) was used to cause localized DSBs along a defined track within the nucleus. The cells were incubated for 25, 45, 53 and 90 min after damage, fixed and then co-IF stained for TopBP1, Api5, and γH2AX (using γH2AX antibody Millipore 16-202A at a dilution of 1:200). During imaging, cells showing γH2AX tracks were scored as the ones having endured DSBs, and enrichment of TopBP1 and Api5 along the same tracks was looked for (Fig 5.2.3G). This method has the unique advantage of providing internal control; the region of the nucleus along laser track is the one that has localized DNA damage, whereas the other regions of the same nucleus don't bear damage as serve as an internal control. TopBP1 was observed to be enriched along the laser tracks marked with γH2AX in almost all the nuclei (Fig 5.2.3G 25,45,53 and 90 minutes) whereas Api5 did not show any enrichment and was rather excluded from ~ 25% of all such tracks that showed γH2AX and TopBP1 enrichment (Fig 4.2.3G 90 minutes) (n=24). This experiment showed that Api5 does not form DDR foci even at short time span after DSB whereas TopBP1 does, as evidenced by its co-localization with γH2AX DSB foci along the laser track.

A

B

% of Nuclei showing TopBP1 foci

p=0.0076

C

	Hoechst	Api5	TopBP1	Api5 + TopBP1
-UV				
+UV				

D

	Hoechst	TopBP1	53BP1	TopBP1 + 53BP1
-CPT				
+CPT				

E

% of Nuclei showing TopBP1 foci

ns

- ■ -UV
- ■ +UV

p=0.5341

%

Treatment Groups

F

% TopBP1 foci co-localizing with 53BP1 foci

**

%

Treatment groups

100

G
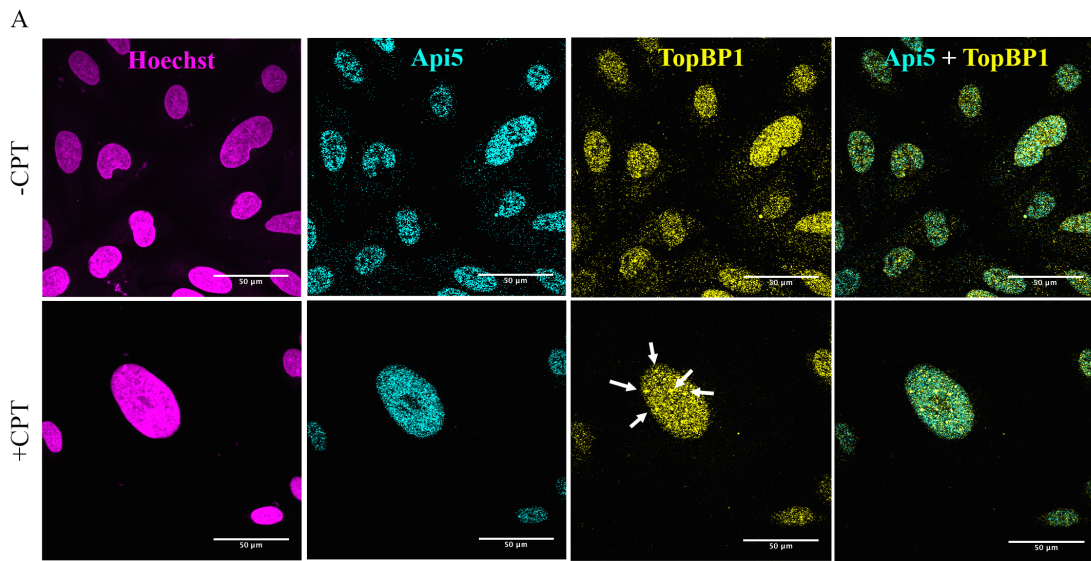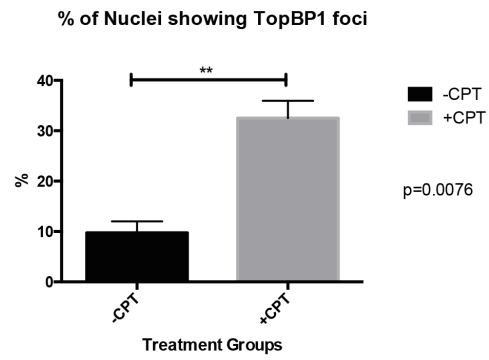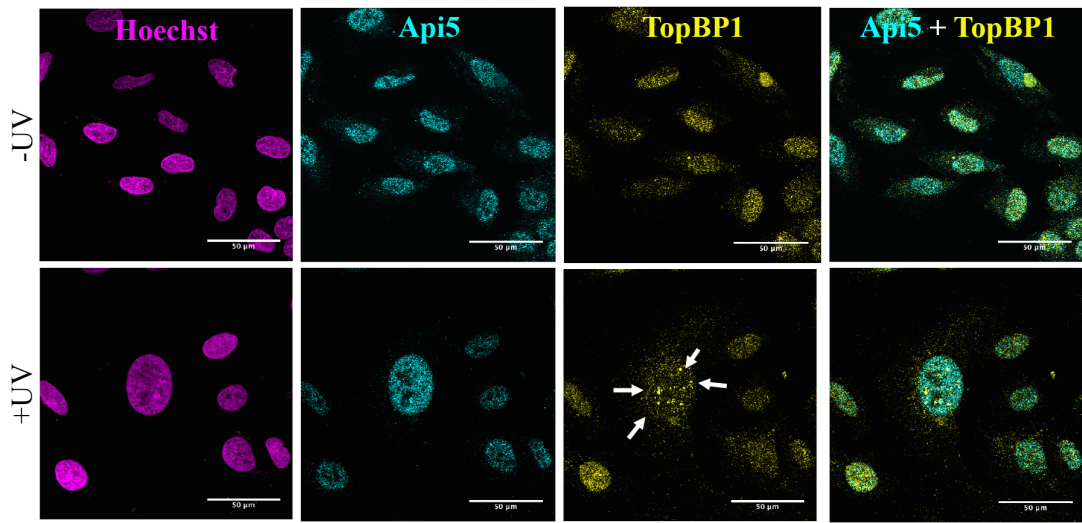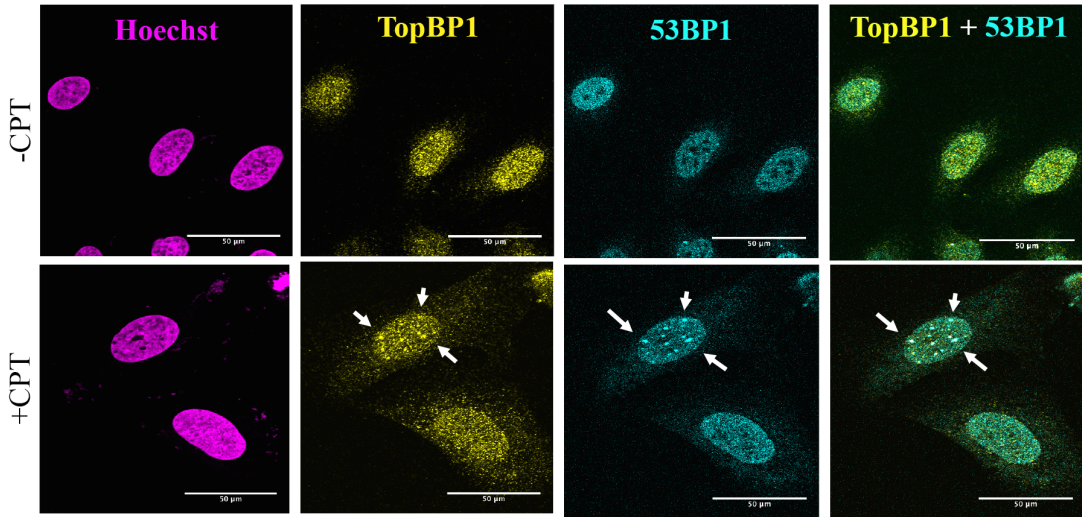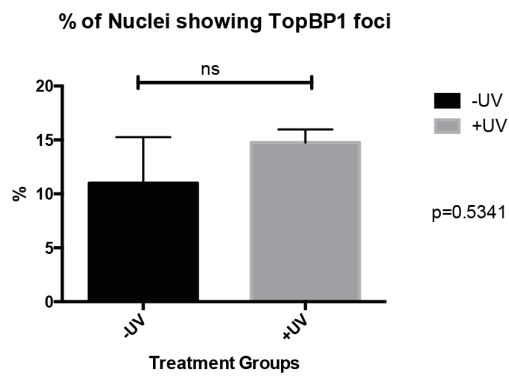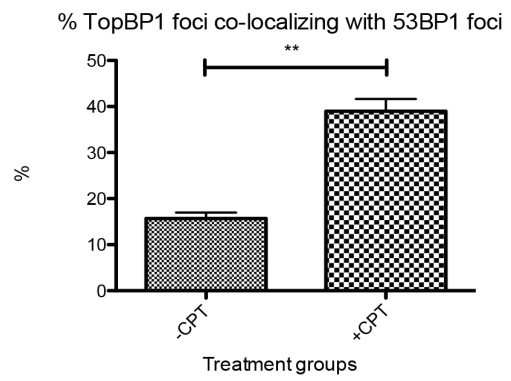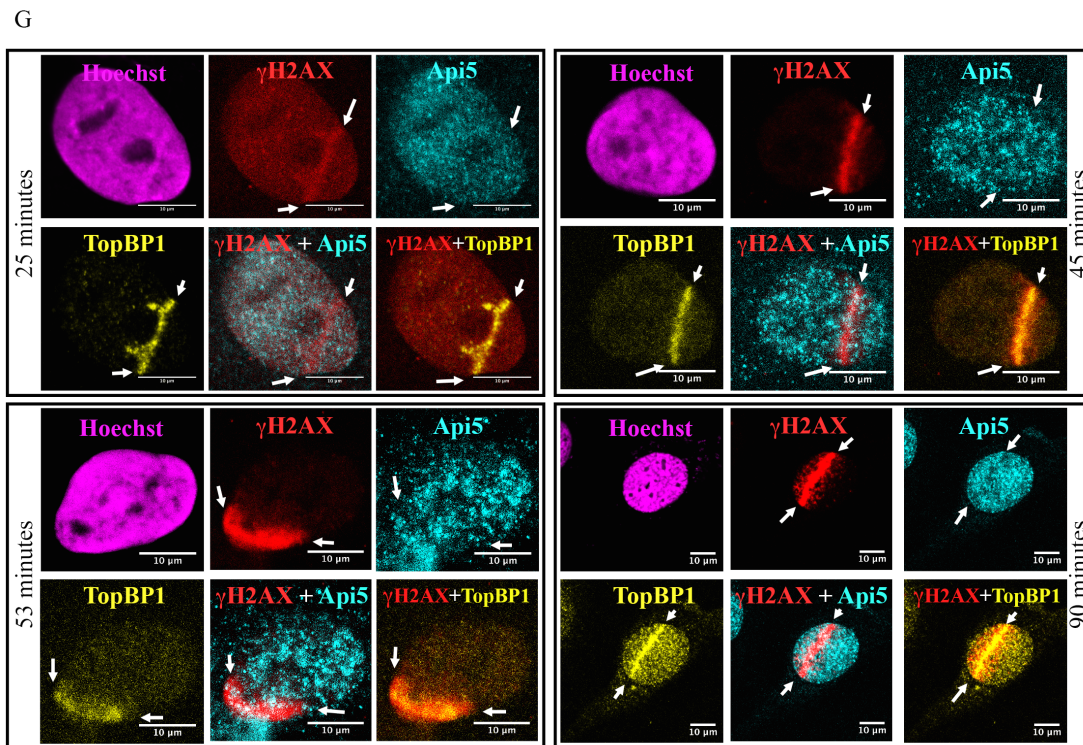
Figure 5.2.3: Api5 does not form nuclear foci or co-localize with TopBP1 DDR foci.

(A) U2OS cells were treated without or with 10μM CPT for 16 hours, fixed, IF stained for Api5 and TopBP1 and imaged under confocal microscope, arrows mark TopBP1 foci (B) quantification showing percentage of all the cells showing TopBP1 foci in figure A (N=3, n >150, p=0.0076; two-tailed t-test) (C) U2OS cells were irradiated or not with 50 J/m^2 of UV for 6 seconds, incubated for 2 hours, fixed, IF stained for Api5 and TopBP1 and imaged under confocal microscope, arrows mark TopBP1 foci (D) U2OS cells were treated without or with 10μM CPT for 16 hours fixed, IF stained for TopBP1 & 53BP1 and imaged under confocal microscope, arrows mark TopBP1, 53BP1 foci and their co-localization (E) quantification showing percentage of all the cells showing TopBP1 foci in figure C (N=3, n >150, p=0.5341; two-tailed t-test) (F) quantification showing percentage of TopBP1 foci across all the cells colocalizing with 53BP1 foci in figure D (N=3, n >150, p=0.0014; two-tailed t-test) (G) Single nucleus confocal images of U2OS cells fixed and IF stained for γH2AX, Api5, and TopBP1 at indicated time points after being subject to UV laser induced localized damage post photosensitization with BrdU, arrows mark UV laser tracks within the nucleus. While TopBP1 was enriched in almost all the nuclei along

101

the laser tracks marked with γH2AX (for example 25,45,53 and 90 minutes), Api5 was not enriched along the same tracks and was rather excluded from ~25% of the nuclei (for example in 90 minute) (n=24).

5.2.4 U2OS cells released after G2/M synchronization were arrested at G1 upon damage and underwent cell death after 12 hours

U2OS cells were synchronized to G2/M phase of the cell cycle by thymidine-nocodazole (T-N) block. They were harvested and released from the block by reseeding into fresh media in pairs of 60mm dishes containing coverslip. CPT to a final concentration of 10μM was added to one amongst the pair, while an equal volume of DMSO was added to the other dish. The dishes were incubated for 4,8,12,16 and 20 hours respectively. Coverslip containing the growing cells from a pair of dishes (with or without CPT) at each time point was removed, fixed and IF stained for TopBP1 and Api5 as described in the previous section. The remaining cells of the dish were harvested, fixed and stored at 4°C. The cells were rinsed with PBS, stained with propidium iodide (PI) and analyzed by FACS to observe their cell cycle profile.

PI fluorescence peak height vs peak area scatter plot represented the distribution of cells according to their DNA content (Fig 5.2.4A). The two prominent clusters represent cells containing DNA content corresponding to that at G1 and G2/M (double the amount at G1) respectively. Cell scatter beyond G2/M cluster represent cell clumps whereas the scatter before G1 (sub-G1) represent apoptotic cells (as the apoptotic cells undergo DNA fragmentation and hence have DNA content lesser than that of living cells). Two kinds of DNA histograms were plotted out of this scatter plot: first one with a gate around the G1 and G2/M clusters representing the distribution of live single cell population across the cell cycle (Fig 5.2.4A upper lane) and the second type without any gate representing the distribution of the entire population (Fig 5.2.4A lower lane). The sub-G1 peak in the second kind of histogram represented the apoptotic cell population.

Most of the cells in asynchronous culture were observed to be in G1 indicated by the first peak, followed by G2/M indicated by the third peak and a very small number in S phase as indicated by the small peak in between G1 and G2/M peaks. T-N synchronization achieved almost a complete synchronization of single cell population at G2/M in comparison to the cell cycle profile of asynchronous cells (Fig5.2.4A)

A

B

Figure 5.2.4: G2/M synchroniztion and release cell cycle profiles with or without CPT damage.

(A) Scatter plot representing the distribution of FACS sample according to their DNA content, DNA histograms (FACS profile) for asynchronous cell culture and synchronized culture fixed immediately after thymidine-nocodazole blockage; gated DNA histograms represent the cell cycle profile of the two cultures, whereas the corresponding ungated DNA histograms reveal the sub-G1 peak indicating the

apoptotic cell population. (B) FACS profiles (gated as well as ungated) at indicated time points after T-N blockage release both in presence and absence of 10μM CPT.

G2/M synchronized cells proceeded to G1 phase 4 hours after T-N release both in presence and absence of CPT. Cells further started moving into S phase after 8 hours without damage whereas they mostly remained stuck at G1 with damage. After 12 hours, the cells started moving back to G2 without damage, whereas with damage, they started entering apoptosis as indicated by the emergence of the sub-G1 peak in the ungated histogram and the remaining live cells still were mostly stuck in G1. At 16 and 20 hours post T-N block without damage, cells were in G2 and G1 respectively, but they also started undergoing apoptosis. In the corresponding time points with CPT damage, cells were increasingly undergoing apoptosis while those alive were still stuck at G1, as inferred from the increasing sub-G1 peak in ungated histograms and decreasing height of G1 peak in the gated histograms.

5.2.5 Api5 did not form cell cycle dependent foci in presence or absence of DNA damage, unlike TopBP1.

U2OS cells released for 4,8,12,16 and 20 hours after G2/M synchronization with and without 10μM CPT and growing on coverslips as described in section 5.2.4 were fixed, co-IF stained with TopBP1 and Api5 as described earlier and imaged (Fig 5.2.5A). Api5 did not appear to form discernable foci at any phase of the cell cycle with or without damage. It only appeared as speckles. TopBP1 did form foci across the experimental set, its foci were counted using ImageJ and quantified (Fig 5.2.5B).

A

B
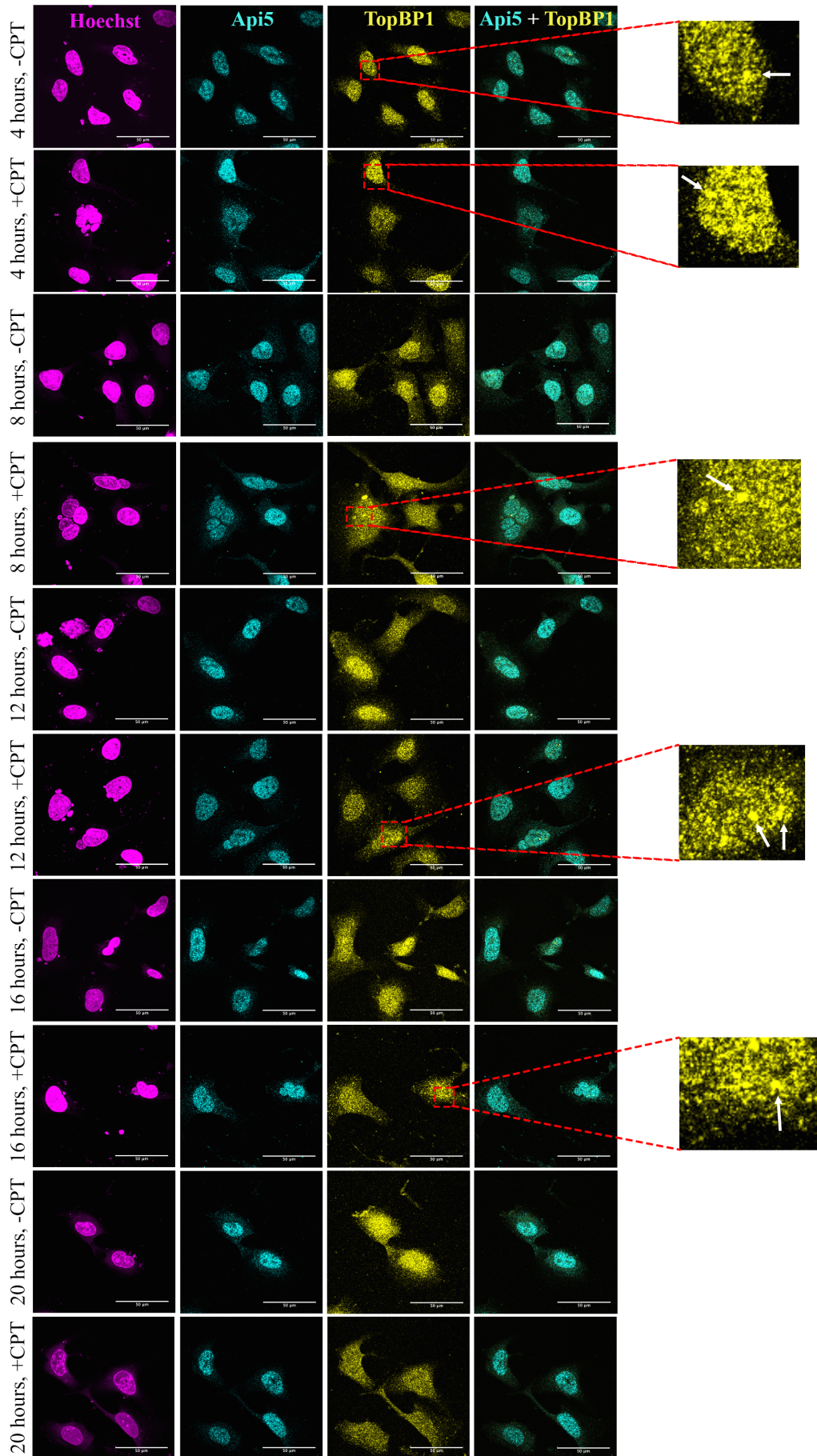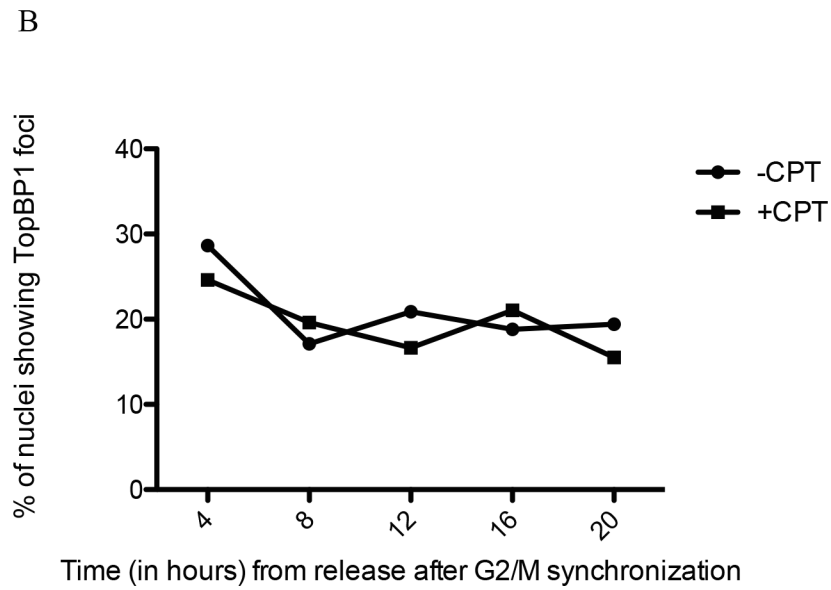
Figure 5.2.5: Api5 does not form nuclear foci across the cell cycle with or without damage.

(A) U2OS cells synchronized at G2/M and released for 4,8,12,16 and 20 hours with or without 10μM CPT were IF stained with TopBP1 and Api5 and imaged using a confocal microscope. Representative images zoomed in to show TopBP1 foci marked with arrows. (B) Plot showing the percentage of the total number of nuclei counted showing TopBP1 foci for each experimental set (N=3, n>150).

5.2.6 Recombinant Api5 did not form DDR foci upon sustained or instantaneous DNA damage

IF staining of endogenous Api5 protein did not show foci formation. Presence or absence of global and prolonged exposure to CPT damage or localized quick laser inflicted DNA damage upon asynchronous or synchronized cultures only yielded speckle kind of staining pattern for Api5. To rule out the cause of such an observation to be an artifact of antibody staining, another approach was taken.

Api5 mVenusC1 plasmid was transfected into U2OS cells growing on coverslips so as to express Api5 mVenusC1 fluorescently tagged protein and was subjected to DNA damage inflicted by 10μM of CPT for 16 hours. The coverslip was removed, fixed, mounted and imaged under a confocal microscope immediately.

Api5 mVenus protein appeared homogenous inside the nucleus both with or without DNA damage and did not show foci formation in either of the circumstances (Fig 5.2.6A)

A
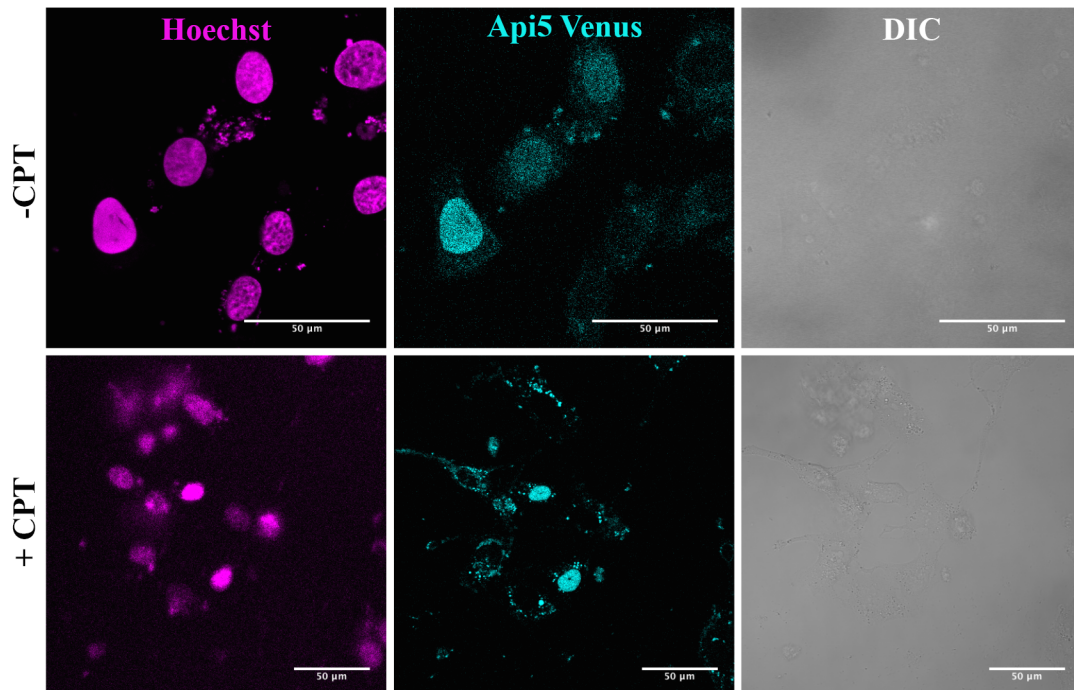
B
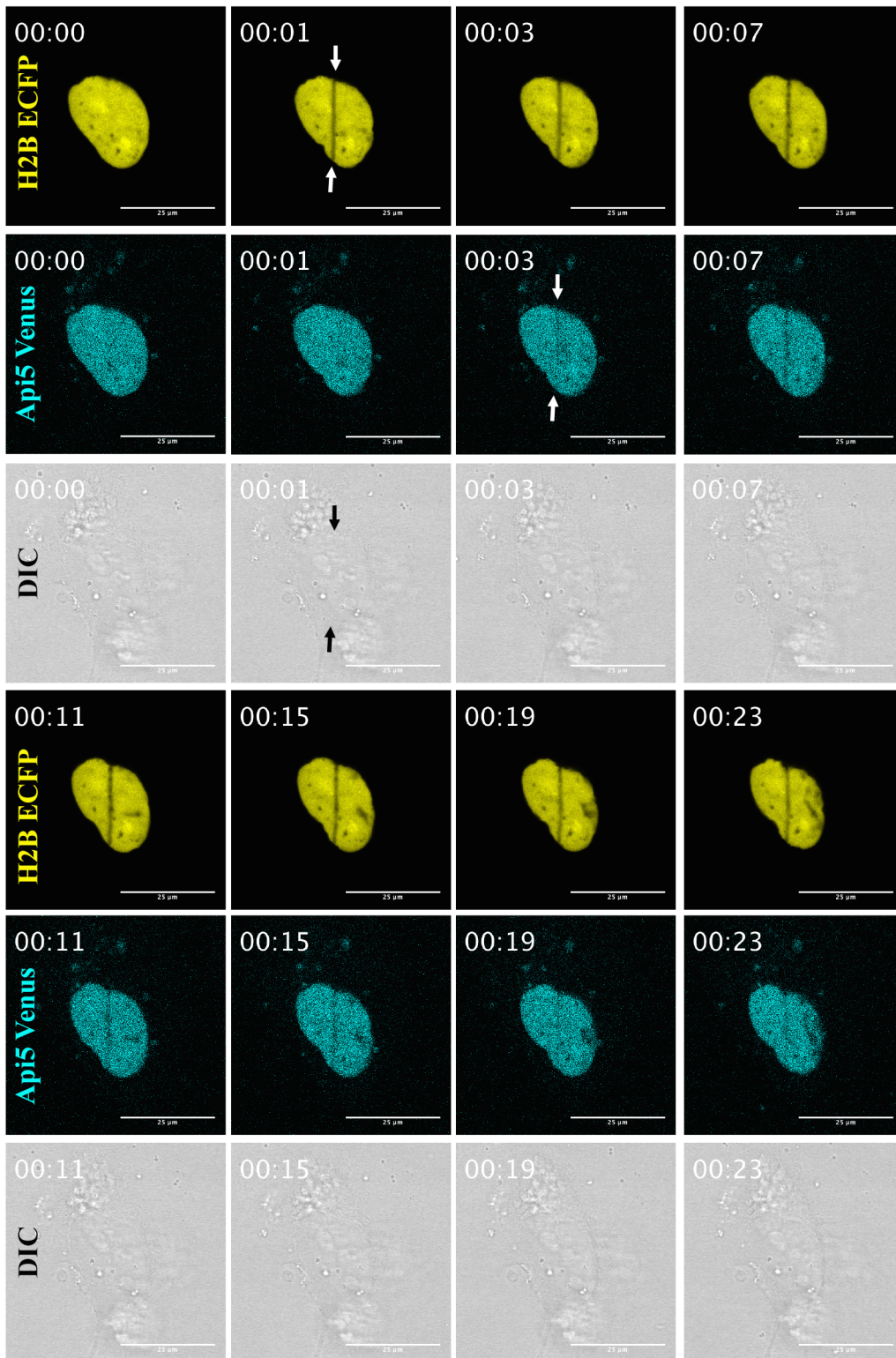
Figure 5.2.6: Fluorescently tagged and overexpressed Api5 also does not form DDR foci.

109

(A) U2OS cells transfected with Api5 mVenusC1 plasmid were treated with or without 10μM for 16 hours. The cells were fixed, counterstained with Hoechst DNA stain, mounted and imaged immediately (B) U2OS cells were grown on chamber coverglass, co-transfected with H2B-ECFP & Api5 mVenusC1 plasmids, photosensitized with BrdU and live cell imaged upon laser inflicted DNA damage. Time stamps indicate the time point in minutes and arrows mark the laser tracks

The possibility of transient and short-lived nature of Api5 foci upon DNA damage was also explored with overexpressed Api5 protein. Api5 mVenusC1 and H2B-ECFP plasmids were co-transfected into U2OS cells to express the respective fluorescent fusion proteins. H2B-ECFP served as a nuclear marker for live cell imaging. Cells were photosensitized with BrdU for 24 hours and then subject to live cell imaging under a Carl Zeiss confocal microscope. The multiphoton laser of the microscope was used as a source of DNA damage. Its energy was optimized on a higher side just as much as not to physically damage/disrupt the nucleus (as visible under the DIC channel) but result in ablation of H2B-ECFP along the laser track. A single nucleus was focussed, damaged by the laser while imaging and the recovery were tracked. Snapshots of a representative experiment in which the laser was inflicted at 1 min since the beginning of imaging and its recovery was tracked till 24 minutes showed that the damage was inflicted at 1 min along the laser track (marked with white arrows in H2B-ECFP channel) while not causing physical damage to the cell (arrow marks on the DIC channel), Api5 mVenus got excluded from the side of damage at 2 min (marked with arrows on Api5 mVenus channel) and remained so even till 24 min after damage (Fig 5.2.6B). The experiment was repeated several times with different laser energies and recovery times up to 45 min, but still, Api5 mVenus protein was never seen to localize at sites of laser damage at any time point.

5.3 Discussion

The current studies proved univocally that Api5 does not form nuclear foci under any circumstance of DNA damage or cell cycle phase. Neither did global and prolonged DNA damage caused by CPT nor localized and instantaneous damage caused by laser made Api5 to form cytologically discernible "foci" anywhere close to those formed by TopBP1 or γH2AX under such circumstance. It did not form foci across the cell cycle with or without damage. Both the endogenous and overexpressed Api5 proteins did not form nuclear foci.

Our previous studies show an interaction between Api5 and TopBP1 that increases upon DNA damage. The presence of Api5, as well as TopBP1 on the chromatin whereas an absence of TopBP1 in the cytoplasm, hints towards their interaction possibly on the chromatin. This interaction might not be cytologically "visible" in the face of a failure of Api5 to form nuclear foci, but it could be described on the lines of several DNA damage proteins that are known to bind to chromatin together with other DDR proteins but still do not form visible foci.

EMSA studies clarified that Api5 need not depend on other proteins (like TopBP1) to get recruited at chromatin as it has the DNA binding potential by itself, though its recruitment to DNA because of its association with TopBP1 or some other protein can not be ruled out at the moment. EMSA also showed that Api5 has more affinity towards undamaged DNA in comparison to transient structures that are formed upon fork stalling. Preference of Api5 towards normal DNA or damaged DNA can further be investigated by using DNA probes that represent ssDNA-dsDNA junctions.

Having established the interaction of Api5 with TopBP1 upon DNA damage that doesn't happen at visible DNA damage foci, the next step is to elucidate the role of Api5 protein in the DDR induced apoptosis signaling.

5.4 Summary

The current study set out to investigate the foci formation by Api5 given its interaction with TopBP1 upon DNA damage which is known to form DDR foci. Using a combination of imaging techniques, it was established that Api5 does not form DDR foci under any circumstance of DNA damage or cell cycle phase or co-localise with TopBP1 DDR foci. EMSA studies also established that Api5 can bind to DNA by itself resting earlier ambiguity about its DNA binding potential. Chromatin fractionation studies showed that Api5 is chromatin bound *in vivo* and given its interaction with TopBP1 and inability to form visually distinct foci, it can be argued that the interaction happens on the chromatin in a way that is not cytologically discernible, possibly in a way similar to that of some of those in the DDR pathway like checkpoint and DNA repair proteins.

Chapter 6: Functional characterization of Api5 in response to DNA damage

6.1 Background

As mentioned in Chapter1, Api5 is an anti-apoptotic protein that is known to save the cells from undergoing growth factor withdrawal as well as DNA damage-induced apoptosis and inhibits Acinus mediated apoptotic DNA fragmentation.

Acinus is a late player in the apoptosis signaling that can be activated by several types of stresses including, DNA damage. As discussed earlier, DNA damage triggers the checkpoint signaling, activating its various effector proteins that function in conjunction to carry out either DNA repair or apoptosis (Abraham, 2001). Interestingly, Api5 is known to affect the functions of one of these effectors, namely E2F1.

E2F1 is the first member of the E2F family of transcription factors. E2F1-3 function as transcriptional activators, while E2F4-8 are repressors(Wu et al., 2009). The transcriptional regulation function of these proteins is kept in control by the association with their respective "pocket binding" proteins, Rb is that candidate for E2F1 and keeps it functions in check (Iaquinta and Lees., 2007). E2Fs mostly regulate transcription of proteins involved in cell cycle regulation, for example, the different cyclins, Chk1, TopBP1 to name a few, and thus regulate cell proliferation (Ginsberg, 2002; Mueller et al., 2001; Mundle and Saberwal, 2003). E2F1 is unique in that respect as it regulates expression of proteins associated with the apoptosis pathway as well in addition to those of cell cycle control. For example, it upregulates transcription of p14^{ARF}, APAF-1, p73, pro-apoptotic BH3 only proteins (BIM, PUMA, NOXA), and Caspases while it represses transcription of the anti-apoptotic Bcl-2 family of proteins like Bcl-2 and MCL-1 (Wu et al., 2009; Iaquinta and Lees., 2007). E2F1 thus has arguably opposing functions of regulating cell proliferation as well as apoptosis. The choice of transcriptional regulation targets of E2F1, that is. cell cycle or apoptosis pathway proteins, is believed to be regulated by alternative post-translational modification (majorly phosphorylation and acetylation) states of E2F1, which in turn is a response to stimuli the cell experiences, for example, kind and extent of DNA damage (Biswas and Johnson, 2012; Carnevale et al., 2012). E2F1

transcription regulation function is a subject of the influence of other proteins as well, by mechanisms that are sometimes well characterized, as in the case of TopBP1 or not so elaborately understood, as for Api5 and discussed below.

Api5 is known to influence both the cell cycle regulation as well as the apoptosis induction functions of E2F1 (Arconde et al., 2013; Morris et al., 2006). Protein levels of both Api5 and E2F1 show a similar profile across the cell cycle, peaking at G1 (Arconde et al., 2013). Neither do they interact with each other nor are they involved in transcriptional regulation of expression of each other. Api5 has been shown to contribute to the E2F1 control of G1/S cell cycle phase transition by contributing to the transcriptional activation of E2F1 cell cycle targets like cyclin E, cyclin D1, and Cdk2 as Api5 depletion significantly decreases transcription of above genes even in presence of E2F1. Such role of Api5 in influencing E2F1 mediated transcription is however contradicted by another report which suggests that Api5 does not influence transcription of E2F1 cell cycle target cyclin E and apoptosis target p14[ARF] as over-expression of Api5 did not prevent E2F1 overexpression mediated increase in levels of the mentioned proteins (Morris et al., 2006). Interestingly, over-expression of Api5 still manages to inhibit E2F1 overexpression mediated apoptosis indicating that Api5 might be functioning downstream of E2F1 mediated transcriptional control, at least of apoptosis target genes (Morris et al., 2006). Api5 was indeed shown to negatively influence one such E2F1 downstream apoptotic transcriptional target APAF-1, which is involved in the formation of apoptosome (Mayank et al., 2015). It is possible that Api5 might affect other E2F1 downstream apoptotic players that might be it's direct or indirect transcriptional target(s). Other than the Rb-E2F1 pathway, MDM2-p53 is the other key pathway that is activated by checkpoint signaling (Yoshida and Miki, 2010). Both of them have extensive crosstalk between each other and determine the cell fate; survival or apoptosis (Polager and Ginsberg, 2009). E2F1 signals the transcription of p14[ARF], that is an inhibitor of MDM2: the E3 ubiquitin ligase of p53. E2F1 thus brings about the stabilization of the downstream p53 indirectly which otherwise undergoes constant turnover by MDM2 (Beckerman and Prives, 1995; Fridman and Lowe, 2003; Haupt et al., 2003; Oren, 1999; Yoshida and Miki, 2010).

E2F1 and p53 are two key tumor suppressors in the cell and their functions overlap, both regulate cell cycle as well as apoptosis induction by working as transcription factors to regulate overlapping sets of proteins. Upon low level of DNA damage,

checkpoint pathway phosphorylates p53, disrupting its interaction with its degrader MDM2, hence stabilizing it (Moll et al., 2003). p53 upregulates p21 transcriptionally bringing about G1 arrest so as to buy time for the DNA repair to happen (Garner and Raj, 2008; Rodier et al., 2007). If however, the extent of damage is high, p53 accumulates above a particular threshold and now functions to instead up-regulate the transcription of pro-apoptotic proteins like BAX, PUMA, NOXA, FAS. (which can also be transcribed by E2F1 independently as discussed earlier) (Roos and Kaina, 2013). p53 is mutant in almost fifty percent of human cancers (Liu et al., 2011) and E2F1 ensures that apoptosis is induced in such cases as well by transcriptionally activating p53 homolog p73 (Haupt et al., 2003; Roos and Kaina, 2013). p73, in turn, has similar apoptosis transcriptional targets as p53 (Elmore, 2007).

Interestingly, TopBP1, that we identified as an interactor of Api5 upon DNA damage is one protein that is known to inhibit the apoptosis induction function of both E2F1 and p53 (Liu et al., 2003, 2004, 2009a ;) Yoshida and Inoue, 2004). TopBP1 interacts through its BRCT6 with the amino terminal of E2F1 (Liu et al., 2003). TopBP1 recruits chromatin remodeling complex components Brg1/Brm at E2F1 responsive cell cycle and apoptosis promoters and inhibits their firing (Liu et al., 2004). TopBP1 thus inhibits E2F1 mediated apoptosis by inhibiting its transcription regulation function. The inhibition of E2F1 transcriptional regulation by TopBP1 is independent of inhibition by its regular pocket binding protein Rb (Liu et al., 2003). E2F1, in turn, activates the transcription of TopBP1 by binding to its promoter, thus completing a feedback regulation between E2F1 and TopBP1 (Yoshida and Inoue, 2004).

TopBP1 keeps p53 activities in check during normal growth by interacting with the DNA binding domain of p53 through its BRCT7-8 domains (Liu et al., 2009a). This brings about inhibition of promoter binding capacity of p53, without affecting its protein levels. TopBP1 keeps activation of both, p53 cell cycle targets like p21 and apoptosis targets like BAX, PUMA, NOXA, MDM2 among others, under check after DNA damage as well because its depletion leads to their up-regulation. TopBP1 inhibits p53-induced apoptosis in this way. As mentioned earlier, half of the cancers in which p53 is mutant, p63/p73 (induced by E2F1) take up the function of activating p53 cell cycle and apoptosis targets. In such cases also, TopBP1 facilitates the interaction of mutant p53 with p63/73 and inhibits the apoptotic transcriptional targets (Liu et al., 2011).

TopBP1 is thus known to inhibit E2F1 as well as p53 induced apoptosis at a transcriptional level, whereas Api5 is known to inhibit E2F1 mediated apoptosis, but how exactly it targets the apoptosis signaling downstream of E2F1 is not very clear. Given the interaction between TopBP1 and Api5 as reported earlier, and the role of TopBP1 in controlling the E2F1-p53 apoptosis pathways, it will be interesting to find out how Api5 affects this axis.

This can be done by Api5 knockdown and rescue studies in conjunction with the TopBP1 knockdown to compare and elucidate the place of Api5 in the molecular pathway that gets activated in response to DNA damage and connects checkpoint signaling with apoptosis signaling. After elucidating this, the other important aspect will be to do the structural characterization of Api5 so as to find which region(s) of the protein is critical and/or responsible for carrying out the function of Api5 in the signaling as discovered in the previous objective. This can be achieved by Api5 knockdown and rescue with several truncation mutants of Api5 in comparison with that by the full-length protein.

6.2 Results

6.2.1 Functional characterization of the role of Api5 in apoptosis signaling upon DNA damage

6.2.1.1 Cloning and site-directed mutagenesis of Api5-mVenus-C1 construct

One of the robust ways of carrying out functional studies of a target gene in cell culture system is by knockdown and rescue. The target gene can be knocked down/out and subject to the stimulus for example, DNA damage, and a range of relevant phenotypes can be compared between the knockdown and wild-type experimental sets so as to identify phenotype(s) that show a differential pattern. The phenotype could be at a cellular level for example, effect on cell cycle, apoptosis or necrosis, or at a molecular level for example, up-regulation or down-regulation of certain protein(s) levels or their certain PTM states. Identification of such a molecular read-out may point to the role of that protein in a certain molecular signaling pathway and its place in that signaling cascade by looking for the proteins that are affected vs not affected by the knockdown of the target. This elucidation can be counterchecked by doing the rescue experiment, i.e, reversal of the identified phenotype upon re-introduction of the target gene exogenously in the background of endogenous gene knockdown.

The knockdown and rescue can be transient or permanent. Gene knockout can be achieved by using genomic editing tools like CRISPR-Cas, permanent knockdown can be achieved by shRNA transfections or lentiviral transduction against the target gene. However, an easier method for performing transient knockdown is by transfecting with siRNA against the target gene, which can be rescued by co-transfecting with the target gene cDNA sequence cloned into a suitable mammalian expression vector. Since our experiment only involved with looking at the levels of different proteins in the checkpoint-apoptosis pathway after CPT-induced DNA damage, it didn't require knockdown or overexpression in prolonged culture, so siRNA-mediated knockdown and cloned vector-mediated rescue was the method of choice.

Api5 was cloned into a fluorescent Venus expressing mammalian plasmid mVenusC1. The 1575 bp cDNA was PCR amplified using Fluor Api5 For (IDT) and

Fluor Api5 Rev (IDT) primers and cloned between BglII and EcoRI restriction sites respectively in the plasmid. The clones were screened by colony PCR using the same primers that were used for amplifying Api5 to be used for cloning and were confirmed by restriction digestion with the same RE and looking for release of Api5 insert of the same size i.e. 1575bp, which is same as that of the PCR amplicon used for cloning initially (Fig 6.2.1.1A)

siRNA against the target gene is designed against a short sequence (20-22 bases) of its mRNA, such that it can bind and degrade the mRNA transcript of the gene. But, when coupling the siRNA knockdown with the plasmid-mediated rescue of the target gene expression, the same siRNA can also theoretically target the exogenous transcript of the target gene cloned in the vector. To avoid this from happening, the target gene sequence in the plasmid requires being mutagenized to destroy its complementarity with the siRNA sequence such that siRNA can no longer bind to its transcripts and degrade them. This is achieved by mutating a few bases, taking advantage of codon degeneracy so as to avoid overall change in amino acid composition of the protein (Fig 6.2.1.1B)

mutApi5-1F and mutApi5-1R (IDT) primers were used for the site-directed mutagenesis (SDM) PCR of Api5 mVenusC1 construct so as to make it resistant to siApi5-1 siRNA (Sigma). This mutagenesis changed amino acids D225E and E227D while not affecting L226. The swapping of D (Aspartic acid) with E (Glutamic acid) and vice versa is not supposed to change the overall properties of Api5 protein much as both the amino acids exhibit similar properties of being negatively charged. The mutagenized clone mut-1 Api5 mVenusC1 was confirmed by sequencing.
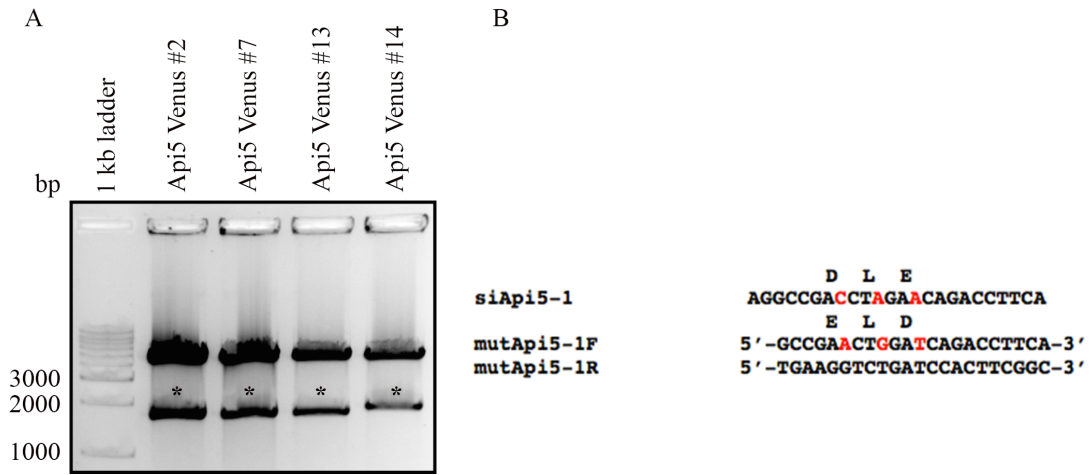
Figure 6.2.1.1: Cloning and site-directed mutagenesis of Api5 mVenusC1.

(A) EtBr-stained agarose gel imaged under UV trans-illuminator showing restriction digestion release of 1575bp Api5 fragment (marked with the asterisk) from the mVenusC1 vector for four different Api5 mVenusC1 clones. (B) siApi5-1 is the sequence of siRNA that targets Api5. mutApi5-1 F and R are the site-directed mutagenesis primers, red letters indicate the changed bases from the siRNA sequence that alter the corresponding amino acids.

6.2.1.2 Api5 knockdown did not influence activation of checkpoint pathways induced by Camptothecin mediated DNA damage

Our aim is to study the role of Api5 upon DNA damage. The DNA damage is first detected by the checkpoint pathway which gets activated to trigger several downstream effectors like p53, E2F1 as mentioned earlier. So, U2OS cells were subjected to siRNA-mediated knockdown of LacZ (as control), Api5 and TopBP1 respectively with or without 10μM CPT-mediated DNA damage for 16 hours. Activation of Chk1, Chk2, and levels of E2F1 was monitored (Fig 6.2.1.2)

DSB activate the ATM-Chk2 pathway that leads to the phosphorylation of Chk2 at Thr68, whereas SSB and replication fork arrest activate the ATR-Chk1 pathway by phosphorylating Chk1 at S345 or S317 depending upon the source of damage (Kastan and Bartek, 2004; Liang et al., 2009; Liu et al., 2000; Zhou and Elledge, 2000). TopBP1 works as a mediator in the ATR-Chk1 pathway (Kumagai et al., 2006). E2F1 is an important common downstream effector of either arm of the checkpoint signaling and has important functions in controlling cell cycle and apoptosis, as discussed earlier.

CPT-induced DNA damage activated both Chk1 and Chk2 in the siLacZ control. This is consistent with the knowledge that CPT induces transient SSB, permanent DSBs leading to replication fork collapse as discussed in Chapter 3. TopBP1 knockdown failed to activate Chk1 whereas it had no effect on activation of Chk2. This observation was in line with the known role of TopBP1 as a mediator in ATR-Chk1 pathway. Api5 knockdown interestingly didn't have any effect on the activation of either Chk1 or Chk2 as both of them showed phosphorylation comparable to that in siLacZ controls. This proved that Api5 must be working at any level below the apical kinase (ATM/ATR) - effector kinase (Chk1/Chk2) axis of the checkpoint signaling. E2F1 protein didn't show any difference in levels across the treatment groups. This showed that neither TopBP1 nor Api5 is involved in the expression or degradation of E2F1 with or without damage. Of note, however, is that E2F1 is involved in the expression of TopBP1 as mentioned earlier.

120
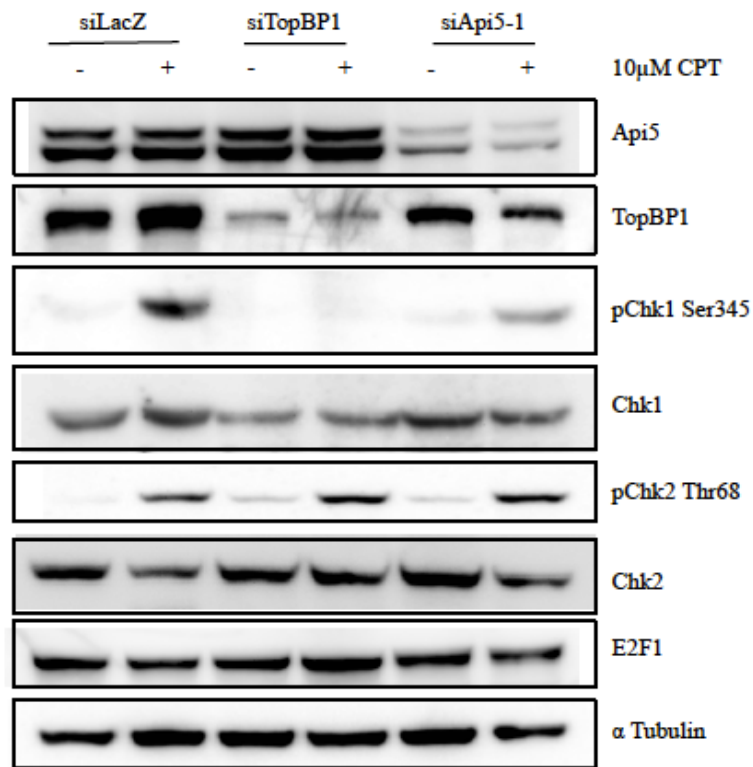
Figure 6.2.1.2: Api5 knockdown does not affect checkpoint activation or E2F1 protein levels.

U2OS cells were transfected with siLacZ (lanes1-2), siApi5-1 (lanes 3-4), siTopBP1 (lanes 5-6), and each pair was treated without or with 10μM CPT for 16 hours. Western blots were probed with antibodies against Api5 (1st panel), TopBP1 (2nd panel), pChk1 S^{345} (3rd panel), Chk1 (4th panel), pChk2 Thr^{68} (5th panel), Chk2 (6th panel), E2F1 (7th panel), α Tubulin (8th panel).

6.2.1.3 Camptothecin caused time-dependent activation of apoptotic pathway

The main aim of the current objective is to study how Api5 possibly regulates the apoptotic pathway in the face of DNA damage. CPT has been shown in previous sections to activate both the arms of canonical checkpoint signaling, induce TopBP1 foci formation and induce its interaction with Api5 at 10μM concentration for 16 hrs. Api5 is an anti-apoptotic protein and is supposed to function at a threshold of damage that is just on the verge of inducing apoptosis and not high enough to push the cells already into robust apoptosis or further, necrosis.

So, to determine that dosage of CPT-induced DNA damage, U2OS cells were treated with 10μM of CPT and harvested after increasing time points of incubation: 0.5,1,2,4,6,8,9,10,11,12,16 hours. They were subject to WB and probed for two markers of apoptosis: active Caspase 3 (cleaved p17 fragment) and active Caspase 9 (cleaved p37 fragment).

As observed in Fig 6.2.1.3A, both the active caspases showed robust activation at 16 hours. Fig 6.2.1.3 B and C represent fold change of densitometric quantification of WB for three biological replicates for active Caspase 3 and 9 respectively for the treatment groups over that for without CPT. From this, it was concluded that CPT caused robust activation of Capase3 and Caspase 9 by 16 hours in comparison to without CPT or earlier time points.

12 hours time point was chosen for further functional studies, as caspases did not show that robust an activation as was observed by 16 hours. The activation state of apoptosis pathway markers caused by 12 hours of 10μM CPT damage was considered as a control for the functional studies experiment. Since the experimental scheme involves transfections as a means of achieving target gene knockdown or over-expression, siLacZ was transfected into this "control" set so as to normalize for the effect of transfections. The effect of target gene knockdown/overexpression was elucidated by comparing the levels of protein/activation of the marker proteins with that of the aforementioned control. Any difference that was observed over the control could be attributed to the target gene by a suitable cause and effect relationship, thus revealing the function of the target gene in the apoptosis pathway.
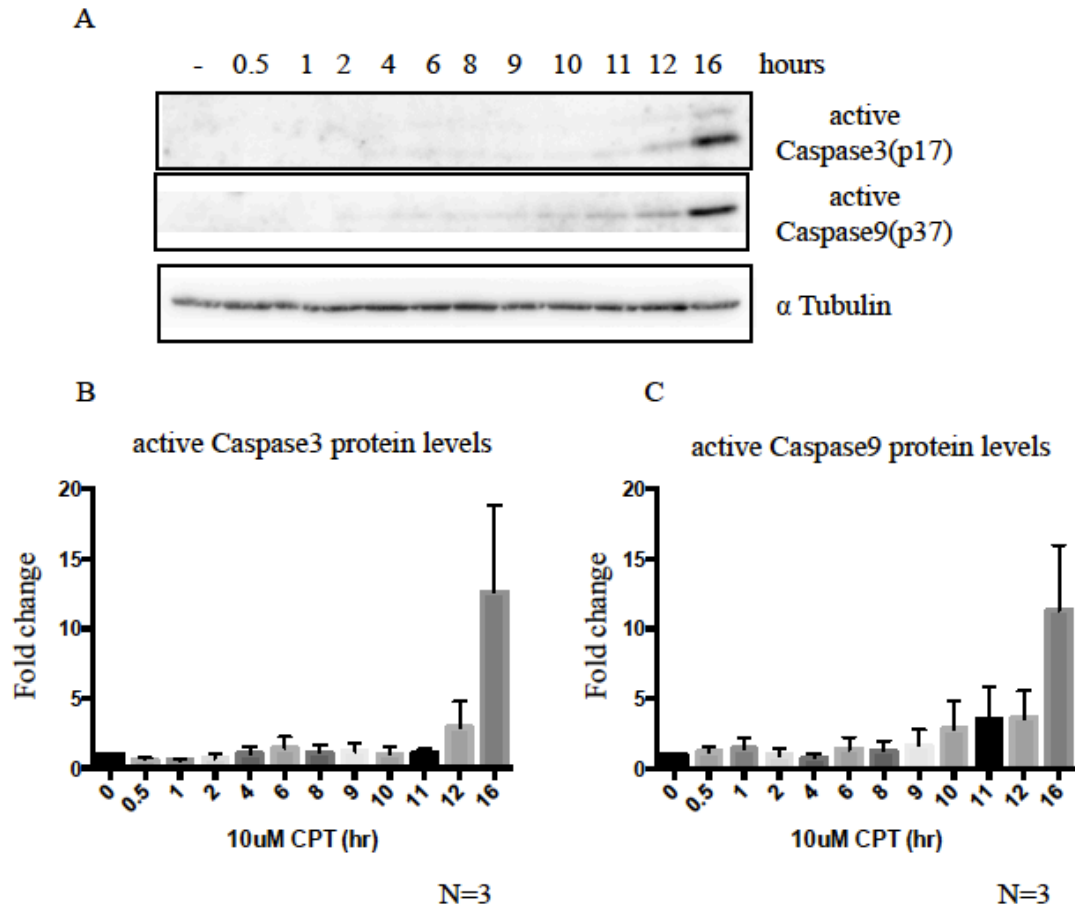
Figure 6.2.1.3: Camptothecin caused time-dependent activation of the apoptotic pathway as observed by Caspase activation.

(A)U2OS cells treated without or with 10μM CPT and harvested after 0.5,1,2,4,6,8,9,10,11,12 and 16 hours subjected to WB and probed for active Caspase 3, active Caspase 9 and αTubulin (upper, middle and lower panels). (B and C) plots showing fold change in active caspase 3 and 9 protein levels respectively across the treatment group over without CPT as quantified by densitometry of western blots (N=3, error bars represent SEM)

6.2.1.4: Ectopically expressed Api5 showed a decrease in protein levels upon CPT treatment

Api5 protein exhibits an elongated all α helical structure, its N, and C termini resemble HEAT and ARM repeats respectively and hence it is predicted to be functioning as a scaffolding protein (Han et al., 2012a). It is supposed to be carrying out its anti-apoptotic function as an outcome of its stability in response to stimuli, which may be regulated by its acetylation status. Han et al. predicted that Api5 is readily acetylated and thus stabilized after its synthesis and remains inactive. However, apoptotic stimuli generating from serum starvation can deacetylate the protein, leading to its degradation and carry out its anti-apoptotic function in the way. However, specific acetyltransferases, deacetylases or ubiquitination of Api5 are not known yet.

Functional studies of Api5 were performed at all three levels of the protein: knockdown of endogenous protein by transfecting with siApi5-1, the rescue of protein levels by co-transfecting siApi5-1 with mut-1 Api5 mVenusC1 plasmid, as well as overexpression of the protein over and above its endogenous level by co-transfecting siLacZ with mut-1 Api5 mVenusC1. TopBP1 was studied only at its endogenous level (siLacZ) and knockdown (siTopBP1). All the transfection sets were performed in the pair without and with damage.

Near complete knockdown of Api5 and TopBP1 were achieved by siApi5-1 (lanes 5,6,7,8) and siTopBP1 (lanes 9,10) siRNAs (Fig 6.2.1.4 A, B, C). mut-1 Api5 mVenus expressed Api5 mVenus protein both in the background of siLacZ (lanes3,4) and siApi5-1 (lanes 7,8) as detected by the GFP antibody at expected size, indicating that the mutagenesis was successful in rendering the Api5 construct siRNA-resistant.

Ectopically expressed Api5 exhibited a significant decrease in protein levels upon damage in comparison to without it (Fig 6.2.1.4 A, D, E). Change in protein levels in response to stimuli can be an outcome of alteration of either its transcription or degradation/stabilization. It is not immediately clear which of the two is responsible for this observation, it is clear however that this is caused by CPT-induced damage as it was observed upon LacZ as well as endogenous Api5 knockdown. This observation of a decrease in Api5 levels upon DNA damage is unique because previous studies have reported similar observation upon serum starvation and linked with its anti-apoptotic function.

124
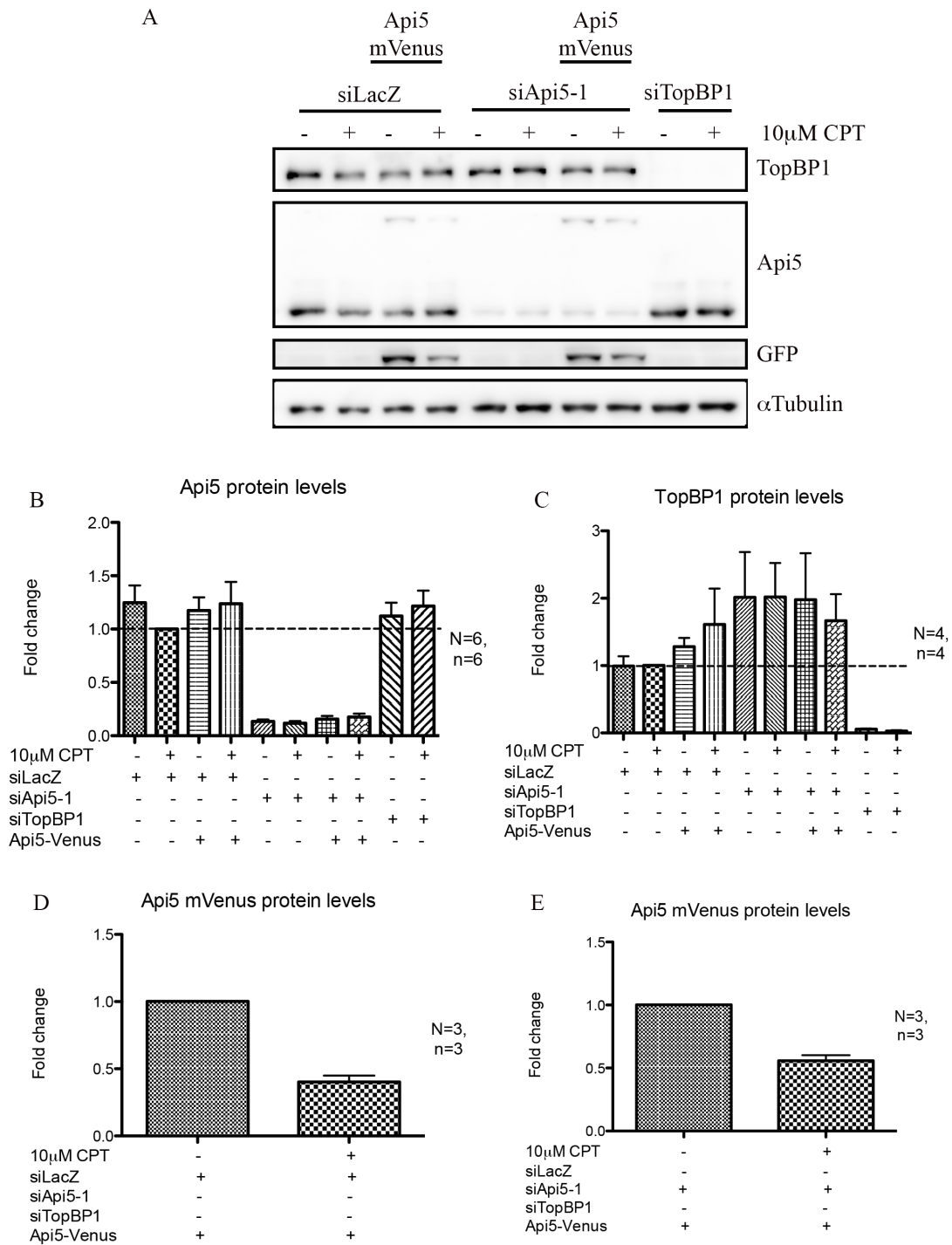
Figure 6.2.1.4: Ectopically expressed Api5 shows a decrease in protein levels upon damage.

(A) U2OS cells were transfected with siLacZ (lanes1-2), siLacZ and mut-1 Api5 mVenusC1 (lanes 3-4), siApi5-1 (lanes 5-6), siApi5 and mut-1 Api5 mVenusC1 (lanes 7-8), siTopBP1 (lanes 9-10), and each pair was treated without or with 10μM CPT for 12 hours. Western blots were probed with antibodies against TopBP1 (1st panel), Api5 (2nd panel), GFP (3rd panel), and α Tubulin (4th panel). Plots showing fold change in Api5 protein levels (B) and TopBP1 protein levels (C) across the treatment groups over siLacZ+CPT set as quantified by densitometry of WB, fold change in levels of Api5 mVenus protein upon damage in the background of LacZ knockdown (D) and Api5 knockdown (E). (N=biological replicates, n= technical replicates, error bars represent SEM)

6.2.1.5: Api5 inhibits DNA damage-induced apoptosis

As mentioned earlier, one of the important markers of Apoptosis is activation of Caspases. Under the intrinsic pathway of apoptosis that gets activated in response to DNA damage, in response to apoptotic stimuli, pro-apoptotic Bcl2 family proteins oligomerize at the Mitochondrial surface, creating pores and release of Cytochrome c and Inhibitors of apoptosis (IAPs) antagonists like Smac/DIABLO (Bratton and Salvesen, 2010; Elmore, 2007). Cytochrome c, together with APAF-1 and pro-caspase9 constitute Apoptosome (Fulda and Debatin, 2006). Pro-caspase 9 undergoes autolytic cleavage at Asp 315 to create partially active caspase 9 p35/p12 fragments (Srinivasula et al., 1998). The p12 fragment is prone to inhibition by IAPs like XIAP, survivin (Api4) (Parrish et al., 2016; Salvesen and Duckett, 2002; Silke and Meier, 2013). That, however, is taken care of, by IAP antagonists as mentioned earlier. The activated p35/p12 Caspase9 species trigger the downstream caspase activation cascade leading to apoptosis. They cleave pro-caspase3 at Asp 175 to create active caspase 3 p19/p17 fragments. The active caspase3 works in a feed-forward loop to cleave procaspase 9 at Asp 330 to create fully active p37/p10 caspase9 (Srinivasula et al., 1998; Twiddy and Cain, 2007; Zou et al., 2003). The p10 fragment is resistant from inhibition by IAPs (Zou et al., 2003). The active caspase9 p37 species is thus, a downstream cleavage product of active caspase3.

Activated caspases bring about proteolytic cleavage of a number of downstream proteins like ICAD, Acinus and PARP1 that carry out different functions leading to apoptosis and their cleavage are commonly used as markers or readouts for the

occurrence of apoptosis. PARP1 is a nuclear protein that gets activated upon DNA damage and brings about ADP-ribosylation of its targets primarily in DNA repair but also in gene transcription, immune responses, inflammation, learning, memory, synaptic functions, angiogenesis and aging (Chaitanya et al., 2010). Large amounts of DNA damage sends PARP1 on an overdrive, leading to energy deficiency within the cell and thus triggering necrosis (D'Amours et al., 2001; Soldani and Scovassi, 2002). When the DNA damage is not high enough to trigger necrosis, or low enough to be repaired, apoptosis is induced and caspases are activated. Caspase3 primarily, but also caspase7 cleaves the 113kDa PARP1 protein into a 89 kDa C-terminal fragment containing its catalytic domain and another 24 kDa N-terminal domain containing its DNA binding domain, thus inactivating the PARP1 ADP-ribosylation function (Chaitanya et al., 2010; D'Amours et al., 2001; Gobeil et al., 2001; Soldani and Scovassi, 2002).

To investigate the role of Api5 in inhibiting DNA damage induced apoptosis, levels of active caspase3 (p17), active caspase9 (p37) and PARP1 cleavage were looked at upon Api5 knockdown and rescue. Api5 overexpression decreased caspase3 activation upon DNA damage in the siLacZ background (lanes 2,4, fig 6.2.1.5 A, B). Api5 knockdown increased caspase3 activation in comparison to LacZ, whereas its rescue brought down active caspase 3 to levels close to that in siLacZ (lanes 2, 6, 8 fig 6.2.1.5A, B). TopBP1 knockdown triggered robust activation of caspase 3 and PARP1 cleavage upon damage, though it did not activate caspase9 much (lane 10, fig 6.2.1.5 A, B, C). Api5 knockdown increased capspase9 activation and PARP1 cleavage in comparison to siLacZ upon damage, but Api5 rescue and overexpression interestingly increased their levels even more rather than decreasing. This could just be an outcome of a non-linear and multi-factorial regulation between active caspase3 and caspase9 (p37) and PARP1 cleavage that could be affected by the presence of Api5. This study validates earlier reports that Api5 can inhibit DNA damage-induced apoptosis.
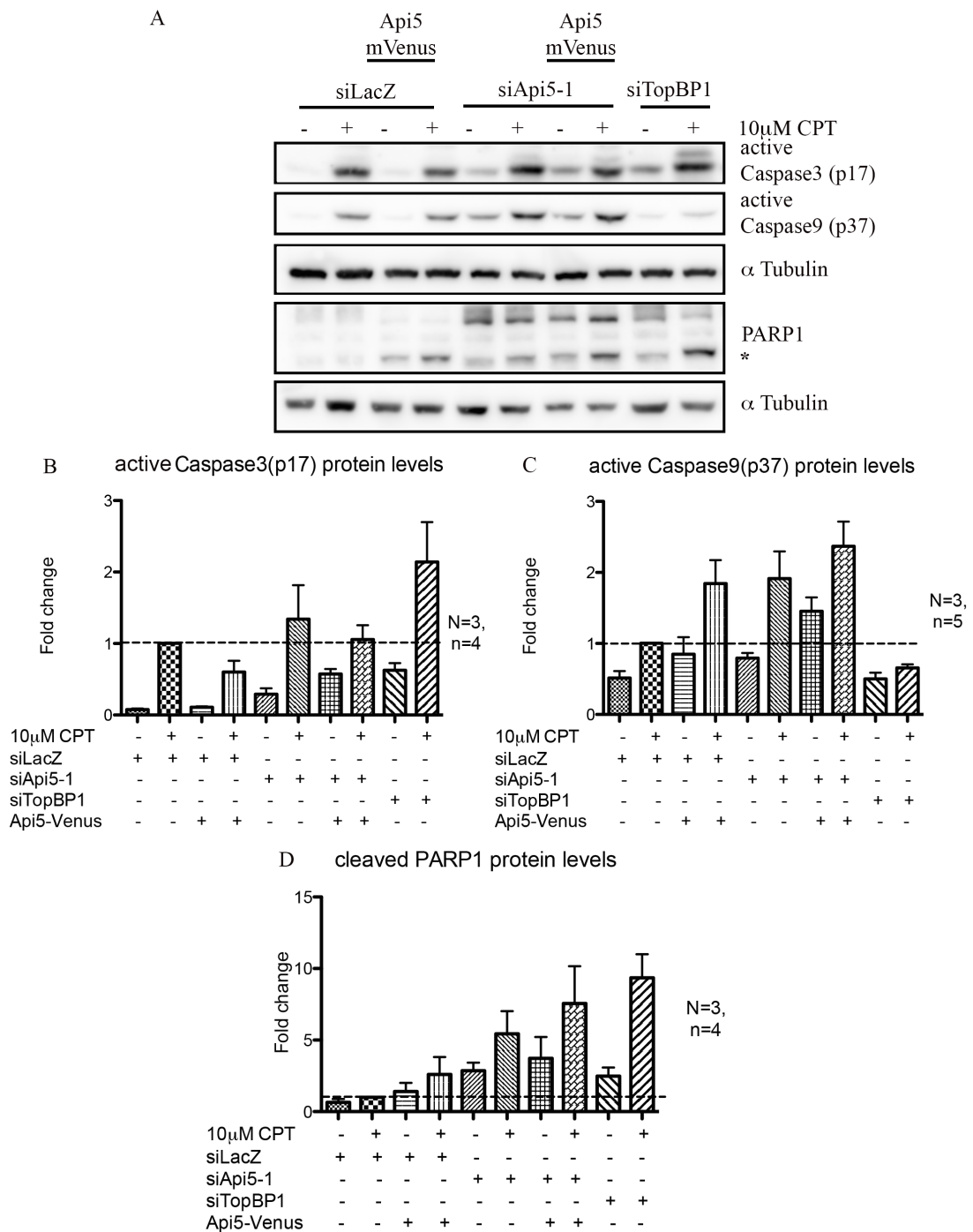
Figure 6.2.1.5: Api5 inhibits DNA damage-induced apoptosis.

(A) U2OS cells were transfected with siLacZ (lanes1-2), siLacZ+mut-1 Api5 mVenusC1 (lanes 3-4), siApi5-1 (lanes 5-6), siApi5+mut-1 Api5 mVenusC1 (lanes 7-8), siTopBP1 (lanes 9-10), and each pair was treated without or with 10μM CPT for

128

12 hours. Western blots were probed with antibodies against active Caspase3 p17 fragment (1st panel), active Caspase9 p37, (2nd panel), α Tubulin for the first two panels (3rd panel), PARP1 (4th panel) and α Tubulin for the 4th panel (5th panel). Upper band in PARP1 plot represents full-length PARP1, the lower band marked with an asterisk represents cleaved PAPR1 89kDa fragment. Plots showing fold change in active Caspase 3 protein levels (B), active Caspase 9 (C) and PARP1 protein levels (D) across the treatment groups over siLacZ+CPT as quantified from densitometry of WB. (N=biological replicates, n= technical replicates, error bars represent SEM)

6.2.1.6 Api5 knockdown led to a significant increase in p53

As mentioned earlier, Api5 inhibits E2F1 mediated apoptosis by working downstream of it. As observed in section 6.2.1.2, Api5 knockdown or rescue did not affect E2F1 protein levels itself. The next important tumor suppressor and an important regulator of apoptosis downstream of E2F1 is p53. Having established a role of Api5 in DNA damage-induced apoptosis, and a prediction of its regulatory function at a level below E2F1, it was logical to investigate how Api5 regulates p53.

p53 is phosphorylated at S15 in response to DNA damage induced checkpoint pathway activation, particularly by ATM, which leads to its stabilization (Yoshida and Miki, 2010). In our knockdown experiments, Api5 knockdown was observed to significantly increase the levels of p53 over and above its stabilization with siLacZ knockdown upon DNA damage, while Api5 rescue brought p53 levels down (lanes 2,6,8 Fig 6.2.1.6 A, C). Interestingly TopBP1 knockdown didn't have a significant effect upon p53 levels as much as Api5 did. Activation of p53 at S15 was observed in the treatment groups with CPT as expected and its profile did not reflect the effect of different transfections to levels similar to that observed for total p53 protein levels. This led us to conclude that Api5 negatively regulates p53 protein levels without much affecting its activity. The increase in p53 levels upon Api5 knockdown might be a result of either stabilization from its degradation or transcriptional up-regulation and this needs to be looked into.
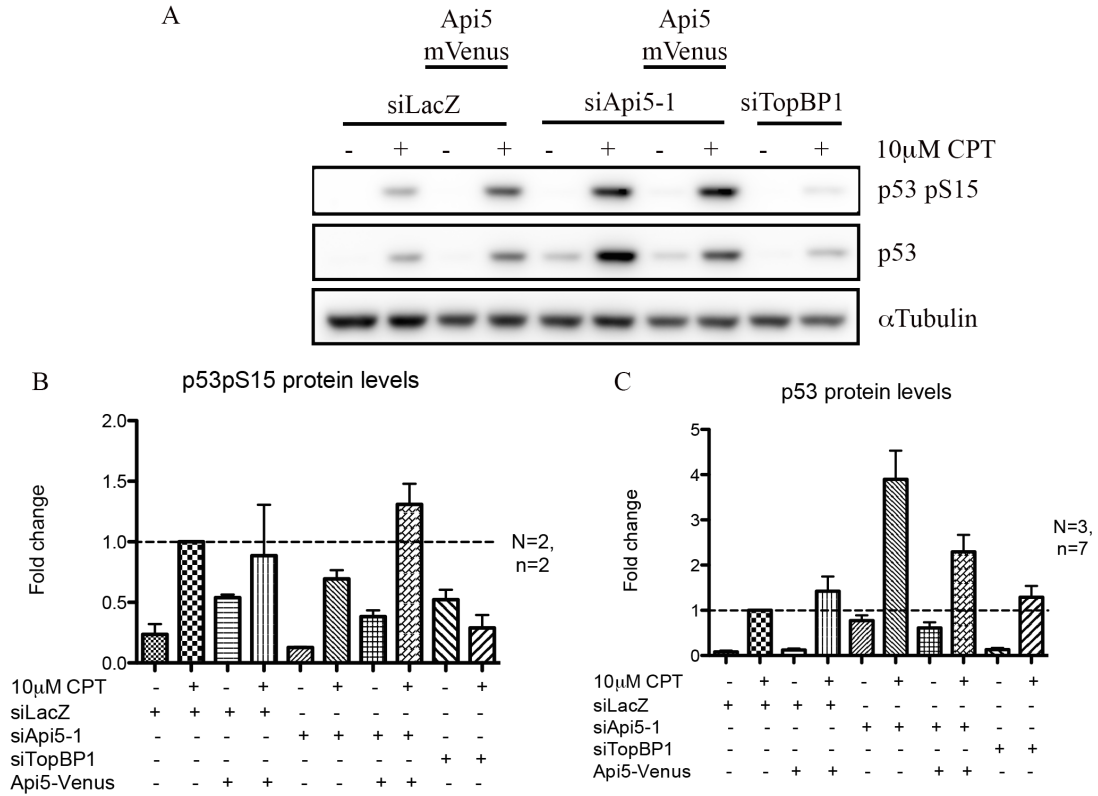
Figure 6.2.1.6: Api5 knockdown led to a significant increase in p53.

(A) U2OS cells were transfected with siLacZ (lanes1-2), siLacZ+mut-1 Api5 mVenusC1 (lanes 3-4), siApi5-1 (lanes 5-6), siApi5+mut-1 Api5 mVenusC1 (lanes 7-8), siTopBP1 (lanes 9-10), and each pair was treated without or with 10μM CPT for 12 hours. Western blots were probed with antibodies against p53 pS15 (1st panel), p53 (2nd panel) and α Tubulin (3rd panel). Plots showing fold change in p53 pS15 protein levels (B) and p53 (C) across the treatment groups over siLacZ+CPT as quantified from densitometry of WB. (N=biological replicates, n= technical replicates, error bars represent SEM)

6.2.1.7 Api5 knockdown did not cause significant difference in MDM2 protein levels upon DNA damage

As discussed in section 6.1, MDM2 binds and ubiquitinates p53 through its C-terminal E3 ubiquitin transferase, upon damage, both of them are phosphorylated by the checkpoint pathway leading to their loss of interaction and subsequent stabilization of p53 (Moll et al., 2003). MDM2 in turn is under the transcriptional control of p53, whereas p53 mediated activation of downstream Caspases lead to cleavage of the full length MDM2 (p90) to release the C-terminal E3 Ubiquitin ligase subunit and form a p60 species of MDM2 that can bind to p53 and stabilize it instead, thus completing a feedback regulation between p53 and MDM2 (Oliver et al., 2011; Pochampally et al., 1998, 1999). Bax is one of the apoptotic transcriptional targets of p53 that gets relocalized at the nuclear membrane leading to the release of Cytochrome c, thus contributing to apoptosome formation and initiating the intrinsic pathway of apoptosis upon DNA damage (Elmore, 2007; Parrish et al., 2016).

Api5 knockdown and rescue led to an insignificant (less than 2 fold) change in p53 degrading MDM2 p90 and p53 stabilizing MDM2 p60 species (lanes 2,4,6,8 Fig 6.2.1.7 A, B, C). The difference was even less significant in the case of TopBP1 knockdown (lane 10 Fig 6.2.1.7 A, B, C). Api5 knockdown, however, led to a significant increase in Bax levels upon damage, whereas TopBP1 knockdown didn't have much effect (lanes 2, 6, 10 Fig 6.2.1.7 A, D). This pattern was similar as seen for p53 in section 6.2.6. This could be explained as happening because of increase in Bax transcription from elevated levels of p53 caused by Api5 knockdown. Upregulation of pro-apoptotic Bax because of knockdown to Api5 is another evidence of its anti-apoptotic function upon DNA damage. Api5 did not significantly affect MDM2, the upstream degrader of p53, hence the increase in p53 levels upon Api5 knockdown could be a result of its transcriptional activation rather than stabilization from MDM2. Several regions of Api5 are known to have a transcriptional regulation function, but no targets are known as yet (Berghe et al.,2000). The observations from this section, however, make it interesting to look for Api5 as a negative regulator of p53 transcription.
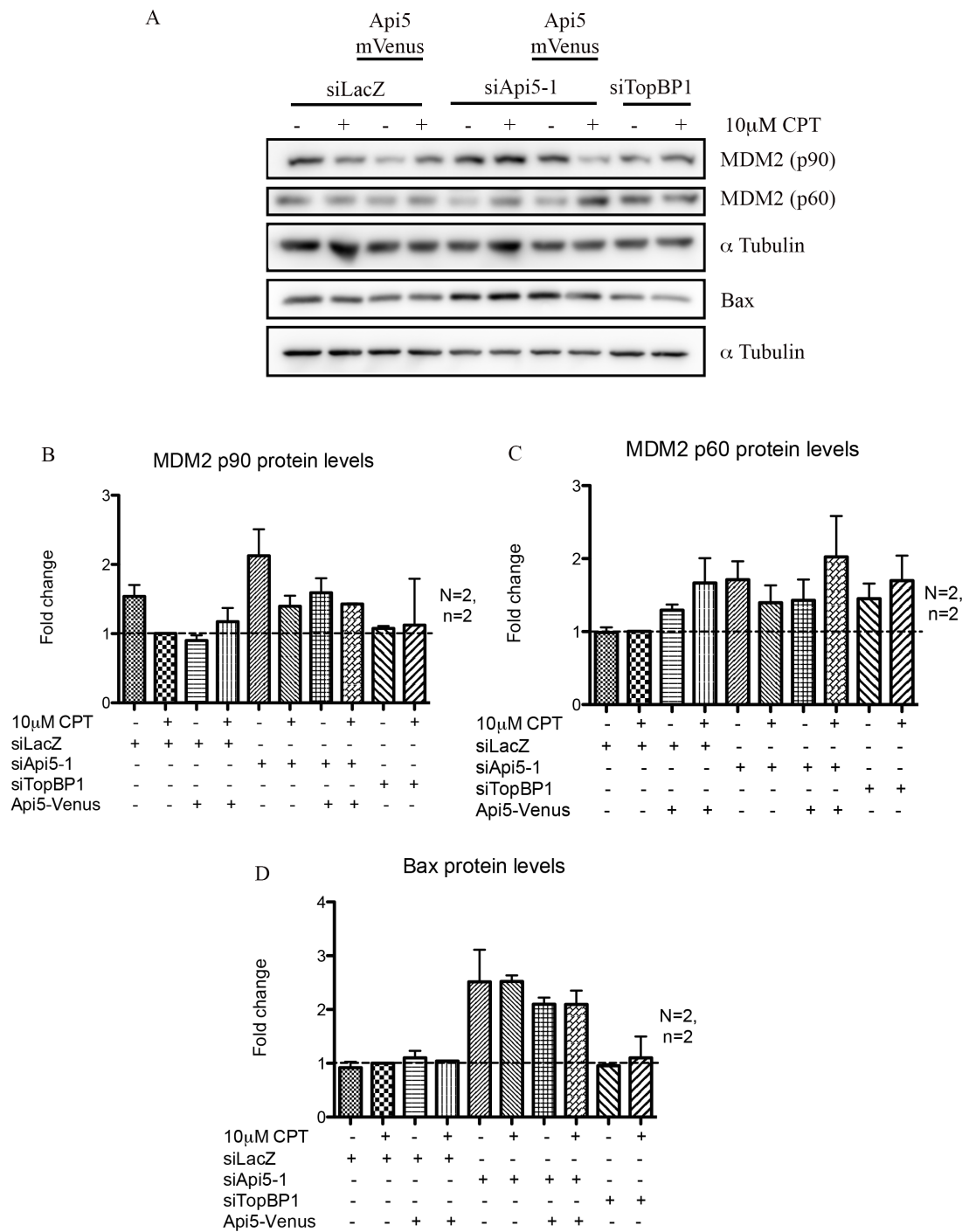
Figure 6.2.1.7: Api5 knockdown did not cause significant difference in MDM2 protein levels upon DNA damage.

(A) U2OS cells were transfected with siLacZ (lanes1-2), siLacZ+mut-1 Api5 mVenusC1 (lanes 3-4), siApi5-1 (lanes 5-6), siApi5+mut-1 Api5 mVenusC1 (lanes 7-8), siTopBP1 (lanes 9-10), and each pair was treated without or with 10μM CPT for

12 hours. Western blots were probed with antibodies against MDM2 p90 (1st panel), MDM2 p60 (2nd panel) α Tubulin for the above two (3rd panel), Bax (4th panel), α Tubulin for Bax (5th panel). Plots showing fold change in MDM2 p90 (B), MDM2 p60 (C) and Bax (D) protein levels across the treatment groups over siLacZ+CPT as quantified from densitometry of WB. (N=biological replicates, n= technical replicates, error bars represent SEM)

6.2.2 Elucidating the region of Api5 involved in its anti-apoptotic regulation function.

6.2.2.1 Cloning the different Api5 deletion mutants into mVenus C1 plasmid vector

To elucidate the region of Api5 protein involved in carrying out its anti-apoptosis function as discovered in section 6.2.1, several truncation mutants of Api5 were designed, so as to use them for rescue experiments and then look for recovery of phenotype to a level similar to that achieved by the full-length Api5 protein.

These were designed so as to include or exclude the LZD in combination with rest of the regions of the protein (Fig 6.2.2.1A). The full-length Api5 consisted of 524 amino acids. The deletion constructs designed were as follows:

- i) Api5 Δ2-3: portion of Api5 from before the beginning of LZD, comprising of 358 amino acids spanning between 1-358
- ii) Api5 LZD: only the LZD portion, comprising of 31 amino acids spanning between 358-389
- iii) Api5 Δ1-2: portion of Api5 after the LZD, comprising of 135 amino acids spanning between 389-524
- iv) Api5 Δ3: portion of Api5 without the region after LZD, comprising of 389 amino acids spanning between 1-389
- v) Api5 Δ1: portion of Api5 from LZD to the end, comprising of 166 amino acids spanning between 358-524

Api5 pGEX 4T11 was used as a template to PCR-amplify the different regions and cloned between BglII and EcoRI sites of the mVenusC1 plasmid. Api5 has an NLS near its C-terminal end. Some of the truncation mutants like Δ2-3, LZD and Δ3 missed the endogenous NLS of Api5. This would hamper the nuclear localization of

these mutants and hence their supposed function. Therefore, an NLS sequence: GAAGAAGAAGCGAAAGGTA coding for NLS peptide MDYKDDD was appended to each of the forward primers so as to introduce NLS sequence into each of the truncation mutants. Api5 Δ2-3 was amplified using Api5 mVenusC1 NLS for (Sigma) and Api5 mVenusC1 NLS d2-3 rev (Sigma) primer pair, Api5 LZD was amplified with Api5 mVenusC1 NLS LZD for (Sigma) and Api5 mVenusC1 NLS LZD rev (Sigma) primer pair, Api5 Δ1-2 was amplified using Api5 mVenusC1 NLS d1-2 for (Sigma) and Fluor Api5 Rev (IDT) primer pair, Api5 Δ3 was amplified using Api5 mVenusC1 NLS for (Sigma) and Api5 mVenusC1 NLS LZD rev (Sigma) primer set and lastly Api5 Δ1 was amplified using Api5 mVenusC1 NLS LZD for (Sigma) and Fluor Api5 Rev (IDT) primer pair. The clones obtained were confirmed by restriction digestion with BglII and EcoRI and looking for insert release at expected size (Fig 6.2.2.1 C, D, E, F, G). The clones prepared were transfected into U2OS cells and their expression was confirmed by western blotting against GFP antibody (Section 6.2.2.2). The transfected cells were also fixed and imaged under the microscope, all the constructs showed nuclear localization (data not shown).
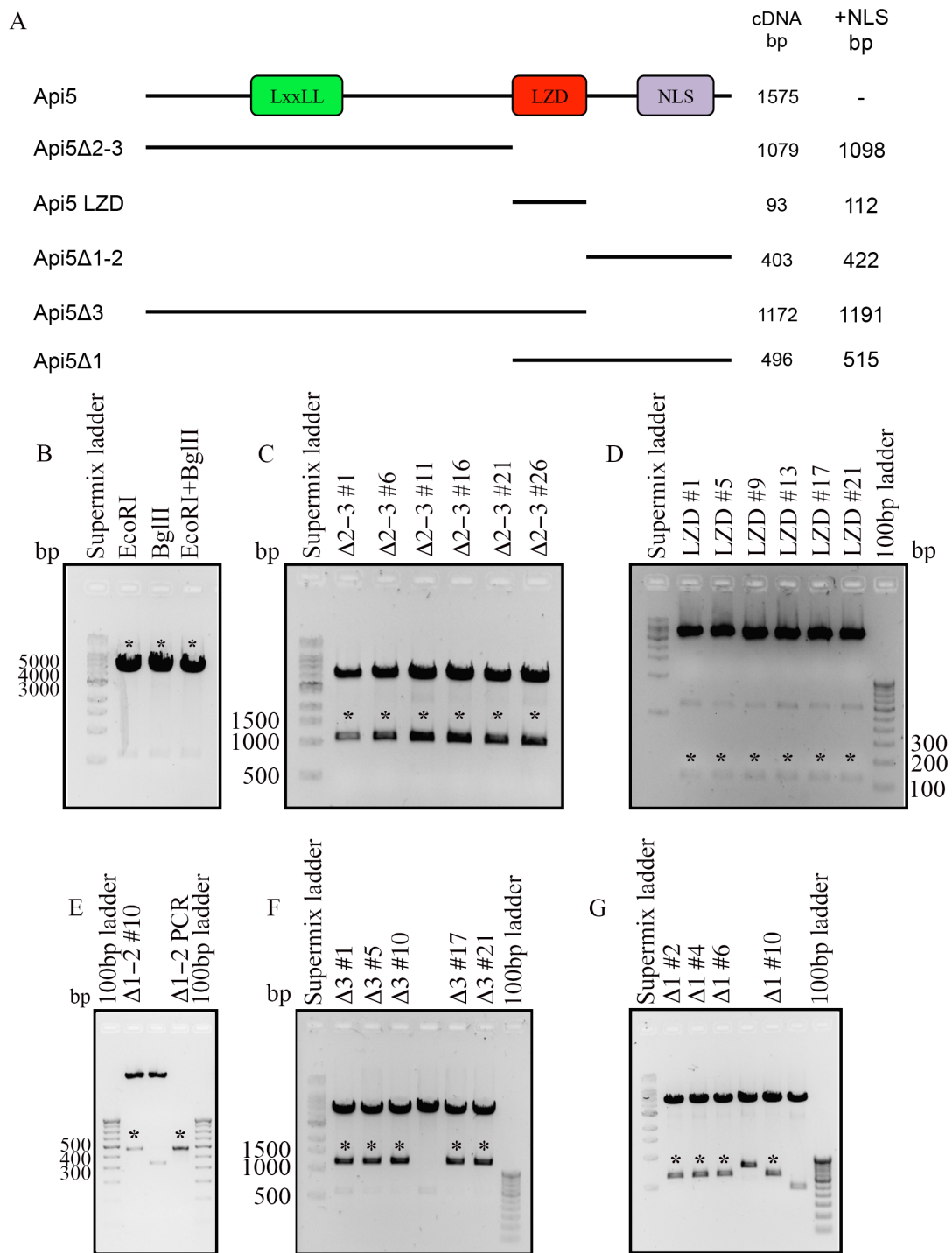
Figure 6.2.2.1: Cloning of Api5 deletion constructs into mVenusC1.

(A) Schematic of Api5 and its deletion constructs indicating each of their cDNA sizes and corresponding sizes of amplicon after addition of NLS used for cloning as well as the size of fragment release upon restriction digestion to confirm the cloning. EtBr-stained agarose gels imaged under UV trans-illuminator showing single and double

digestion profile of empty mVenusC1 plasmid (B); asterisks mark insert release from mVenusC1 vector upon restriction digestion: (C) six different positive clones of Δ2-3 construct showing release of 1098 bp fragment, (D) six different positive clones of LZD construct showing release of 112 bp fragment, (E) two different positive clones of Δ1-2 construct showing release of 422 bp fragment and (F) five different positive clones of Δ3 construct showing release of 1191 bp fragment and (G) four different positive clones of Δ1 showing a release of 515 bp

6.2.2.2 Region of Api5 protein between its N-terminal and LZD was critical for its stability upon DNA damage

For carrying out Api5 knockdown and rescue with truncation mutants experiment, the knockdown was carried out by two different siRNAs so as to avoid the requirement of mutating each of the five different truncation constructs so as to make them siRNA-resistant. While siApi5-1 targets "AGGCCGACCTAGAACAGACCTTCA" Api5 sequence, which lies in a region between N-terminal and LZD, siApi5-3 targets "AACAGAAGAGAACAAGATTAAAGT" Api5 sequence in a region between LZD and C-terminal. Both the siRNAs were able to knock down Api5 to comparable levels (lanes 3-12, 15-20 Fig 6.2.2.2 B, C, D).

U2OS cells were transfected with the different Api5 mVenusC1 NLS truncation mutants prepared in section 6.2.2.1. All the mutants expressed recombinant Api5 deletion proteins at expected size as analyzed after WB with GFP antibody (Fig 6.2.2.2 A, B).

The transfectants were treated without or with 10μM CPT-induced damage for 12 hours. Full-length, as well as the deletion constructs, showed a decrease in Api5 levels upon DNA damage. The Δ1-2, Δ1 and LZD deletion constructs that lacked the region of Api5 between its N-terminal and LZD showed a significant decrease in protein levels upon DNA damage in comparison to those containing the above region namely, Δ2-3 and Δ3 (Fig 6.2.2.2 F, G, H, I, J).

This proves the region between its N-terminal and LZD is important for the stability of protein. This could be explained due to the presence of a LxxLL motif in that region which is supposed to impart stability to the protein structure (Han et al., 2012a).

A

	protein kDa	+Venus kDa
Api5	60	89
Api5Δ2-3	40	69
Api5 LZD	3	32
Api5Δ1-2	14	43
Api5Δ3	44	73
Api5Δ1	18	47

B

137
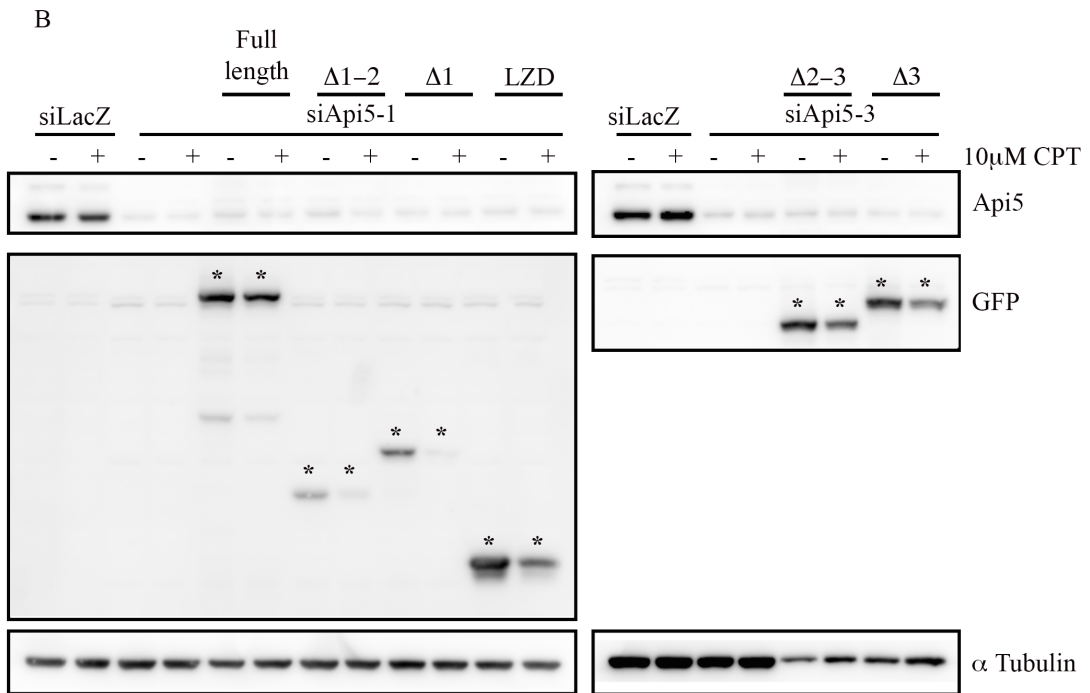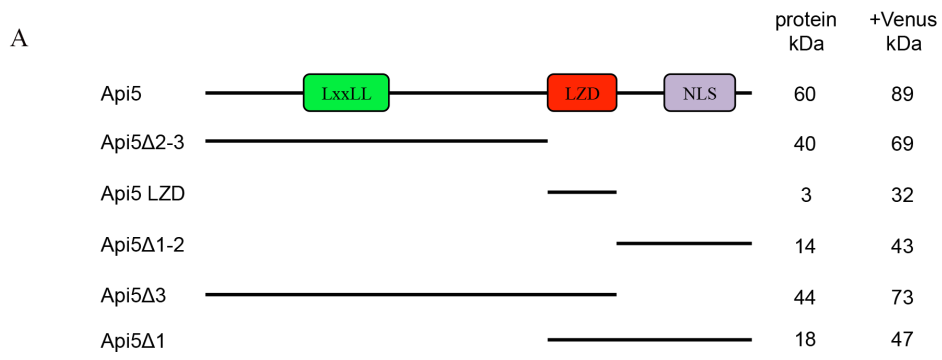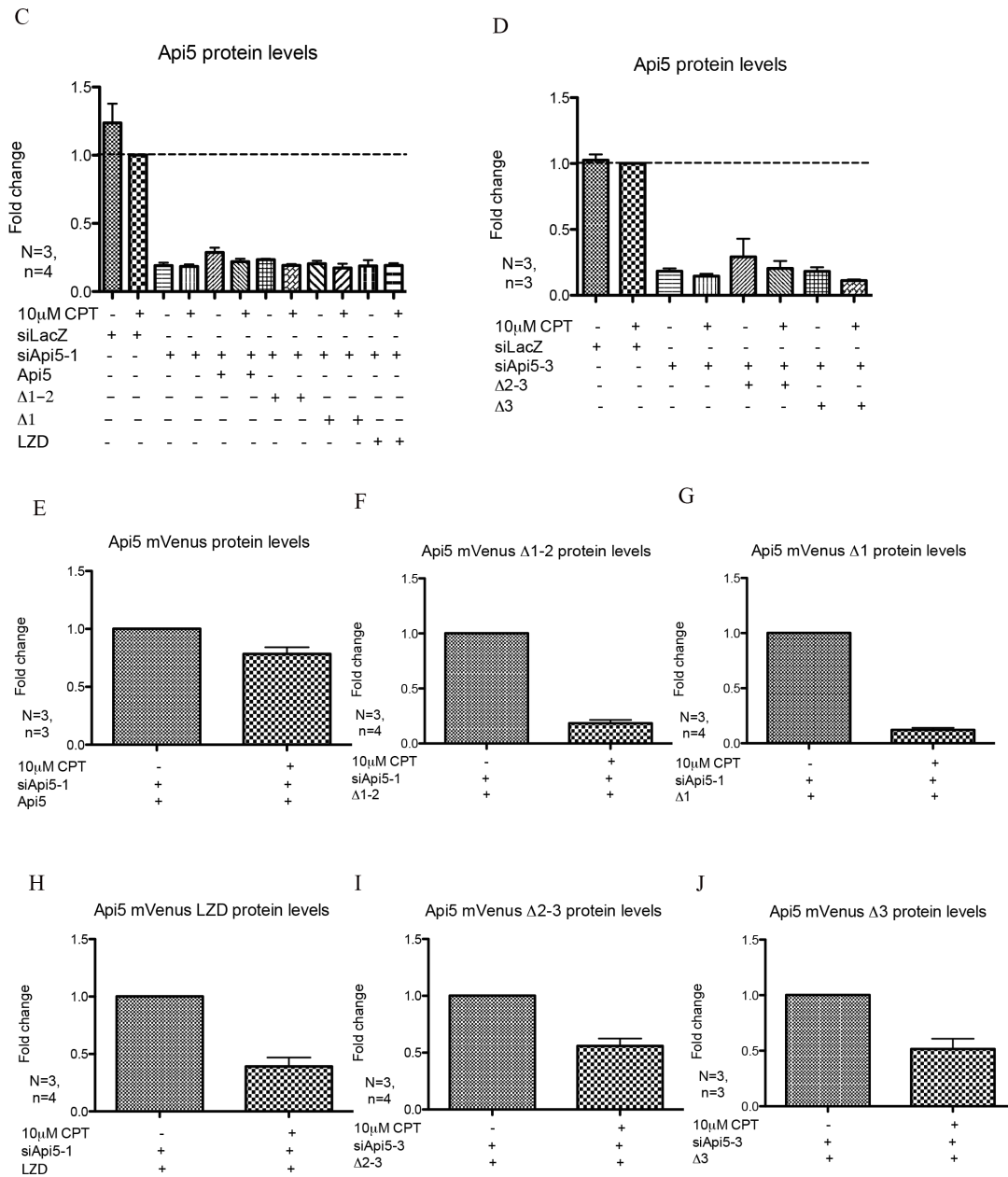
Figure 6.2.2.2: Api5 knockdown and rescue with truncation mutants.

(A) Schematic of Api5 and its truncation mutants indicating the molecular weight of proteins. mVenus fusion adds additional 29 kDa to each of the proteins and the molecular weights of each of the mVenus recombinant Api5 truncation mutants is also mentioned (B) U2OS cells were transfected with siLacZ (lanes1-2), siApi5-1 (lanes 3-4), siApi5-1+mut-1 Api5 mVenusC1 (lanes 5-6), siApi5-1+Api5 Δ1-2 mVenusC1 NLS (lanes 7-8), siApi5-1+ Api5 Δ1 mVenusC1 NLS (lanes 9-10), siApi5-1+Api5 LZD mVenusC1 NLS (lanes 11-12), siLacZ (lanes 13-14), siApi5-3

(lanes 15-16), siApi5-3+Api5 Δ2-3 mVenusC1 NLS (lanes 17-18), siApi5-3+Api5 Δ3 mVenusC1 NLS (lanes 19-20) and each pair was treated without or with 10μM CPT for 12 hours. Western blots were probed with antibodies against Api5 (upper panels), GFP (middle panels) and α Tubulin (bottom panels). Plots showing fold change in Api5 (B and C) protein levels across the treatment groups over the siLacZ+CPT set as quantified from densitometry of WB. Plots showing fold change in levels of Api5 mVenus full length (D), Δ1-2 (E), Δ1 (F), LZD (G), Δ2-3 (H), Δ3 (I) recombinant proteins upon DNA damage over without damage in the background of endogenous Api5 knockdown (N=biological replicates, n= technical replicates, error bars represent SEM)

6.2.2.3 The region between N-terminal and LZD of Api5 was responsible for its anti-apoptotic activity.

Api5 was knocked down and rescued using its different deletion constructs as mentioned earlier. Api5 knockdown led to an increase in active caspase 3 upon damage in comparison to siLacZ (lanes 2,4, 14, 16 Fig 6.2.2.3 A, B, C). Rescue with Δ2-3 and Δ3 brought down the levels of active caspase 3 much more than LZD or Δ1-2 and Δ1, which intriguingly appeared to raise active caspase 3 levels over siApi5-1 upon damage (Fig 6.2.2.3 A, B, C). From this, it can be concluded that the 1st region of Api5 between its N-terminal and LZD is responsible for carrying out apoptosis inhibition function as the deletion constructs that lacked this region were not able to reduce the levels of active caspase 3 in the background of endogenous Api5 knockdown, as is done by the full-length Api5 protein.
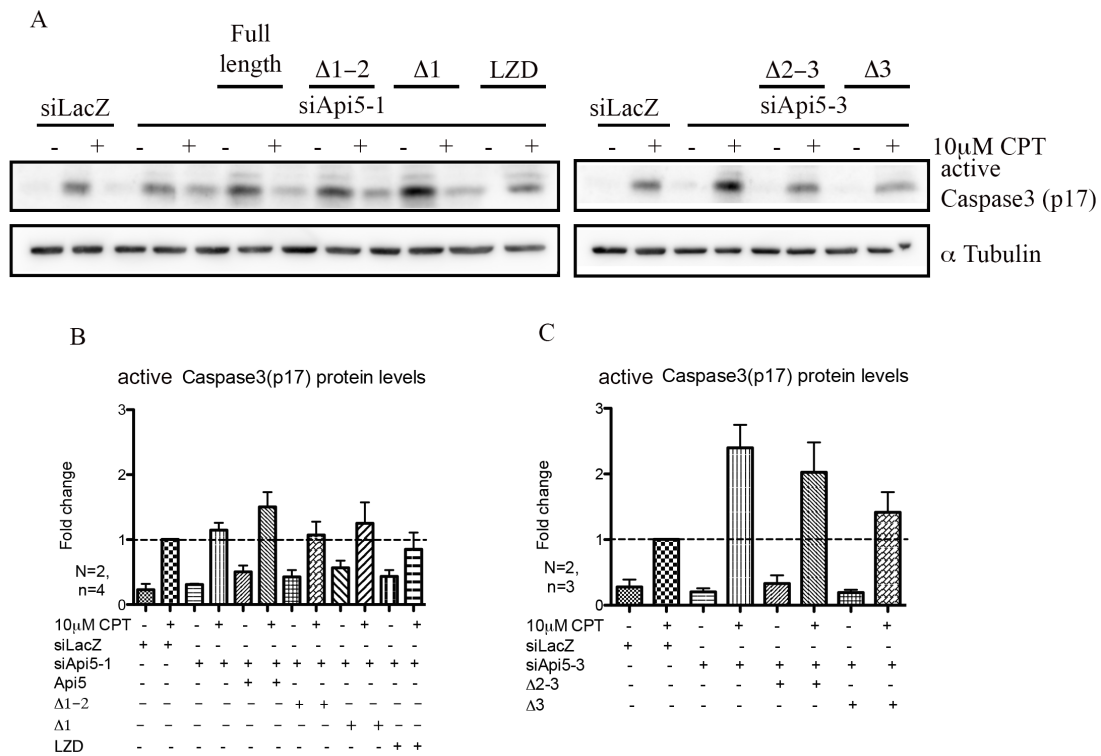
Figure 6.2.2.3: The region between N-terminal and LZD of Api5 was responsible for its anti-apoptotic activity.

U2OS cells were transfected with siLacZ (lanes1-2), siApi5-1 (lanes 3-4), siApi5-1+mut-1 Api5 mVenusC1 (lanes 5-6), siApi5-1+Api5 Δ1-2 mVenusC1 NLS (lanes 7-8), siApi5-1+ Api5 Δ1 mVenusC1 NLS (lanes 9-10), siApi5-1+Api5 LZD mVenusC1 NLS (lanes 11-12), siLacZ (lanes 13-14), siApi5-3 (lanes 15-16), siApi5-3+Api5 Δ2-3 mVenusC1 NLS (lanes 17-18), siApi5-3+Api5 Δ3 mVenusC1 NLS (lanes 19-20) and each pair was treated without or with 10μM CPT for 12 hours. Western blots were probed with antibodies against active Caspase 3 (upper panels) and α Tubulin (bottom panels). Plots showing fold change in active Caspase 3 (B and C) protein levels across the treatment groups over siLacZ+CPT as quantified by densitometry of WB. (N=biological replicates, n= technical replicates, error bars represent SEM)

140

6.2.2.4 Different regions of Api5 were able to rescue the p53 phenotype observed upon Api5 knockdown to different extents

Elevation of total p53 protein levels upon Api5 knockdown over and above its stabilization caused by DNA damage was one important discovery we made earlier. Rescue with full-length exogenous Api5 was able to revert this phenotype as shown earlier. To elucidate which region of Api5 is responsible for such regulation of p53, the rescue was performed with the different constructs as well as with full-length Api5. Interestingly, all the deletion constructs of Api5 were able to reduce the levels of p53 in the background of endogenous Api5 knockdown to levels comparable to that by ectopically expressed full-length Api5 (Fig 6.2.2.4 A, B, C). From this observation, it can be concluded that each of the three regions of Api5 or an additive combination of them is sufficient to bring about the negative regulation of p53 protein levels.
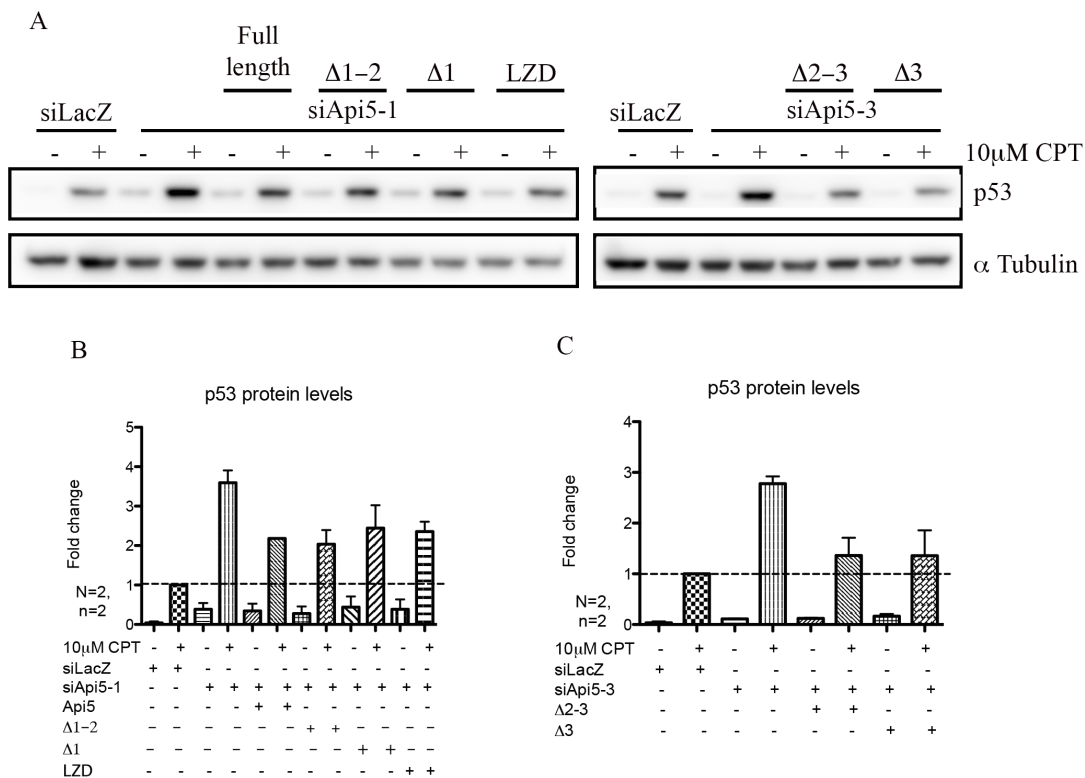
Figure 6.2.2.4: Different regions of Api5 were able to rescue the p53 phenotype observed upon Api5 knockdown to different extents.

U2OS cells were transfected with siLacZ (lanes1-2), siApi5-1 (lanes 3-4), siApi5-1+mut-1 Api5 mVenusC1 (lanes 5-6), siApi5-1+Api5 Δ1-2 mVenusC1 NLS (lanes 7-8), siApi5-1+ Api5 Δ1 mVenusC1 NLS (lanes 9-10), siApi5-1+Api5 LZD mVenusC1 NLS (lanes 11-12), siLacZ (lanes 13-14), siApi5-3 (lanes 15-16), siApi5-3+Api5 Δ2-3 mVenusC1 NLS (lanes 17-18), siApi5-3+Api5 Δ3 mVenusC1 NLS (lanes 19-20) and each pair was treated without or with 10μM CPT for 12 hours. Western blots were probed with antibodies against active p53 (upper panels) and α Tubulin (bottom panels). Plots showing fold change of active p53 (B and C) protein levels across the treatment groups over siLacZ+CPT as quantified from densitometry of WB. (N=biological replicates, n= technical replicates, error bars represent SEM)

142

6.3 Discussion

This section set out with finding the role of Api5 in the signaling cascade that gets activated at the level of checkpoints and leads to apoptosis upon DNA damage. Earlier reports had shown Api5 to be probably working downstream of E2F1 inhibiting the apoptosis signaling initiated by it. Only one downstream target of E2F1 that is, APAF-1 was identified to be targeted by Api5, but there was no information on other important regulators of apoptosis pathway that work downstream of E2F1. As discussed earlier, p53 is an important tumor suppressor that works downstream of E2F1 and regulates cell process like cell cycle and apoptosis in conjunction with E2F1. We identified p53 as a major target of Api5 regulation upon DNA damage. Api5 was identified as a negative regulator of p53 protein as its knockdown led to a sharp increase, whereas rescue led to decrease in levels of p53. This change in protein levels was over and above that seen because of stabilization vs degradation of p53 with or without damage. Surprisingly Api5 knockdown and rescue didn't alter the levels of the MDM2 significantly, which is the upstream regulator of p53. Given the literature suggesting Api5 as having a putative transcription regulation function, the possibility of transcriptional inhibition of p53 by Api5 can't be ruled out and makes it an interesting avenue to explore. Negative regulation of p53 by Api5 also mirrored in that of its apoptotic transcriptional target Bax, however, the effect on other targets need to be explored.

TopBP1 is known to inhibit both E2F1 and p53 apoptosis transcriptional targets without affecting their protein levels directly. Our studies showed that while Api5 does not affect the levels of E2F1, it does affect the levels of p53. Owing to the interaction between the Api5 and TopBP1, it is possible that they cooperatively regulate the E2F1-p53 apoptosis signaling axis. This can be addressed by carrying out TopBP1/Api5 double knockdown experiments and look for redundant or additive readouts on apoptosis markers (preferably E2F1/p53 transcriptional targets). Double knockouts could, however, be lethal to the cells owing to major anti-apoptotic roles of both the proteins. Rescue with deletion mutants further revealed that each of the three regions of Api5 that were incorporated into the mutants was capable of exhibiting that regulation of p53 protein levels which was observed for the full-length protein. However, the region of Api5 between its N-terminal and LZD was responsible for

carrying out the anti-apoptosis function upon DNA damage as revealed by the Caspase activation studies.

6.4 Summary

Using a combination of knockdown and rescue, this chapter addressed the functional characterization of Api5 in apoptosis signaling. Api5 knockdown was shown to activate the caspases upon DNA damage over and above that without any gene knockdown, and this was rescued upon Api5 re-introduction to prove that Api5 inhibits DNA damage-induced apoptosis. Api5 was also identified as a negative regulator of p53 protein levels, which is an important downstream regulator of E2F1 initiated apoptosis signaling. Api5 was thus discovered to be functioning at a level below E2F1 at the level of p53.

Chapter 7: Discussion

The primary objective of every life form is to pass on its genetic material to the next generation, intact and without undesirable changes. At the organism level, this faithful transmission of genetic material is achieved by meiosis or mitosis depending upon whether the organism follows sexual or asexual reproduction. At the cellular level, cell division is required not only for the production of gametes ensuring passage of the genome to next generation but is also important for normal growth and maintenance of the body. The efficacy of cell division in delivering genetic material to its daughter cells may be compromised if the genome has acquired mutations arising from DNA damage. This threat is real as each of the ~10^3 cells of human body receives tens of thousands of DNA lesions per day, sources of which can be intrinsic as well as extrinsic (Jackson and Bartek, 2010). DNA damage is a kind of stress, which if not taken care of might lead to accumulation of undesirable mutations in the genome that can disturb cellular homeostasis.

Cells mount a DNA damage response (DDR) to tackle the onslaught of DNA damage on their genomic integrity and cellular homeostasis. DDR is a comprehensive response that involves activation of an intricate network of pathways achieved by concomitant modulation of chromatin remodeling, gene transcription, protein synthesis, post-translational modifications (PTMs), protein degradation, translocation, nuclear export/import as well as metabolism (Shiloh, 2001). This leads to activation and synchronized interplay between checkpoint signaling, DNA repair, and apoptosis pathways as discussed earlier and failure of either of them leads to accumulation of mutations, leading to genomic instability which is one of the major causal agents of cancer.

The importance of DDR pathway in maintaining genomic integrity is evidenced by the fact that a number of key players of the signaling pathway are mutagenized in a wide variety of cancers and these mutations lead not only to initiation but also development and metastasis of cancers; whole genome sequencing has revealed mutations in components of DDR with a high frequency in a large number and variety of human cancers (Weber and Ryan, 2015). A number of cancerous diseases have been known to be historically associated with mutations in components of DDR pathways. For example, xeroderma pigmentosum (XP) is caused my mutations in

nucleotide excision repair (NER) pathway proteins, Lynch syndrome is caused by mutations in human mismatch repair proteins (Msh2/Msh6), 50% of all human cancers are known to harbor p53 loss of function mutations, BRCA1, and 2 mutations are associated with hereditary breast cancer (Broustas and Lieberman, 2014; Deng, 2006; Jeggo et al., 2016; Ozaki and Nakagawara, 2011). Accumulation of genomic instability because of mutations in DDR pathway not only potentiates cancer but can also lead to several metabolic situations like neurodegeneration, progeroid diseases, inflammation, cardiovascular diseases and diabetes (Shimizu et al., 2014).

Inhibiting DDR components is an attractive therapeutic strategy, as resistance to chemo or radiotherapy is often attributed to mutation(s) in components of DDR signaling (Weber and Ryan, 2015). The accepted model for cancer development is that it can not merely be induced by a single initiator mutation because of existence of parallel and alternative DDR signaling pathways, but is instead a multistep process that involves simultaneous or stepwise gain of function or loss of function mutations of oncogene and tumor suppressor genes respectively (Jeggo et al., 2016). Cancer therapeutics takes advantage of this and uses approaches of synthetic lethality. For example, PARP inhibitors are used to kill breast and ovarian cancers already harboring BRCA mutations (O'Connor, 2015).

Current study deals with two important components of DDR: TopBP1, which is a mediator in the ATR-Chk1 arm of checkpoint signaling, and Api5, which is an inhibitor of apoptosis.

As discussed earlier TopBP1 is a BRCT rich protein. A BRCT domain is composed of ~95 amino acids which fold as an autonomous globular domain with the secondary structure element alignment as βαββαβα: four stranded parallel β sheets, surrounded by α1 and α3 on one side and α2 on the other side (Wu et al., 2015; Zhang et al., 1998). BRCT domains can occur as single as well as canonical pairs, single BRCT domains do not, but canonical pairs do have the potential to recognize and bind phosphorylated proteins at sequence motif pSXXF (Wu et al., 2015; Zhang et al., 1998). TopBP1 was observed to interact with Api5 *in vivo* that showed an enhancement upon DNA damage (Fig 4.2.2). Protein phosphorylation prediction databases (UniProt and PhosphSite Plus) predict phosphorylation of Api5 at multiple residues and considering the phospho-protein binding nature of TopBP1, it could be speculated that interaction between the two may be dependent upon this PTM.

However, the dependence of their interaction on phosphorylation of Api5 can be ruled out by the findings of *in vitro* interaction studies which showed that the two *in bacto* purified recombinant proteins interacted with each other as shown by far western blotting analysis (Fig 3.2.1.3). Interestingly, BRCT 7 and 8 of TopBP1 were involved in this interaction (Fig 3.2.2.6) that form a canonical pair and are supposed to bind with phosphorylated proteins. However, there are known exceptions to this: the tandem BRCT repeats of BRCA1 interact with DNA-PKcs in a phospho-independent manner (Davis et al., 2014).

Api5 on the other hand interacts with TopBP1 through a region between its N-terminal and LZD encompassing α1 to α17 (Fig 3.2.2.4). α1-α11 of Api5 resemble HEAT repeat, whereas the region beyond from α12 to α19 till its C-terminal resembles ARM repeats. It can be concluded that both the HEAT and ARM-like regions of Api5 are involved in its interaction with TopBP1. HEAT and ARM repeat motifs are composed of tandem repeats of closely packed α helices, each 50 amino acid long. They have arisen because of gene duplication, are phylogenetically related and have similar structures as well. In both the motifs, the repeats stack together to form a single domain in the shape of an elongated helix with a continuous hydrophobic core and concave surface. They are known as protein scaffolding motifs that are involved in protein-protein interactions (Andrade et al., 2001; Neuwald and Hirano, 2000b).

Cell fractionation studies showed that Api5 is bound to chromatin (Fig 5.2.2) and this could be because of its direct binding to DNA as evidenced by EMSA studies (Fig 5.2.1 A,B,C) proving that lack of basic DNA binding region in its LZD does not limit its interaction with DNA as it happens anyway.

Api5 is believed to be a nuclear protein, just like TopBP1 but it was observed to be present in the cytoplasmic fraction as well unlike TopBP1 (Fig 5.2.2). This is important because protein translocation and nuclear export is a way just like its transcription or PTM to modulate its function as mentioned earlier. Nuclear export of Api5 could be felicitated either by piggybacking on some other protein or its direct export. Considering the known interactors of Api5, FGF2 is found in nucleus as well as cytoplasm, but the interaction happens exclusively in the nucleus (Berghe et al., 2000; Sinowatz et al., 2000), Acinus is a nuclear protein, which is part of spliceosomes, exon junction complexes (EJC) as well as apoptosis and splicing-

147

associated protein (ASAP) complexes, it undergoes caspase-mediated cleavage which then potentiates itself to carry chromatin condensation, interaction with Api5 again happens in the nucleus (Joselin et al., 2006; Rigou et al., 2009; Sahara et al., 1999; Schwerk et al., 2003; Tange et al., 2005). ALC1 is a chromatin remodeling enzyme similar to the SNF2 family of chromatin modifiers which are found in the nucleus as well (Ahel et al., 2009; Mohrmann and Verrijzer, 2005). Owing to the nuclear localization of the interaction of Api5 with all its known interactors, its putative nuclear export can't be expected by virtue of them. Export of proteins from the nucleus is modulated by their transport through the CRM-1 pathway which identifies a consensus nuclear export signal (NES) L-x(2,3)-[LIVFM]-x(2,3)-L-x-[LI] where x is any amino acid while L,I,V,F,M are hydrophobic amino acids (Kosugi and Hasebe, 2008). Interestingly, analysis of Api5 revealed a peptide sequence LQVYIRQLRL between 388th and 397th residues that quite closely resemble the NES consensus signal. So it will be interesting to investigate putative nuclear export of Api5, correlate it with its activity and the role of this sequence in the process, though the role of some unknown interactor in its nuclear export felicitation cannot be ruled out at the moment.

Api5 did not form nuclear foci with or without damage or across any of the cell cycle phases unlike TopBP1 (Fig 5.2.3, 5.2.5, 5.2.6) even though it was chromatin-bound (Fig 5.2.2). Not all proteins form foci. Ku70 and 80 are one of them even if they are bound to DNA.

Ectopically expressed Api5 showed a decrease in protein levels upon DNA damage (Fig 6.2.1.4) and this was even more pronounced in the deletion constructs that did not have the region between its N-terminal and LZD (Fig 6.2.2.2). The decrease in protein levels can either happen because of repression of transcription or because of degradation of the protein. Prior reports, however, support the concept of Api5 degradation as a means of its function upon apoptotic stimuli, whereas the deletion construct observation is supported by the fact that the constructs showing more degradation lack the LxxLL motif that has been reported to be important for providing stability to the protein.

Api5 knockdown led to an increase in active Caspase 3 levels upon DNA damage which were reduced upon Api5 rescue, proving negative regulation of DNA damage-

148

induced apoptosis by Api5 (Fig 6.2.1.5). The region between N-terminal and LZD was responsible for this anti-apoptotic activity (Fig 6.2.2.3)

Api5 knockdown increased the levels of p53 significantly over and above its stabilization upon DNA damage without much affecting its activation measured by its phosphorylation at S15, however, TopBP1 didn't have that effect (Fig 6.2.1.6). This effect could either be because of a comparable down-regulation of its primary degrador MDM2 or because of its transcriptional up-regulation. MDM2, however, did not show a concomitant change in levels (Fig 6.2.1.7) under the same experimental conditions as would be expected to bring about the change in p53 levels that was observed. Hence the possibility of transcriptional up-regulation of p53 because of Api5 knockdown could not be ruled out.

Induction of p53 response upon stress is largely dependent upon alterations in its total protein levels, which in turn is mostly governed by its PTMs like ubiquitination or phosphorylation by its regulators, changes in the rate of transcription of TP53 gene are supposed to play a minor role, however they can not be dismissed (Boggs and Reisman, 2007; Hale and Braithwaite, 1995; Oren, 1999). c-MYC/MAX was identified as an important transcriptional regulator of murine p53, which is a basic helix loop helix (bHLH) protein just like Api5 and the p53 promoter element required for its binding has an analog in human p53 promoter as well (Reisman et al., 1993). Rice Api5 was observed to interact with two DEAD-box ATP-dependent RNA helicases API5-INTERACTING PROTEIN 1 and 2 (AIP1/2) and had common function with a bHLH transcription factor TAPETUM DEGENERATION RETARDATION (TDR) in regulating transcription of rice cysteine protease gene CP1 (Fu et al., 2014; Li et al., 2011). In light of these evidences of role of bHLH proteins as transcriptional regulators, our observations of role of Api5 in negatively regulating p53 protein levels upon damage, and earlier reports of human Api5 being HLH protein, regions of which have transcription regulation function, it will be interesting to investigate whether Api5 negatively regulates p53 transcription and if so how. Interestingly wild-type p53 has been reported to repress Api5 transcription, whereas gain of function p53 mutants, as is found in the majority of cancers activates Api5 transcription (Scian et al., 2004). If transcriptional regulation of p53 by Api5 is indeed found to be true, it will make for a negative feedback transcriptional regulation between the two proteins independent of the regulation between MDM2 and p53.

149

As discussed earlier, Api5 is known to interact with Acinus, ALC1 in humans and AIP1/2 in rice. The metazoan homolog of rice AIP1/2 is UAP56 (Kammel et al., 2013). Both UAP56 and Acinus are components of exon junction complex (EJC) (Le Hir and Andersen, 2008). EJC is deposited upstream of exon-exon junctions in pre-spliced mRNA and is a key modulator of spliced mRNA (Tange et al., 2005). ALC1 (Amplified in liver cancer 1), also known as CHD1L is a component of SNF chromatin remodeling complex (Ahel et al., 2009).

Chromatin is tightly packed in the nucleus wound over nucleosomes. Gene expression requires an opening of the DNA to make access to the transcriptional machinery (Narlikar et al., 2013). This process is tightly controlled. Histone modification enzymes recognize and covalently modify specific residues on histone tails by acetylation, methylation, phosphorylation, ribosylation, and ubiquitination. ATP-dependent chromatin remodeling complexes recognize these histone marks, undergo ATP hydrolysis to mobilize the chromatin, exchanging or ejecting the nucleosome and recruiting the transcription machinery (Clapier and Cairns, 2009). These complexes are large (more than 1 MDa) multi-subunit complexes consisting of 4-17 components including characteristic ATPase subunit among others (Tang et al., 2010). They have four families: SWI/SNF, ISWI, CHD, INO80 (Längst and Manelyte, 2015). SWI/SNF family of chromatin remodeling enzymes are highly conserved across the eukaryotes: SWI/SNF (switching defective/ sucrose non-fermenting) in yeasts, BAP (Brahma associated protein) in *Drosophila*, BAF (Brg1 associated factor) in Humans (Kadoch and Crabtree, 2015). In humans, the BAF complex can have one of the two distinct ATPase subunits: hBRM (Brahma) or BRG1 (Brahma-related gene 1)(Mohrmann and Verrijzer, 2005).

Interactions of Api5 with components of exon junction and chromatin remodeling complex suggest possible roles of Api5 at transcriptional level. p53 may be one such novel target, by down-regulating which, it inhibits apoptosis.

Interestingly, TopBP1 has also been reported to inhibit E2F1 transcriptional targets by recruiting Brg1/Brm to E2F1 responsive promoters. Interactions of TopBP1 and Api5 with different components of SWI/SNF complex and with each other as shown in this study, may point towards them working in a protein complex with the multiple components of chromatin remodeling complex so as to aid and complement each

other in bringing about transcriptional regulation of apoptotic promoters leading to inhibition of apoptosis in the face of DNA damage.

Chapter 8. Future perspectives

Api5 was observed to interact with BRCT 7-8 tandem repeats of TopBP1 through a region between its N-terminal and LZD. This region of Api5 has a sequence that resembles both the HEAT and ARM protein-protein interaction motifs towards the N terminal and C terminal respectively as mentioned in Chapter 1. It will be interesting to elucidate which amongst the two regions is responsible/sufficient for its interaction with TopBP1. This can be achieved by making Api5 truncation mutants that span across α1-α11 and α12-α17 respectively and using the far western blotting approach using purified recombinant proteins. If the HEAT region of Api5 is found to be interacting with TopBP1, the role of LxxLL motif nested within the region in α6 can further be investigated as Api5 is known to interact with one of its interactors: FGF2 though that motif.

EMSA studies were performed with annealed oligos to generate dsDNA and intermediate structures like fork and bubble. It will be useful to broaden the repertoire of DNA structures tested for their binding to purified Api5 protein as different kinds of genotoxic damages can produce a wide variety of DNA damage structures which are not limited to stalled forks and bubbles; varying lengths of ssDNA-dsDNA junctions will be of particular interest.

Several approaches will be required to investigate nuclear export of Api5 as a means of its physiological function. Api5 truncation mutants can be made so as to include or exclude the putative NES in different combinations which can then be transfected into mammalian cells and the subcellular localization of the recombinant proteins studied by both biochemical approaches like sub-cellular fraction and imaging of fluorescently tagged recombinant protein. Exposing one set to DNA damage can add another dimension, as the behavior of protein upon damage, in comparison to that without damage can tell about the intracellular translocation of the protein when it is supposedly activated by DNA damage to carry anti-apoptosis function. The putative NES can further be validated by carrying out point mutations of its vital hydrophobic residues in the construct and investigate whether that abrogates the export potential of recombinant protein.

As mentioned in Chapter 1, Api5 is predicted to undergo de-acetylation for carrying out its anti-apoptotic function in which otherwise is acetylated at Lys 251 soon after

its synthesis. Validation of this will be useful in establishing the role of Api5 acetylation in its anti-apoptotic function, and this can be done by IP of Api5 form sets of cells treated with a deacetylase inhibitor like Suberoylanilide hydroxamic acid, with or without damage and probing the immunoprecipitate with an acetyl-Lysine antibody. The role of Lys 251 acetylation in its anti-apoptotic function can further be studied by knocking down endogenous Api5 and re-introducing acetylation-deficient K251R, acetylation mimic K251Q or uncharged K251A recombinant Api5 point mutants and looking for the rescue of any phenotype like caspase activation or p53 protein accumulation upon DNA damage.

Recombinant Api5 was observed to be undergoing degradation upon DNA damage, but the mechanism of this is still unknown. It will be interesting to investigate the occurrence of PTMs like ubiquitination or SUMOylation of Api5 in response to DNA damage that could mark it for degradation. It will further be pertinent to look for the pathway of degradation that it undertakes.

The transcriptional regulation studies of p53 by Api5 needed to validated by looking at transcript levels of p53 by qRT-PCR as mRNA level is a direct read out of effects of transcriptional regulation in comparison to protein levels as judged by western blotting because it has the possibility of another level of regulation by PTMs. The next step would be looking for Api5 occupancy on p53 promoter elements, which could be achieved by utilizing chromatin immunoprecipitation (ChIP) strategies. The transcriptional regulation function of Api5 on other target promoters can further be explored *in vitro* by employing luciferase reporter assays.

The possibility of Api5 and TopBP1 in a complex with other components of SWI/SNF chromatin remodeling complex can be validated by performing an Api5 IP and looking for co-immunoprecipitation of TopBP1 as well as other SWI/SNF components.

Bibliography

Abraham, R.T. (2001). Cell cycle checkpoint signaling through the ATM and ATR kinases. Genes Dev. *15*, 2177–2196.

Ahel, D., Hořejší, Z., Wiechens, N., Polo, S.E., Garcia-Wilson, E., Ahel, I., Flynn, H., Skehel, M., West, S.C., Jackson, S.P., et al. (2009). Poly(ADP-ribose)–Dependent Regulation of DNA Repair by the Chromatin Remodeling Enzyme ALC1. Science. *325*, 1240–1243.

Alves, C., and Cunha, C. (2012) Electrophoretic Mobility Shift Assay : Analyzing Protein – Nucleic Acid Interactions., Gel Electrophoresis - Advanced Techniques, Dr. Sameh Magdeldin (Ed.).

Andrade, M.A., Petosa, C., O'Donoghue, S.I., Müller, C.W., and Bork, P. (2001). Comparison of ARM and HEAT protein repeats. J. Mol. Biol. *309*, 1–18.

Arconde, T., Touriol, C., Perez, G., Navarro, M.G., and Lacazette, E. (2013). Api5 Contributes to E2F1 Control of the G1 / S Cell Cycle Phase Transition. PLOS One *8*, 1-10.

Beckerman, R., and Prives, C. (1995). Transcriptional Regulation by p53. J. Biol. Chem. *270*, 6966–6974.

Berggård, T., Linse, S., and James, P. (2007). Methods for the detection and analysis of protein-protein interactions. Proteomics *7*, 2833–2842.

Berghe, V. Den, Laurell, H., Huez, I., Zanibellato, C., and Cedex, T. (2000). FIF [Fibroblast Growth Factor-2 (FGF-2) -Interacting-Factor], a Nuclear Putatively Antiapoptotic Factor , Interacts Specifically with FGF-2. Mol. Endo. *2*, 1709–1724.

Bino, G. Del, Bruno, S., Yit, P.N., and Darzynkiewicz, Z. (1992). Apoptotic cell death triggered by camptothecin or teniposide . The cell cycle specificity and effects of ionizing radiation. Cell Prolif. *25*, 537–548.

Biology, C., Wu, Z., Zheng, S., and Yu, Q. (2009). The E2F family and the role of E2F1 in apoptosis. Int. J. Biochem. *41*, 2389–2397.

Biswas, A.K., and Johnson, D.G. (2012). Transcriptional and nontranscriptional functions of E2F1 in response to DNA damage. Cancer Res. *72*, 13–17.

Boggs, K., and Reisman, D. (2007). C/EBP β participates in regulating transcription of the p53 gene in response to mitogen stimulation. J. Biol. Chem. *282*, 7982–7990.

Boner, W., Taylor, E.R., Tsirimonaki, E., Yamane, K., Campo, M.S., and Morgan,

I.M. (2002). A Functional interaction between the human papillomavirus 16 transcription/replication factor E2 and the DNA damage response protein TopBP1. J. Biol. Chem. *277*, 22297–22303.

Brady, C.A., D, L., and Attardi, L.D. (2010). p53 at a glance. J. Cell Sci. *123*, 2527–2532.

Bratton, S.B., and Salvesen, G.S. (2010). Regulation of the Apaf-1-caspase-9 apoptosome. J. Cell Sci. *123*, 3209–3214.

Broustas, C.G., and Lieberman, H.B. (2014). DNA damage response genes and the development of cancer metastasis. Radiat. Res. *181*, 111–130.

Carey, M.F., Peterson, C.L., and Smale, S.T. (2012). Experimental Strategies for the Identification of DNA-Binding Proteins. Cold Spring Harbor Protoc. 18–34.

Carnevale, J., Palander, O., Seifried, L.A., and Dick, F.A. (2012). DNA Damage Signals through Differentially Modified E2F1 Molecules To Induce Apoptosis. Mol Cell Biol. *32*, 900–912.

Cescutti, R., Negrini, S., and Kohzaki, M. (2010). TopBP1 functions with 53BP1 in the G1 DNA damage checkpoint. EMBO J. *29*, 3723–3732.

Chaitanya, G. V, Steven, A.J., and Babu, P.P. (2010). PARP-1 cleavage fragments: signatures of cell-death proteases in neurodegeneration. Cell Commun. Signal *8*, 31.

Chen, J. Analysis of protein-protein interaction by in vivo quantitative proteomics in Caenorhabditis elegans. (2015). D i s s e r t a t i o n.

Chen, J., Rhee, S.Y., Frommer, W.B., Lalonde, S., Ehrhardt, D.W., and Loque, D. (2008). Molecular and cellular approaches for the detection of protein − protein interactions : latest techniques and current limitations. The Plant Journ. *53*, 610–635.

Choudhary, C., Kumar, C., Gnad, F., Nielsen, M.L., Rehman, M., Walther, T.C., Olsen, J. V, and Mann, M. (2012). Lysine Acetylation Targets Protein Complexes and Co-Regulates Major Cellular Functions. Science *325*, 834-840.

Christmann, M. (2003). Mechanisms of human DNA repair: an update. Toxicology *193*, 3–34.

Ciccia, A., and Elledge, S.J. (2010). Review The DNA Damage Response : Making It Safe to Play with Knives. Mol. Cell *40*, 179–204.

Clapier, C.R., and Cairns, B.R. (2009). The biology of chromatin remodeling complexes. Annu. Rev. Biochem. *78*, 273–304.

D'Amours, D., Sallmann, F.R., Dixit, V.M., and Poirier, G.G. (2001). Gain-of-

function of poly(ADP-ribose) polymerase-1 upon cleavage by apoptotic proteases: implications for apoptosis. J. Cell Sci. *114*, 3771–3778.

Davis, A.J., Chi, L., So, S., Lee, K.J., Mori, E., Fattah, K., Yang, J., and Chen, D.J. (2014). BRCA1 modulates the autophosphorylation status of DNA-PKcs in S phase of the cell cycle. Nucleic Acids Res. *42*, 11487–11501.

DeGregori, J., Leone, G., Miron, A., Jakoi, L., and Nevins, J.R. (1997). Distinct roles for E2F proteins in cell growth control and apoptosis. Proc. Natl. Acad. Sci. U. S. A. *94*, 7245–7250.

Deng, C.X. (2006). BRCA1: cell cycle checkpoint, genetic instability, DNA damage response and cancer evolution. Nucleic Acids Res *34*, 1416–1426.

Donehower, L. a, Harvey, M., Slagle, B.L., McArthur, M.J., Montgomery, C. a, Butel, J.S., and Bradley, a (1992). Mice deficient for p53 are developmentally normal but susceptible to spontaneous tumours. Nature *356*, 215–221.

Duncan, T., Trewick, S.C., Koivisto, P., Bates, P. a, Lindahl, T., and Sedgwick, B. (2002). Reversal of DNA alkylation damage by two human dioxygenases. Proc. Natl. Acad. Sci. U. S. A. *99*, 16660–16665.

Elmore, S. (2007). Apoptosis: A Review of Programmed Cell Death. Toxicol. Pathol. NIH Public Access. *35*, 495–516.

Erol, A. (2011). Deciphering the intricate regulatory mechanisms for the cellular choice between cell repair , apoptosis or senescence in response to damaging signals. Cell. Signal. *23*, 1076–1081.

Faye, A., and Poyet, J. (2010). Targeting AAC-11 in cancer therapy. Expert Opin. Ther. Targets *14*, 15–17.

Fishel, M.L., He, Y., Smith, M.L., and Kelley, M.R. (2007). Manipulation of base excision repair to sensitize ovarian cancer cells to alkylating agent temozolomide. Clin. Cancer Res. *13*, 260–267.

Flynn, R.L., and Zou, L. (2011). ATR : a master conductor of cellular responses to DNA replication stress. Trends Biochem. Sci. *36*, 133–140.

Forma, E., Brys, M., and Krajewska, W.M. (2010). TopBP1 in DNA Damage Response. DNA Repair. Dr. Inna Kruman (Ed.) *15*, 281-304.

Fridman, J.S., and Lowe, S.W. (2003). Control of apoptosis by p53. Oncogene *22*, 9030–9040.

Fu, D., Calvo, J.A., and Samson, L.D. (2012). Balancing repair and tolerance of DNA

damage caused by alkylating agents. Nat. Rev. Cancer *12*, 104–120.

Fu, Z., Yu, J., Cheng, X., Zong, X., Xu, J., Chen, M., Li, Z., Zhang, D., and Liang, W. (2014). The Rice Basic Helix-Loop-Helix Transcription Factor TDR INTERACTING PROTEIN2 Is a Central Switch in Early Anther Development. Plant Cell *26*, 1512–1524.

Fulda, S., and Debatin, K.-M. (2006). Extrinsic versus intrinsic apoptosis pathways in anticancer chemotherapy. Oncogene *25*, 4798–4811.

Garcia, V., Furuya, K., and Carr, A.M. (2005). Identification and functional analysis of TopBP1 and its homologs. DNA Repair *4*, 1227–1239.

Garner, E., and Raj, K. (2008). Protective mechanisms of p53-p21-pRb proteins against DNA damage-induced cell death. Cell Cycle 1–6.

Giglia-mari, G., Zotter, A., and Vermeulen, W. (2011). DNA Damage Response. Cold Spring Harb. Perspect. Biol. *3*, 1-19.

Ginsberg, D. (2002). E2F1 pathways to apoptosis. FEBS Lett. *529*, 122–125.

Gobeil, S., Boucher, C.C., Nadeau, D., and Poirier, G.G. (2001). Characterization of the necrotic cleavage of poly(ADP-ribose) polymerase (PARP-1): implication of lysosomal proteases. Cell Death Differ *8*, 588–594.

Greer, D.A., Besley, B.D.A., Kennedy, K.B., and Davey, S. (2003). hRad9 Rapidly Binds DNA Containing Double-Strand Breaks and Is Required for Damage-dependent Topoisomerase II β Binding Protein 1 Focus Formation. Cancer Res. *63*, 4829–4835.

Hale, T.K., and Braithwaite, A.W. (1995). Identification of an upstream region of the mouse p53 promoter critical for transcriptional expression. Nucleic Acids Res. *23*, 663–669.

Han, B., Kim, K.H., Lee, S.J., Jeong, K., Cho, J., Hee, K., Woo, T., Kim, S., Yoon, H., Suh, S.W., et al. (2012a). Helical Repeat Structure of Apoptosis Inhibitor 5 Reveals Protein-Protein Interaction Modules * □. J. Biol. Chem. *287*, 10727–10737.

Han, B., Kim, K.H., Lee, S.J., Jeong, K., Cho, J., Hee, K., Woo, T., Kim, S., Yoon, H., Suh, S.W., et al. (2012b). Helical Repeat Structure of Apoptosis Inhibitor 5 Reveals Protein-Protein Interaction Modules * □. J. Biol. Chem. *287*, 10727–10737.

Hanahan, D., and Weinberg, R.A. (2011). Review Hallmarks of Cancer : The Next Generation. Cell *144*, 646–674.

Haupt, S., Berger, M., Goldberg, Z., and Haupt, Y. (2003). Apoptosis - the p53

network. J. Cell Sci. *116*, 4077–4085.

Hellman, L. M., and Fried, M. G. (2007). Electrophoretic mobility shift assay (EMSA) for detecting protein-nucleic acid interactions. Nature protocols *2*, 1849-61.

Helwa, R., and Hoheisel, J. D. (2010). Analysis of DNA-protein interactions: From nitrocellulose filter binding assays to microarray studies. Analytical and Bioanalytical Chemistry *398*, 2551-2561.

Hongmei, Z. (2012). Extrinsic and Intrinsic Apoptosis Signal Pathway Review Scientist. Apoptosis Med. 3–22.

Horwitz, S.B, Chang, C.K., Grollman, A.P. (1971). Studies on Camptothecin: I. Effects on Nucleic Acid and Protein Synthesis. Mol. Pharmacol. *7*, 632-644.

Hsiang, Y., Lihou, M.G., and Liu, L.F. (1989). Arrest of Replication Forks by Drug-stabilized Topoisomerase I-DNA Cleavable Complexes as a Mechanism of Cell Killing by Camptothecin. Cancer Res *47*, 5077–5082.

Hsiang, Y.H., Hertzberg, R., Hecht, S., and Liu, L.F. (1985). Camptothecin induced protein-linked DNA breaks via mammalian DNA topoisomerase. J. Biol. Chem. *260*, 14873–14878.

Huang, X., King, M. A., Halicka, H. D., Traganos, F., Okafuji, M., and Darzynkiewicz, Z. (2004). Histone H2AX phosphorylation induced by selective photolysis of BrdU-labeled DNA with UV light: Relation to cell cycle phase. Cytometry Part A *62*, 1-7.

Iaquinta, P.J., and Lees, J.A. (2007). Life and death decisions by the E2F transcription factors. Curr. Opin. Cell Biol. *19*, 649-657.

Iijima, K., Ohara, M., Seki, R., Tauchi, H., and Nbs, A.T.M. (2008). Dancing on Damaged Chromatin : Functions of ATM and the RAD50 / MRE11 / NBS1 Complex in Cellular Responses to DNA Damage. DNA Repair (Amst). *49*, 451–464.

Imre, G., Berthelet, J., Heering, J., Kehrloesser, S., Melzer, I.M., Lee, B. Il, Thiede, B., Dötsch, V., and Rajalingam, K. (2017). Apoptosis inhibitor 5 is an endogenous inhibitor of caspase- 2. EMBO reports.1–12.

Jackson, S.P., and Bartek, J. (2010). The DNA-damage response in human biology and disease. Nature *461*, 1071–1078.

Jagot-Lacoussiere, L., Kotula, E., Villoutreix, B.O., Bruzzoni-Giovanelli, H., and Poyet, J.L. (2016). A cell-penetrating peptide targeting AAC-11 specifically induces cancer cells death. Cancer Res. *76*, 5479–5490.

158

Jeggo, P.A., Pearl, L.H., and Carr, A.M. (2016). DNA repair, genome stability and cancer: a historical perspective. Nat. Rev. Cancer *16*, 35–42.

Jensen, E.C., (2013). Overview of Live-Cell Imaging : Requirements and Methods The Anatomical Record. *8*, 1–8.

Jensen, O.N. (2004). Modification-specific proteomics : characterization of post-translational modifications by mass spectrometry. Curr. Opin. Chem. Biol. *8*, 33-41.

Johnson, R.D., and Jasin, M. (2000). Sister chromatid gene conversion is a prominent double-strand break repair pathway in mammalian cells. EMBO J. *19*, 3398–3407.

Johnson, N., Ng, T.T.C., and Parkin, J.M. (1997). Camptothecin causes cell cycle perturbations within T-lymphoblastoid cells followed by dose dependent induction of apoptosis. Leuk. Res. *21*, 961–972.

Joselin, A.P., Schulze-Osthoff, K., and Schwerk, C. (2006). Loss of acinus inhibits oligonucleosomal DNA fragmentation but not chromatin condensation during apoptosis. J. Biol. Chem. *281*, 12475–12484.

Kadoch, C., and Crabtree, G.R. (2015). Mammalian SWI/SNF chromatin remodeling complexes and cancer: Mechanistic insights gained from human genomics. Sci. Adv. *1*, e1500447–e1500447.

Kammel, C., Thomaier, M., Sørensen, B.B., Schubert, T., Längst, G., Grasser, M., and Grasser, K.D. (2013). Arabidopsis DEAD-Box RNA Helicase UAP56 Interacts with Both RNA and DNA as well as with mRNA Export Factors. PLoS One *8*, 1-12.

Kanu, N., and Behrens, A. (2007). ATMIN defines an NBS1-independent pathway of ATM signalling. EMBO J. *26*, 2933–2941.

Karve, T.M., and Cheema, A.K. (2011). Small Changes Huge Impact : The Role of Protein Posttranslational Modifications in Cellular Homeostasis and Disease. Jour. of Amino Acids *2011*, 1-13.

Kastan, M.B., and Bartek, J. (2004). Cell-cycle checkpoints and cancer. Nature *432*, 316–323.

Koci, L., Chlebova, K., Hyzdalova, M., Hofmanova, J., Jira, M., Kysela, P., Kozubik, A., Kala, Z., and Krejci, P. (2012). Apoptosis inhibitor 5 (API-5; AAC-11; FIF) is upregulated in human carcinomas in vivo. Oncol. Lett. *3*, 913–916.

Kollenstart, L. (2009). A focus on foci : How spatio-temporal regulation of the DNA damage response is crucial for DDR activation and cell fate. 1–22.

Kops, G.J.P.L., Weaver, B. a a, and Cleveland, D.W. (2005). On the road to cancer:

aneuploidy and the mitotic checkpoint. Nat. Rev. Cancer *5*, 773–785.

Koster, D. a, Croquette, V., Dekker, C., Shuman, S., and Dekker, N.H. (2005). Friction and torque govern the relaxation of DNA supercoils by eukaryotic topoisomerase IB. Nature *434*, 671–674.

Kosugi, S., and Hasebe, M. (2008). Nuclear Export Signal Consensus Sequences Defined Using a Localization-Based Yeast Selection System. Traffic *9*, 2053–2062.

Krejci, P., Pejchalova, K., Rosenbloom, B.E., Rosenfelt, F.P., Tran, E.L., Laurell, H., and Wilcox, W.R. (2007). The antiapoptotic protein Api5 and its partner, high molecular weight FGF2, are up-regulated in B cell chronic lymphoid leukemia. J. Leukoc. Biol. *82*, 1363–1364.

Kumagai, A., Lee, J., Yoo, H.Y., and Dunphy, W.G. (2006). TopBP1 activates the ATR-ATRIP complex. Cell *124*, 943–955.

Kuo, L. J., and Yang, L.-X. (2008). Gamma-H2AX - a novel biomarker for DNA double-strand breaks. In vivo (Athens, Greece) *22*, 305-9.

Längst, G., and Manelyte, L. (2015). Chromatin remodelers: From function to dysfunction. Genes (Basel). *6*, 299–324.

Le Hir, H., and Andersen, G.R. (2008). Structural insights into the exon junction complex. Curr. Opin. Struct. Biol. *18*, 112–119.

Leung, C.C.Y., and Glover, J.N.M. (2011). BRCT domains: Easy as one, two, three. Cell Cycle *10*, 2461–2470.

Li, X., Gao, X., Wei, Y., Deng, L., Ouyang, Y., Chen, G., Li, X., Zhang, Q., and Wu, C. (2011). Rice APOPTOSIS INHIBITOR5 coupled with two DEAD-box adenosine 5'-triphosphate-dependent RNA helicases regulates tapetum degeneration. Plant Cell *23*, 1416–1434.

Liang, Y., Charles, Æ.S.L.Æ.F., Goss, J., and Li, Æ.K. (2009). DNA Damage Response Pathways in Tumor Suppression and Cancer Treatment. World J. Surg. *33*, 661–666.

Lin, S.J., Wardlaw, C.P., Morishita, T., Miyabe, I., Chahwan, C., Caspari, T., Schmidt, U., Carr, A.M., and Garcia, V. (2012). The Rad4TopBP1 ATR-activation domain functions in G1/S phase in a chromatin-dependent manner. PLoS Genet. *8*, 1-14.

Liu, K., Lin, F., Ruppert, J.M., and Lin, W. (2003). Regulation of E2F1 by BRCT Domain-Containing Protein TopBP1. Mol. and cell. biol. *23*, 3287–3304.

Liu, K., Luo, Y., Lin, F., and Lin, W. (2004). TopBP1 recruits Brg1 / Brm to repress E2F1-induced apoptosis , a novel pRb-independent and E2F1-specific control for cell survival. Genes Dev. *18*, 673–686.

Liu, K., Paik, J.C., Wang, B., Lin, F.-T., and Lin, W.-C. (2006). Regulation of TopBP1 oligomerization by Akt/PKB for cell survival. EMBO J. *25*, 4795–4807.

Liu, K., Bellam, N., Lin, H.-Y.Y., Wang, B., Stockard, C.R., Grizzle, W.E., and Lin, W.-C.C. (2009). Regulation of p53 by TopBP1: a potential mechanism for p53 inactivation in cancer. Mol Cell Biol *29*, 2673-2693.

Liu, K., Ling, S., and Lin, W. (2011). TopBP1 Mediates Mutant p53 Gain of Function through NF-Y and p63 / p73   . Mol Cell Biol *31*, 4464–4481.

Liu, K., Graves, J.D., Scott, J.D., Li, R., and Lin, W.-C. (2013). Akt switches TopBP1 function from checkpoint activation to transcriptional regulation through phosphoserine binding-mediated oligomerization. Mol. Cell. Biol. *33*, 4685–4700.

Liu, Q., Guntuku, S., Cui, X., Matsuoka, S., Cortez, D., Tamai, K., Luo, G., Carattini-rivera, S., Demayo, F., Bradley, A., et al. (2000). Chk1 is an essential kinase that is regulated by Atr and required for the G 2 / M DNA damage checkpoint. Genes Dev. *14*, 1448–1459.

M.E.Wall, Wani, C.E. Cook, K.H. Palmer, A.T. McPhail, G. a. S. (1966). Plant anitumor agents I. The isolation and structure of camptothecin, a novel alkaloidal leukemia and tumor inhibitor from camptotheca acuminata. Jounal Am. Chem. Soc. *18*, 3888–3890.

Maecker, H.L., Koumenis, C., and Giaccia, A.J. (2000). p53 promotes selection for Fas-mediated apoptotic resistance. Cancer Res. *60*, 4638–4644.

Makiniemi, M., Hillukkala, T., Tuusa, J., Reini, K., Vaara, M., Huang, D., Pospiech, H., Majuri, I., Westerling, T., Makela, and T.P., Syvaoja, J.E. (2001). BRCT Domain-containing Protein TopBP1 Functions in DNA Replication and Damage Response. Journ. Biol. Chem. *276*, 30399–30406.

Malumbres, M., and Barbacid, M. (2009). Cell cycle, CDKs and cancer: a changing paradigm. Cancer *9*, 153-66.

Mann, M., and Jensen, O.N. (2003). Proteomic analysis of post-translational modifications. Nat. biotechnology *21*, 255–261.

Massagué, J. (2004). G1 cell-cycle control and cancer. Nature *432*, 298–306.

Mayank, A.K., Sharma, S., Nailwal, H., and Lal, S.K. (2015). Nucleoprotein of

influenza A virus negatively impacts antiapoptotic protein API5 to enhance E2F1-dependent apoptosis and virus replication. Cell Death Dis *6*, 1–11.

Méndez, J., and Stillman, B. (2000). Chromatin association of human origin recognition complex, cdc6, and minichromosome maintenance proteins during the cell cycle: assembly of prereplication complexes in late mitosis. Mol. Cell. Biol. *20*, 8602–8612.

Mesquita, R.D., Woods, N.T., Seabra-Junior, E.S., and Monteiro, a. N. a. (2010). Tandem BRCT Domains: DNA's Praetorian Guard. Genes Cancer *1*, 1140–1146.

Miernyk, J.A., and Thelen, J.J. (2008). Biochemical approaches for discovering protein – protein interactions. The Plant Journal. *53*, 597–609.

Mirakabadi, A.Z., Sarzaeem, A., Moradhaseli, S., Sayad, A., and Negahdary, M. (2012). Necrotic effect versus apoptotic nature of Camptothecin in human cervical cancer cells. Iran. J. Cancer Prev. *5*, 109–116.

Modrich, P., and Lahue, R. (1996). Mismatch repair in replication fidelity, genetic recombination, and cancer biology. Annu. Rev. Biochem. *65*, 101–133.

Mohrmann, L., and Verrijzer, C.P. (2005). Composition and functional specificity of SWI2/SNF2 class chromatin remodeling complexes. Biochim. Biophys. Acta - Gene Struct. Expr. *1681*, 59–73.

Moldovan, G., Pfander, B., and Jentsch, S. (2007). PCNA , the Maestro of the Replication Fork. Cell *129*, 665–679.

Moll, U.M., Petrenko, O., Moll, U.M., and Petrenko, O. (2003). The MDM2-p53 Interaction The MDM2-p53 Interaction. Mol. Can. Res *1*, 1001–1008.

Mordes, D.A., Nam, E.A., and Cortez, D. (2008). Dpb11 activates the Mec1-Ddc2 complex. Proc. Natl. Acad. Sci. U. S. A. *105*, 18730–18734.

Moreland, J.L., Gramada, A., Buzko, O. V, Zhang, Q., Bourne, P.E., Kraulis, P., DeLano, W., Sayle, R., Milner-White, E., Guex, N., et al. (2005). The Molecular Biology Toolkit (MBT): a modular platform for developing molecular visualization applications. BMC Bioinformatics *6*, 21.

Morishima, K., Sakamoto, S., Kobayashi, J., and Izumi, H. (2007). TopBP1 associates with NBS1 and is involved in homologous recombination repair. Biochem. Biophys. Res Comm. *362*, 872–879.

Morris, E.J. (1996). Topoisomerase-I : Evidence for Cell Cycle-independent Toxicity. Cell *134*, 757–770.

Morris, E.J., Michaud, W.A., Ji, J., Moon, N., Rocco, J.W., and Dyson, N.J. (2006). Functional Identification of Api5 as a Suppressor of E2F-Dependent Apoptosis In Vivo. PLoS Genetics *2*, 1834-1848.

Mueller, H., Bracken, A.P., Vernell, R., Moroni, M.C., Christians, F., Grassilli, E., Prosperini, E., Vigo, E., Oliner, J.D., and Helin, K. (2001). E2Fs regulate the expression of genes involved in differentiation , development , proliferation , and apoptosis. Genes Dev. *2*, 267–285.

Mundle, S.D., and Saberwal, G. (2003). Evolving intricacies and implications of E2F1 regulation. FASEB J. *17*, 569–574.

Nakano, K., Vousden, K.H., Ashcroft, M., Taya, Y., Vousden, K.H., Ashkenazi, A., Dixit, V.M., Bates, S., Vousden, K.H., Bennett, M., et al. (2001). PUMA, a novel proapoptotic gene, is induced by p53. Mol. Cell *7*, 683–694.

Narlikar, G.J., Sundaramoorthy, R., and Owen-Hughes, T. (2013). Mechanisms and functions of ATP-dependent chromatin-remodeling enzymes. Cell *154*, 490–503.

Neuwald, A.F., and Hirano, T. (2000a). HEAT Repeats Associated with Condensins , Cohesins , and Other Complexes Involved in Chromosome-Related Functions. Genome Res *10*, 1445-1452.

Noh, K.H., Kim, S., and Kim, J.H. (2014). API5 Confers Tumoral Immune Escape through FGF2-Dependent Cell Survival Pathway. Cancer Res. *74(13)*, 3556–3566.

Nyberg, K.A., Michelson, R.J., Putnam, C.W., and Weinert, T.A. (2002). TOWARD MAINTAINING THE GENOME : DNA Damage and Replication Checkpoints. Annu. Rev. Genet. *36*, 617-56.

O'Connor, M.J. (2015). Targeting the DNA Damage Response in Cancer. Mol. Cell *60*, 547–560.

Oda, K., Arakawa, H., Tanaka, T., Matsuda, K., Tanikawa, C., Mori, T., Nishimori, H., Tamai, K., Tokino, T., Nakamura, Y., et al. (2000). p53AIP1, a potential mediator of p53-dependent apoptosis, and its regulation by Ser-46-phosphorylated p53. Cell *102*, 849–862.

Oliver, T.G., Meylan, E., Chang, G.P., Xue, W., Burke, J.R., Humpton, T.J., Hubbard, D., Bhutkar, A., and Jacks, T. (2011). Caspase-2-Mediated Cleavage of Mdm2 Creates a p53-Induced Positive Feedback Loop. Mol. Cell *43*, 57–71.

Oren, M. (1999). Regulation of the p53 tumor suppressor protein. J. Biol. Chem. *274*, 36031–36034.

Ozaki, T., and Nakagawara, A. (2011). Role of p53 in cell death and human cancers. Cancers (Basel). *3*, 994–1013.

Parchment, R., and Pessina, A. (1998). Topoisomerase I inhibitors and drug resistance. Cytotechnology *27*, 149–164.

Parrish, A.B., Freel, C.D., and Kornbluth, S. (2013). Cellular Mechanisms Controlling Caspase Activation and Function. Cold Spring Harb. Perspect. Biol. *5*, 1–24.

Pawson, T., and Nash, P. (2000). Protein – protein interactions define specificity in signal transduction. Genes Dev. *14*, 1027–1047.

Phizicky, E.M., and Fields, S. (1995). Protein-protein interactions: methods for detection and analysis. Microbiol. Rev. *59*, 94–123.

Piehler, J. (2005). New methodologies for measuring protein interactions in vivo and in vitro. Curr. Opin. Str. Biol. *15*, 4–14.

Plevin, M.J., Mills, M.M., and Ikura, M. (2005). The LxxLL motif : a multifunctional binding sequence in transcriptional regulation. TRENDS Biochem. Sci. *30*, 66–69.

Pochampally, R., Fodera, B., Chen, L., Shao, W., Levine, E. a, and Chen, J. (1998). A 60 kd MDM2 isoform is produced by caspase cleavage in non-apoptotic tumor cells. Oncogene *17*, 2629–2636.

Pochampally, R., Fodera, B., Chen, L., Lu, W., and Chen, J. (1999). Activation of an MDM2-specific caspase by p53 in the absence of apoptosis. J. Biol. Chem. *274*, 15271–15277.

Polager, S., and Ginsberg, D. (2009). p53 and E2f : partners in life and death a V. Nat. Rev. Cancer *9*, 738–748.

Polo, S.E., and Jackson, S.P. (2011). Dynamics of DNA damage response proteins at DNA breaks : a focus on protein modifications. Genes Dev. *25*, 409–433.

Pommier, Y. (2009). DNA Topoisomerase I Inhibitors: Chemistry, Biology and Interfacial Inhibition. Chem Rev *109*, 2894–2902.

Rappold, I., Iwabuchi, K., Date, T., and Chen, J. (2001). Tumor Suppressor p53 Binding Protein 1 (53BP1) Is Involved in DNA Damage-signaling Pathways. Journ. Cell Biol. *153*, 613–620.

Rastogi, R.P., Kumar, A., Tyagi, M.B., and Sinha, R.P. (2010). Molecular Mechanisms of Ultraviolet Radiation-Induced DNA Damage and Repair. *2010*, 1-32.

Reisman, D., Elkind, N.B., Roy, B., Beamon, J., and Rotter, V. (1993). c-Myc Trans-activates the p53 Promoter through a Required Downstream CACGTG Motif. Cell

Growth & Differentiation *4*, 57–65.

Ren, K., Zhang, W., Shi, Y., and Gong, J. (2010). Pim-2 activates API-5 to inhibit the apoptosis of hepatocellular carcinoma cells through NF-kappaB pathway. Pathol. Oncol. Res. *16*, 229–237.

Rigou, P., Piddubnyak, V., Faye, A., Rain, J.-C., Michel, L., Calvo, F., and Poyet, J.-L. (2009). The antiapoptotic protein AAC-11 interacts with and regulates Acinus-mediated DNA fragmentation. EMBO J. *28*, 1576–1588.

Robles, A.I., Bemmels, N.A., Foraker, A.B., and Harris, C.C. (2001). APAF-1 is a transcriptional target of p53 in DNA damage-induced apoptosis. Cancer Res. *61*, 6660–6664.

Rodier, F., Campisi, J., and Bhaumik, D. (2007). Two faces of p53 : aging and tumor suppression. Nucleic Acids Res. *35*, 7475–7484.

Roos, W.P., and Kaina, B. (2013). DNA damage-induced cell death : From specific DNA lesions to the DNA damage response and apoptosis. Cancer Lett. *332*, 237–248.

Rothenberg, M.L. (1997). Topoisomerase I inhibitors: review and update. Ann. Oncol. *8*, 837–855.

Rothkamm, K., Barnard, S., Moquet, J., Ellender, M., Rana, Z., and Burdak-rothkamm, S. (2015). Review DNA Damage Foci : Meaning and Significance. Environmental and Molecular Mutagenesis *56*, 491-504.

Ryan, A.J., Squires, S., Strutt, H.L., and Johnson, R.T. (1991). Camptothecin cytotoxicity in mammalian cells is associated with the induction of persistent double strand breaks in replicating DNA. Nucleic Acids Res. *19*, 3295–3300.

Sahara, S., Aoto, M., Eguchi, Y., Imamoto, N., Yoneda, Y., and Tsujimoto, Y. (1999). Acinus is a caspase-3 -activated protein required for apoptotic chromatin condensation. Nature *401*, 168-173.

Salvesen, G.S., and Duckett, C.S. (2002). IAP proteins: blocking the road to death's door. Nat. Rev. Mol. Cell Biol. *3*, 401–410.

Sancar, A., and Kemp, M.G. (2011). Multiple ATR-Chk1 Pathway Proteins Preferentially Associate with Checkpoint-Inducing DNA Substrates. PLoS One *6*, 1-10.

Sasaki, H., Moriyama, S., Yukiue, H., Kobayashi, Y., Nakashima, Y., Kaji, M., Fukai, I., Kiriyama, M., Yamakawa, Y., and Fujii, Y. (2001). Expression of the antiapoptosis gene, AAC-11, as a prognosis marker in non-small cell lung cancer. Lung Cancer *34*,

53–57.

Schultz, L.B., Chehab, N.H., Malikzay, A., and Halazonetis, T.D. (2000). p53 Binding Protein 1 (53BP1) Is an Early Participant in the Cellular Response to DNA Double-Strand Breaks. *151*, 1381–1390.

Schwerk, C., Prasad, J., Degenhardt, K., Erdjument-Bromage, H., White, E., Tempst, P., Kidd, V.J., Manley, J.L., Lahti, J.M., and Reinberg, D. (2003). ASAP, a novel protein complex involved in RNA processing and apoptosis. Mol. Cell. Biol. *23*, 2981–2990.

Scian, M.J., Stagliano, K.E.R., Ellis, M.A., Hassan, S., Bowman, M., Miles, M.F., Deb, S.P., and Deb, S. (2004). Modulation of gene expression by tumor-derived p53 mutants. Cancer Res. *64*, 7447–7454.

Shaheen, M., Shanmugam, I., and Hromas, R. (2010). The Role of PCNA Posttranslational Modifications in Translesion Synthesis. Journ. Nucleic Acids. *2010*, 1-8.

Sheng, Z., and Zhao, Y. Evolutionary Bioinformatics Functional evolution of BRCT Domains from Binding DNA to protein. Evolutionary Bioinformatics *2011*, 87–97.

Shiloh, Y. (2001). ATM (ataxia telangiectasia mutated): expanding roles in the DNA damage response and cellular homeostasis. Biochem. Soc. Trans. *29*, 661–666.

Shimizu, I., Yoshida, Y., Suda, M., and Minamino, T. (2014). DNA damage response and metabolic disease. Cell Metab. *20*, 967–977.

Shiotani, B., and Zou, L. (2009). Single-Stranded DNA Orchestrates an ATM-to-ATR Switch at DNA Breaks. Mol. Cell *33*, 547–558.

Shoemaker, B.A., and Panchenko, A.R. (2007). Deciphering Protein–Protein Interactions. Part I. Experimental Techniques and Databases. PLoS Comp. Biol. *3*, 0337-0344.

Silke, J., and Meier, P. (2013). Inhibitor of Apoptosis (IAP) Proteins – Modulators of Cell Death and Inflammation. Cold Spring Harb Perspect Biol *5*, 1-19.

Sinowatz, F., Schams, D., Einspanier, R., Arnold, G., Pfeffer, M., Temmim-Baker, L., Amselgruber, W., and Plendl, J. (2000). Cellular localization of fibroblast growth factor 2 (FGF-2) in benign prostatic hyperplasia. Histol Histopathol *15*, 475–481.

Soldani, C., and Scovassi, A.I. (2002). Poly (ADP-ribose) polymerase-1 cleavage during apoptosis : An update Cell death mechanisms : Necrosis and apoptosis. Apoptosis *7*, 321–328.

Song, K., Cho, H., Kim, S., Lee, H., Oh, S.J., Woo, S.R., Hong, S., Jang, H.S., Noh, K.H., Choi, C.H., et al. (2017). API5 confers cancer stem cell-like properties through the FGF2-NANOG axis. Oncogenesis *6*, 1-13.

Song, K., Kim, S., Noh, K.H., Bae, H.C., Kim, J.H., Lee, H., and Song, J. (2015). Apoptosis inhibitor 5 increases metastasis via Erk-mediated MMP expression. BMB Rep. *48*, 330–335.

Spektor, T.M., and Rice, J.C. (2009). Identification and characterization of posttranslational modification-specific binding proteins in vivo by mammalian tethered catalysis. Proc. Natl. Acad. Sci. U. S. A. *106*, 14808–14813.

Srinivasula, S.M., Ahmad, M., Fernandes-Alnemri, T., and Alnemri, E.S. (1998). Autoactivation of procaspase-9 by Apaf-1-mediated oligomerization. Mol. Cell *1*, 949–957.

Suzuki, K., Yamauchi, M., Oka, Y., and Suzuki, M. (2010). A novel and simple micro-irradiation technique for creating localized DNA double-strand breaks. Nucleic Acids Res. *38*, 1–11.

Suzuki, K., Yamauchi, M., Oka, Y., Suzuki, M., and Yamashita, S. (2011). Creating localized DNA double-strand breaks with microirradiation. Nat. Protoc. *6*, 134–139.

Tang, L., Nogales, E., and Ciferri, C. (2010). Structure and function of SWI / SNF chromatin remodeling complexes and mechanistic implications for transcription. Prog. Biophys. Mol. Biol. *102*, 122–128.

Tange, T.Ø., Shibuya, T., Jurica, M.S., and Moore, M.J. (2005). Biochemical analysis of the EJC reveals two new factors and a stable tetrameric protein core. RNA *11*, 1869–1883.

Tewari, M., Yu, M., Ross, B., Yu, M., Dean, C., Giordano, A., and Rubin, R. (1997). AAC-11 , a Novel cDNA That Inhibits Apoptosis after Growth Factor Withdrawal. Cancer Res. *57*, 4063–4069.

Tewari, R., Bailes, E., Bunting, K.A., and Coates, J.C. (2010). Armadillo-repeat protein functions : questions for little creatures. Trends Cell Biol. *20*, 470–481.

Thompson, C.L., and Sancar, A. (2002). Photolyase/cryptochrome blue-light photoreceptors use photon energy to repair DNA and reset the circadian clock. Oncogene *21*, 9043–9056.

Tobergte, D. R., and Curtis, S. (2013). Advances in Biochemical Engineering Biotechnology (Springer). Journal of Chemical Information and Modeling. *53*, 1689-

1699.

Toshiyuki, M., and Reed, J.C. (1995). Tumor suppressor p53 is a direct transcriptional activator of the human bax gene. Cell *80*, 293–299.

Turinetto, V., and Giachino, C. (2015). Multiple facets of histone variant H2AX : a DNA double-strand-break marker with several biological functions. Nucleic Acids Res. *43*, 2489-2498.

Twiddy, D., and Cain, K. (2007). Caspase-9 cleavage, do you need it? Biochem. J. *405*, e1.

Walsh, C.T., Garneau-tsodikova, S., and Gatto, G.J. (2005). Protein Chemistry Protein Posttranslational Modifications : The Chemistry of Proteome Diversifications Angewandte Chemie - International Edition *44*, 7342–7372.

Ward, I.M., Minn, K., Jorda, K.G., and Chen, J. (2003). Accumulation of Checkpoint Protein 53BP1 at DNA Breaks Involves Its Binding to Phosphorylated Histone H2AX. The Journ. of Biol. Chem. *278*, 19579-19582.

Wardlaw, C.P., Carr, A.M., and Oliver, A.W. (2014). TopBP1 : A BRCT-scaffold protein functioning in multiple cellular pathways. DNA Repair (Amst). *22*, 165–174.

Warmerdam, O., and Kanaar, R. (2010). Mutation Research / Reviews in Mutation Research Dealing with DNA damage : Relationships between checkpoint and repair pathways. DNA Repair (Amst). *704*, 2–11.

Weber, A.M., and Ryan, A.J. (2015). ATM and ATR as therapeutic targets in cancer. Pharmacol. Ther. *149*, 124–138.

Westermarck, J., Ivaska, J., and Corthals, G.L. (2013). Identification of Protein Interactions Involved in Cellular Signaling. MCP *12*, 1752–1763.

Wolff, S., Erster, S., Palacios, G., and Moll, U.M. (2008). p53's mitochondrial translocation and MOMP action is independent of Puma and Bax and severely disrupts mitochondrial membrane integrity. Cell Res. *18*, 733–744.

Wood, R.D., Wood, R.D., Mitchell, M., Sgouros, J., and Lindahl, T. (2011). Human DNA Repair Genes. Science *1284*, 241–283.

Wright, R.H.G., Dornan, E.S., Donaldson, M.M., and Morgan, I.M. (2006). TopBP1 contains a transcriptional activation domain suppressed by two adjacent BRCT domains. Biochem. J. *400*, 573–582.

Wu, Q., Jubb, H., and Blundell, T.L. (2015). Phosphopeptide interactions with BRCA1 BRCT domains: More than just a motif. Prog. Biophys. Mol. Biol. *117*, 143–

148.

Wu, Y., Li, Q., and Chen, X.-Z. (2007). Detecting protein-protein interactions by Far western blotting. Nat. Protoc. *2*, 3278–3284.

Xing, S., Wallmeroth, N., Berendzen, K.W., and Grefen, C. (2016). Techniques for the Analysis of Protein-Protein Interactions in Vivo. Plant physiology. *171*, 727–758.

Yamane, K., and Tsuruo, T. (1999). Conserved BRCT regions of TopBP1 and of the tumor suppressor BRCA1 bind strand breaks and termini of DNA. Oncogene *18*, 5194–5203.

Yamane, K., Wu, X., and Chen, J. (2002). A DNA Damage-Regulated BRCT-Containing Protein , TopBP1 , Is Required for Cell Survival. Molecular and cellular biology *22*, 555–566.

Yan, S., and Michael, W.M. (2009). TopBP1 and DNA polymerase α-mediated recruitment of the 9-1-1 complex to stalled replication forks. Cell Cycle *8*, 2877–2884.

Yoo, H.Y., Kumagai, A., Shevchenko, A., and Dunphy, W.G. (2007). Ataxia-telangiectasia Mutated (ATM) -dependent Activation of ATR Occurs through Phosphorylation of TopBP1 by ATM * □. J. Biol. Chem. *282*, 17501–17506.

Yoo, H.Y., Kumagai, A., Shevchenko, A., Shevchenko, A., and Dunphy, W.G. (2009). The Mre11-Rad50-Nbs1 Complex Mediates Activation of TopBP1 by ATM. Molecular Biology of the Cell *20,* 2351–2360.

Yoshida, K., and Inoue, I. (2004). Expression of MCM10 and TopBP1 is regulated by cell proliferation and UV irradiation via the E2F transcription factor. Oncogene *23*, 6250–6260.

Yoshida, K., and Miki, Y. (2010). The cell death machinery governed by the p53 tumor suppressor in response to DNA damage. Cancer Sci. *101*, 831–835.

Zeng, L., Hu, Y., and Li, B. (2005). Identification of TopBP1 as a c-Abl-interacting protein and a repressor for c-Abl expression. J. Biol. Chem. *280*, 29374–29380.

Zhang, X., Moréra, S., Bates, P.A., Whitehead, P.C., Coffer, A.I., Hainbucher, K., Nash, R.A., Sternberg, M.J.E., Lindahl, T., and Freemont, P.S. (1998). Structure of an XRCC1 BRCT domain: A new protein-protein interaction module. EMBO J. *17*, 6404–6411.

Zhou, B.S., and Elledge, S.J. (2000). The DNA damage response: putting checkpoints in perspective. Nature *408*, 433–439.

Zou, H., Yang, R., Hao, J., Wang, J., Sun, C., Fesik, S.W., Wu, J.C., Tomaselli, K.J., and Armstrong, R.C. (2003). Regulation of the Apaf-1/caspase-9 apoptosome by caspase-3 and XIAP. J. Biol. Chem. *278*, 8091–8098.

Appendix

PCR reactions and buffer compositions

PCR reaction for amplifying Api5 and its deletion mutants:

Template plasmid	1.0 μl
10X Pfu buffer	5.0 μl
Forward primer (25μM)	1.0 μl
Reverse primer (25μM)	1.0 μl
dNTPs (2.5 mM each)	2.5 μl
Pfu Pol	1.0 μl
milliQ water	38.5 μl

PCR thermo-cycling conditions for cloning of Api5 and its deletion mutants:

Step1. Initital denaturation:	95° C – 2 minutes	
Step2. Denaturation:	95°C – 1 minute	
Step3. Primer annealing:	60°C – 1 minute	30 cycles
Step4*. Extension:	72°C – 3 minutes	
Step5. Final extension:	72°C – 6 minutes	
Step6. Hold:	4°C - ∞	

* For amplifying LZD, Step 4 was for 1 minute

PCR reaction for site directed mutagenesis of Api5:

Template plasmid	1.0 μl
10X Pfu buffer	5.0 μl
Forward primer (25μM)	1.0 μl
Reverse primer (25μM)	1.0 μl
dNTPs (2.5 mM each)	4.0 μl
Pfu Pol	1.0 μl
milliQ water	37.0 μl

PCR thermo-cycling conditions for site directed mutagenesis of Api5

Step1. Initial denaturation: 95°C – 1 minute

Step2. Denaturation: 95°C – 30 seconds

Step3. Primer annealing: 55°C – 1 minute   } 18 cycles

Step4. Extension: 68°C – 15 minutes

Step6. Hold: 4°C - ∞

10X PBS pH7.4 (500ml)

NaCl	40g
KCl	1g
Na_2HPO_4	7.2g
KH_2PO_4	1.2g

50X TAE buffer (1litre)

Tris base	242g
Glacial acetic acid	57.1ml
0.5M EDTA pH8.0	100ml

TE buffer (1litre)

1M Tris pH7.4	100ml
0.5M EDTA pH8.0	20ml

5X TBE (1litre)

Tris base	54g
Boric acid	27.5g
0.5M EDTA pH8.0	20ml

Western blotting buffers:

10X SDS running buffer (1litre)

Tris base	30.3g
Glycine	144g
SDS	10g

10X Transfer buffer (2litres)

Tris base 58g

Glycine 293g

20 X TBS (1litre)

Tris base 60g

NaCl 160g

KCl 4g

pH7.6 with HCl

6X Laemmli buffer (10ml)

1M Tris pH6.8	3.5ml
DTT	0.93g
Glycerol	3.6ml
SDS	1.1g
1% bromo-phenol blue	0.6ml

Far western (AC) buffers composition:

Guanidine HCl concentration (M)	6	3	1	0.1	0
Glycerol (ml)	2.5	2.5	2.5	2.5	2.5
5M NaCl (ml)	0.5	0.5	0.5	0.5	0.5
1M Tris pH7.5 (ml)	0.5	0.5	0.5	0.5	0.5
0.5M EDTA (ml)	0.05	0.05	0.05	0.05	0.05
Tween-20 (ml)	0.025	0.025	0.025	0.025	0.025
1M DTT (ml)	0.025	0.025	0.025	0.025	0.025
dH$_2$O (ml)	2.45	12.82	18.07	20.89	21.20
NFDM (g)	0.5	0.5	0.5	0.5	0.5
8M Guanidine HCl (ml)	18.75	9.30	3.13	0.31	0
Total volume (ml)	25	25	25	25	25
Incubation time/ temperature	30 min/RT	30 min/RT	30 min/RT	30 min/4°C	Overnight/ 4°C

Table 1: List of antibodies

S No	Cat No	Vendor	Antibody	Source	Dilution	Purpose
1	ab2302	Abcam	active Caspase 9	Rabbit	1:1000	WB
2	ab31930	Abcam	ORC2 SB46	Mouse	1:500	WB
3	ab290	Abcam	GFP	Rabbit		WB
4	PAB7951	Abnova	Api5	Rabbit	1:2500 1:1000	WB IF
5	611874	BD Biosciences	TopBP1	Mouse	1:200	IF
6	A300-111A	Bethyl Laboraties	TopBP1	Rabbit	1:5000	WB
7	A300-247A	Bethyl Laboratories	p53	Rabbit	1:10,000	WB
8	AM30	Calbiochem	PARP1	Mouse	1:100	WB
9	2348S	Cell Signaling Technology	pChk1 S345 133D3	Rabbit	1:5000	WB
10	2661S	Cell Signaling Technology	pChk2 T68	Rabbit	1:2500	WB
11	9271S	Cell Signaling Technology	Chk2 1C12	Mouse	1:1000	WB
12	9284S	Cell Signaling Technology	p53 pS15	Rabbit	1:1000	WB
13	9664S	Cell Signaling Technology	cleaved Caspase 3 Asp 175 5A1E	Rabbit	1:1000	WB
14	2772S	Cell Signaling Technology	Bax	Rabbit	1:1000	WB
15	4937S	Cell Signaling Technology	53BP1	Rabbit	1:100	IF
16	05-782	Merck Millipore	GST	Mouse	1:5000	WB
17	16-202A	Merck Millipore	γ H2AX-FITC	Mouse	1:200	IF
18	sc8408	Santacruz Biotechnology	Chk1 G4	Mouse	1:1000	WB
19	sc193	Santacruz Biotechnology	E2F1 C20	Rabbit	1:2000	WB
20	sc-813	Santacruz Biotechnology	MDM2	Rabbit	1:800	IF
21	G9545	Sigma Aldrich	GAPDH	Rabbit	1:20,000	WB
22	T6199	Sigma Aldrich	α Tubulin	Mouse	1:20,000	WB
23	115-035-003	Jackson ImmunoResearch	Peroxidase AffiniPure Goat Anti-Mouse IgG (H+L)	Goat	1:10,000	WB

24	111-035-003	Jackson ImmunoResearch	Peroxidase AffiniPure Goat Anti-Rabbit IgG (H+L**)**	Goat	1:10,000	WB
25	A-11034	Invitrogen	Goat anti-Rabbit IgG (H+L) Secondary Antibody, Alexa Fluor 488	Goat	1:1000	IF
26	A-11004	Invitrogen	Goat anti-Mouse IgG (H+L) Secondary Antibody, Alexa Fluor 568	Goat	1:1000	IF
27	A-21071	Invitrogen	Goat anti-Rabbit IgG (H+L) Secondary Antibody, Alexa Fluor 633	Goat	1:1000	IF

Table 2: List of oligos

S No	Oligo name	Sequence	Application
1	Api5 for2	CATGATCCATGGATGCCGACAGTAGAGGAGCT	Cloning
2	LZD rev2	ATCGGAATTCCAAAATCTGGAAGTTTTCGGCCC	Cloning
3	GSLZDfor	CATGCCATGGACTTAACAGCCAAACTGAATGC	Cloning
4	GSLZDErev	ATCGGAATTCAAGTTGTCTGATATAAACTTGC	Cloning
5	GS-6 for	CATGCCATGGTTCGCTTAGCTCTCCAGGGTA	Cloning
6	GST Api5 rev	CCAGAATTCTCAGTAGAGTCTTCCCCGAC	Cloning
7	Fluor Api5 For	GGAAGATCTATGCCGACAGTAGAGGAGCT	Cloning
8	Fluor Api5 Rev	CCGGAATTCTCAGTAGAGTCTTCCCCGAC	Cloning
9	Api5 mVenusC1 NLS for	GGAAGATCTCCGAAGAAGAAGCGAAAGGTAATGCCGACAGTAGAGGAGCT	Cloning
10	Api5 mVenusC1 NLS d2-3 rev	CCGGAATTCAAATCTGGAAGTTTTCGGCC	Cloning
11	Api5 mVenusC1 NLS LZD for	GGAAGATCTCCGAAGAAGAAGCGAAAGGTATTCTTAACAGCCAAACTGAA	Cloning
12	Api5 mVenusC1 NLS LZD rev	CCGGAATTCAGTTGTCTGATATAAACTTG	Cloning
13	Api5 mVenusC1 NLS d1-2 for	GGAAGATCTCCGAAGAAGAAGCGAAAGGTACTTCGCTTAGCTCTCCAGGG	Cloning
14	mut Api5 1-F	GCCGAACTGGATCAGACCTTCA	SDM
15	mut Api5 1-R	TGAAGGTCTGATCCACTTCGGC	SDM
16	Api5-1 mutseqchk	TAACAAAGGAAGTGGAAGAGC	Sequencing
17	TopBP1 BRCT7-8 pGEX-2Tkcs For	CGGGATCCACTCATGAAGAATTAAAAAAACAGT	Cloning

18	TopBP1 pGEX-2Tkcs Rev	CGGAATTCTTAGTGTACTCTAGGTCGTTTGATT	Cloning
19	ds70-1	TGCAGCTGGCACGACAGGTTTTAATGAATCGGCCAACGCGCGGGGAGAGGCGGTTTGCGTATTGGGCGCT	EMSA
20	ds70-2	ACGTCGACCGTGCTGTCCAAAATTACTTAGCCGGTTGCGCGCCCCTCTCCGCCAAACGCATAACCCGCGA	EMSA
21	70-fork	ACGTCGACCGTGCTGTCCAATCGCGGGTTATGCGTTTGGCGGAGAGGGGCGCGCAACCGGCTAAGTAATT	EMSA
22	70-bubble	ACGTCGACCGTGCTGTCCAATTAATGAATCGGCCAACGCGCGGGGAGAGGGCCAAACGCATAACCCGCGA	EMSA
23	si LacZ	Sense: CGUACGCGGAAUACUUCGA Antisense: UCGAAGUAUUCCGCGUACG	Knockdown
24	si Api5-1	Sense: GACCUAGAACAGACCUUCAUU Antisense: UUCUGGAUCUUGUCUGGAAGU	Knockdown
25	si Api5-3	Sense: CAGAAGAGAACAAGAUUAAUU Antisense: UUGUCUUCUCUUGUUCUAAUU	Knockdown
26	si TopBP1	Sense: GUGGUUGUAACAGCGCAUCUU Antisense: GAUGCGCUGUUACAACCACUU	Knockdown